UNIVERSITAT ROVIRA I VIRGILI
BOTTOM-UP SURFACE ENGINEERING FOR THE CONSTRUCTION OF (BIO) SENSORING SYSTEMS: DESIGN STRATEGIES AND ANALYTICAL APPLICATIONS
Hossam Metwally Ahmed Nassef
ISBN:978-84-692-3235-4/DL:T-932-2009

Hossam Metwally Ahmed Nassef

BOTTOM-UP SURFACE ENGINEERING FOR THE CONSTRUCTION OF (BIO)SENSORING SYSTEMS: DESIGN STRATEGIES AND ANALYTICAL APPLICATIONS

DOCTORAL THESIS

Department of Chemical Engineering

UNIVERSITAT ROVIRA I VIRGILI

UNIVERSITAT ROVIRA I VIRGILI
BOTTOM-UP SURFACE ENGINEERING FOR THE CONSTRUCTION OF (BIO) SENSORING SYSTEMS: DESIGN STRATEGIES AND ANALYTICAL APPLICATIONS
Hossam Metwally Ahmed Nassef
ISBN:978-84-692-3235-4/DL:T-932-2009

UNIVERSITAT ROVIRA I VIRGILI
BOTTOM-UP SURFACE ENGINEERING FOR THE CONSTRUCTION OF (BIO) SENSORING SYSTEMS: DESIGN STRATEGIES AND ANALYTICAL APPLICATIONS
Hossam Metwally Ahmed Nassef
ISBN:978-84-692-3235-4/DL:T-932-2009

UNIVERSITAT ROVIRA I VIRGILI
BOTTOM-UP SURFACE ENGINEERING FOR THE CONSTRUCTION OF (BIO) SENSORING SYSTEMS: DESIGN STRATEGIES AND ANALYTICAL APPLICATIONS
Hossam Metwally Ahmed Nassef
ISBN:978-84-692-3235-4/DL:T-932-2009

UNIVERSITAT ROVIRA I VIRGILI
BOTTOM-UP SURFACE ENGINEERING FOR THE CONSTRUCTION OF (BIO) SENSORING SYSTEMS: DESIGN STRATEGIES AND ANALYTICAL APPLICATIONS
Hossam Metwally Ahmed Nassef
ISBN:978-84-692-3235-4/DL:T-932-2009

Hossam Metwally Ahmed Nassef

BOTTOM-UP SURFACE ENGINEERING FOR THE CONSTRUCTION OF (BIO)SENSORING SYSTEMS: DESIGN STRATEGIES AND ANALYTICAL APPLICATIONS

DOCTORAL THESIS

Supervised by

Dr. Ciara K. O´Sullivan & Dr. Alex Fragoso

Department of Chemical Engineering

Tarragona

2009

UNIVERSITAT ROVIRA I VIRGILI
BOTTOM-UP SURFACE ENGINEERING FOR THE CONSTRUCTION OF (BIO) SENSORING SYSTEMS: DESIGN STRATEGIES AND ANALYTICAL APPLICATIONS
Hossam Metwally Ahmed Nassef
ISBN:978-84-692-3235-4/DL:T-932-2009

UNIVERSITAT ROVIRA I VIRGILI
BOTTOM-UP SURFACE ENGINEERING FOR THE CONSTRUCTION OF (BIO) SENSORING SYSTEMS: DESIGN STRATEGIES AND ANALYTICAL APPLICATIONS
Hossam Metwally Ahmed Nassef
ISBN:978-84-692-3235-4/DL:T-932-2009

Department of Chemical Engineering
University of Rovira I Virgili,
Avinguda Països Catalans, 26
43007, Tarragona, Spain.
Tel: +34-977-558740/8722
Fax: +34-977-559621/8205

Dra. Ciara K. O´Sullivan i Dr. Alex Fragoso, professores titular del Departament d'Enginyeria Química de la Universitat Rovira i Virgili,

CERTIFICO:

Que el present treball, titulat “Bottom-up surface engineering for the construction of (bio)sensoring systems: Design strategies and analytical applications”, que presenta Hossam Metwally Ahmed Nassef per a l’obtenció del títol de Doctor, ha estat realitzat sota la meva direcció al Departament Enginyeria Química d’aquesta universitat i que acompleix els requeriments per poder optar a Menció Europea.

Tarragona, 30 de Enero de 2009

Dra. Ciara K. O´Sullivan Dr. Alex Fragoso

UNIVERSITAT ROVIRA I VIRGILI
BOTTOM-UP SURFACE ENGINEERING FOR THE CONSTRUCTION OF (BIO) SENSORING SYSTEMS: DESIGN STRATEGIES AND ANALYTICAL APPLICATIONS
Hossam Metwally Ahmed Nassef
ISBN:978-84-692-3235-4/DL:T-932-2009

UNIVERSITAT ROVIRA I VIRGILI
BOTTOM-UP SURFACE ENGINEERING FOR THE CONSTRUCTION OF (BIO) SENSORING SYSTEMS: DESIGN STRATEGIES AND ANALYTICAL APPLICATIONS
Hossam Metwally Ahmed Nassef
ISBN:978-84-692-3235-4/DL:T-932-2009

Department of Chemical Engineering
University of Rovira i Virgili,
Avinguda Països Catalans, 26
43007, Tarragona, Spain.
Tel: +34-977-558740/8579
Fax: +34-977-559621/8205

Dr. Ciara K. O´Sullivan and Dr. Alex Fragoso, professors of the Department of Chemical Engineering of the Rovira i Virgili University,

Certify that:

The present work entitled with "Bottom-up surface engineering for the construction of (bio)sensoring systems: Design strategies and analytical applications", presented by Hossam Metwally Ahmed Nassef to obtain the degree of doctor by the University Rovira i Virgili, has been carried out under my supervision at the Chemical Engineering Departament, and that it fulfills the requirements to obtain the Doctor Europeus Mention.

Tarragona, January, 30, 2009

Dr. Ciara K. O´Sullivan Dr. Alex Fragoso

UNIVERSITAT ROVIRA I VIRGILI
BOTTOM-UP SURFACE ENGINEERING FOR THE CONSTRUCTION OF (BIO) SENSORING SYSTEMS: DESIGN STRATEGIES AND ANALYTICAL APPLICATIONS
Hossam Metwally Ahmed Nassef
ISBN:978-84-692-3235-4/DL:T-932-2009

UNIVERSITAT ROVIRA I VIRGILI
BOTTOM-UP SURFACE ENGINEERING FOR THE CONSTRUCTION OF (BIO) SENSORING SYSTEMS: DESIGN STRATEGIES AND ANALYTICAL APPLICATIONS
Hossam Metwally Ahmed Nassef
ISBN:978-84-692-3235-4/DL:T-932-2009

Acknowledgement

Al Hamdu to ALLAH in the beginning and end.

I am grateful to **Dr. Ciara K. O´Sullivan** and **Dr. Alex Fragoso**, for suggesting the point of research, valuable and expert supervision, continuous advice and encouragement during the experimental work and preparation of the thesis.

I would like to thank **Prof. A. Radi**, for his supervision and efforts during the early stages of the experimental work.

I would like also to thank **Mr. Hany Nassif** for his kind support and help for making a good weather for me during the last stage of writing the thesis.

Finally, I would like to thank **my wife, my kids and my son** who have tolerate and provided much over the years including love and support to me. I would like also to thank **my parents and my brothers** for their support. Special thanks to **NBG** and **BBG** group members, and all staff members of the department of chemical engineering, university of Rovira i Virgili, for their unique help and support. I would like to thank **URV** for the financial support (BRDI scholarship).

H. M. Nassef

UNIVERSITAT ROVIRA I VIRGILI
BOTTOM-UP SURFACE ENGINEERING FOR THE CONSTRUCTION OF (BIO) SENSORING SYSTEMS: DESIGN STRATEGIES AND ANALYTICAL APPLICATIONS
Hossam Metwally Ahmed Nassef
ISBN:978-84-692-3235-4/DL:T-932-2009

UNIVERSITAT ROVIRA I VIRGILI
BOTTOM-UP SURFACE ENGINEERING FOR THE CONSTRUCTION OF (BIO) SENSORING SYSTEMS: DESIGN STRATEGIES
AND ANALYTICAL APPLICATIONS
Hossam Metwally Ahmed Nassef
ISBN:978-84-692-3235-4/DL:T-932-2009

Resumen

El trabajo descrito en la presente tesis ha sido organizado en capitulos en los que se detallan diferentes artículos publicados, enviados para su publicación o en preparacion en los cuales esta basada la tesis.

El **Capitulo 1** es una introducción en la que se presenta el estado del arte del tema y los objetivos de la tesis.

En los **Capítulos 2 a 4** se evalúan las propiedades electrocatalíticas de diferentes mediadores (hidracina, NADH y ácido ascórbico) que podrían ser utilizados en reacciones de reciclado de substratos enzimáticos en estrategias de amplificación de señal en biosensores. La hidracina es usada como antioxidante y agente reductor, el NADH es fundamental para el funcionamiento de oxidorreductasas y deshidrogenasas y el ácido ascórbico (AA, vitamina C) es de gran importancia como antioxidante. Las propiedades electrocatalíticas de monocapas de o-aminofenol (o-AP) en superficies de carbón vítreo fueron empleadas en la caracterización electroquímica de estos mediadores con el objetivo de seleccionar el mediador más adecuado. Para ello se determinaron diferentes parámetros cinéticos asociados empleando voltametría cíclica e hidrodinámica, así como cronoamperometría y cronocoulometría de doble potencial, siendo el acido ascórbico es mas adecuado en términos de coste, respuesta electroquímica y estabilidad.

Teniendo en cuenta estas propiedades del AA, se decidió explorar otras posibles aplicaciones clínicas y en análisis de alimentos de este sistema. En primer lugar se estudio la determinación de acido úrico en presencia de AA, el cual coexiste en diferentes fluidos biológicos y se estudió su determinación en muestras reales de orina (Capítulo 4).

En los **Capítulos 5 y 6** se detalla la utilización de electrodos desechables modificados con o-AP fabricados con la técnica de *screen-printing* en la determinación de AA de ácido ascórbico en una amplia variedad de frutas y vegetales frescos y zumos comerciales. La selectividad, reproducibilidad y estabilidad de estos electrodos fueron también estudiadas.

En la segunda parte de la tesis se evalúan diferentes estrategias para la inmovilización de anticuerpos para la construcción de inmunosensores. Estas estrategias

UNIVERSITAT ROVIRA I VIRGILI
BOTTOM-UP SURFACE ENGINEERING FOR THE CONSTRUCTION OF (BIO) SENSORING SYSTEMS: DESIGN STRATEGIES
AND ANALYTICAL APPLICATIONS
Hossam Metwally Ahmed Nassef
ISBN:978-84-692-3235-4/DL:T-932-2009

consisten en la deposición de los anticuerpos en superficies de oro mediante autoensamblaje de compuestos tiolados o la electrodeposición de sales de diazonio.

En el **Capítulo 7** se compara el uso de dos compuestos ditiolados para la modificación de superficies de oro. Estos compuestos se emplearon para la inmovilización de anticuerpos en la construcción de un inmunosensor electroquímico para la detección de gliadina en muestras reales.

El **Capítulo 8** es la continuación del trabajo anterior y está basado en la adsorción espontánea de fragmentos de anticuerpos o anticuerpos tiolados en superficies de Au para la detección de gliadina. Para ello se compararon las respuestas amperométricas de ambos sistemas, observándose una excelente sensibilidad en el caso de los fragmentos de anticuerpos, asi como una mayor estabilidad (hasta 60 dias a 4ºC) de este sistema.

En el **Capítulo 9**, se estudia una alternativa consistente en la electrodeposición de sales de diazonio conjugadas a anticuerpos. Para ello se estudiaron diferentes métodos de deposicion (electroquímicos o adsorción espontánea), siendo la deposición empleando voltametría ciclica la más adecuada. Sin embargo, esta metodología requirió de un gran número de pasos de lavado para la eliminaciñon de compuestos adsorbidos no específicamente. A pesar de esto, el anticuerpo inmovilizado mostró una buena afinidad hacia la gliadina al ser evaluada por amperometría con una excelente especificidad.

El **Capítulo 10** consiste en las conclusiones generales y un plan de trabajo para el futuro.

De forma general, este trabajo ha contribuido significativamente a la culminación de una estrategia que evita pasos de lavado y de adición de reactivo en el diseño de inmunosensores. Para ello se la seleccionado el mediador más adecuado para coencapsulación con fosfatasa alcalina en liposomas para la regeneración de sustratos inmovilizados en superficies, lo cual facilita su reciclado, así como incrementa la sensibilidad y disminuye los limites de detección. Paralelamente, se han estudiado diferentes superficies para la inmovilización de anticuerpos consistentes en la deposición de los anticuerpos y sus fragmentos en superficies de oro mediante autoensamblaje de compuestos tiolados o la electrodeposición de sales de diazonio. Se propone en el futuro combinar ambas estrategias en la construcción de plataformas inmunosensoras de fácil operatividad y ultrasensibles.

UNIVERSITAT ROVIRA I VIRGILI
BOTTOM-UP SURFACE ENGINEERING FOR THE CONSTRUCTION OF (BIO) SENSORING SYSTEMS: DESIGN STRATEGIES
AND ANALYTICAL APPLICATIONS
Hossam Metwally Ahmed Nassef
ISBN:978-84-692-3235-4/DL:T-932-2009

Summary

Specifically outlining the work achieved in this PhD thesis, the work is organised into separate articles that have been published, submitted or are under preparation for submission.

Chapter 1 is an introduction, in which the state of the art and objectives are presented.

In **Chapters 2-4**, different potential mediators that could be used for the catalytic interaction with the enzymatic product o-AP were evaluated and due to their well characterized properties, hydrazine, NADH and ascorbic acid were selected for further study. Hydrazine is used as an antioxidant and reducing agent; NADH plays an important rule in oxidoreductases and dehydrogenase systems and ascorbic acid (vitamin C) is an antioxidant whose detection is important in clinical and food applications. The electrocatalytic properties of o-aminophenol films grafted on glassy carbon surfaces have been employed for the electrochemical evaluation of hydrazine, NADH and ascorbic acid, to select the most relevant as a recycling mediator in the planned signal amplification strategy. To evaluate the best mediator, the reaction kinetics between mediators and the o-AP/o-QI were extensively studied using different techniques such as cyclic voltammetry, hydrodynamic voltammetry, double potential step chronoamperometry, and double potential step chronocoulometry.

Of them, ascorbic acid was selected as the mediator for regeneration of the o-AP film and substrate recycling. We had thus demonstrated an interesting catalytic system for the oxidation of ascorbic acid, which is stable, sensitive and reproducible, and we decided to explore this system for clinical and food applications. In the first application, we targeted the determination of uric acid (UA) in the presence of ascorbic acid (AA), which commonly co-exist in biological fluids of humans, mainly in blood and urine (Chapter 4). In **Chapters 5 and 6**, the selective electrocatalytic properties of the grafted o-AP film toward ascorbic acid were also applied to its detection in real samples of fruits and vegetables using disposable one-shot screen printed electrodes. The o-AP modified screen printed electrodes showed high catalytic responses toward the electrocatalytic

UNIVERSITAT ROVIRA I VIRGILI
BOTTOM-UP SURFACE ENGINEERING FOR THE CONSTRUCTION OF (BIO) SENSORING SYSTEMS: DESIGN STRATEGIES
AND ANALYTICAL APPLICATIONS
Hossam Metwally Ahmed Nassef
ISBN:978-84-692-3235-4/DL:T-932-2009

oxidation of ascorbic acid. The o-AP SPE sensor exhibited high sensitivity and selectivity toward ascorbic acid with excellent storage and operational stability, as well as a quantitatively reproducible analytical performance.

In the second part of the thesis, different surface engineering strategies of antibody immobilization for immunosensor construction using a linker or via direct attachment onto a Au surface using a strategy of self assembly were evaluated and compared. An alternative strategy explored was the direct anchoring of the antibody with or without a linker via the electrochemical reduction of their diazonium cations.

In **Chapter 7**, a comparison between these different surface chemistries methodologies for the construction of immunosensors towards the model analyte of coeliac toxic gliadin was carried out. Firstly, the self-assembled monolayer approach was evaluated based on the modification of gold surfaces with two bipodal carboxylic acid terminated thiols (thioctic acid and a benzyl alcohol disubstituted thiol, DT2). A stable SAM of DT2 was rapidly immobilized (3 h) on Au as compared with thioctic acid (100 h), although both surface chemistries resulted in highly sensitive electrochemical immunosensors for gliadin detection using an anti-gliadin antibody (CDC5), with detection limits of 11.6 and 5.5 ng/mL, respectively. The developed immunosensors were then applied to the detection of gliadin in commercial gluten-free and gluten-containing food products, showing an excellent correlation when compared to results obtained with ELISA.

In **Chapter 8**, another approach was explored to further improve immunosensor sensitivity and stability and furthermore to reduce the time necessary for sensor preparation was investigated looking at the direct attachment of the SATA modified full length antibody, and their F(ab) fragments onto Au electrodes. Spontaneously adsorbed SAMs of Fab-SH and CDC5-SH onto Au were rapidly formed in less than 15 minutes. The amperometric immunosensors based on Fab fragments exhibited a vastly improved detection limit as compared to the thiolated antibody with a highly sensitive response toward gliadin detection (LOD, 3.29 ng/ml for amperometric detection and 0.42 μg/ml for labelless (impedimetric) detection). Moreover, the self-assembled monolayer of F(ab) fragments was extremely stable with almost no loss in response after 60 days storage at 4^{o}C.

UNIVERSITAT ROVIRA I VIRGILI
BOTTOM-UP SURFACE ENGINEERING FOR THE CONSTRUCTION OF (BIO) SENSORING SYSTEMS: DESIGN STRATEGIES
AND ANALYTICAL APPLICATIONS
Hossam Metwally Ahmed Nassef
ISBN:978-84-692-3235-4/DL:T-932-2009

In **Chapter 9**, an alternative surface chemistry approach was explored for the modification of Au electrodes via electrochemical and spontaneous reduction of diazonium cations of a conjugate prepared from the monoclonal full length anti-gliadin antibody (CDC5) and the linker 3,5-bis(aminophenoxy)benzoic acid (DAPBA). Cylic voltammetry was chosen for surface modification via applying three potential cycles, but it was observed that an extensive washing process was necessary after each potential cycle to remove the non-specifically adsorbed molecules or formed multilayers. The affinity of the immobilized antibody toward gliadin was studied using EIS and amperometry. The modified CDC5-DAPBA surface showed a reasonable amperometric response after incubation with 5 μg/ml gliadin, and exhibited excellent specificity with no response observed in the absence of the analyte.

In **Chapter 10**, general conclusions and future work are presented.

From the different surface chemistry strategies evaluated in this work we can conclude that the best approach is the immunosensor based on the spontaneous adsorption of thiolated F(ab) fragments on gold. This surface is easy and fast to prepare, very stable and sensitive and can be stored for long times in the appropriate conditions without lost of affinity. A good alternative to this approach seems to be the electrodeposition of antibody-diazonium conjugates, although further work is needed in order to optimize this system.

Overall, this work has contributed significantly to the vision we have for an immunosensor that avoids washes and reagent addition, where we have selected an excellent mediator for co-encapsulation with alkaline phosphatase enzymes within liposome reporter molecules, for regeneration of surface immobilised substrate following enzymatic dephosporylation, facilitating substrate recycling and increase in sensitivity and reduction in detection limit. Furthermore, we have selected an optimum surface chemistry for co-immobilisation of capture antibody molecules and enzyme substrate via the formation of self-assembled monolayers of antibody fragments on gold surfaces. Future work will focus on combining the selected mediator and surface chemistry into a sandwich immunosensor with a target sensitive liposome reporter molecule, to demonstrate a reagentless, washless ultrasesensitive immunosensing platform.

UNIVERSITAT ROVIRA I VIRGILI
BOTTOM-UP SURFACE ENGINEERING FOR THE CONSTRUCTION OF (BIO) SENSORING SYSTEMS: DESIGN STRATEGIES AND ANALYTICAL APPLICATIONS
Hossam Metwally Ahmed Nassef
ISBN:978-84-692-3235-4/DL:T-932-2009

Table of Contents

UNIVERSITAT ROVIRA I VIRGILI
BOTTOM-UP SURFACE ENGINEERING FOR THE CONSTRUCTION OF (BIO) SENSORING SYSTEMS: DESIGN STRATEGIES AND ANALYTICAL APPLICATIONS
Hossam Metwally Ahmed Nassef
ISBN:978-84-692-3235-4/DL:T-932-2009

UNIVERSITAT ROVIRA I VIRGILI
BOTTOM-UP SURFACE ENGINEERING FOR THE CONSTRUCTION OF (BIO) SENSORING SYSTEMS: DESIGN STRATEGIES AND ANALYTICAL APPLICATIONS
Hossam Metwally Ahmed Nassef
ISBN:978-84-692-3235-4/DL:T-932-2009

CHAPTER 1:

Introduction

UNIVERSITAT ROVIRA I VIRGILI
BOTTOM-UP SURFACE ENGINEERING FOR THE CONSTRUCTION OF (BIO) SENSORING SYSTEMS: DESIGN STRATEGIES
AND ANALYTICAL APPLICATIONS
Hossam Metwally Ahmed Nassef
ISBN:978-84-692-3235-4/DL:T-932-2009

1. Introduction

1.1. Definition of biosensor

A biosensor is a self-contained integrated device, which is capable of providing specific quantitative or semi-quantitative analytical information using a biological recognition element (biochemical receptor) which is retained in direct spatial contact with transduction element (usually physical, chemical or electrical) capable of detecting the biological reaction and converting it into a signal which can be processed in response to the concentration or level of either a single analyte or a group of analytes [1]. The biological sensing material may be a protein such as an enzyme or antibody, a nucleic acid (DNA, RNA or PNA), antibody fragment, a whole microbial cell, or even a plant or animal tissue [2], and biosensors can be divided into catalytic (enzyme) and affinity (antibodies, lectine, DNA) sensors.

1.2. Definition of immunosensor

An immunosensor is an affinity ligand-based biosensor solid-state device that uses antibodies or antigens as the specific sensing element, in which the immunochemical reaction is coupled to a signal transducer which detects the binding of the complementary species providing concentration-dependent signals [3]. The fundamental basis of all immunosensors is the specificity of the molecular recognition of antigens by antibodies to form a stable complex [4]. An indirect immunosensor uses a separate labelled species that is detected after binding and a direct immunosensor detects immunocomplex formation by a change in potential difference, current, resistance, mass, heat, or optical properties. Although indirect immunosensors may encounter fewer problems due to nonspecific binding effects, direct immunosensors are capable of real-time monitoring of the antigen-antibody reaction [5].

There are various transduction systems, such as electrochemical, optical, piezoelectric, and nanomechanics methods, which have been used for the design and fabrication of immunosensors [6]. In conventional solid-phase immunoassays, reagents are generally used only once, whereas immunosensors can facilitate the regeneration of

UNIVERSITAT ROVIRA I VIRGILI
BOTTOM-UP SURFACE ENGINEERING FOR THE CONSTRUCTION OF (BIO) SENSORING SYSTEMS: DESIGN STRATEGIES
AND ANALYTICAL APPLICATIONS
Hossam Metwally Ahmed Nassef
ISBN:978-84-692-3235-4/DL:T-932-2009

the immobilized component by using the reversibility of the antibody-antigen reaction. Thus, the bioactive surface of the biosensor can be regenerated to enable continual monitoring of the measured signal. Regeneration of the sensing surface is usually performed by displacement of the immunoreaction [7,8], using agents that are able to break the antibody-analyte association-organic solvents with acidic buffers [9], chaotropic agents [10] or digesting enzymes [11] or a combination of two or more of these methods.

1.3. Classification of immunosensors

The biorecognition element determines the degree of selectivity or specificity of the biosensor, whereas the sensitivity of the biosensor is greatly influenced by the transducer [12]. According to the transduction mechanism, immunosensors can be classified into four types: electrochemical (potentiometric, amperometric or conductometric/capacitative), optical (luminescent, fluorescent, reflective, ellipsometric, surface plasmon resonance (SPR), and waveguide), microgravimetric (piezoelectric or acoustic wave), thermometric (calorimetric) and nanomechanic immunosensors [5,6].

There is a great variety of labels which have been applied in indirect immunosensors, such as enzymes (e.g. glucose oxidase, horseradish peroxidase (HRP), β-galactosidase, alkaline phosphatase, catalase, luciferase), nanoparticles, and fluorescent or electrochemiluminescent probes [13-17], and electroactive compounds such as ferrocene. Among the fluorescent labels rhodamine, fluorescein, Cy5, ruthenium diimine complexes, phosphorescent porphyrin dyes and the most widely used [18-22]. Although the indirect immunosensors are usually more sensitive, they are not capable of real-time monitoring of the Ab–Ag reaction and increase both development and operational costs compared to label-free immunosensors.

The vital advantage of the direct (non-labelled) immunosensors is the simple, single-stage reagentless operation. However, such direct immunosensors are often inadequate to generate a highly sensitive signal resulting from Ab–Ag binding interactions and often fail to meet the demand of sensitive detection.

UNIVERSITAT ROVIRA I VIRGILI
BOTTOM-UP SURFACE ENGINEERING FOR THE CONSTRUCTION OF (BIO) SENSORING SYSTEMS: DESIGN STRATEGIES
AND ANALYTICAL APPLICATIONS
Hossam Metwally Ahmed Nassef
ISBN:978-84-692-3235-4/DL:T-932-2009

1.4. Electrochemical Immunosensors

Electrochemical transducers are the oldest and most common methods used in biosensors. In immunosensors, the principle is based on the electrical properties of the electrode or buffer that is affected by Ab–Ag interaction. They can determine the level of antigen by measuring the change of potential, current, conductance, or impedance caused by the immunoreaction. They combine the high specificity of traditional immunoassay methods with high sensitivity, possibility of multiplexing and low cost of electrochemical measurement systems, and thus exhibit great advantages. They are not affected by sample turbidity, quenching, or interference from absorbing and fluorescing compounds commonly found in biological samples, as is the case with optical immunosensors. However, a high-performance, cost-effective field analysis system still remains a big challenge. In the work reported in this thesis, electrochemical transduction is exploited and to this end the different possible electrochemical transducing strategies are detailed below.

1.4.1. Potentiometric immunosensors

Potentiometric transducer electrodes are based on the principle of the accumulation of a membrane potential as a result of the selective binding of ions to a sensing membrane, and are capable of measuring surface potential alterations at near-zero current flow, are being constructed by applying the following methodologies:

Transmembrane potential. This transducer principle is based on the accumulation of a potential across a sensing membrane. Ion-selective electrodes (ISE) use ion-selective membranes which generate a charge separation between the sample and the sensor surface. Analogously, antigen or antibody immobilized on the membrane binds the corresponding compound from the solution at the solid-state surface and changes the transmembrane potential.

Electrode potential. This transducer is similar to the transmembrane potential sensor. An electrode by itself, however, is the surface for the immunocomplex construction, changing the electrode potential in relation to the concentration of the analyte.

Field-effect transistor(FET). The FET is a semiconductor device used for monitoring of charges at the surface of an electrode, which have accumulated on its metal gate

ISBN:978-84-692-3235-4/DL:T-932-2009

between the so-called source and drain electrodes. The surface potential varies with the analyte concentration. The integration of an ISE with FET is realized in the ion-selective field-effect transistor (ISFET), and can also be applied to immunosensors.

Potentiometric immunosensors are based on the fact that proteins in aqueous solution behave as polyelectrolytes and subsequently the electrical charge of an antibody can be affected by binding the corresponding antigen. Measuring the changes in potential induced by the label used, which occur after the specific binding of the Ab–Ag, a logarithmic relationship between potential and concentration is revealed. The first description of the use of potentiometric transducers for monitoring an immunochemical reaction was published in 1975 [23]. Examples of these kinds of immunosensors for the determination of the pesticides 2,4-dichlorophenoxyacetic acid (2,4-D) and 2,4,5-trichlorophenoxyacetic acid (2,4,5-T) have been reported [24,25], as well as an ISFET-immunosensor for the determination of the simazine herbicide [26].

A biosensor for detecting *Candida albicans* has been developed based on a field-effect transistor (FET) in which a network of single-walled carbon nanotubes (SWCNTs) acts as the conductor channel. Monoclonal anti-*Candida* antibodies were adsorbed onto the SWCNT to provide specific binding sites for fungal antigens [27], the SWCNTs modified with anti-*Salmonella* antibodies were used for detection of *Salmonella* [28]. Rius and coworkers has developed another FET biosensor for bisphenol A detection in water in which a network of single-walled carbon nanotubes (SWCNTs) acts as the conductor channel. SWCNTs are functionalized with a nuclear receptor, the estrogen receptor alpha (ER-α), which is adsorbed onto the SWCNTs and acts as the sensing part of the biosensor which detect picomolar concentrations of BPA in 2 min [29].

An advantage of potentiometric sensors is the simplicity of operation, which can be used for automation, and the small size of the solid-state FET sensors. Conversely, potentiometric immunosensing has several problems such as, signal-to-noise ratio is low because the charge density on most biomolecules is low compared with background interferences (e.g., ions), and there is a marked dependence of signal response on conditions as pH and ionic strength [3]. One significant problem associated with ion-selective potentiometric transducers is that the measured potential is related only to the activity of the ion. Furthermore, ISEs are vulnerable to interferences from other ions,

ISBN:978-84-692-3235-4/DL:T-932-2009

which also reduces the specificity of the sensor [5,30]. Thus, a trend moving away from these techniques for immunosensing has been observed in the last few years. Only the ISFET may be seen as a candidate for ultrasensitive clinical immunosensor applications, in particular, when the novel concept of differential ISFET-based measurement of the zeta potential is used [31].

1.4.2. Amperometric immunosensors

Amperometric sensors are designed to measure the concentration-dependent current generated by an electrochemical reaction at constant voltage after immuno-complex formation [32]. The resulting current is directly proportional to specific antibody–antigen binding. However, many molecules (e.g. proteins) are not intrinsically electroactive and cannot be directly detected amperometrically. Therefore, electrochemically active labels (enzymes) are incorporated to catalyze redox reactions that facilitate the production of electroactive species, which then can be determined electrochemically. A series of enzymes have been used for substrate transformation in amperometric systems [33], such as alkaline phosphatase, which catalyzes the dephosphorylation of phenyl phosphate or *p*-aminophenyl phosphate (4-APP) compounds, resulting in electrochemically active phenol or *p*-aminophenol [34]. Horseradish peroxidase (HRP) catalyses the oxidation of H_2O_2 in presence of different redox mediators such as aminophenols, phenylenediamine derivatives, and hydroquinones, but most of HRP mediators are unstable and require fast enzymatic assay. Glucose oxidase, glucose-6-phosphate dehydrogenase, have also been applied as labels [35].

The main disadvantages of amperometric immunosensors of having an indirect sensing system is compensated by an excellent sensitivity of the system, with linear concentration dependence (compared with a logarithmic relationship in potentiometric systems), and low interferences from matrix components, can be obtained by altering the electrode potential independently of the sample buffer capacity, making the system well suited for immunochemical sensing. Finally, this system has been applied for the simultaneous analysis of several analytes/samples using only one device via a multichannel immunosensor [36].

UNIVERSITAT ROVIRA I VIRGILI
BOTTOM-UP SURFACE ENGINEERING FOR THE CONSTRUCTION OF (BIO) SENSORING SYSTEMS: DESIGN STRATEGIES
AND ANALYTICAL APPLICATIONS
Hossam Metwally Ahmed Nassef
ISBN:978-84-692-3235-4/DL:T-932-2009

1.4.3. Other types of electrochemical immunosensors

The concepts of impedance, conductance, capacitance, and resistance are inter-related [37]. Impedance immunosensors measure the changes of an electrical field. These changes could be overall electrical conductivity of the solution and/or capacity alteration due to an Ab–Ag interaction on the electrode surface. Conductimetric immunosensor transducers measure the change of the electrical conductivity in a solution at constant voltage, caused by biochemical (enzymatic) reactions which specifically generate or consume ions. For example, when urea is converted to ammonium cations by the enzyme urease which can also be used as an enzyme label [38], the increase in solution conductance measured is proportional to urea concentration [39]. Variations in ionic strength and buffer capacity of measured samples have caused problems [40] with this type of biosensor in the past, but these drawbacks have been overcome with more recent designs [41], by using an ion-channel conductance immunosensor, mimicking biological sensory functions [42], in which the conductance of a population of molecular ion channels, built of tethered gramicidin A and aligned across a lipid bilayer membrane, is changed by the antibody–antigen binding event. In another reported approach the measurement of changes of the surface conductivity. Yagiuda et al. [43] developed a conductometric immunosensor for the determination of methamphetamine (MA) in urine. Anti-MA antibodies were immobilized onto the surface of a pair of platinum electrodes. The immunocomplex formation caused a decrease in the conductivity between the electrodes. In an alternate approach, reported, the changes in the effective dielectric thickness of an insulating layer, with antibodies linked to an alkylthiol layer, during antigen binding,. where a marked decrease of the electrical capacitance is observed and is used to quantify the analyte, such as the determination of albumin by Mirsky et al. [44]. Conductimetric sensors may however have problems with non-specificity of measurements, as the resistance of a solution is determined by the migration of all ions present.

Electrochemical impedance spectroscopy (EIS) is a sensitive technique, which detects the electrical response of the system after application of a periodic small amplitude AC signal. Impedance spectroscopy allows the detection of capacitance changes at the interfaces that originate from biorecognition events. These capacitance changes can be

ISBN:978-84-692-3235-4/DL:T-932-2009

derived from the imaginary part, Z_{im}, of the complex impedance spectra. Formation of antigen-antibody complexes on conductive supports yields a chemically modified film on the surface that alters the impedance features of the interface, and perturbs the double-charged layer existing at the electrode/electrolyte interface resulting in the increase of its thickness, and the insulation of the electrode surface in respect to redox labels added to the solution. This results in the capacitance change and electron transfer resistance change at the interface, respectively [45].

In recent years, the electrochemical impedance immunosensors have attracted extensive interest in the sensing formation of Ag–Ab [46-49]. EIS in connection with immunochemical methods was tested for the direct determination of the herbicide 2,4-D [50,51].

Non-Faradaic impedance spectroscopy in the absence of a redox probe was applied to follow the biorecognition events at functionalized electrode surfaces [52]. Impedimetric techniques are also used as a characterization method for most of the enzyme-based impedimetric biosensors. A biosensor for collagenase detection was developed, which detected the change in impedance caused by the proteolytic digestion of gelatin-coated interdigitated gold electrodes [53].

Affinity-binding based impedimetric biosensors are attracting increasing interest, since they are direct and label-free electrochemical immunosensors and have many potential advantages with respect to speed, the use of unskilled analysts and the potential development of multi-analyte sensors. In recent years, many novel designs of affinity-binding-based impedimetric biosensors have been reported.

Protein multilayer films were also investigated by impedance spectroscopy in the presence of a redox probe. The multilayer film was composed of avidin and biotin-labeled antibody (bio-Ab) on a gold surface, which was prepared by layer-by-layer assembly technology. A significant difference in the impedance spectra was observed upon the stepwise formation of the multi-layers [54].

Impedance spectroscopy was used to characterize the structure of biomaterial layers on the gate surface of ISFET devices, and to elucidate antigen-antibody binding interactions on the gate interface. The ability to characterize the thickness of layered protein assemblies on the gate interface of ISFET devices by means of impedance

spectroscopy not only provided a method for the structural characterization of the systems, but also yielded an analytical method to probe and sense bio-recognition events that occurred on the gate surface of the ISFET [55].

1.5. Surface Engineering of Biosensors

The development of an immunosensor requires immobilization of antibody (or in some cases antigen) on the transducer surface. Many studies have compared methods of antibody attachment to biosensor surfaces including physicochemical adsorption and covalent attachment [56,57]. The disadvantage of physicochemical adsorption biosensors is that the binding of sensor surfaces and antibodies is not strong enough, and, subsequently, the sensitivity of the biosensors will continuously decrease due to loss of biocomponent from the surface. Moreover, the antibody will not be oriented and this leads to both poor reproducibility and non-optimal detection limits. To improve the uniformity and reproducibility of immobilised antibodies, chemical crosslinking has been used for the covalent immobilisation of proteins onto different solid substrate surfaces using defined linkages such as glutaraldehyde, carbodiimide, and other reagents such as succinimide esters, maleiimides, and periodate [58,59]. However, linkage strategies that selectively form covalent bonds with the lysine residues randomly present in the antibodies, give rise to a random orientation of the receptor molecules immobilised on the sensor surface [59,60]. Therefore, the antibodies will be partially oriented with their antigen binding site towards the sensor surface and thus will not all be accessible for antigen binding, and also may lead to loss of the biological activity of the antibody [61].

1.5.1. Self assembled monolayer strategy.

Gold electrodes are very useful for electrochemical immunosensors as they are chemically inert and have a prolonged double-layer potential region in aqueous solutions [62] and the oriented immobilization of antibodies onto the gold is critical for a rational design of immunosensors. The well established strategy of formation of a self-assembled monolayer for immobilization of biomolecules onto gold surfaces are based on the strong attachment of thiol (SH) or disulfide (-S-S-) functional groups to Au (Figure 1).

UNIVERSITAT ROVIRA I VIRGILI
BOTTOM-UP SURFACE ENGINEERING FOR THE CONSTRUCTION OF (BIO) SENSORING SYSTEMS: DESIGN STRATEGIES
AND ANALYTICAL APPLICATIONS
Hossam Metwally Ahmed Nassef
ISBN:978-84-692-3235-4/DL:T-932-2009

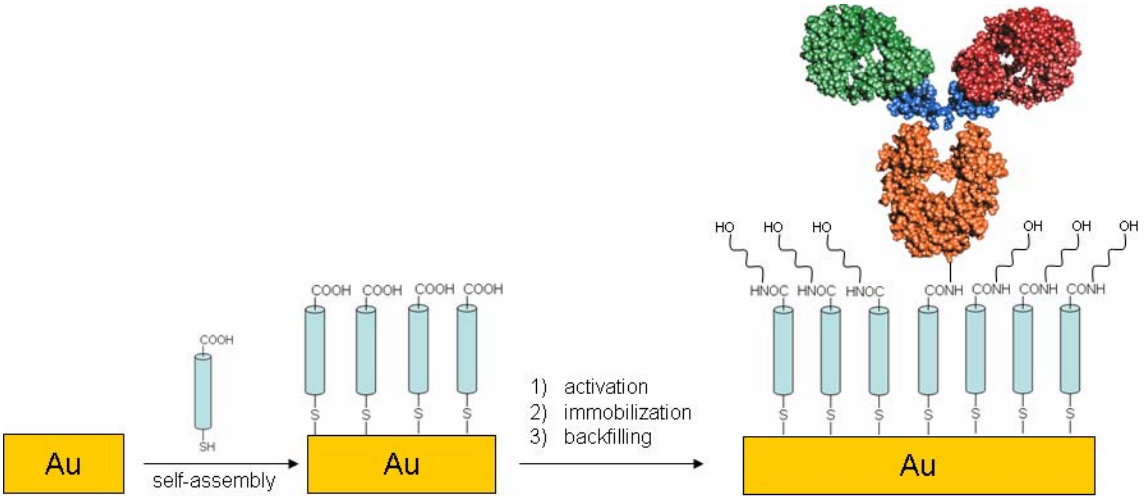

Figure 1. Immunosensor construction based on self-assembled monolayers of thiols on gold.

Alkanethiol SAMs are most commonly used to covalently immobilize a biorecognition molecule (typically an enzyme, antibody or nucleic acid sequence) onto the surface of the transducer since they offer the possibility of controlling the orientation, distribution and spacing of the sensing element while reducing non-specific interactions [63]. However, whilst long chain SAMs are very stable and effective in reducing/eliminating non-specific binding [64,65] they have limited applicability in electrochemical biosensors since they show a low permeability to electron transfer, with a blocking of the electrochemical response. This disadvantage could be circumvented with the use of alkanethiol mixtures having different chain lengths but the low biomolecule immobilisation capacity of these surfaces negatively influences the performance of the sensor [66].

Carboxylic acid terminated SAMs are a popular way of incorporating a biorecognition molecule to the transducer surface. These SAMs can be activated via carbodiimide chemistry and react with amino groups of the biomolecule, generating a robust surface able to operate in a wide range of samples [67]. Another strategy has been developed for glycoprotein immobilization, based on the targeted functionalization of carbohydrate residues with disulfide "anchors" which able to be spontaneously chemisorbed onto gold without prefunctionalization of Au surface [68]. The specificity of the chemical reaction, for disulfide introduction, toward carbohydrate moieties prevents

any cross-reaction with other functional groups present in the protein structure [68]. However, as previously mentioned, amino groups are usually randomly located in the biomolecule, the recognition sites are thus arbitrarily orientated over the surface, which can hinder biosensor sensitivity. The opposite arrangement using amino-terminated SAMs requires pre-activation of the carboxylic acid groups of the antibody. In this step, intermolecular crosslinking reactions can take place between the activated carboxylates and antibody amino groups resulting in the formation of polymeric materials of uncontrolled composition. Our group has recently described the use of SAMs of dithiolated scaffolds derived from 3,5-dihydroxybenzyl alcohol for the construction of an impedimetric immunosensor for the detection of a cancer marker protein [69]. These molecules contain two identical alkylthiol substituents attached to a phenyl ring through phenolate bridges that provide two attachment points on the metallic surface, similar to thioctic acid, but having the potential of far-enhanced stability. This bipodal alkanethiol also contains a polyethylene glycol moiety, useful for the preventing of non-specific adsorption of proteic substances. It can be anticipated that these molecules will generate more stable SAMs than monothiols due to a multivalent mechanism of interaction and also provide a more adequate spacing of an immobilised biomolecule thus allowing an improved mobility and flexibility at the recognition terminus [70]. This structure, with a dithiol anchor and a single tail, should have less insulating properties than alkanethiol SAMs and therefore are expected to be permeable to electron transfer, making these molecules attractive candidates for the construction of electrochemical biosensors [71].

This problem of orientation is critical as immunosensor sensitivity is strongly dependent on the density of the free active epitopes immobilised per surface area. As an alternative to use alkanethiol SAMS, followed by cross-linking, the use of smaller and well-oriented antibody fragments, such as Fab fragments, which contain a thiol group that would orientate the fragment to have the antigen binding site exposed, as bioreceptor molecules should facilitate lower detection limits due to this improved orientation, as well as the increased number of active binding sites available.

Fab fragments can be directly generated using thiol proteases such as papain or ficin, or, alternatively, $F(ab')_2$ fragments can be generated using bromelain, pepsin, or ficin,

ISBN:978-84-692-3235-4/DL:T-932-2009

and the disulphide hinge subsequently cleaved using a reducing agent, generating Fab fragments[72,73]. Pepsin is not applicable to all antibody types (e.g. it cannot be used for mouse IgG1 subclasses) and the low pH required for pepsin digestion can destroy antibodies.[74] Bromelain or ficin provide significantly higher yields than pepsin[75], and with more rapid and reproducible digestion[76] . The $F(ab')_2$ fragments are dimeric structures of two Fab units linked together by a disulfide bridge that can be cleaved generating two Fab fragments with active thiol groups, which are located on the opposite side of the molecule with respect to the binding site [77]. These thiol groups can interact with gold surfaces leading to a monolayer of Fab fragments displaying a highly controlled orientation that is expected to maximize their antigen-binding efficiency with a concomitant increase in sensitivity and selectivity [78,79] when compared to randomly immobilized whole antibodies[66]. The density of the immobilized Fab depends on the distribution ratio of the SH or SS on the applied modified surface [66,80].

Several strategies have been used to immobilize antibody Fab fragments on different substrate surfaces for application in immunosensing. As outlined, it is preferable that antibody fragments be immobilized with highly controlled orientation so as to maximize their antigen-binding efficiency and attain ultimate sensitivity and selectivity of immunoassay [78,79]. In one report, where the authors crosslink Fab fragments to a mixed SAM, not even taking advantage of an increased density of binding sites, but simply due to an improved orientation, there is a >2-fold increase of the antigen binding signals compared to randomly covalently immobilised full-length antibodies [66]. Lu et. al, has also demonstrated that the antigen binding activity of Fab fragments immobilized in oriented form on derivatized silica surfaces is 2.7 times higher than the random form [78].

Lu et. al, have demonstrated that the antigen binding activity of the Fab fragments immobilized in oriented form on derivatized silica surfaces is 2.7 times higher than that of the random form[78]. Vikholm-Lundin[81] reported on a generic platform where the spaces in between chemisorbed Fab fragments is filled with the disulfide bearing polymer of *N*-[tris(hydroxyl-methyl)methyl]-acrylamide, resulting in a marked decrease in non-specific binding. The same group went on to apply the developed platform to the detection of C-reactive protein, comparing $F(ab')_2$ and Fab immunocapture layers, with a

UNIVERSITAT ROVIRA I VIRGILI
BOTTOM-UP SURFACE ENGINEERING FOR THE CONSTRUCTION OF (BIO) SENSORING SYSTEMS: DESIGN STRATEGIES
AND ANALYTICAL APPLICATIONS
Hossam Metwally Ahmed Nassef
ISBN:978-84-692-3235-4/DL:T-932-2009

five-fold improvement in specific binding observed with the Fab monolayer [82]. The self assembly of Fab onto a gold surface, followed by surface plasmon resonance transduction was applied to the detection of insulin [83], with another report detailing the detection of differentiated leukocyte antigens for immunophenotyping of acute leukaemia via the direct adsorption of Fab fragments onto gold nano-particles with piezoelectric transduction [84]. In last two examples, the authors did not compare their approach with a full length antibody strategy.

In some cases, the use of $F(ab')_2$ fragments has resulted in lower detection limits as compared to whole antibodies [85]. There have also been reports of the exploitation of Fab fragments, but without taking direct advantage of the ordered monolayer that can be formed via the direct chemisorption of the thiolated Fab onto a gold surface, but rather focusing on antibody orientation as a means of increasing sensitivity. Examples of this are the immobilization of biotinylated anti-atrazine Fab on neutravidin modified gold electrodes [51,86] for the detection of atrazine, and monobiotinylated Fab against human chorionic gonadotropin and using surface plasmon fluorescence measurements, the biotin-Fab achieved a detection limit of 6×10^{-13} M as compared to 4×10^{-12} M when biotinylated whole antibody was used [87]. Additionally, exchange reactions between disulfide-terminated SAMs and thiolated Fab fragments have also been employed to generate sensor surfaces with well oriented Fab fragments [66,78-80]. However, the preferred method for Fab immobilization is the spontaneous adsorption of Fab motifs on gold, giving rise to surfaces of higher epitope density, high antigen-binding constants and operational stability or adhesion [88-90].

1.5.2. Surface modification via the electrochemical reduction of diazonium salts.

Diazonium salts ($R\text{-}N{\equiv}N^+ X^-$) are a class of organic compounds prepared by the treatment of aromatic amines with sodium nitrite in the presence of a mineral acid. Grafting and electrografting of diazonium salts on carbon (including nanotubes and diamond), metals, and metal oxides as well as hydrogenated silicon provide an easy and efficient way to covalently modify the surface of these materials.

In 1992, Pinson and his coworkers investigated the modification of carbon surfaces based on electrochemical reduction of diazonium salts (4-nitropheny1)diazonium

UNIVERSITAT ROVIRA I VIRGILI
BOTTOM-UP SURFACE ENGINEERING FOR THE CONSTRUCTION OF (BIO) SENSORING SYSTEMS: DESIGN STRATEGIES
AND ANALYTICAL APPLICATIONS
Hossam Metwally Ahmed Nassef
ISBN:978-84-692-3235-4/DL:T-932-2009

tetrafluoroborate in acetonitrile), which leads to a strong covalent binding of the 4-nitrophenyl group on the carbon surface rather than mere adsorption (Figure 2).

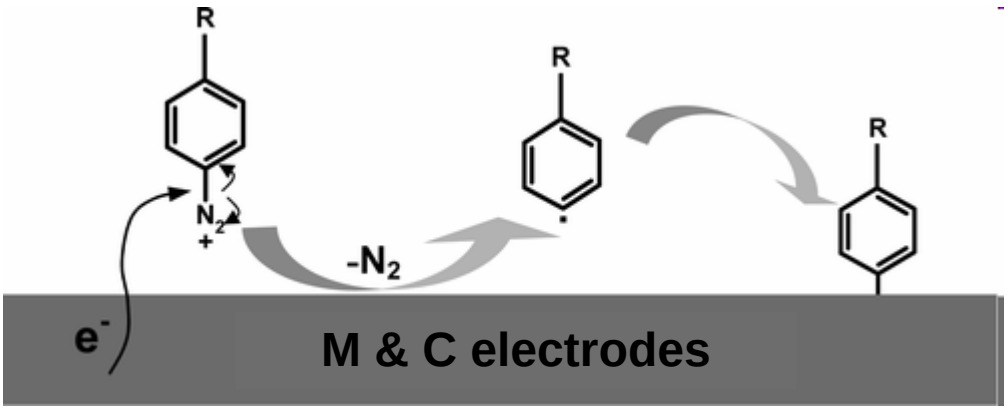

Figure 2. Mechanism of diazonium salt electrografting on metal and carbon surfaces.

The versatility of the method is based on the possibility of grafting a large variety of functionalized aryl groups, hence allowing the attachment of a broad spectrum of substances [91]. Pinson et al. have assigned the covalent attachment of the aryl groups to the binding of the aryl radical produced upon one-electron reduction of the diazonium salt to the carbon surface. Two factors favour such a reaction: (i) the diazonium salt is adsorbed prior to its reduction, and (ii) the aryl radical is not reduced at the very positive reduction potential of the diazonium salt [91]. The reduction mechanism of the diazonium cation has been studied, the electron transfer concerted with the cleavage of the C-N bond furnishes the aryl radical; this radical undergoes two competitive reactions: reduction at the electrode and H-atom transfer [92]. The surface coverage can be controlled through diazonium concentration and electrolysis duration [93,94]. Mechanistic investigations have shown that the electrochemical reduction process increases the adherence between the carbon surfaces and the matrix [95]. In 2005, Belanger and Baranton studied the derivatization of a glassy carbon electrode surface via electrochemical reduction of in situ generated diazonium cations. This deposition method, which involves simple reagents and does not require the isolation and purification of the diazonium salt, enabled the grafting of covalently bound layers which exhibited properties very similar to those of layers obtained by the classical derivatization method involving isolated diazonium salt dissolved in acetonitrile or aqueous acid solution [96].

ISBN:978-84-692-3235-4/DL:T-932-2009

The formation of maleimide-functionalized surfaces using maleimide-activated aryl diazonium salts have been studied via the electrodeposition of N-(4-diazophenyl)maleimide tetrafluoroborate on gold electrodes, the electrodeposition conditions were used to control film thickness and yielded submonolayer-to-multilayer grafting [97]. The structure and properties of thin organic films electrografted to conducting surfaces by this method are not well understood. Electrochemistry and contact angle measurements have been used to characterize multilayer carboxyphenyl and methylphenyl films grafted to Au surfaces. The charge associated with Au oxide reduction was used to estimate the upper limit for surface concentration of modifiers directly attached to the surface after careful preparation of the Au surface prior to and after grafting [98].

1.5.2.1. Biosensors based on diazonium deposition.

The covalent attachment of biosensing moieties onto electrodes surfaces via the electrochemical reduction of diazonium salts has a great importance in biosensing and analytical applications. This can be achieved by two main routes (Figure 3):

- The transducer surface is previously modified with functionalized aryl groups by electrografting of the corresponding diazonium salts followed by biomolecule incorporation with the formation of a covalent bond.
- Biomolecule-diazonium salt conjugates are first prepared and isolated, followed by electrografting on the transducer surface.

The first technique has been used for covalent immobilization of glucose oxidase onto electrically conductive ultrananocrystalline diamond (UNCD) thin films. For this aminophenyl functional groups were previously grafted to UNCD surface by electrochemical reduction of an aryl diazonium salt [99], and onto GCE using different linkers such as cinnamic acid [100], cross-linked hydrogel [101], and a mixed monolayer of 4-carboxyphenyl and a 20 Å oligo(phenylethynyl) molecular wire [102].

The immobilization of biomolecules such as glucose oxidase onto 4-phenylacetic modified GCE through electrochemical reduction of the corresponding diazonium salt [103], DNA onto 4-nitrobenzene modified Si (100) [104], alkaline phosphatase [105], and horseradish peroxidase [106], have been demonstrated. Diazonium chemistry has

UNIVERSITAT ROVIRA I VIRGILI
BOTTOM-UP SURFACE ENGINEERING FOR THE CONSTRUCTION OF (BIO) SENSORING SYSTEMS: DESIGN STRATEGIES
AND ANALYTICAL APPLICATIONS
Hossam Metwally Ahmed Nassef
ISBN:978-84-692-3235-4/DL:T-932-2009

also been shown to be suitable for the electrically addressable biomolecular functionalization of single-walled carbon nanotubes, in which nitro groups on specific nanostructures are reduced to amino groups and then used to covalently link DNA to vertically aligned carbon fiber electrodes, and was used for DNA detection [107].

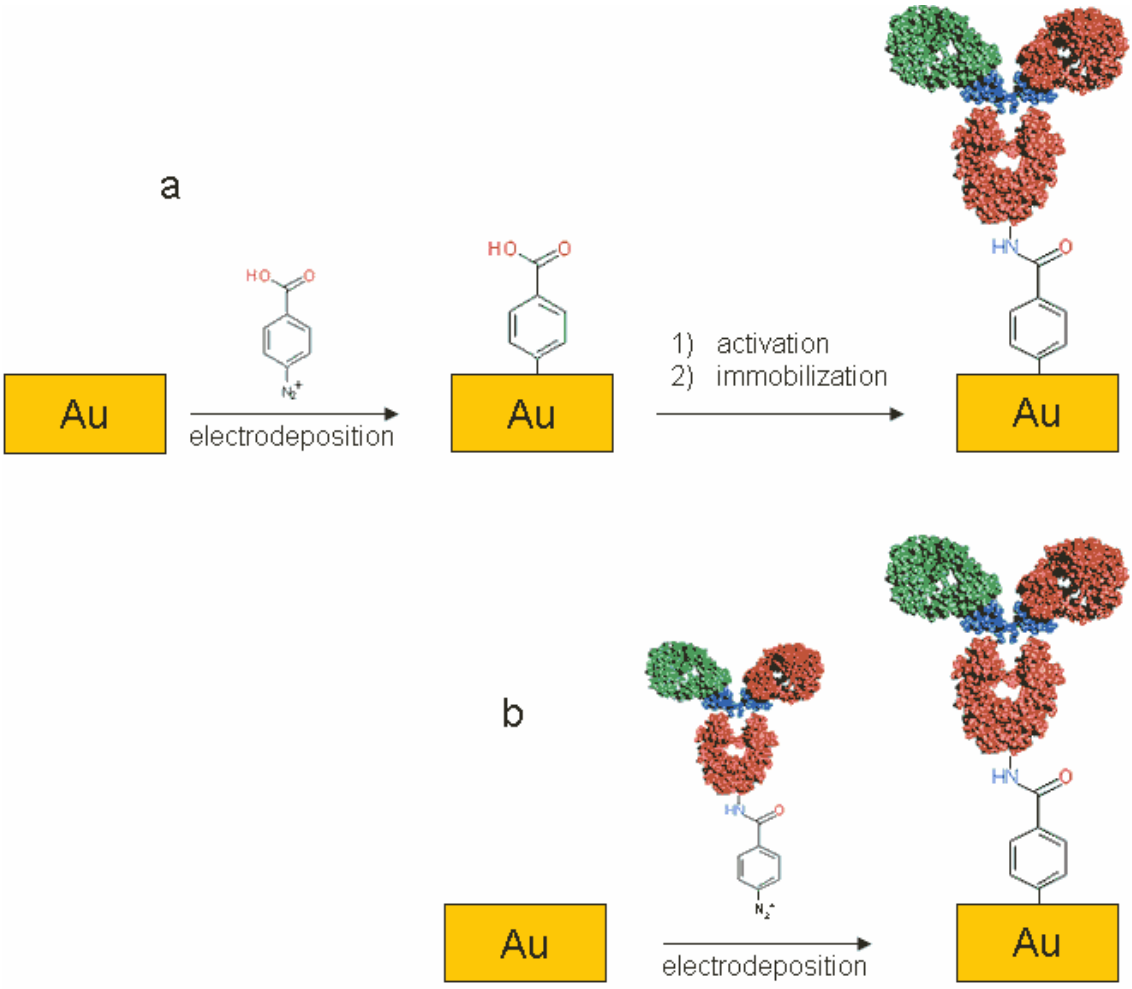

Figure 3. Strategies for immunosensor construction based on diazonium salts: a) covalent attachment of antibodies on diazonium functionalized surfaces; b) direct electrografting of antibody-diazonium conjugates.

The direct electrically addressable deposition of diazonium-modified antibodies has been demonstrated for immunosensing applications, in which the immobilized antibodies can be detected by the use of electroactive enzyme tags and gold-nanoparticle labeling, where chemiluminescence was used as the transduction method, and electrochemistry for

ISBN:978-84-692-3235-4/DL:T-932-2009

biopatterning. The individually and selectively addressed closely spaced microelectrodes for multi-target protein detection in an array format has been reported [108]. Recently, Marquette and coworkers introduced a technique for the direct and electroaddressable immobilization of proteins onto screen-printed graphite electrode microarrays via coupling 4-carboxymethylaniline to antibodies followed by diazotation of the aniline derivative to form an aryl diazonium functional group, the immuno-biochip has been used for the specific detection of anti-rabbit IgG antibodies [109]. Selective immobilization of rabbit and human immunoglobulins onto screen-printed graphite electrodes was demonstrated using chemiluminescence. The electroactive enzyme horseradish peroxidase (HRP) can also be modified with 4-carboxybenzenediazonium for addressable electrodeposition onto glassy carbon electrodes [110].

The deposition of diazonium functionalised horseradish peroxidase facilitates direct electron transfer between the enzyme and electrode, the modified electrode showed high non-mediated catalytic activity toward H_2O_2 reduction [110]. McNeil's group has developed different biosensors based on the direct deposition of enzymes such as HRP [111] for biotin detection via competitive binding of biotin and biotinylated glucose oxidase. Hydrogen peroxide was generated upon addition of glucose. Direct electron transfer between the electrodes and HRP is related to H_2O_2. The immunosensor showed greatest sensitivity over the range of biotin concentrations 0.07 to 2 μg ml^{-1} in the presence of 10 μg μg ml^{-1} excess of biotinylated glucose oxidase in the bulk solution [111]. With using cytochrome *c* covalently immobilised at N-acetyl cysteine modified gold electrode, the electron transfer rate constant (k_{et}) of enzymatic and cellular production of the superoxide anion radical was 3.4 ± 1.2 s^{-1} [112,113], while with using HRP, current sensitivity for peroxide was 637 nA μM^{-1} cm^{-2} , with heterogeneous rate constant (k'_{ME}) of 5.3 × 10^{-3} cm s^{-1} [112]. The attachment of hemoglobin and cytochrome c onto functionalized GCE with 4-carboxyphenyl diazonium groups have been also applied for the amperometric detection of H_2O_2 at a fairly mild potential of 0 V without any mediators [114].

A proof of concept procedure for the electroaddressable covalent immobilization of DNA and protein on arrayed electrodes along with simultaneous detection of multiple targets in the same sample solution has been reported [115]. Carboxyphenyldiazonium

UNIVERSITAT ROVIRA I VIRGILI
BOTTOM-UP SURFACE ENGINEERING FOR THE CONSTRUCTION OF (BIO) SENSORING SYSTEMS: DESIGN STRATEGIES
AND ANALYTICAL APPLICATIONS
Hossam Metwally Ahmed Nassef
ISBN:978-84-692-3235-4/DL:T-932-2009

was selectively deposited onto five of nine individually addressable electrodes in an array via bias assisted assembly. Amine functionalized DNA probes were covalently coupled to the carboxyl surface via carbodiimide chemistry. This was followed by the covalent immobilization of diazonium-antibody conjugates into the remaining four electrodes via cyclic voltammetry. Simultaneous electrochemical detection of a DNA sequence related to the breast cancer BRCA1 gene and the human cytokine protein interleukin-12, which is a substantial component in the immune system response and attack of tumor cells has been investigated [115]. Another example of DNA-sensing platforms were prepared by covalently attaching oligonucleotide capture probes onto p-aminophenyl-functionalized carbon surfaces and applied to the determination of an amplified herpes virus DNA sequence in an electrochemical hybridization assay [105].

1.5.3. Comparison between thiol and diazonium based strategies.

The attractiveness of Au-thiol chemistry is that well ordered and densely-packed monolayers can be easily formed, with a reasonably strong bond formed between the immobilized molecule and the electrode, and furthermore, a diverse range of molecules can be synthesized with a vast number of functional groups to modify the electrode surface [116-118]. One of the disadvantages of the Au-thiol system is that alkanethiols can be oxidatively or reductively desorbed at potentials typically outside the window defined by -800 to +800 mV versus Ag/AgCl [119], as well as the fact that alkanethiols are desorbed at temperatures over 100 ºC [120,121]. Additionally, as gold is a highly mobile surface, this results in monolayers moving across the electrode surface. Furthermore, the Au-thiolate bond is prone to UV photooxidation [122] and the Au/thiol junction creating large tunneling barrier (≈ 2 eV) which affects on the rate of electron transfer from the organic monolayer to the electrode [123]. Furthermore, the formation of a stable alkanethiol based SAM can require between 3 and 120 hours to allow organisation into an energetically favourable monolayer [71]. SAM are prone to displacement by other thiols [124].

As shown above, the electrochemical reduction of aryl diazonium salts is one possible alternative which has recently been reported as a method for the covalent derivatization of carbon or gold electrodes, forming a covalent bond which is strong, stable over both

UNIVERSITAT ROVIRA I VIRGILI
BOTTOM-UP SURFACE ENGINEERING FOR THE CONSTRUCTION OF (BIO) SENSORING SYSTEMS: DESIGN STRATEGIES
AND ANALYTICAL APPLICATIONS
Hossam Metwally Ahmed Nassef
ISBN:978-84-692-3235-4/DL:T-932-2009

time and temperature, non-polar and conjugated [119]. The irreversible interaction between diazonium derived aryl films and carbon has also led to the application of this method to other materials such as metals [125] and semiconductors [126].

The advantages of the diazonium reduction approach as compared to alkanethiol self-assembled monolayers include a highly stable surface over time and over a wide potential window, ease of preparation, and the ability to synthesize diazonium salts with a wide range of functional groups [93,127]. In addition, the ability to create a diazonium-modified surface by the application of a potential bias allows the selective functionalization of closely spaced microelectrode surfaces. While the use of carbon surfaces have dominated the majority of studies relating to the electrodeposition of aryl diazonium salts, Au surfaces have also been shown to be suitable for diazonium grafting [125,128]. The selective functionalization of Au electrodes with control over surface functional group density and electron transfer kinetics employing diazonium chemistry has been reported [129]. In contrast to the more common thiol–Au chemistry, diazonium modification on Au surfaces yields increased stability with respect to long-term storage in air, potential cycling under acidic conditions, and a wider potential window for subsequent electrochemistry [130], which has been proved by the calculated bonding energy; 24, 70, and 105 kcal/mol on Au, Si, and carbon, respectively [131,132]. The reductive deposition of aryl diazonium salts onto gold electrodes is superior for electrochemical sensors than either alkanethiol modified gold electrodes or aryl diazonium salt modified GC electrodes [130].

Some obvious advantages of the use of diazonium-functionalized antibodies and the electrically addressable deposition procedure are simplicity, fewer reagents and preparation steps; a strong covalent bond between antibody and electrode; the ability to selectively coat and control deposition onto electrode platforms and finally, a reduced number of chemical reactions on a surface relative to attaching a protein to a surface that has been diazonium-functionalized. The use of diazonium modification also allows for attachment to a variety of substrates including conducting and semiconducting substrates as well as carbon nanotubes [108]. The main disadvantage for diazonium approach is the multilayer formation [133-135]. Combellas et al, has prevented the layer from growing by hindering different positions of the diazonium ions [136] while Harper et al. exploited

UNIVERSITAT ROVIRA I VIRGILI
BOTTOM-UP SURFACE ENGINEERING FOR THE CONSTRUCTION OF (BIO) SENSORING SYSTEMS: DESIGN STRATEGIES
AND ANALYTICAL APPLICATIONS
Hossam Metwally Ahmed Nassef
ISBN:978-84-692-3235-4/DL:T-932-2009

the disadvantages of multilayer formation to immobilize two diverse molecules on a single gold electrode via consecutive electrodeposition of nitrophenyl and phenylboronic acid pinacol ester diazonium salts to form a thin film with dual binding functionality [137].

1.6. Washless/separation free biosensors

In most immunosensors using direct, or indirect approaches with labeled antibodies, the analyte detection consists of three steps; the first step is the addition of the analyte to a electrode biofunctionalised with anchored capture antibody, the second is the incubation with a labeled antibody and the final step is the addition of the substrate which is converted by the enzyme label to an electrochemically oxidisable/reducible product. In this format, several washing steps are necessary after each of the first two steps to remove non-specifically bounded molecules to the immunosensor surface [138,139].

It is desirable to eliminate the need for washing, as this would not only simplify the immunosensor use, but would also decrease the time required for measurement, as well as eliminating possible operator errors and sources of irreproducibility and erroneous results. To overcome the requirement for addition of substrate, this substrate could be co-immobilised with the immobilized capture antibody.

There are some research groups that have been investigated the construction of washless immunosensors. Ho et al. reported on a non-separation washless thick-film immunosensor using screen printed electrodes with immobilized capture antibodies and horseradish peroxidase (HRP) as an indicator enzyme. Only H_2O_2 generated near the electrode surface was detected and catalase was added to destroy the excess of H_2O_2 in the bulk to prevent interference generated by unbound labelled antibodies [140]. In 1998, the same group developed another separation-free washless electrochemical immunosensor for the detection of the pesticide atrazine via a competitive immunoassay using disposable screen printed horseradish peroxidase modified electrodes as a detecting element in conjunction with atrazine immuno-membranes. The assay is based on competition for available binding sites between free atrazine and an atrazine–glucose

ISBN:978-84-692-3235-4/DL:T-932-2009

oxidase conjugate. In the presence of glucose, H_2O_2 formed by the conjugate was reduced by enzyme-channelling via the HRP electrode [14].

Heller's group has developed a separationless washless amperometric immunosensor, in which the electrodes were not washed after their incubation with a biotinylated antibody or after any other step. The platform of the sensor is an electron-conducting redox hydrogel in which avidin and choline oxidase are co-immobilized, the hydrogel is immobilized on a vitreous carbon electrode. In this immunosensor, the H_2O_2 substrate of the immunolabeling enzyme is generated in the coating of an electrode and is not significantly decomposed by added catalase [141].

A separation free immunosensor has been developed via the covalent immobilization of the capture monoclonal antibody on the gold-coated microporous nylon membranes via a self-assembled monolayer of thioctic acid [142]. In the separation free sandwich assay, both model analyte protein and alkaline phosphatase labelled antibody are incubated simultaneously with the immobilized capture antibody. The enzyme substrate (4-aminophenyl phosphate) was introduced through the back side of the porous membrane, where it first encounters bound ALP-Ab at the gold surface, the enzymatically generated product, aminophenol, is detected immediately by oxidation at the gold electrode [142], and by careful optimisation of the time at which measurement is taken, the response due to enzyme label in the bulk solution can be separated from the local electrode response.

An amperometric immunosensor was developed by Lu et al [143] based on a non-diffusional redox polymer co-immobilised with anti-HRP antibody onto the sensing surface, used for transferring electrons between the electrode surface and HRP antigen bound to the anti-HRP antibody. The sensor showed LOD for HRP of 0.01 pg ml^{-1}, which is one order of magnitude lower than that obtained with ELISA [143].

Another type of separation-free channelling immunosensor has been developed from a disposable, polymer-modified, carbon electrode on which enzyme is co-immobilized with a specific antibody that binds the corresponding antigen. Another enzyme conjugate is introduced in the bulk solution, and the immunological reaction brings the two enzymes into close proximity at the electrode surface, and the signal is amplified through enzyme channeling. The localization of both enzymes on the electrode

surface limits the enzymatic reactions to the polymer/membrane/electrode interface [144].

Additionally, an amperometric immunosensor for creatinine detection has been developed using anti-creatinine antibodies, redox-labeled creatinine and a glassy carbon electrode covered with a semipermeable cellulose membrane. Creatinine from the sample competes with redox-labeled creatinine for the antigen binding sites of the antibody. Unbound conjugate passes through the membrane and is indicated at the electrode whereas antibody bound conjugate is size excluded [145]. The same phenomena has been used for the construction of enzyme biosensor in which amino acid oxidase was immobilized with glutaraldehyde and polyethylenimine on a working electrode made of rodinised carbon, and a protease was immobilized on an immunodyne membrane and was placed on the electrode. In the presence of protein sample, amino acids is liberated in the presence of the protease, and in turn the hydrogen peroxide produced by the immobilized amino acid oxidase was detected [146].

1.7. Reagentless biosensors

The vast majority electrochemical immunosensors rely on a reporter label linked to either antigen or antibody, which necessitates the addition of substrate following immunocomplex formation, thus taking away from the advantages of biosensors, where it is desirable that the only required end-user intervention be the addition of sample. One approach for reagentless detection, one of the more stringent in biosensor development relies on an unimolecular sensing format in which the meadiator is connected to the electrode surface through a stable chemical bond [147-149]. This not only simplifies the immunsensor procedure, accelerates the electrode response and decreases the analytical time but also increases the reproducibility and minimizes leaching of molecules in microsystem packaged biosensors [150,151].

Further examples of reagentless immunosensors have been constructed via several strategies. One of these strategies is based on the direct oxidation of HRP via measurement of the electron transfer between labelled HRP and the electrode surface [152]. In 2003, Dai and coworkers proposed a strategy for a reagentless and mediatorless immunosensor for the detection of carcinoma antigen-125 (CA125) by detecting the

UNIVERSITAT ROVIRA I VIRGILI
BOTTOM-UP SURFACE ENGINEERING FOR THE CONSTRUCTION OF (BIO) SENSORING SYSTEMS: DESIGN STRATEGIES AND ANALYTICAL APPLICATIONS
Hossam Metwally Ahmed Nassef
ISBN:978-84-692-3235-4/DL:T-932-2009

direct electrochemical signal of HRP labeled to immunoreagent [153]. Wu et al. developed a screen-printed reagentless immunosensor array, via immobilisation of gold nanoparticles linked to horseradish peroxidase labeled antibodies modified in biopolymer/sol-gel modified electrodes to obtain direct electrochemical responses of HRP using DPV. Upon the formation of immunocomplexes, the DPV responses decreased due to increasing spatial blocking and impedance (Scheme 1) [154], and has been applied to the fabrication of a reagentless immunosensor array by individually embedding 4 different HRP labeled antibody-modified gold nanoparticles in a designed biopolymer/sol-gel matrix formed on screen-printed carbon electrodes [155].

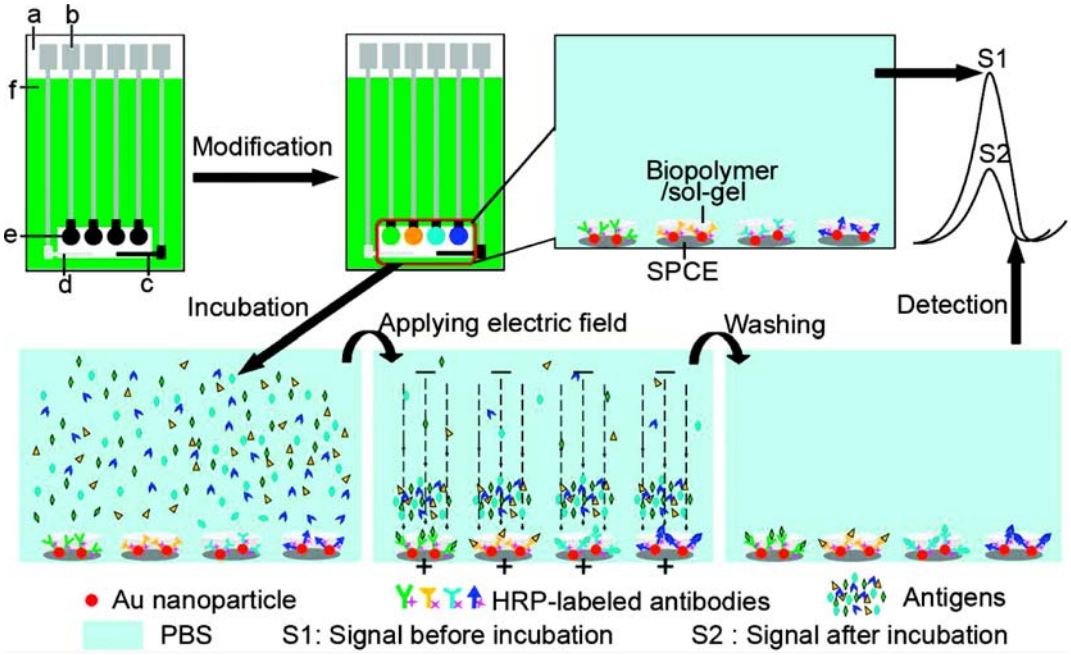

Scheme 1. Schematic representation of ECIA and the electrochemical multiplexed immunoassay with an electric field-driven incubation process. (a) Nylon sheet, (b) silver ink, (c) graphite auxiliary electrode, (d) Ag/AgCl reference electrode, (e) graphite working electrode, and (f) insulating dielectric [154].

In a similar approach, Dan and co-workers reported a reagentless immunosensor for the determination of the carbohydrate antigen 19-9 (CA19-9) in human serum based on the immobilization of antibody in colloidal gold nanoparticle modified carbon paste electrode, and the direct electrochemistry of HRP labeled to a CA19-9 antibody, resulted

ISBN:978-84-692-3235-4/DL:T-932-2009

in significant peak current decrease of HRP, after the formation of antigen–antibody complex, due to blocking of electron transfer of HRP toward electrode [156]. Chorionic gonadotrophin (HCG) antigen has also been determined using a reagentless immunosensor, based on the direct electron transfer of the HRP of horseradish peroxidase-labeled human chorionic gonadotrophin antibody (HRP-anti-HCG) encapsulated in a titania sol–gel thin film [151,157], and in three-dimensional ordered nanoporous organically modified silicate (ormosil sol-gel) material [158,159]. Upon the formation of immunocomplex the direct electron transfer signal of the immobilized HRP was decreased due to the increasing spatial blocking and dielectric constant of the microenvironment around HRP molecules. A reagentless immunosensor for determination of α-1-fetoprotein (AFP) in human serum has also been developed, via immobilization of α-1-fetoprotein antibody (AFP Ab) onto the glassy carbon electrode modified by gold nanowires (Au NWs) and ZnO nanorods (ZnO NRs) composite film. A sandwich immunocomplex format was employed to detect AFP with horseradish peroxidase (HRP)-labeled AFP as tracer and hydrogen peroxide as enzyme substrate. The determination of AFP was established by chronoamperometry to record the reduction current response of H_2O_2 catalysed HRP by means of the direct electron-transfer of Au NWs between HRP and electrode without addition of mediators or non immunoreagents [160].

An alternative approach to direct electron transfer from HRP enzyme labels, is based on the entrapping of the redox mediator into Nafion film, such as entrapping of 3,3´,5,5´-tetramethylbenzidine into Nafion film modified glassy carbon electrode for the detection of mouse IgG antigen [161]. Thionine (Thi) into Nafion (Nf) is also entrapped to form a composite Thi/Nf membrane, which yields an interface containing amine groups to assemble gold nanoparticles layer for immobilization of α-1-fetoprotein antibody (anti-AFP) and the specific binding of anti-AFP to AFP in serum has been directly detected by the decrease in the current response [162]. The redox mediator could also be directly immobilized on the electrode surface, such as deposition of Prussian blue PB on bare platinum electrode, which forms a negatively charged surface to immobilize positively charged TiO_2 nanoparticles, and consequently immobilize nano-Au. The

UNIVERSITAT ROVIRA I VIRGILI
BOTTOM-UP SURFACE ENGINEERING FOR THE CONSTRUCTION OF (BIO) SENSORING SYSTEMS: DESIGN STRATEGIES
AND ANALYTICAL APPLICATIONS
Hossam Metwally Ahmed Nassef
ISBN:978-84-692-3235-4/DL:T-932-2009

deposited nano-Au layer was used to immobilize a higher amount of alpha-fetoprotein antibody which easily detect alpha-fetoprotein (Scheme 2) [163].

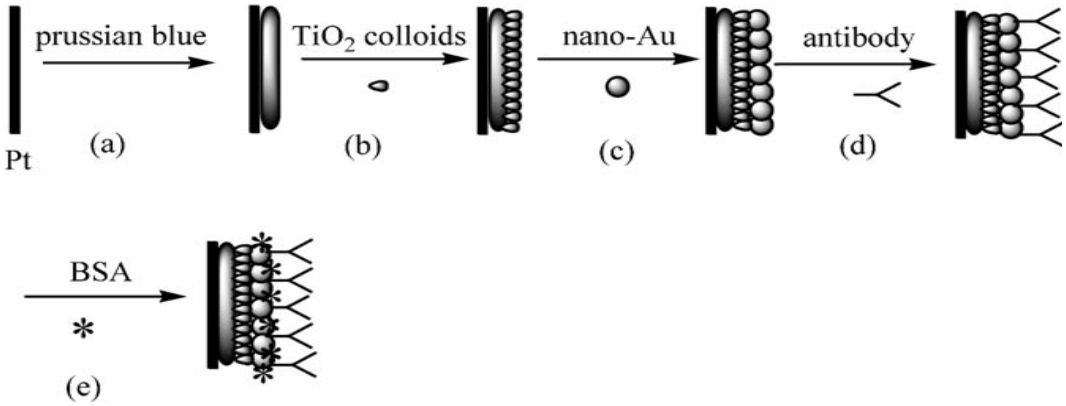

Scheme 2 Example of reagentless biosensor based on nanoparticle deposition [163].

Liu and coworkers recently reported a reagentless amperometric immunosensor for the determination of carcinoembryonic antigen (CEA) by employing a novel organic–inorganic composite film coupled with gold nanoparticles. Prussian blue was deposited on GCE and then a porous organic material synthesized with 3,4,9,10-perylenetetracarboxylicdianhydride (PTCDA) and ethanediamine was coated on the surface of Prussian blue film, followed by the immobilization of nano-Au as a substrate for anti-CEA immobilization [164].

There is a series of reagentless biosensors based on redox polymers, in which a variety of nitrogen donor groups containing co-polymers entrapped with an enzyme (HRP) are used to coordinate with a ligand (Os-bis-*N*,*N*-(2,2′-bipyridil)-dichloride). The ligand exchange reaction assures an efficient electron-transfer pathway between the polymer-entrapped horseradish peroxidase and the electrode surface [165]. A water-soluble Os-poly(vinyl-imidazole) redox hydrogel is deposited on a graphite electrode by drop-coating (i.e. manually) followed by the electrochemically-induced deposition of an enzyme-containing non-conducting polymer film. In the presence of quinohemoprotein alcohol dehydrogenase (QH-ADH), the polymer precipitation leads to an entrapment of the redox enzyme within the polymer film. Simultaneously, the water-soluble Os-poly(vinyl-imidazole) redox hydrogel, which slowly dissolves from the electrode surface after addition of the electrolyte, is co-entrapped within the precipitating polymer layer.

UNIVERSITAT ROVIRA I VIRGILI
BOTTOM-UP SURFACE ENGINEERING FOR THE CONSTRUCTION OF (BIO) SENSORING SYSTEMS: DESIGN STRATEGIES
AND ANALYTICAL APPLICATIONS
Hossam Metwally Ahmed Nassef
ISBN:978-84-692-3235-4/DL:T-932-2009

This provides the pre-requisite for an efficient electron-transfer pathway from the redox enzyme via the polymer-bound redox centers to the electrode surface [166]. Another polymerization strategy based on oxidative electropolymerisation of dicarbazole derivative functionalised by a N-hydroxysuccinimide group in acetonitrile, leading to the formation of electroactive poly(dicarbazole) films on the electrode surface. The subsequent chemical functionalisation of the poly(dicarbazole) film was easily performed by successive immersions in aqueous enzyme and mediator solutions. The amperometric responses of the poly(dicarbazole) films grafted with polyphenol oxidase (PPO) and thionine showed sensitive response toward catechol detection [167]. Three types of glucose sensors were prepared by electrochemical deposition of glucose oxidase (GOD), $[Os(bpy)_2(PVP)_{10}Cl]Cl$ (Os-polymer) (*bpy* = 2,2'-*bipyridyl*, *PVP* = *poly*(4-*vinylpyridine*)) within polyphenol (PPh) films on a platinum electrode. The enzyme and Os-polymer were entrapped in PPh films. The sensors has been applied for glucose detection [168]. Another reagentless glucose biosensor based on the codeposition of glucose oxidase enzyme with the redox polymer $[Os(bpy)_2(PVP)_{10}Cl]Cl$ (bpy = bipyridyl, PVP = poly-4-vinylpyridine) and glutaradehyde on the surface of a platinum electrode, and subsequently covered with an electropolymerized layer of pyrrole. The electron transfer from the reduced $FADH_2$ group in the core of the enzyme to the electrode surface is facilitated via the redox polymer/polypyrrole system [169]. The main disadvantage attached to biosensors based on the redox polymer is the non-specific adsorption of different materials present in the same media due to the charge of the polymer which attract non-specific molecules.

Reagentless fructose and alcohol biosensors have been developed with a versatile enzyme immobilisation technique mimicking natural interactions and the flexibility of living systems. The electrode architecture was built up on electrostatic interactions by the sequential layer-by-layer adsorption of a cationic redox polyelectrolyte (poly[(vinylpyridine)$Os(bpy)_2Cl$]) and redox enzymes (fructose dehydrogenase, horseradish peroxidase (HRP) and a combination of HRP and alcohol oxidase). In this way, an efficient transformation of substrate fluxes into electrocatalytic currents was achieved due to the intimate contact of both catalytic unit and mediator. The sensitivities

obtained for each biosensor were 19.3, 58.1 and 10.6 mA M^{-1} cm^{-1} for fructose, H_2O_2 and methanol, respectively [170].

1.8. Ultra-sensitive and substrate/enzymatic recycling based biosensors

Signal amplification and noise reduction are crucial for obtaining low detection limits in biosensors. The need for ultrasensitive detection systems is exemplified in the case of certain proteins that signal the presence of various diseases. Most current protein detection methods only allow detection after protein levels reach critical threshold concentrations. At these concentrations the disease is often significantly advanced. More sensitive methods that allow for early detection of protein markers could potentially revolutionize physician treatment moving from purely therapeutic and aggressive strategies to prevention and disease monitoring, increasing quality of life and patient survival rates and reducing the high economic burden of the healthcare sector.

1.8.1. Amplification via liposomes

There are several strategies that have been applied for the construction of ultra-sensitive biosensors. One of these strategies exploits the use of liposomes. Liposomes exhibit outstanding features such as easy preparation, high resistance to non-specific adsorption as well as being versatile carriers of various functional molecules with liposomes having a large internal volume and outer surface area where thousands of reporter molecules can be entrapped or immobilized and the release of reporter molecules is controllable [171-173]. Thus, the development of liposome-based immunosorbent assays has been studied for signal enhancement [174]. Zheng and coworkers developed a highly sensitive chemiluminescence immunosensor for the detection of prostate-specific antigen (PSA) based on amplification with the enzyme encapsulating liposomes. Horseradish peroxidase (HRP) encapsulated and antibody-modified liposome act as the carrier of a large number of markers and specific recognition label for the amplified detection of PSA. In the detection of PSA, the analyte was first bound to the specific capture antibody immobilized on the microwell plates, and then sandwiched by the antibody-modified liposomes encapsulating HRP. The encapsulated markers, HRP

molecules were released by the lysis of the specifically bound liposomes in the microwell with Triton X-100 solution and the concentration of the analyte PSA is determined via the chemiluminescence signal of HRP-catalyzed luminol/peroxide/enhancer system [175]. Furthermore, Chen and coworkers [176], developed an ultrasensitive chemiluminescence biosensor for the detection of cholera toxin, based on ganglioside-functionalized supported lipid membrane as sensing surface and the HRP/GM1-functionalized liposome as detection probe. The implementation of liposome-based detection probe allowed for an efficient incorporation of the GM1 receptor and covalent conjugation of multiple biocatalytic amplifier HRP through common phospholipid components. The application of enhanced chemiluminescence reaction in the detection of HRP-bearing liposome afforded signal amplification via effective immobilization of multiple biocatalytic amplifiers with LOD 0.8 pg mL^{-1} [176].

1.8.2. Enzymatic Amplification

An alternative approach strategy for signal amplification, based on enzymatic recycling, has recently been reported [177]. This immunosensor was used for detection of phycotoxins such as okadaic acid (OA), in which OA–ovalbumin (OA–OVA) conjugate was immobilised on screen-printed electrodes, then secondary antibodies labelled with alkaline phosphatase or horseradish peroxidase were used for signal generation. Electrochemical signal amplification was achieved using the enzyme diaphorase (DI) for recycling the signal arising from an ALP-labelled secondary antibody. Detection was based on the dephosphorylation of p-APP by ALP and the oxidation of the corresponding electroactive p-AP to p-iminoquinone (p-IQ) on the electrode surface, and the regeneration of p-IQ by DI, decreasing the LOD to 0.03 μg L^{-1} and enlarging the working range by two orders of magnitude [177]. ALP and DI (Scheme 3) was also used for signal amplification for microcystin detection and the amplification expanded the linear range by more than four orders of magnitude and decreased the limit of detection from 37.75 to 0.05 μg/L [178].

UNIVERSITAT ROVIRA I VIRGILI
BOTTOM-UP SURFACE ENGINEERING FOR THE CONSTRUCTION OF (BIO) SENSORING SYSTEMS: DESIGN STRATEGIES AND ANALYTICAL APPLICATIONS
Hossam Metwally Ahmed Nassef
ISBN:978-84-692-3235-4/DL:T-932-2009

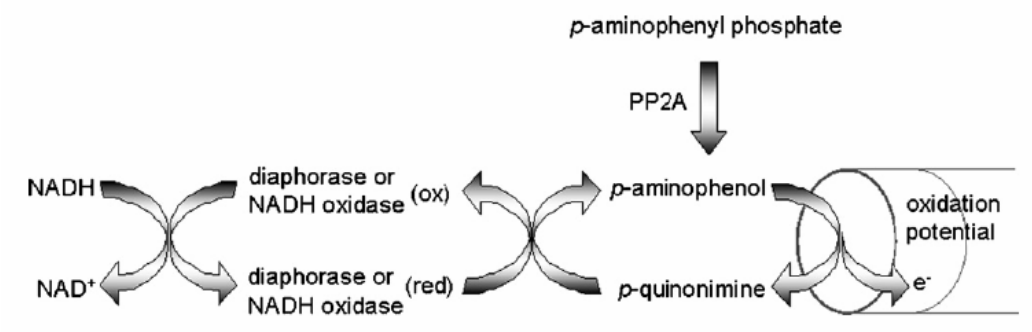

Scheme 3 Example of enzymatic substrate recycling for signal amplification [178].

A highly selective and sensitive amperometric system of trace amounts of glutamate has been reported, the system includes a microdialysis probe, immobilized enzyme reactor, and poly(1,2-diaminobenzene)-coated platinum electrode. The enzyme reactor prepared by the co-immobilization of glutamate oxidase and glutamate dehydrogenase were employed to enhance the sensitivity of glutamate as an on-line amplifier based on the substrate recycling. The -glutamate in the dialysate from the probe are recycled enzymatically during passage through the reactor in the presence of sufficient amounts of NADH and oxygen to produce a large amount of hydrogen peroxide, which is detected if selectively at a downstream poly(1,2-diaminobenzene)-coated platinum electrode. Glutamate is determined with a 160-fold increase in sensitivity (LOD 0.5×10^{-7} M) compared with the unamplified responses [179].

A sensitive potentiometric enzyme electrode for lactate determination has been developed based on the bienzyme system lactate oxidase-peroxidase co-immobilized on the surface of carbonic material. Enzymatic oxidation of lactate results in the formation of hydrogen peroxide. The latter leads to a shift in the electrode potential due to mediatorless peroxidase catalysis of hydrogen peroxide electroreduction. For increasing the sensitivity, a recycling system containing additionally co-immobilized lactate dehydrogenase has been realized. In the presence of NADH, lactate dehydrogenase catalyses the reduction of pyruvate formed by lactate oxidation. In this way lactate oxidase and lactate dehydrogenase co-immobilized on the electrode surface form an enzyme recycling system, which has a higher sensitivity towards lactate. The detection limit of lactate is 100 nM [180].

UNIVERSITAT ROVIRA I VIRGILI
BOTTOM-UP SURFACE ENGINEERING FOR THE CONSTRUCTION OF (BIO) SENSORING SYSTEMS: DESIGN STRATEGIES
AND ANALYTICAL APPLICATIONS
Hossam Metwally Ahmed Nassef
ISBN:978-84-692-3235-4/DL:T-932-2009

An amperometric flow-injection system with a glucose-6-phosphate dehydrogenase-lactate dehydrogenase-lactate oxidase co-immobilized reactor that gives responses amplified by substrate recycling was employed for the highly sensitive detection of NAD^+ and NADH. Both NAD^+ and NADH are recycled enzymatically during the passage through the reactor in the presence of sufficient glucose-6-phosphate and pyruvate in the carrier solution. As a result of this recycling reaction, a large amount of L-lactate is generated in the reactor and the L-lactate produced is subsequently converted back to pyruvate to produce a large amount of hydrogen peroxide by co-immobilized lactate oxidase, which is detected amperometrically at a downstream platinum electrode. Both NAD^+ and NADH are determined with a 400-fold increase in sensitivity compared with the unamplified responses. The detection limit is 0.1 pmol for both coenzymes [181].

1.8.3. Amplification via substrate recycling

The sensitivity of enzyme electrodes can also be increased substantially by incorporation of a substrate recycling scheme. where the analyte is not only measured once but is reconverted to be measured again leading to an amplification of the transduction signal [182,183]. A substrate recycling assay for phenolic compounds was developed using tyrosinase, a copper-containing enzyme, in excess NADH. The reaction of various phenols with the enzyme produced an *o*-quinone, which was then detected by recycling between reactions with the enzyme and NADH. The recycling of quinones by excess NADH to their original reduced forms prevented the problems of subsequent quinone polymerization and product inactivation which occur in nonrecycling assays. Absorbance measurements of the NADH consumption rate enhanced the assay sensitivity for catechol 100-fold compared to nonrecycling *o*-quinone detection, giving a detection limit of 240 nM. Fluorescence NADH monitoring permitted a 10-fold improvement over absorbance, with a detection limit of 23 nM [184].

1.8.4. Other methods of amplification

Another approach to achieve ultrasensitive detection is based on the potentiometric detection of enzyme labelled immuno-complexes formed at the surface of a polypyrrole

coated screen printed gold electrodes [185], or at negatively charged platinum electrode modified with colloidal nanosized gold and polyvinyl butyral (PVB sol-gel) [186]. Hepatitis B surface antibody (HBsAb) was immobilized onto the modified surfaces via self-assembly (SA) and opposite-charged adsorption (OCA) techniques. These types of potentiometric immunosensors have been applied to the determination of hepatitis B surface antigen (HBsAg). Detection is mediated by the immunoreaction that produces charged products, the shift in potential is measured at the sensor surface, caused by local changes in redox state, pH and/or ionic strength. The magnitude of the difference in potential is related to the concentration of the formed receptor-target complex. The immunosensor showed a fast potentiometric response (< 3 min) to HBsAg, with LOD 2.3 ng mL^{-1} [186].

The use of polymer based biosensors have been extensively used for signal amplification. The electrochemiluminescence behaviour of luminol and H_2O_2 system on a poly(diallyldimethyl ammonium chloride) (PDDA)–chitosan-modified glassy carbon electrode for the ultrasensitive detection of H_2O_2 was evaluated and the PDDA greatly enhanced the ECL intensity of luminol [187], resulting in improved sensitivity and detection limit.

Tang and his coworkers developed an ultrasensitive immunosensor based on a carbon fiber microelectrode (CFME) covered with a well-ordered anti-CEA/protein A/nanogold architecture for the detection of carcinoembryonic antigen (CEA). The signal amplification strategy was based on the use of thionine (TH)-doped magnetic gold nanospheres as labels and horseradish peroxidase (HRP) as enhancer. The magnetic gold nanospheres amplified the surface coverage of HRP-bound anti-CEA, and the bound bionanospheres catalyze the reduction of H_2O_2 in the presence of the doped thionine, as a mediator, with amplified signal output, and the noise is reduced by employing the CFME electrode and the hydrophilic immunosensing layer [188]. A further example of an ultrasensitive immunosensor is based on the use of superparamagnetic nanoparticles and a “microscope” based on a high-transition temperature dc superconducting quantum interference device (SQUID) [189], in which a suspension of magnetic nanoparticles carrying antibodies is added to a mylar film containing targets. Pulses of magnetic field are applied parallel to the SQUID, during the application of magnetic field, the

UNIVERSITAT ROVIRA I VIRGILI
BOTTOM-UP SURFACE ENGINEERING FOR THE CONSTRUCTION OF (BIO) SENSORING SYSTEMS: DESIGN STRATEGIES
AND ANALYTICAL APPLICATIONS
Hossam Metwally Ahmed Nassef
ISBN:978-84-692-3235-4/DL:T-932-2009

nanoparticles develop a net magnetization. Unbound nanoparticles relax rapidly and contribute no measurable signal. Nanoparticles that are bound to the target are immobilized and undergo Néel relaxation, producing a slowly decaying magnetic flux detected by the SQUID [189].

1.9. Objectives of the thesis.

Surface engineering relies on the modification of materials from the molecular scale with the aim of providing a biointerface of enhanced performance and improved physical and (bio)chemical properties. This is especially relevant for the construction of biosensors where the challenge is to rationally design and engineer the surface functional groups in order to control the communication between the device and its bioenvironment.

The overall objective of the thesis is to contribute to the development of washless, reagentless, highly sensitive immunosensors exploiting surface immobilised substrate and target sensitive reporter encapsulating liposomes.

The principle for a reagentless, washless and ultrasensitive immunosensor is depicted in Scheme 4, where the substrate (o-aminophenylphosphate, o-APP) is co-immobilized with capture antibodies. Target sensitive liposomes (TSL) linked to the secondary antibody and the sample containing the target to be detected are simultaneously added to the functionalised electrode. TSL are stable structures in solution even when linked to the target analyte. When the complete immunocomplex is formed with the immobilised capture antibody, TSL lose flexibility, becoming rigid, and spontaneously collapse, rapidly releasing its encapsulated contents [190]. No washing step is thus necessary as liposome-Ab or liposome-Ab-target are stable and it is only when the full immunocomplex forms that the liposomes open and signal is generated (Scheme 4a).

UNIVERSITAT ROVIRA I VIRGILI
BOTTOM-UP SURFACE ENGINEERING FOR THE CONSTRUCTION OF (BIO) SENSORING SYSTEMS: DESIGN STRATEGIES AND ANALYTICAL APPLICATIONS
Hossam Metwally Ahmed Nassef
ISBN:978-84-692-3235-4/DL:T-932-2009

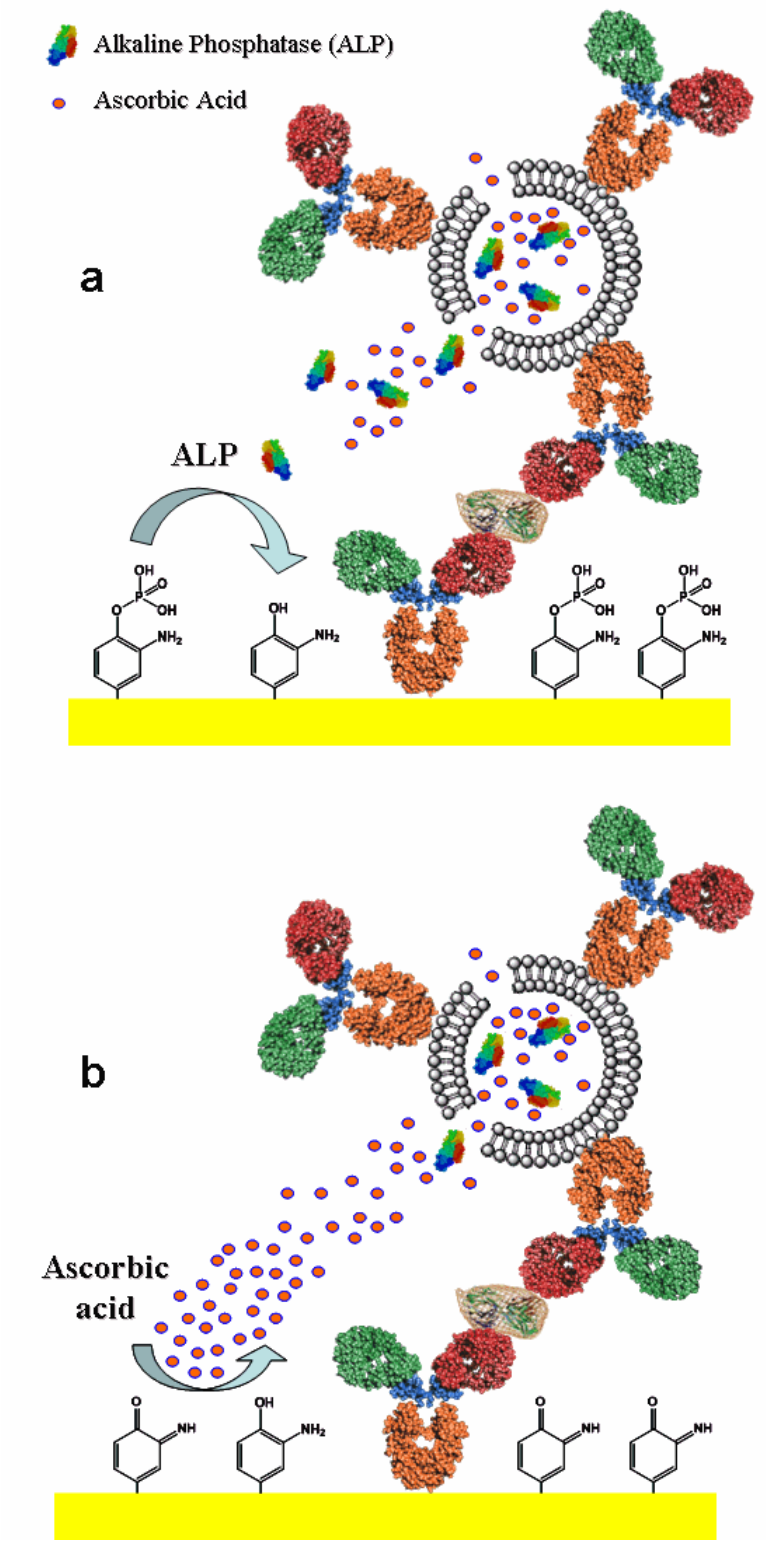

Scheme 4. Principle for a reagentless, washless and ultrasensitive immunosensor: a) target sensitive release of liposome contents; b) amplification reaction.

UNIVERSITAT ROVIRA I VIRGILI
BOTTOM-UP SURFACE ENGINEERING FOR THE CONSTRUCTION OF (BIO) SENSORING SYSTEMS: DESIGN STRATEGIES
AND ANALYTICAL APPLICATIONS
Hossam Metwally Ahmed Nassef
ISBN:978-84-692-3235-4/DL:T-932-2009

In a further amplification step, it is envisaged that the electrode surface contains a mixed layer of antibody and ALP substrate, with the liposomes encapsulating ALP as well as a mediator that can be used to recycle the surface using substrate recycling. After dephosphorylation of the substrate by ALP, the immobilized substrate film is transformed into o-aminophenol (o-AP) which could be used for the recycled catalytic oxidation of mediators such as hydrazine, NADH or ascorbic acid (Scheme 4b) This designed model could produce a double amplification of the reaction signals; first by using high amount of enzyme encapsulated into liposomes as compared with only one enzyme molecule attached per one antibody; the second amplification will be obtained from the recycling process of the electrocatalytic oxidation of ascorbic acid using the produced o-AP film by the first enzymatic reaction [177,191] .

The thesis has the following specific objectives (Scheme 5):

1. Study the electrochemical behaviour of different mediators which could be used in signal amplification and recycling process in the enzymatic reactions of ALP.
2. Study the construction of a biosensor model based on SAM using different types of dithiols as a substrate (or linker) for protein attachment on Au surfaces.
3. Study the construction of a biosensor model based on the direct attachment of proteins such as Fab and thiol-modified antibodies on Au surfaces.
4. Study the construction of a biosensor model based on the attachment of the proteins through a linker on Au surfaces via the electrochemical reduction of their corresponding diazonium salts.
5. Evaluate the analytical application of the studied models.

UNIVERSITAT ROVIRA I VIRGILI
BOTTOM-UP SURFACE ENGINEERING FOR THE CONSTRUCTION OF (BIO) SENSORING SYSTEMS: DESIGN STRATEGIES
AND ANALYTICAL APPLICATIONS
Hossam Metwally Ahmed Nassef
ISBN:978-84-692-3235-4/DL:T-932-2009

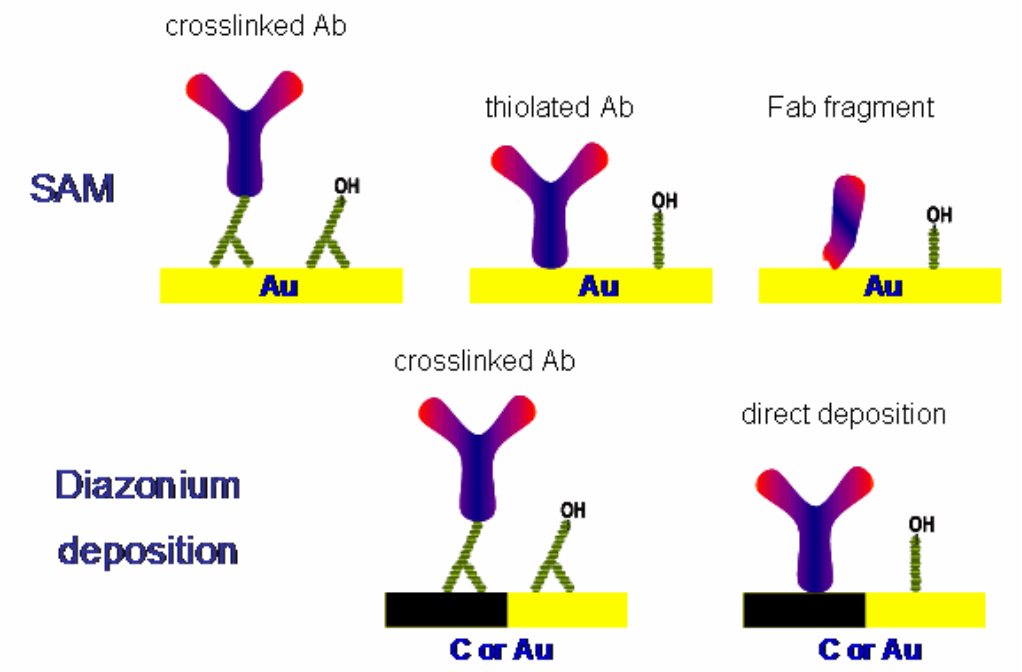

Scheme 5. Strategies for surface modification studied in this thesis.

As previously explained, ALP is a specific enzyme routinely used for immunosensing. Numerous approaches have been reported for its sensitive detections, which consistently require the addition of such reagents. Our group previously studied the grafting of o-aminophenylphosphate (o-APP), the substrate for ALP, film onto GCE by the electrochemical reduction of the corresponding nitrophenyl phosphate diazonium salt in acidic aqueous solution [192], facilitating the reagentless detection of ALP.

Specifically outlining the work achieved in this PhD thesis, the work is organised into separate articles that have been published, submitted or are under preparation for submission.

In the first three of these Articles (Chapters 2-4), different potential mediators that could be used for the catalytic interaction with the enzymatic product o-AP were evaluated and due to their well characterized properties, hydrazine, NADH and ascorbic acid were selected for further study. Hydrazine is used as an antioxidant and reducing agent; NADH plays an important rule in oxidoreductases and dehydrogenase systems and ascorbic acid (vitamin C) is an antioxidant whose detection is important in clinical and food applications. The electrocatalytic properties of o-aminophenol films grafted on glassy carbon surfaces have been employed for the electrochemical evaluation of

UNIVERSITAT ROVIRA I VIRGILI
BOTTOM-UP SURFACE ENGINEERING FOR THE CONSTRUCTION OF (BIO) SENSORING SYSTEMS: DESIGN STRATEGIES
AND ANALYTICAL APPLICATIONS
Hossam Metwally Ahmed Nassef
ISBN:978-84-692-3235-4/DL:T-932-2009

hydrazine, NADH and ascorbic acid, to select the most relevant as a recycling mediator in the planned signal amplification strategy. To evaluate the best mediator, the reaction kinetics between mediators and the o-AP/o-QI were extensively studied using different techniques such as cyclic voltammetry, hydrodynamic voltammetry, double potential step chronoamperometry, and double potential step chronocoulometry.

Of the three mediators evaluated, hydrazine is flammable, detonable, corrosive and highly toxic [193-195] and therefore difficult to handle. On the other hand, NADH is unstable and expensive [196,197] and electrode surfaces are easily fouled by the accumulation of reaction products during NADH oxidation [198]. Finally, ascorbic acid is cheap, easy to handle, safe, showed excellent electrocatalytic behavior, and is compatible with hydrolases such as ALP for co-encapsulation purposes [177,191]. Therefore, ascorbic acid was selected as the mediator for regeneration of the o-AP film and substrate recycling. We had thus demonstrated an interesting catalytic system for the oxidation of ascorbic acid, which is stable, sensitive and reproducible, and we decided to explore this system for clinical and food applications. In the first application, we targeted the determination of uric acid (UA) in the presence of ascorbic acid (AA), which commonly co-exist in biological fluids of humans, mainly in blood and urine (Chapter 4). It is difficult to electrochemically differentiate between UA and AA at bare electrodes, while the o-AP surface facilitates a selective catalytic activity towards ascorbic acid and was used for the detection of ascorbic acid in the presence of uric acid and vice versa, and applied to the detection of uric acid in a real urine sample.

In Articles 4 and 5 (Chapters 5 and 6), the selective electrocatalytic properties of the grafted o-AP film toward ascorbic acid were also applied to its detection in real samples of fruits and vegetables using disposable one-shot screen printed electrodes. The o-AP modified screen printed electrodes showed high catalytic responses toward the electrocatalytic oxidation of ascorbic acid. The o-AP SPE sensor exhibited high sensitivity and selectivity toward ascorbic acid with excellent storage and operational stability, as well as a quantitatively reproducible analytical performance. exhibited excellent correlation with the standard spectrophotometric method in the testing of food samples [199].

UNIVERSITAT ROVIRA I VIRGILI
BOTTOM-UP SURFACE ENGINEERING FOR THE CONSTRUCTION OF (BIO) SENSORING SYSTEMS: DESIGN STRATEGIES
AND ANALYTICAL APPLICATIONS
Hossam Metwally Ahmed Nassef
ISBN:978-84-692-3235-4/DL:T-932-2009

In the second part of the thesis, different surface engineering strategies of antibody immobilization for immunosensor construction using a linker or via direct attachment onto a Au surface using a strategy of self assembly (scheme 5) were evaluated and compared. An alternative strategy explored was the direct anchoring of the antibody with or without a linker via the electrochemical reduction of their diazonium cations (scheme 5).

In Article 6 (Chapter 7), a comparison between these different surface chemistries methodologies for the construction of immunosensors towards the model analyte of coeliac toxic gliadin was carried out. Firstly, the self-assembled monolayer approach was evaluated based on the modification of gold surfaces with two bipodal carboxylic acid terminated thiols (thioctic acid and a benzyl alcohol disubstituted thiol, DT2). A stable SAM of DT2 was rapidly immobilized (3 h) on Au as compared with thioctic acid (100 h), although both surface chemistries resulted in highly sensitive electrochemical immunosensors for gliadin detection using an anti-gliadin antibody (CDC5), with detection limits of 11.6 and 5.5 ng/mL, respectively. The developed immunosensors were then applied to the detection of gliadin in commercial gluten-free and gluten-containing food products, showing an excellent correlation when compared to results obtained with ELISA.

In Article 7 (Chapter 8), another approach was explored to further improve immunosensor sensitivity and stability and furthermore to reduce the time necessary for sensor preparation was investigated looking at the direct attachment of the SATA modified full length antibody, and their F(ab) fragments onto Au electrodes. Spontaneously adsorbed SAMs of Fab-SH and CDC5-SH onto Au were rapidly formed in less than 15 minutes. The amperometric immunosensors based on Fab fragments exhibited a vastly improved detection limit as compared to the thiolated antibody with a highly sensitive response toward gliadin detection (LOD, 3.29 ng/ml for amperometric detection and 0.42 μg/ml for labelless (impedimetric) detection). Moreover, the self-assembled monolayer of F(ab) fragments was extremely stable with almost no loss in response after 60 days storage at 4^{o}C.

In Chapter 9, an alternative surface chemistry approach was explored for the modification of Au electrodes via electrochemical (i.e. CV at different potential cycling

UNIVERSITAT ROVIRA I VIRGILI
BOTTOM-UP SURFACE ENGINEERING FOR THE CONSTRUCTION OF (BIO) SENSORING SYSTEMS: DESIGN STRATEGIES
AND ANALYTICAL APPLICATIONS
Hossam Metwally Ahmed Nassef
ISBN:978-84-692-3235-4/DL:T-932-2009

or via application of fixed potential at different deposition times) and spontaneous reduction (via dipping at different exposure times) in diazonium cations of a conjugate prepared from the monoclonal full length anti-gliadin antibody (CDC5) and the linker 3,5-bis(aminophenoxy)benzoic acid (DAPBA). Cylic voltammetry was chosen for surface modification via applying three potential cycles, but it was observed that an extensive washing process was necessary after each potential cycle to remove the non-specifically adsorbed molecules or formed multilayers. The affinity of the immobilized antibody toward gliadin was studied using EIS and amperometry. The modified CDC5-DAPBA surface showed a reasonable amperometric response after incubation with 5 μg/ml gliadin, and exhibited excellent specificity with no response observed in the absence of the analyte.

The approaches of surface modification via the electrochemical deposition of diazonium salts, either by modification of the surface with a linker and followed by cross-linking with the full length antibody, or via one step immobilization of the prepared antibody-linker conjugate, are time consuming and very laborious requiring extensive washing, and further exploration is required to understand how to control deposition to avoid complex multiplayer formation.

From the different surface chemistry strategies evaluated in this work we can conclude that the best approach is the immunosensor based on the spontaneous adsorption of thiolated F(ab) fragments on gold. This surface is easy and fast to prepare, very stable and sensitive and can be stored for long times in the appropriate conditions without lost of affinity. A good alternative to this approach seems to be the electrodeposition of antibody-diazonium conjugates, although further work is needed in order to optimize this system.

Overall, this work has contributed significantly to the vision we have for an immunosensor that avoids washes and reagent addition, where we have selected an excellent mediator for co-encapsulation with alkaline phosphatase enzymes within liposome reporter molecules, for regeneration of surface immobilised substrate following enzymatic dephosporylation, facilitating substrate recycling and increase in sensitivity and reduction in detection limit. Furthermore, we have selected an optimum surface chemistry for co-immobilisation of capture antibody molecules and enzyme substrate via

UNIVERSITAT ROVIRA I VIRGILI
BOTTOM-UP SURFACE ENGINEERING FOR THE CONSTRUCTION OF (BIO) SENSORING SYSTEMS: DESIGN STRATEGIES
AND ANALYTICAL APPLICATIONS
Hossam Metwally Ahmed Nassef
ISBN:978-84-692-3235-4/DL:T-932-2009

the formation of self-assembled monolayers of antibody fragments on gold surfaces. Future work will focus on combining the selected mediator and surface chemistry into a sandwich immunosensor with a target sensitive liposome reporter molecule, to demonstrate a reagentless, washless ultrasesensitive immunosensing platform.

UNIVERSITAT ROVIRA I VIRGILI
BOTTOM-UP SURFACE ENGINEERING FOR THE CONSTRUCTION OF (BIO) SENSORING SYSTEMS: DESIGN STRATEGIES
AND ANALYTICAL APPLICATIONS
Hossam Metwally Ahmed Nassef
ISBN:978-84-692-3235-4/DL:T-932-2009

Bibliography

[1] D.R. Theâvenot, K. Toth, R.A. Durst, G.S. Wilson, Pure Appl. Chem. 71 (1999) 2333.

[2] A.P.F. Turner, I. Karube, G.S. Wilson, in Biosensors: Fundamentals and Applications, Oxford University Press, Oxford, 1987.

[3] J. North, Trends Biotechnol. 3 (1985) 180.

[4] P.B. Luppa, L.J. Sokoll, D.W. Chan, Clinica Chimica Acta 314 (2001) 1.

[5] C.L. Morgan, D.J. Newman, C.P. Price, Clinical Chemistry 42 (1996) 193.

[6] X. Jiang, D. Li, X. Xu, Y. Ying, Y. Li, Z. Ye, J. Wang, Biosens. Bioelect., 23 (2008) 1577.

[7] J.P. Whelan, A.W. Kusterbeck, G.A. Wemhoff, R. Bredehorst, F.S. Ligler, Anal. Chem. 65 (1993) 3561.

[8] P.T. Charles, D.W. Conrad, M.S. Jacobs, J.C. Bart, A.W. Kusterbeck, Bioconjug. Chem. 6 (1995) 691.

[9] P. Orozlan, C. Thommen, M. Wehrli, D. Gert, M. Ehrat, Anal. Methods Instrum. 1 (1993) 43.

[10] F.V. Bright, T.A. Betts, K.S. Litwiler, Anal. Chem. 62 (1990) 1065.

[11] F.F. Bier, R.D. Schmid, Analyst 119 (1994) 437.

[12] B. Leca-Bouvier, L.J. Blum, Anal. Lett. 38 (2005) 1491.

[13] R. Wilson, M.H. Barker, D.J. Schiffrin, R. Abuknesha, Biosens. Bioelectron. 12 (1997) 277.

[14] R.W. Keay, C.J. McNeil, Biosensors and Bioelectronics 13 (1998) 963.

[15] B. Danielsson, I. Surugiu, A. Dzgoev, M. Mecklenburg, K. Ramanathan, Anal. Chim. Acta 426 (2001) 227.

[16] M. Seydack, Biosens. Bioelectron. 20 (2005) 2454.

[17] M.S. Wilson, Anal. Chem. 77 (2005) 1496.

[18] L.J. Sokoll, D.W. Chan, Anal. Chem. 71 (1999) 356.

[19] R.P. Ekins, Clin. Chem. 44 (1998) 2015.

[20] L.J. Kricka, Clin. Chem. 44 (1998) 2008.

[21] J.L. Bock, Am. J. Clin. Pathol. 113 (2000) 628.

ISBN:978-84-692-3235-4/DL:T-932-2009

[22] D.J. Li, L.J. Sokoll, D.W. Chan, J. Clin. Ligand Assay 21 (1998) 377.

[23] J. Janata, J. Am. Chem. Soc. 97 (1975) 2914.

[24] M.F. Yulaev, R.A. Sitdycov, N.M. Dmitrieva, B.B. Dzantiev, A.V. Zherdev, K.A. Askarov, J. Anal. Chem. 50 (1995) 194.

[25] B.B. Dzantiev, A.V. Zherdev, M.F. Yulaev, R.A. Sitdikov, N.M. Dmitrieva, I.Y. Moreva, Biosens. Bioelectron. 11 (1996) 179.

[26] N.F. Starodub, B.B. Dzantiev, V.M. Starodub, A.V. Zherdev, Anal. Chim. Acta 424 (2000) 37.

[27] R.A. Villamizar, A. Maroto, F.X. Rius, Sensors and Actuators B-Chemical 136 (2009) 451.

[28] R.A. Villamizar, A. Maroto, F.X. Rius, I. Inza, M.J. Figueras, Biosensors and Bioelectronics 24 (2008) 279.

[29] Z.C. Sanchez-Acevedo, J. Riu, F.X. Rius, Biosensors and Bioelectronics In Press, Corrected Proof (2009).

[30] J.E. Pearson, A. Gill, P. Vadgama, Ann. Clin. Biochem 37 (2000) 119.

[31] S. Koch, P. Woias, L.K. Meixner, S. Drost, H. Wolf, Biosens. Bioelectron. 14 (1999) 413.

[32] G.S. Wilson, in Fundamentals of amperometric sensors. In: Turner APF, Karube I, Wilson GS, eds. Biosensors. Fundamentals and applications, Oxford University Press, Oxford, 1987, p. 165.

[33] A.L. Ghindilis, P. Atanasov, M. Wilkins, E. Wilkins, Biosens. Bioelectron. 13 (1998) 113.

[34] M. Aizawa, Adv. Clin. Chem. 31 (1994) 247.

[35] C.J. McNeil, D. Athey, R. Renneberg, EXS 81 (1997) 17.

[36] P. Skládal, T. Kaláb, Anal. Chim. Acta 316 (1995) 73.

[37] K.R. Milner, A.P. Brown, D.W.E. Allsopp, W.B. Betts, Electron. Lett. 34 (1998) 66.

[38] W.O. Ho, S. Krause, C.J. McNeil, J.A. Pritchard, R.D. Armstrong, D. Athey, K. Rawson, Analytical Chemistry 71 (1999) 1940.

[39] L. Watson, P. Maynard, D. Cullen, R. Sethi, I. Brettle, C. Lowe, Biosensors 3 (1988) 101.

[40] H.C. Berney, J. Alderman, W.A. Lane, J.K. Collins, J. Mol. Recognit. 11 (1998) 175.

[41] A.A. Shulga, A.P. Soldatkin, A.V. El'skaya, S.V. Dzyadevich, S.V. Patskovsky, V.I. Strikha, Biosens. Bioelectron. 9 (1994) 217.

[42] B.A. Cornell, V.L.B. Braach-Maksvytis, L.G. King, Nature 387 (1997) 580.

[43] K. Yagiuda, A. Hemmi, S. Ito, Biosens. Bioelectron. 11 (1996) 703.

[44] V.M. Mirsky, M. Riepl, O.S. Wolfbeis, Biosensors and Bioelectronics 12 (1997) 977.

[45] O. Pänke, T. Balkenhohl, J. Kafka, D. Schäfer, F. Lisdat, in T. Scheper (Editor), Advances in Biochemical Engineering/Biotechnology, Springer-Verlag Berlin Heidelberg, 2008, p. 209.

[46] O.A. Sadik, H. Xu, E. Gheorghiu, D. Andreescu, C. Balut, M. Gheorghiu, D. Bratu, Anal. Chem. 74 (2002) 3142.

[47] F. Darain, D.S. Park, J.S. Park, Y.B. Shim, Biosens. Bioelectron. 19 (2004) 1245.

[48] L. Yang, Y. Li, Biosens. Bioelectron. 20 (2005) 1407.

[49] H. Chen, J. Jiang, Y. Huang, T. Deng, J. Li, G. Shen, R. Yu, Sens. Actuators B 117 (2006) 211.

[50] I. Navrátilová, P. Skládal, Bioelectrochemistry 62 (2004) 11.

[51] S. Hleli, C. Martelet, A. Abdelghani, N. Burais, N. Jaffrezic-Renault, Sensors and Actuators, B: Chemical 113 (2006) 711.

[52] J. Rickert, W. Göpel, W. Beck, G. Jung, P. Heiduschka, Biosensors and Bioelectronics 11 (1996) 757.

[53] A.G.E. Saum, R.H. Cumming, F.J. Rowell, Biosensors and Bioelectronics 13 (1998) 511.

[54] X. Cui, R. Pei, Z. Wang, F. Yang, Y. Ma, S. Dong, X. Yang, Biosensors and Bioelectronics 18 (2003) 59.

[55] A.B. Kharitonov, J. Wasserman, E. Katz, I. Willner, The Journal of Physical Chemistry B 105 (2001) 4205.

[56] R. Danczyk, Krieder, B., et al., Biotechnol. Bioeng 84 (2003) 215.

[57] M. Shinkai, et al., J. Biosci. Bioeng 94 (2002) 606.

[58] T. Cass, Ligler, F.S., in Immobilized Biomolecules in Analysis: A Practical Approach, Oxford University Press, New York., 1998.

[59] G.T. Hermanson, in Bioconjugate Techniques, Academic Press, San Diego, 1996.

[60] R.A. Vijayendran, Leckband, D.E., Anal. Chem. 73 (2001) 471.

[61] S. Babacam, Pivarnik, P., et. al, , Biosensors and Bioelectronics 15 (2000) 615.

[62] A. Hamelin, Double-layer properties at sp and sd metal single-crystal electrodes., in Modern Aspects of Electrochemistry; B.E. Conway, R.E. White, J. O`M. Bokris, Eds., Plenum Press, New York & London, 1985, 16, p. 1.

[63] J.J. Gooding, D.B. Hibbert, Trends Anal. Chem. 18 (1999) 525.

[64] E. Ostuni, L. Yan, G.M. Whitesides, Colloids Surf. B 15 (1999) 3.

[65] F. Frederix, K. Bonroy, G. Reekmans, W. Laureyn, A. Campitelli, M.A. Abramov, W. Dehaen, G. Maes, J. Biochem. Biophys. Methods 58 (2004) 67.

[66] K. Bonroy, Frederix, F., Reekmans, G., Dewolf, E., De Palma, R., Borghs, G., Declerck, P., Goddeeris, B., Journal of Immunological Methods 312 (2006) 167.

[67] N. Patel, M.C. Davies, M. Hartshorne, R.J. Heaton, C.J. Roberts, S.J.B. Tendler, P.M. Williams, Langmuir 13 (1997) 6485.

[68] G. Suarez, R.J. Jackson, J.A. Spoors, C.J. McNeil, Analytical Chemistry 79 (2007) 1961.

[69] A. Fragoso, N. Laboria, D. Latta, C.K. O'Sullivan, Analytical Chemistry 80 (2008) 2556.

[70] W. Spangler, B.D. Spangler, E.S. Tarter, Z. Suo, Polym. Preprints 45 (2004) 524.

[71] H.M. Nassef, M.C. Bermudo Redondo, P.J. Ciclitira, H.J. Ellis, A. Fragoso, C.K. O'Sullivan, Analytical Chemistry 80 (2008) 9265.

[72] A. Coulter, R. Harris, J. Immunol. Methods 59 (1983) 199.

[73] J. Rousseaux, G. Biserte, H. Bazin, Molecular Immunology 17 (1980) 469.

[74] D. Beale, Developmental and Comparative Immunology 11 (1987) 287.

[75] M. Bia, W. Li, L. Lia, Z. Yian, Y. Zo, Chin Med Sci J 10 (1995) 78.

[76] M. Mariant, M. Camagna, L. Tarditi, E. Seccamani, Molecular Imminology 28 (1991) 69.

[77] D. Saerens, L. Huang, K. Bonroy, S. Muyldermans, Sensors 8 (2008) 4669.

[78] B. Lu, J. Xie, C. Lu, C. Wu, Y. Wei, Anal. Chem. 67 (1995) 83.

[79] I. Vikholm, Albers, W.M., Välimäki, H., Helle, H., Thin Solid Films 643 (1998) 327.

[80] P. Ihalainen, J. Peltonen, Langmuir 18 (2002) 4953.

[81] I. Vikholm-Lundin, Langmuir 21 (2005) 6473.

[82] I. Vikholm-Lundin, W.M. Albers, Biosensors & Bioelectronics 21 (2006) 1141.

[83] W. Lee, B.K. Oh, W.H. Lee, J.W. Choi, Colloids and Surfaces B: Biointerfaces 40 (2005) 143.

[84] H. Wang, H. Zeng, Z. Liu, Y. Yang, T. Deng, G. Shen, R. Yu, Analytical Chemistry 76 (2004) 2203.

[85] S. Song, B. Li, L. Wang, H. Wu, J. Hu, M. Li, C. Fan, Molecular Biosystems 3 (2007) 151.

[86] C. Esseghaier, Helali, S., Fredj, H.B., Tlili, A., Abdelghani, A., Sensors and Actuators, B: Chemical 131 (2008) 584.

[87] M.M.L.M. Vareiro, J. Liu, W. Knoll, K. Zak, D. Williams, A.T.A. Jenkins, Analytical Chemistry 77 (2005) 2426.

[88] J.C. O'Brien, V.W. Jones, M.D. Porter, C.L. Mosher, E. Henderson, Anal. Chem. 72 (2000) 703.

[89] Y. Harada, Kuroda, M., Ishida, A., Langmuir 16 (2000) 708.

[90] K.L. Brogan, Wolfe, K.N., Jones, P.A., Schoenfish, M.H., Anal. Chim. Acta 496 (2003) 73.

[91] M. Delamar, R. Hitmi, J. Pinson, J.M. Saveant, J. Am. Chem. Soc. 114 (1992) 5883.

[92] C.P. Andrieux, J. Pinson, Journal of the American Chemical Society 125 (2003) 14801.

[93] P. Allongue, M. Delamar, B. Desbat, O. Fagebaume, R. Hitmi, J. Pinson, J.M. Save?ant, Journal of the American Chemical Society 119 (1997) 201.

[94] J.K. Kariuki, M.T. McDermott, Langmuir 15 (1999) 6534.

[95] M. Delamar, G. Desarmot, O. Fagebaume, R. Hitmi, J. Pinsonc, J.M. Saveant, Carbon 35 (1997) 801.

[96] S. Baranton, D. Be?langer, Journal of Physical Chemistry B 109 (2005) 24401.

[97] J.C. Harper, R. Polsky, D.R. Wheeler, S.M. Brozik, Langmuir 24 (2008) 2206.

[98] M.G. Paulik, P.A. Brooksby, A.D. Abell, A.J. Downard, J. Phys. Chem. C 111 (2007) 7808.

[99] J. Wang, J.A. Carlisle, Diamond and Related Materials 15 (2006) 279.

[100] X. Yang, S.B. Hall, S.N. Tan, Electroanalysis 15 (2003) 885.

[101] M. Pellissier, D. Zigah, F. Barriere, P. Hapiot, Langmuir 24 (2008) 9089.

[102] G. Liu, M.N. Paddon-Row, J. Justin Gooding, Electrochemistry Communications 9 (2007) 2218.

[103] C. Bourdillon, M. Delamar, C. Demaille, R. Hitmi, J. Moiroux, J. Pinson, Journal of Electroanalytical Chemistry 336 (1992) 113.

[104] A. Shabani, A.W.H. Mak, I. Gerges, L.A. Cuccia, M.F. Lawrence, Talanta 70 (2006) 615.

[105] A. Ruffien, M. Dequaire, P. Brossier, Chemical Communications (2003) 912.

[106] G. Liu, J.J. Gooding, Langmuir 22 (2006) 7421.

[107] C.-S. Lee, S.E. Baker, M.S. Marcus, W. Yang, M.A. Eriksson, R.J. Hamers, Nano Letters 4 (2004) 1713.

[108] R. Polsky, J.C. Harper, D.R. Wheeler, S.M. Dirk, D.C. Arango, S.M. Brozik, Biosensors and Bioelectronics 23 (2008) 757.

[109] B.P. Corgier, C.A. Marquette, L.J. Blum, J. Am. Chem. Soc. 127 (2005) 18328.

[110] R. Polsky, J.C. Harper, S.M. Dirk, D.C. Arango, D.R. Wheeler, S.M. Brozik, Langmuir 23 (2007) 364.

[111] J.D. Wright, K.M. Rawson, W.O. Ho, D. Athey, C.J. McNeil, Biosensors & Bioelectronics 10 (1995) 495.

[112] C.J. McNeil, D. Athey, W.O. Ho, Biosensors & Bioelectronics 10 (1995) 75.

[113] J.M. Cooper, K.R. Greenough, C.J. McNeil, Journal of Electroanalytical Chemistry 347 (1993) 267.

[114] M.C. Liu, Y. Qi, G.H. Zhao, Electroanalysis 20 (2008) 900.

[115] J.C. Harper, R. Polsky, D.R. Wheeler, S.M. Dirk, S.M. Brozik, Langmuir 23 (2007) 8285.

[116] J.A. Rogers, R.J. Jackman, G.M. Whitesides, J. Microelectromech. Syst. 6 (1997) 184.

[117] J.L. Wilbur, G.M. Whitesides, in Self-assembly and Self-assembled Monolayers in Micro and Nanofabrication nanotechnology, Springer-Verlag, New York, 1999, (Chapter 8).

[118] H.O. Finklea, Electroanal. Chem. 19 (1996) 109.

[119] G. Liu, J. Liu, T. Bo?cking, P.K. Eggers, J.J. Gooding, Chemical Physics 319 (2005) 136.

[120] E. Delamarche, B. Michel, H. Kang, C. Gerber, Langmuir 10 (1994) 4103.

[121] A.B. Horn, D.A. Russell, L.J. Shorthouse, T.R.E. Simpson, J. Chem. Soc. Faraday Trans. 92 (1996) 4759.

[122] M.H. Schoenfisch, J.E. Pemberton, J. Am. Chem. Soc. 120 (1998) 4502.

[123] S. Ranganathan, I. Steidel, F. Anariba, R.L. McCreery, Nano Lett. 1 (2001) 491.

[124] C.D. Bain, E.B. Troughton, Y.T. Tao, J. Evall, G.M. Whitesides, R. Nuzzo, J. Am. Chem. Soc. 111 (1989) 321.

[125] M.C. Bernard, A. Chausse, E. Cabet-Deliry, M.M. Chehimi, J. Pinson, F. Podvorica, C. Vautrin-Ul, Chem. Mater. 15 (2003) 3450.

[126] M.P. Stewart, F. Maya, D.V. Kosynkin, S.M. Dirk, J.J. Stapleton, C.L. McGuiness, D.L. Allara, J.M. Tour, J. Am. Chem. Soc. 126 (2004) 370.

[127] A.J. Downard, Electroanalysis 12 (2000) 1085.

[128] A. Laforgue, T. Addou, D. Be?langer, Langmuir 21 (2005) 6855.

[129] J.C. Harper, R. Polsky, S.M. Dirk, D.R. Wheeler, S.M. Brozik, Electroanalysis 19 (2007) 1268.

[130] G. Liu, T. Bocking, J.J. Gooding, Journal of Electroanalytical Chemistry 600 (2007) 335.

[131] D.-e. Jiang, B.G. Sumpter, S. Dai, J. Am. Chem. Soc. 128 (2006) 6030.

[132] D.-e. Jiang, B.G. Sumpter, S. Dai, J. Phys. Chem. B 110 (2006) 23628.

[133] P.A. Brooksby, A.J. Downard, J. Phys. Chem. B 109 (2005) 8791.

[134] F. Anariba, S.H. DuVall, R.L. McCreery, Anal. Chem. 75 (2003) 3837.

[135] J.K. Kariuki, M.T. McDermott, Langmuir 17 (2001) 5947.

[136] C. Combellas, F. Kanoufi, J. Pinson, F.I. Podvorica, J. Am. Chem. Soc. 130 (2008) 8576.

[137] J.C. Harper, R. Polsky, D.R. Wheeler, D.M. Lopez, D.C. Arango, S.M. Brozik, Langmuir 25 (2009) 3282.

[138] C. Price, J.D. Newman, in Principle and Practice of Immunoassay, 2nd ed. Macmillan, New York, 1997.

[139] A.I. Hemmilä, in Applications of Fluorescence in Immunoassay, Wiley, New York, 1991.

[140] W.O. Ho, D. Athey, C.J. McNeil, Biosens. Bioelectron. 10 (1995) 683.

[141] C.N. Campbell, T. de Lumley-Woodyear, A. Heller, Fresenius' Journal of Analytical Chemistry 364 (1999) 165.

[142] C. Duan, M.E. Meyerhoff, Analytical Chemistry 66 (1994) 1369.

[143] B. Lu, E.I. Iwuoha, M.R. Smyth, R. O'Kennedy, Analytica Chimica Acta 345 (1997) 59.

[144] J. Rishpon, D. Ivnitski, Biosensors and Bioelectronics 12 (1997) 195.

[145] A. Benkert, F.W. Scheller, W. Schoessler, B. Micheel, A. Warsinke, Electroanalysis 12 (2000) 1318.

[146] P. Sarkar, Microchemical Journal 64 (2000) 283.

[147] E. Crowley, C. O'Sullivan, G.G. Guilbault, Analytica Chimica Acta 389 (1999) 171.

[148] B.A. Kuznetsov, G.P. Shumakovich, O.V. Koroleva, A.I. Yaropolov, Biosensors and Bioelectronics 16 (2001) 73.

[149] K. Kerman, N. Nagatani, M. Chikae, T. Yuhi, Y. Takamura, E. Tamiya, Analytical Chemistry 78 (2006) 5612.

[150] B. Haghighi, S. Varma, F.M. Alizadeh Sh, Y. Yigzaw, L. Gorton, Talanta 64 (2004) 3.

[151] J. Chen, J. Tang, F. Yan, H. Ju, Biomaterials 27 (2006) 2313.

[152] S.S. Rosatto, L.T. Kubota, G. de Oliveira Neto, Analytica Chimica Acta 390 (1999) 65.

[153] Z. Dai, F. Yan, J. Chen, H. Ju, Analytical Chemistry 75 (2003) 5429.

[154] J. Wu, Y.T. Yan, F. Yan, H.X. Ju, Analytical Chemistry 80 (2008) 6072.

[155] J. Wu, F. Yan, X.Q. Zhang, Y.T. Yan, J.H. Tang, H.X. Ju, Clinical Chemistry 54 (2008) 1481.

[156] D. Dan, X. Xiaoxing, W. Shengfu, Z. Aidong, Talanta 71 (2007) 1257.

[157] J. Chen, F. Yan, Z. Dai, H.X. Ju, Biosensors & Bioelectronics 21 (2005) 330.

[158] F. Tan, F. Yan, H.X. Ju, Biosensors & Bioelectronics 22 (2007) 2945.

[159] F. Tan, F. Yan, H. Ju, Electrochemistry Communications 8 (2006) 1835.

[160] X.X. Lu, H.P. Bai, P. He, Y.Y. Cha, G.M. Yang, L. Tan, Y.H. Yang, Analytica Chimica Acta 615 (2008) 158.

[161] Y. Wu, J.W. Zheng, Z. Li, Y.R. Zhao, Y. Zhang, Biosensors & Bioelectronics 24 (2009) 1389.

[162] Y. Zhuo, R. Yuan, Y.Q. Chai, D.P. Tang, Y. Zhang, N. Wang, X.L. Li, Q. Zhu, Electrochemistry Communications 7 (2005) 355.

[163] Y.R. Yuan, R. Ynan, Y.Q. Chai, Y. Zhuo, Y.T. Shi, X. He, X.M. Miao, Electroanalysis 19 (2007) 1402.

[164] Z.Y. Liu, R. Yuan, Y.Q. Chai, Y. Zhuo, C.L. Hong, X. Yang, Sensors and Actuators B-Chemical 134 (2008) 625.

[165] D.A. Guschin, Y.M. Sultanov, N.F. Sharif-Zade, E.H. Aliyev, A.A. Efendiev, W. Schuhmann, Electrochimica Acta 51 (2006) 5137.

[166] A. Vilkanauskyte, T. Erichsen, L. Marcinkeviciene, V. Laurinavicius, W. Schuhmann, Biosensors and Bioelectronics 17 (2002) 1025.

[167] S. Cosnier, D. Fologea, S. Szunerits, R.S. Marks, Electrochemistry Communications 2 (2000) 827.

[168] M. Pravda, C.M. Jungar, E.I. Iwuoha, M.R. Smyth, K. Vytras, A. Ivaska, Analytica Chimica Acta 304 (1995) 127.

[169] E. Rohde, E. Dempsey, M.R. Smyth, J.G. Vos, H. Emons, Analytica Chimica Acta 278 (1993) 5.

[170] A. Narvaez, G. Suarez, I.C. Popescu, I. Katakis, E. Dominguez, Biosensors & Bioelectronics 15 (2000) 43.

[171] T. Imura, T. Gotoh, K. Otake, S. Yoda, Y. Takebayashi, S. Yokoyama, H. Takebayashi, H. Sakai, M. Yuasa, M. Abe, Langmuir 19 (2003) 2021.

[172] T. Kamidate, N. Kikuchi, A. Ishida, H. Tani, Anal. Sci. 21 (2005) 701.

[173] T. Kamidate, K. Komatsu, H. Tani, A. Ishida, Luminescence 22 (2007) 236.

[174] D. Monroe, J. Liposome Res. 1 (1990) 339.

[175] Y. Zheng, H. Chen, X.P. Liu, J.H. Jiang, Y. Luo, G.L. Shen, R.Q. Yu, Talanta 77 (2008) 809.

[176] H. Chen, Y. Zheng, J.H. Jiang, H.L. Wu, G.L. Shen, R.Q. Yu, Biosensors & Bioelectronics 24 (2008) 684.

[177] M. Campas, P. de la Iglesia, M. Le Berre, M. Kane, J. Diogene, J.L. Marty, Biosensors & Bioelectronics 24 (2008) 716.

[178] M. Campas, M.G. Olteanu, J.L. Marty, Sensors and Actuators B-Chemical 129 (2008) 263.

[179] T. Yao, S. Suzuki, T. Nakahara, H. Nishino, Talanta 45 (1998) 917.

[180] A.L. Ghindilis, A. Makower, F.W. Scheller, Sensors and Actuators B: Chemical 28 (1995) 109.

[181] T. Yao, N. Kobayashi, T. Wasa, Analytica Chimica Acta 248 (1991) 345.

[182] L. Coche-Guérente, V. Desprez, J.P. Diard, P. Labbé, Journal of Electroanalytical Chemistry 470 (1999) 53.

[183] L. Coche-Guérente, V. Desprez, P. Labbé, S. Therias, Journal of Electroanalytical Chemistry 470 (1999) 61.

[184] R.S. Brown, K.B. Male, J.H.T. Luong, Analytical Biochemistry 222 (1994) 131.

[185] D. Purvis, O. Leonardova, D. Farmakovsky, V. Cherkasov, Biosensors & Bioelectronics 18 (2003) 1385.

[186] R. Yuan, D.P. Tang, Y.Q. Chai, X. Zhong, Y. Liu, J.Y. Dai, Langmuir 20 (2004) 7240.

[187] Y. Wang, H. Dai, X. Wu, G. Chen, Luminescence 23 (2008) 98.

[188] D.P. Tang, R. Yuan, Y.Q. Chal, Analytical Chemistry 80 (2008) 1582.

[189] Y.R. Chemla, H.L. Crossman, Y. Poon, R. McDermott, R. Stevens, M.D. Alper, J. Clarke, Proceedings of the National Academy of Sciences of the United States of America 97 (2000) 14268.

[190] R.J.Y. Ho, B.T. Rouse, L. Huang, Biochemistry 25 (1986) 5500.

[191] A.J. Bäumner, R.D. Schmid, Biosens. Bioelectron. 13 (1998) 519.

[192] A.E. Radi, J.M. Montornés, C.K. O'Sullivan, Journal of Electroanalytical Chemistry 587 (2006) 140.

UNIVERSITAT ROVIRA I VIRGILI
BOTTOM-UP SURFACE ENGINEERING FOR THE CONSTRUCTION OF (BIO) SENSORING SYSTEMS: DESIGN STRATEGIES AND ANALYTICAL APPLICATIONS
Hossam Metwally Ahmed Nassef
ISBN:978-84-692-3235-4/DL:T-932-2009

[193] I. Makarovsky, G. Markel, T. Dushnitsky, A. Eisenkraft, Israel Medical Association Journal 10 (2008) 302.

[194] C.J. Waterfield, J. Delaney, M.D.J. Kerai, J.A. Timbrell, Toxicology in Vitro 11 (1997) 217.

[195] A. Tostmann, M.J. Boeree, W.H.M. Peters, H.M.J. Roelofs, R.E. Aarnoutse, A.J.A.M. van der Ven, P.N.R. Dekhuijzen, International Journal of Antimicrobial Agents 31 (2008) 577.

[196] T.W. Barrett, Journal of Raman Spectroscopy 9 (1980) 130.

[197] S.G.A. Alivisatos, F. Ungar, G. Abraham, Nature 203 (1964) 973.

[198] J. Wang, L. Angnes, T. Martinez, Bioelectrochemistry and Bioenergetics 29 (1992) 215.

[199] N. Durust, D.a. Sumengen, Y. Durust, Journal of Agricultural and Food Chemistry 45 (1997) 2085.

UNIVERSITAT ROVIRA I VIRGILI
BOTTOM-UP SURFACE ENGINEERING FOR THE CONSTRUCTION OF (BIO) SENSORING SYSTEMS: DESIGN STRATEGIES
AND ANALYTICAL APPLICATIONS
Hossam Metwally Ahmed Nassef
ISBN:978-84-692-3235-4/DL:T-932-2009

CHAPTER 2: (Art 1)

Electrocatalytic oxidation of hydrazine at *o*-aminophenol grafted modified glassy carbon electrode: Reusable hydrazine amperometric sensor

(Hossam M. Nassef, Abd-Elgawad Radi, Ciara K. O'Sullivan, Journal of Electroanalytical Chemistry 592 (2006) 139–146.)

Available online at www.sciencedirect.com
SCIENCE DIRECT
ELSEVIER
Journal of Electroanalytical Chemistry 592 (2006) 139 146
Journal of Electroanalytical Chemistry
www.elsevier.com/locate/jelechem

Electrocatalytic oxidation of hydrazine at *o*-aminophenol grafted modified glassy carbon electrode: Reusable hydrazine amperometric sensor

Hossam M. Nassef [a], Abd-Elgawad Radi [a,c,*], Ciara K. O'Sullivan [a,b,*]

[a] *Nanobiotechnology and Bioanalysis Group, Department of Chemical Engineering, Universitat Rovira i Virgili, Avinguda Paisos Catalans 26, 43007 Tarragona, Spain*
[b] *Institució Catalana de Recerca i Estudis Avançats, Passeig Lluís Companys 23, 08010 Barcelona, Spain*
[c] *Department of Chemistry, Faculty of Science, Mansoura University, 34517 Dumyat, Egypt*

Received 21 February 2006; received in revised form 4 May 2006; accepted 5 May 2006
Available online 21 June 2006

Abstract

Here, we report a simple and extremely effective method to chemically grafting of *o*-aminophenol film (*o*-AP) onto glassy carbon (GC) electrode by the electrochemical reduction of the corresponding nitrophenyl diazonium salt in acidic aqueous solution for the electrocatalytic detection of hydrazine. The covalently attached *o*-AP enabled hydrazine to be catalytically oxidized at a greatly reduced overpotential and in a wide operational pH range. A quinoneimine structure has been proposed as the electrocatalytically active species. The kinetics of the reaction between the *o*-AP mediator and hydrazine has been characterized using cyclic voltammetry, chronoamperometry, and chronocoulometry and rotating disk electrode voltammetry. The *o*-AP modified electrode as an amperometric sensor has been characterized. The catalytic currents were proportional to the concentration of hydrazine giving rise to calibration curves characterized by two linear segments. The linear segment over the concentration range of 2.0–20.0 μM could be used with analytical purposes to determination of hydrazine with a detection limit of 0.5 μM and a sensitivity of 0.016 μA/μM. The precision of amperometry was found to be 1.7% for replicate determinations ($n = 10$) of a 10 μM solution of hydrazine. The resulting modified electrode retains its initial response for at least one month if stored dry in air.

Keywords: Electrocatalytic oxidation; Hydrazine; Diazonium salt; Surface modification; Hydrazine sensor

1. Introduction

Hydrazine finds widespread usage in rocket fuels, missile systems, weapons of mass destruction and fuel cells [1]. In industrial applications, is also used as catalyst, emulsifier, corrosion inhibitor and reducing agent. It is also used as an oxygen scavenger in industry and has found wide application as an antioxidant, photographic developer and an insecticide [2]. Hydrazine has been recognized as a neurotoxin, carcinogenic mutagenic and hepatotoxic substance, which affects liver and brain glutathione [3]. It is therefore obvious that reliable and sensitive analytical methods for the determination of hydrazine are needed. Numerous methods have been reported for the determination of trace amounts of hydrazine, including titrimetric [4], coulometric [5], potentiometric [6,7], spectrophotometric [8,9] and chromatographic methods [10–12].

Electrochemical techniques offer the opportunity for portable, cheap and rapid methodologies. Much interest has centered on the use of carbon as an inexpensive substrate for electrochemical techniques. However, electrochemical oxidation of hydrazine is kinetically sluggish

* Corresponding authors. Address: Nanobiotechnology and Bioanalysis Group, Department of Chemical Engineering, Universitat Rovira i Virgili, Avinguda Paisos Catalans 26, 43007 Tarragona, Spain. Tel.: +34 977 558740; fax: +34 977 559667.
E-mail addresses: abd.radi@urv.net (A.-E. Radi), ckosulli@etse.urv.es, ciara.osullivan@urv.net (C.K. O'Sullivan).

0022-0728/$ - see front matter © 2006 Elsevier B.V. All rights reserved.
doi:10.1016/j.jelechem.2006.05.007

and a relatively high overpotential is required at carbon electrodes. As such, several approaches have been investigated in an attempt to minimize this high overpotentials problem. One such approach included the application of a pre-anodized glassy carbon electrode to enhance the amperometric detection of hydrazine [13]. Another promising approach is the use of chemically modified electrodes (CMEs) containing specifically selected redox mediators immobilized on conventional electrode materials. Mediators successfully applied include pyrogallol red [14], copper–cobalt hexacyanoferrate [15] chlorogenic acid [16] or metal phthalocyanines [17,18]. Despite the sensitivity and selectivity observed with chemically modified electrodes, the electrodes require regeneration to obtain a reproducible response [19]. As an alternative approach, electrodes such as platinum [20], gold, rhodium [21] and palladium have been reported as being electrocatalytic for the electrochemical oxidation of hydrazine, but such metals are too expensive for practical applications.

The covalent modification of aryl diazonium salts was first developed by Pinson's group [22]. One-electron reduction of aryl diazonium salt at a carbon electrode results in formation of covalent bonding of aryl groups with carbon atoms at the electrode surface. The modification procedure is simple, and the modified electrodes have long-term stability, so various types of electrochemical sensors have been developed by the electrochemical reduction of aryl diazonium salts; for example, an amperometric glucose sensor [22], flow detectors [23], voltammetric differentiation of dopamine and ascorbic acid [24], and detection of alkaline phosphatase [25,26], preparation of quinone modified electrodes with high electrocatalytic activity for reduction of oxygen [27–33].

We have demonstrated recently the electrochemistry of *o*-AP film grafted onto (GC) glassy carbon electrode and a mechanism was also proposed for the electrode surface modification [26]. Accordingly, in continuation of our study, in this work we describe the electrocatalytic behavior of grafted *o*-aminophenol toward the oxidation of hydrazine. In addition, the kinetics of the mediated electrooxidation of hydrazine at *o*-AP of modified glassy carbon electrode is investigated using cyclic voltammetry, chronoamperometry and rotating disk electrode voltammetry. The application of the modified electrode as electrocatalytic sensors in the amperometric detection of hydrazine was also illustrated. The *o*-AP grafted modified glassy carbon electrode not only exhibited strong catalytic activity toward hydrazine but also provided remarkable stable and quantitatively reproducible analytical performance.

2. Experimental

2.1. Reagents

Hydrazine (as hydraziniumhydroxide) purchased from the Sigma Aldrich (Spain) and 2-nitro-4-aminophenol (Acros) were used as received. All other chemicals used for buffer solutions preparation were of analytical-reagent grade. All solutions were prepared with Milli-Q water. Hydrazine solutions were prepared just prior to use.

2.2. Insrtumentation

All electrochemical experiments were carried out using an Autolab model PGSTAT 12 potentiostat/galvanostat controlled with the General Purpose Electrochemical System (GPES) software (Eco Chemie B.V., The Netherlands), equipped with a BASi C-3 Stand (RF-1085) three-electrode cell. This configuration contains a bare or chemically modified glassy carbon working electrode (BAS model MF-2012, 3.0-mm diameter), a platinum wire (BAS model MW-1032) counter electrode and an Ag–AgCl–3 M NaCl (BAS model MF-2078) reference electrode. All potentials were reported with respect to this reference electrode. A magnetic stirrer provided the convective transport during the amperometric experiments. A glassy carbon disk electrode with geometrical area of 0.0314 cm^2 and speed control unit (Pine Instrument Company, USA) were employed for the rotating disk electrode (RDE) measurements.

2.3. Electrode modification

Prior to electrode modification, the electrode was polished to a mirror finish with 0.3 and 0.05 μm alumina slurries (Buehler) and cleaned by sonication in Milli-Q water for 5 min. To a stirred, ice-cold solution of 2-nitro-4-aminophenol (4.624 mg, 0.03 mmol) in 4 ml HCl (2 mM) and sodium nitrite (2.07 mg, 2.0 mmol) were added. After the mixture was stirred for 1.0 h at 4 °C, a polished GC electrode was immersed in the mixture and the potential cycling was carried out between 0.6 and 0.0 V to electrochemically reduce the "in situ" generated *o*-nitrophenol diazonium salt. The electrode was then washed and transferred to 0.1 M H_2SO_4 solution and subjected to 10 potential scanning between 0.0 and −0.85 V at 50 mV s^{-1} for complete reduction of the nitro group to have a grafted film of *o*-aminophenol on the electrode surface [34,35]. The modified electrodes were sonicated in ethanol and water to remove physically adsorbed compounds. O_2-free nitrogen was used to remove oxygen from the solution and a continuous flow of nitrogen was maintained during the voltammetric measurements. All experiments were carried out at ambient temperature.

3. Results and discussion

3.1. Electrochemical characterization of the *o*-AP grafted glassy carbon electrode

Fig. 1 shows the voltammograms of *o*-AP modified glassy carbon electrode in phosphate buffer solution (0.1 M, pH 9.0) at various scan rates. The cyclic voltammetry of the modified GCE shows a well-defined stable reversible redox couple due to *o*-aminophenol/quinoneimine

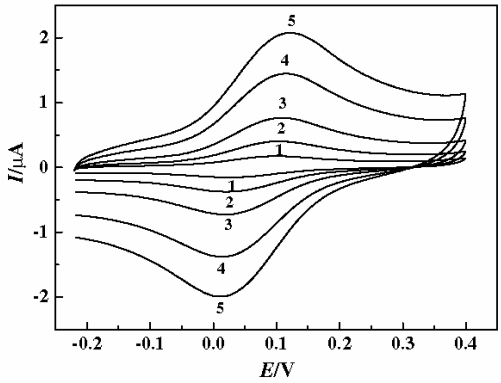

Fig. 1. Cyclic voltammograms of *o*-AP modified GC electrode in phosphate buffer (0.1 M, pH 9.0); sweep rate: 10, 25, 50, 100 and 150 mV s^{-1} (1 5).

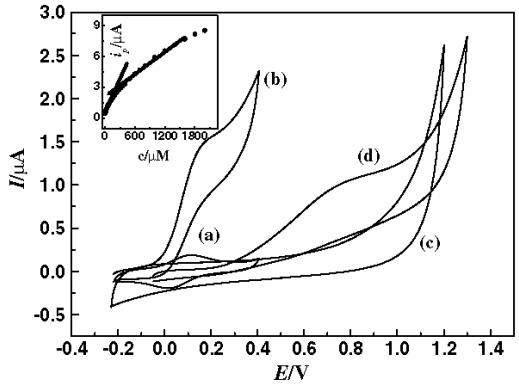

Fig. 2. Cyclic voltammograms of *o*-AP modified (a,b) and bare (c,d) GC electrodes in phosphate buffer (0.1 M, pH 9.0) at a scan rate of 20 mV s^{-1}: (a,c) in the absence and (b,d) in the presence 200 μM hydrazine. Also shown as inset is the current concentration calibration graph.

system. The ratio of anodic to cathodic peak currents obtained at various scan rates is almost constant. Furthermore, the anodic and cathodic currents increase linearly with scans rates up to 200 mV s^{-1}, as expected for a surface-confined redox process. The cyclic voltammograms of the *o*-AP modified GC electrode present a relatively large peak-to-peak separation, even at low sweep rate. The large peak-to-peak separation obtained is unexpected for compounds attached to a surface and indicates that the surface reactions proceed by different routes for redox reaction. These reactions follow electrons and protons transfer steps. The surface coverage was evaluated from the equation $\Gamma = Q/nFA$, where Q is the charge from the area under the *o*-AP oxidation peak corrected for the baseline (at a low scan rate of 10 mV s^{-1}); and other symbols have their usual meanings. In the present case, by assuming the number of electrons exchanged per reactant molecule: $n = 2$, the calculated value of Γ is 1.4×10^{-10} mol cm^{-2}. All experiments reported herein have been carried out with this surface coverage.

To test the electrocatalytic behavior of the grafted *o*-AP, cyclic voltammograms at bare glassy carbon electrode and *o*-AP modified electrodes were recorded at 20 mV s^{-1} in phosphate buffer solution (0.1 M, pH 9.0) in the absence and in the presence of hydrazine, and the results are presented in Fig. 2. Hydrazine oxidation occurs only to a small extent at highly positive overpotential at bare glassy carbon electrode. However, at the modified electrode a significant enhancement in anodic current is achieved at potentials close to the formal potential of *o*-aminophenol/quinoneimine redox couple along with a decrease of the cathodic current, which suggest that *o*-AP is an effective mediator in the electrocatalytic oxidation of hydrazine. The process corresponds to an EC catalytic mechanism, where the *o*-quinoneimine electrochemically formed reacts chemically with hydrazine diffused toward the electrode surface, while the simultaneous oxidation of regenerated *o*-aminophenol causes an increase in the anodic current. For the same reason, the cathodic current of the modified electrode is smaller in the presence of hydrazine. The process could be expressed schematically as shown in Fig. 3.

Quantitative cyclic voltammetry was performed for different concentrations of hydrazine (Fig. 2, inset); two linear relationships were obtained between anodic peak current (I_p) and concentration, from 2 to 200 and from 200 to 1600 μM, respectively. This behavior suggested that the *o*-AP modified electrode might indeed be suitable sensors for the determination of hydrazine.

Since the grafted *o*-AP state changes with pH and protonation is expected to be involved in the catalytic reaction, it is more likely that the solution pH markedly affects the catalytic activity of *o*-AP towards hydrazine oxidation. The modified electrode enabled hydrazine to be catalytically oxidized in a wide operational pH range (pH 7.0–11.0). The catalytic activity almost disappears in solutions having pH < 4.0. The maximum catalytic current is obtained in the pH 9.0. On the other hand, the variation of catalytic oxidation peak potential as a function of solution pH gives a straight line with a slope of 65 mV. This value being very close to the Nernstian slope of 59 mV, indicating an equal number of electrons and protons

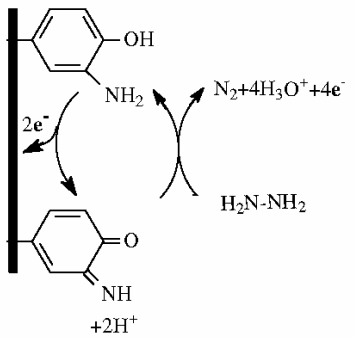

Fig. 3. Schematic diagram for electrocatalytic oxidation of hydrazine at *o*-AP modified GC electrode.

involving in the electrode process. Such an assumption is in accordance with a $4e^- - 4H^+$ proton process, corresponding to the oxidation of the hydrazine to molecular nitrogen.

The cyclic voltammograms for 100 μM hydrazine in phosphate buffer solution (0.1 M, pH 9.0) were recorded at different sweep rates. The catalytic oxidation peak potential gradually shifts towards more positive potentials with increasing the scan rate, suggesting a kinetic limitation for the reaction between the redox site of the *o*-aminophenol and hydrazine. However, the oxidation currents increase linearly with the square root of the scan rate (Fig. 4A, curve a), suggesting that at sufficient overpotential, the reaction is mass-transport controlled. Also, a plot of the scan rate-normalized current $I_p/v^{1/2}$ versus scan rate v (Fig. 4A, curve b), exhibits the characteristic shape typical of an EC_{cat} process [36]. These results show that the overall electrochemical oxidation of hydrazine at modified electrode is controlled by the cross-exchange process between hydrazine and the redox site of the *o*-aminophenol and diffusion of hydrazine.

In order to obtain some information on the rate-determining step, a Tafel-like plot was drawn using the data from the rising part of the current–voltage curve recorded at a scan rate of $5\,mV\,s^{-1}$ for 0.1 mM hydrazine

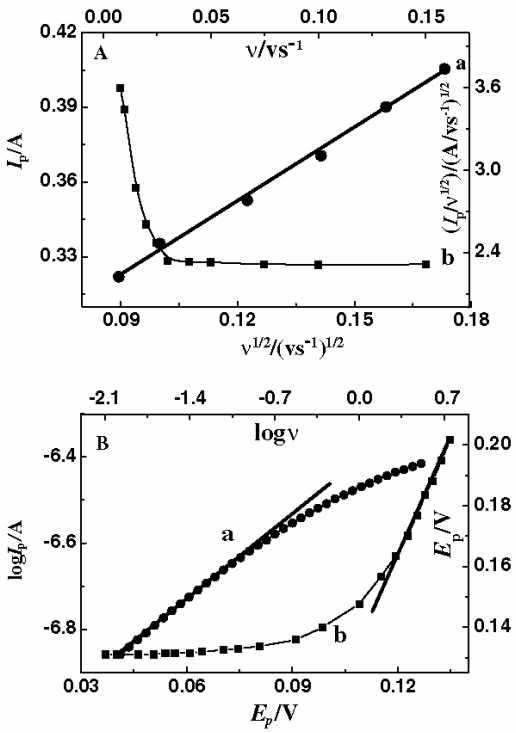

Fig. 4. (A) Curve a: plot of the electrocatalytic current I_p with the square root of scan rate and curve b: plot of the scan rate-normalized current $I_p/v^{1/2}$ with scan rate. (B) Curve a: Tafel plot derived from the rising part of voltammograms recorded at a scan rate $5\,mV\,s^{-1}$ and curve b: plot of E_p versus log v.

(Fig. 4B, curve a). The slope b for the linear part of the plot was estimated as equal to 6.279 mV decade^{-1}.

The transfer coefficient, α, evaluated from the slope was found to be 0.63 assuming that one-electron transfer process is the rate-limiting step. The Tafel slope b can be obtained by another approach using the following equation for a totally irreversible diffusion-controlled process [37]:

$$E_p = \frac{b \log v}{2} + \text{constant} \quad (1)$$

As shown in Fig. 4B (curve b), E_p is linearly dependent on log$v$ for scan rates in the range 10–5000 mV s^{-1}, with a slope of 0.09 V, so, $b = 2 \times 0.09 = 0.180$ V. Assuming the number of electrons transferred in the rate-limiting step one, a transfer coefficient of α was estimated as 0.68. The results obtained from the two different methods are in good agreement.

According to the following equation for a totally irreversible diffusive process [38]:

$$I_p = 3.01 \times 10^5 n[(1-\alpha)n_\alpha]^{1/2} A c_o D^{1/2} v^{1/2} \quad (2)$$

The number of electrons (n) involved in the oxidation of hydrazine calculated from the slope of the linear plot $I_p - v^{1/2}$ was found to be about 4.0, considering $(1-\alpha)n_\alpha = 0.63$, $D = 5.9 \times 10^{-6}\,cm^2\,s^{-1}$, $A = 0.071\,cm^2$ and $c_o = 100$ μM. Concerning the pH dependence of the hydrazine oxidation, the acid–base equilibrium

$$N_2H_5^+ + H_2O \rightleftharpoons N_2H_4 + H_3O^+$$

should be considered. Under solution conditions whereas hydrazine is mainly present in its unprotonated form (the pK_a of hydrazine is 7.9), and the protonated form which presents only to a small extent under these conditions can be neglected concerning the oxidation process, the following mechanism can be proposed for the oxidation of unprotonated hydrazine on the *o*-AP modified GC electrode.

$$N_2H_4 + H_2O \rightarrow N_2H_3 + H_3O^+ + e^- \quad \text{(rate-limiting)}$$

$$N_2H_3 + 3H_2O \rightarrow N_2 + 3H_3O^+ + 3e^- \quad \text{(fast)}$$

In other words, the rate-determining step is a one-electron transfer followed by a three-electron process to give N_2 as a final product. Hence the overall reaction of hydrazine oxidation can be formulated as follows:

$$N_2H_4 + 4H_2O \rightleftharpoons N_2 + 4H_3O^+ + 4e^-$$

The observation that the peak potential of hydrazine oxidation at *o*-AP modified electrode changes with pH (65 mV per pH unit). So that the oxidation process is controlled by thermodynamics rather than kinetics.

3.2. Potential step chronoamperometry

Chronoamperometry was used for the estimation of the diffusion coefficient of hydrazine in the solution [36]. The mean value of D was found to be $5.9 \times 10^{-6}\,cm^2\,s^{-1}$, which is in agreement with values reported in the literature [14–16].

Chronoamperometry can be used for the evaluation of the catalytic rate constant. At intermediate times ($t = 0.4$–2.4 s) the catalytic current i_{cat} is dominated by the rate of the electrocatalyzed oxidation of hydrazine. The rate constant for the chemical reaction between hydrazine and redox sites of the *o*-aminophenol grafted on glassy carbon electrode surface can be evaluated according to the method of Galus [39]

$$\frac{i_{cat}}{i_l} = \gamma^{1/2}\left(\pi^{1/2}\mathrm{erf}\left(\gamma^{1/2}\right) + \frac{\exp(-\gamma)}{\gamma^{1/2}}\right) \quad (3)$$

where i_{cat} is the catalytic current of hydrazine at the modified electrode, i_l the limited current in the absence of hydrazine and $\gamma = kc_o t$ (c_o is the bulk concentration of hydrazine) is the argument of the error function. In the cases where γ exceeds 2 the error function is almost equal to 1 and therefore the above equation can be reduced to

$$\frac{i_{cat}}{i_l} = \pi^{1/2}\gamma^{1/2} = (\pi k c_o t)^{1/2} \quad (4)$$

where t is the time elapsed (s). The above equation can be used to calculate the rate constant of the catalytic process k. Based on the slope of the i_{cat}/i_l versus $t^{1/2}$ plot (Fig. 5), k can be obtained for a given hydrazine concentration. From the values of the slopes an average value of k was found to be 2.0×10^4 M^{-1} s^{-1}.

3.3. Potential step chronocoulometry

The chronocoulometric behavior of *o*-AP modified electrode was also examined by the double potential step technique in the absence and presence of hydrazine. As seen from the corresponding chronocoulograms in Fig. 6A, the modified electrode in the absence of hydrazine, exhibits a chronocoulogram with equal charges consumed for the oxidation Q_f and reduction Q_b of *o*-aminophenol surface-confined sites. However, in the presence of hydrazine, Q_b is significantly smaller than that observed for Q_f and tended to a negligible value after addition of 800 μM hydrazine (not shown). This behavior is typical of that expected for a mediated oxidation. The number of electrons n involved in hydrazine oxidation at the modified electrode is evaluated from the slope of Q versus $t^{1/2}$ plots (Fig. 6B) using the Cottrell equation, i.e.,

$$Q = 2nFAc_o D^{1/2}\pi^{-1/2}t^{1/2} \quad (5)$$

where $c_o = 20$ μM, $A = 0.071$ cm^2 and $D = 5.9 \times 10^{-6}$ cm^2 s^{-1}. The calculated n values are close to 4.0 in agreement with value determined from cyclic voltammetry.

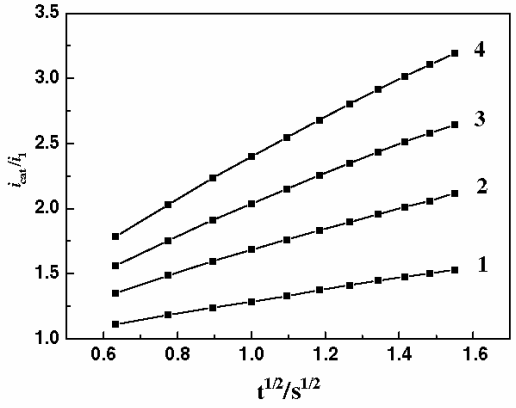

Fig. 5. Plot of i_{cat}/i_l on $t^{1/2}$ as measured from double-potential step chronoamperometry response of *o*-AP modified GC electrode in phosphate buffer solution (0.1 M, pH 9.0) under double voltage steps (from 0.0 to 0.4 to 0.0 V) for different concentrations of hydrazine: 10, 20, 30 and 40 μM (1 4).

3.4. Hydrodynamic voltammetry

RDE voltammetry were used to evaluate the kinetics of the reaction between the hydrazine and the *o*-AP catalyst grafted on GCE. The catalytic current was measured in pH 9.0 at +0.30 V as a function of rotation speed using grafted *o*-AP film rotating disk electrode (Fig. 7A). If solely the mass-transport process in the solution controls the oxidation of hydrazine at the *o*-AP modified electrode, the relationship between the limiting current and rotation rate should obey the Levich equation [40–42]

$$i_l = i_{Lev} = 0.62nFAc_o v^{1/6} D^{2/3}\omega^{1/2} \quad (6)$$

where n, A, c_o, D, v, and ω represent the number of electrons transferred, the electrode area, the bulk concentration of hydrazine in the solution, the hydrazine diffusion coefficient, the kinematic viscosity of the solution (0.01 cm^2 s^{-1}) [43], and the rotation rate, respectively.

From Eq. (6), the plot of the limiting current i_l as a function of the square root of rotation rate $\omega^{1/2}$ should be a straight line intersecting the origin. As shown in Fig. 7B, the plot deviates from linearity at high rates of rotation, indicating kinetic limitations rather than transport control. Slow electron transfer between the grafted *o*-AP and the electrode can be ruled out as rate-limiting taking into account the heterogeneous rate constant values determined earlier [26]. This would suggest that the cross-exchange process between hydrazine and the redox site of the *o*-aminophenol is the rate-determining step. However, under these conditions, there is a linear relationship between the inverse of the limiting current $1/i_l$ and the inverse of the square root of the rotation speed of the electrode $1/\omega^{1/2}$ according to the Koutecky–Levich equation, which is formulated as follows [40–42]

$$\frac{1}{i_l} = \frac{1}{i_{Lev}} + \frac{1}{i_K} = \frac{1}{0.62nFAc_o D^{2/3} v^{-1/6}\omega^{1/2}} + \frac{1}{nFAc_o k\Gamma} \quad (7)$$

where

$$i_K = nFAc_o k\Gamma \quad (8)$$

The Koutecky–Levich plot (Fig. 7C) shows the anticipated linear dependence between $1/i_l$ and $1/\omega^{1/2}$. The calculated number of electrons involved in the oxidation of hydrazine from the slope of the plot was found to be about 4.0 and

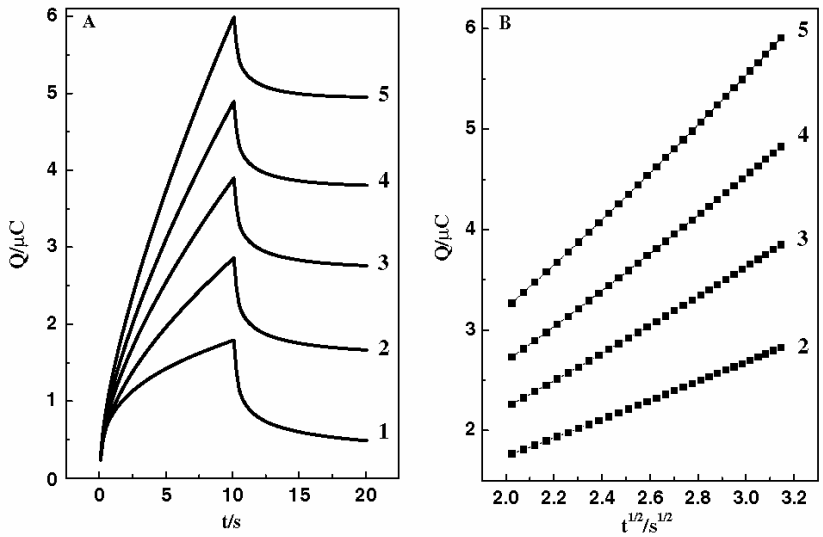

Fig. 6. (A) Double-potential step chronocoulometry response of *o*-AP modified GC electrode in phosphate buffer solution (0.1 M, pH 9.0) in absence (1) and presence of hydrazine (2–4). (B) Plot of Q versus $t^{1/2}$. All conditions as in Fig. 5.

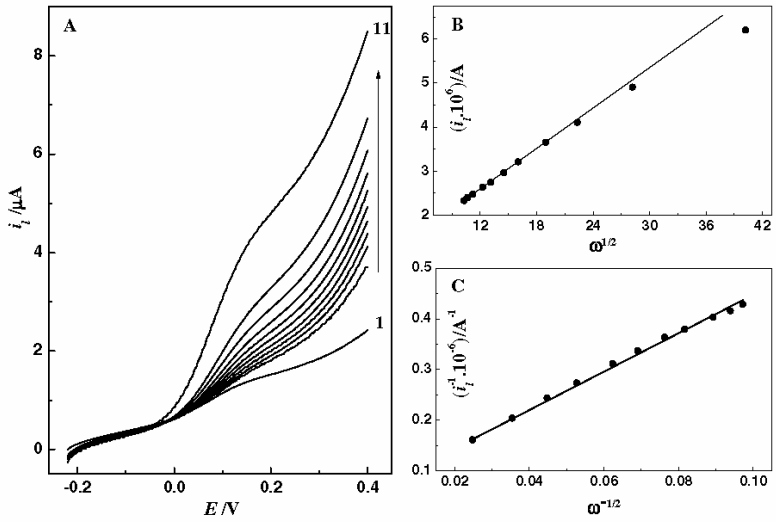

Fig. 7. (A) Hydrodynamic voltammograms of *o*-AP modified GC electrode in phosphate buffer solution (0.1 M, pH 9.0) for 200 μM hydrazine at different rotation rates: 0, 100, 125, 150, 175, 200, 250, 350, 500, 800, and 1600 rpm (1–11); sweep rate: 5 mV s^{-1}. (B) Levich and (C) Koutecky–Levich plots.

the rate constant, k calculated from the value of the intercept was $3.9 \times 10^4\ M^{-1}\ s^{-1}$, which is in the same order of magnitude as that determined from chronoamperometric measurement.

3.5. Amperometric detection of hydrazine

Modified electrode with *o*-AP was tested for the amperometric detection of hydrazine at an applied potential of +0.150 V in a magnetically stirred phosphate buffer solution (0.1 M, pH 9). As shown in Fig. 8 the amperometric sensor shows obvious increase in the oxidation current upon successive additions of hydrazine. The magnitude of the catalytic currents is dependent on the concentration of hydrazine in the solution as can be seen in Fig. 8 (inset), for low (2.0–20.0 μM) and high hydrazine concentrations (20.0–160.0 μM), respectively. A plot of the catalytic peak current versus hydrazine concentration reveals three linear segments with different slopes (Fig. 8, inset). This observation has been previously reported for the electrocatalytic oxidation of hydrazine and is ascribed to a change in the surface conditions due to the generation of molecular nitrogen bubbles [44]. At low hydrazine concentrations the formed N_2 bubbles does not affect the diffusion of new hydrazine molecules to the electrode surface. When hydrazine concentration increases, gas evolution at the sur-

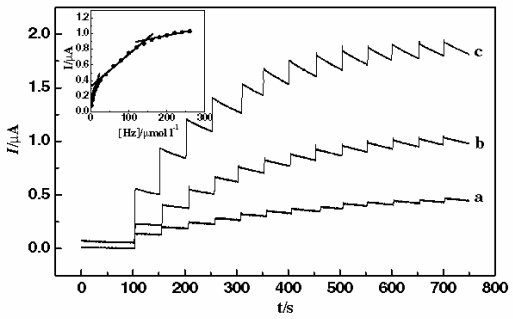

Fig. 8. Amperometric response of *o*-AP modified GC electrode to successive injections of hydrazine concentration in: (a) 0.2 μM, (b) 20 μM and (c) 100 μM steps (final cell concentration) to stirred 5 ml of phosphate buffer solution (0.1 M, pH 9.0). Inset shows current concentration calibration graph.

face affects the normal diffusion of new analyte molecules to the surface, giving rise to decay in the sensitivity of the linear response. Finally, at concentrations higher than 200 μM there is a leveling off in the electrochemical response, which could be ascribed to kinetic limitations. Accordingly, the linear response obtained at low hydrazine concentrations, in that a negligible gas effect is observed, could be used to the construction of a hydrazine sensor. For such conditions, a calibration plot obtained from data of Fig. 8a shows a linear range in the response from 2.0 to 20.0 μM, the sensitivity obtained from the slope of the calibration curve was found to be 0.016 μA/μM and the detection limit obtained (based on a signal-to-noise ratio of 3) was about 0.05 μM. The precision of amperometry was found to be 1.7% for replicate determinations of a 10.0 μM solution of hydrazine ($n = 10$).

A crucial point for analytical applications is the stability of the modified electrodes. Usually, adsorbed low molecular weight mediators are not stable enough. Indeed, the developed modified electrode is stable to solvent sonication and prolonged exposure to air and exhibits a strong and persistent electrocatalytic response. The sensitivity of the sensor showed no observable change after 1 month of storage dry in air or after successive potential cycling from 0.0 to 0.5 V for 5 h in phosphate buffer solutions, indicating that the grafted film of *o*-AP was extremely stable and that the sensor developed in this work could be the most stable sensor developed up to now for hydrazine detection. Undoubtedly, such extreme stability was anticipated based on the fact that the *o*-AP is covalently attached to the electrode surface.

4. Conclusion

We have demonstrated herein the covalent modification of a GC electrode using electrochemical reduction of "in situ" generated *o*-nitrophenol diazonium salt. This modified electrode exhibits excellent and persistent electrocatalytic behavior toward hydrazine oxidation at much lower overpotential compared with the bare GCE. The kinetic parameters such as electron transfer coefficient and catalytic reaction rate constant were also determined using various electrochemical approaches. A mechanism for the electrocatalytic oxidation of hydrazine at the modified electrode has been proposed. The use of *o*-AP modified electrode as the basis of an amperometric sensor for the detection of hydrazine has been illustrated. The simple fabrication, fast response and extreme stability in storage of the modified electrode are obvious advantages. Future investigations are envisaged for possible extension of the modification method for the determination of other high overvoltage analytes.

References

[1] S.D. Zelnick, D.R. Mattie, P.C. Stepaniak, Aviat. Space Environ. Med. 74 (2003) 1285.
[2] S. Garrod, M.E. Bollard, A.W. Nicholls, S.C. Connor, J. Connelly, J.K. Nicholson, E. Holmes, Chem. Res. Toxicol. 18 (2005) 115.
[3] E.H. Vernot, J.D. MacEwen, R.H. Bruner, C.C. Haus, E.R. Kinkead, Fund. Appl. Toxicol. 5 (1985) 1050.
[4] J.S. Budkuley, Mikrochim. Acta 108 (1992) 103.
[5] T.J. Pastor, V.J. Vajgand, N.V. Antonijeic, Mikrochim. Acta 3 (1983) 203.
[6] A.X. Lupea, D. Oprescu, Rev. Chim. 45 (1994) 433.
[7] E. Athanasiou-Malaki, M.A. Koupparis, Talanta 36 (1989) 431.
[8] A. Safavi, A.A. Ensafi, Anal. Chim. Acta 300 (1995) 307.
[9] S. Amlathe, V.K. Gupta, Microchem. J. 42 (1990) 331.
[10] R. Gilbert, R. Rioux, Anal. Chem. 56 (1984) 106.
[11] N.E. Preece, S. Forrow, S. Ghatineh, G.J. Langley, J.A. Timbrell, J. Chromatogr. 573 (1992) 227.
[12] H. Kirchherr, J. Chromatogr. Biomed. Appl. 617 (1993) 157.
[13] K. Ravichandran, R.P. Baldwin, Anal. Chem. 55 (1983) 1782.
[14] A.A. Ensafi, E. Mirmomtaz, J. Electroanal. Chem. 583 (2005) 176.
[15] A. Abbaspour, M.A. Kamyabi, J. Electroanal. Chem. 576 (2005) 73.
[16] S.M. Golabi, H.R. Zare, J. Electroanal. Chem. 465 (1999) 168.
[17] K.M. Korfhang, R. Ravichandran, R.P. Baldwin, Anal. Chem. 56 (1984) 1514.
[18] K.I. Ozoemena, T. Nyokong, Talanta 67 (2005) 162.
[19] P. Anda, J. Weber, L. Dunsch, A.B.P. Lever, Anal. Chem. 68 (1966) 960.
[20] M.D. Garcia-Azorero, M.L. Marcos, J. Gonzalez Velasco, Electrochim. Acta 39 (1994) 1909.
[21] B. Alvarez-Ruiz, R. Gomez, J.M. Orts, J.M. Feliu, J. Electrochem. Soc. 149 (2002) D35.
[22] C. Bourdillon, M. Delamar, C. Demaille, R. Hitmi, H. Moiroux, J. Pinson, J. Electroanal. Chem. 336 (1992) 113.
[23] A.J. Downard, A.D. Roddick, Electroanalysis 9 (1997) 693.
[24] A.J. Downard, A.D. Roddick, A.M. Bond, Anal. Chim. Acta 317 (1995) 303.
[25] M. Dequaire, C. Degrand, B. Limoges, J. Am. Chem. Soc. 121 (1999) 6946.
[26] A. Radi, J.M. Montornes, C.K. O' Sullivan, J. Electroanal. Chem. 587 (2006) 140.
[27] K. Tammeveski, K. Kontturi, R.J. Nichols, R.J. Potter, D.J. Schiffrin, J. Electroanal. Chem. 515 (2001) 101.
[28] A. Sarapuu, K. Vaik, D.J. Schiffrin, K. Tammeveski, J Electroanal. Chem. 541 (2003) 23.
[29] K. Vaik, D.J. Schiffrin, K. Tammeveski, Electrochem. Commun. 6 (2004) 1.
[30] K. Vaik, A. Sarapuu, K. Tammeveski, F. Mirkhalaf, D.J. Schiffrin, J. Electroanal. Chem. 564 (2004) 159.
[31] F. Mirkhalaf, K. Tammeveski, D.J. Schiffrin, Phys. Chem. Chem. Phys. 6 (2004) 1321.

UNIVERSITAT ROVIRA I VIRGILI
BOTTOM-UP SURFACE ENGINEERING FOR THE CONSTRUCTION OF (BIO) SENSORING SYSTEMS: DESIGN STRATEGIES
AND ANALYTICAL APPLICATIONS
Hossam Metwally Ahmed Nassef
ISBN:978-84-692-3235-4/DL:T-932-2009

[32] A. Sarapuu, K. Helstein, D.J. Schiffrin, K. Tammeveski, Electrochem. Solid State Lett. 8 (2005) E30.
[33] K. Vaik, U. Mäeorg, F.C. Maschione, Gilberto Maia, D.J. Schiffrin, K. Tammeveski, Electrochim. Acta 50 (2005) 5126.
[34] E. Theodoridou, J.O. Besenhard, H.P. Fritz, J. Electroanal. Chem. 124 (1981) 87.
[35] K.W. Leitner, B. Gollas, M. Winter1, J.O. Besenhard, Electrochim. Acta 50 (2004) 199.
[36] S.A. Wring, J.P. Hart, B.J. Birch, Analyst 114 (1989) 1563.
[37] J.A. Harrison, Z.A. Khan, J. Electroanal. Chem. 28 (1970) 153.
[38] S. Antoniadou, A.D. Jannakoudakis, E. Theodoridou, Synth. Met. 30 (1989) 295.
[39] Z. Galus, Fundamentals of Electrochemical Analysis, Ellis Horwood, New York, 1994.
[40] C.P. Andrieux, J.M. Dumas-Bouchiat, J.M. Saveant, J. Electroanal. Chem. 131 (1982) 1.
[41] J. Leddy, A.J. Bard, J.T. Maloy, J.M. Saveant, J. Electroanal. Chem. 187 (1985) 205.
[42] C.P. Andrieux, J.M. Saveant, in: R.W. Murray (Ed.), Molecular Design of Electrode Surfaces, Wiley-Interscience, New York, 1992.
[43] D.R. Lide (Ed.), CRC Handbook of Chemistry and Physics, 82 ed., CRC Press, Boca Raton, 2001.
[44] A.J. Bard, Anal. Chem. 35 (1963) 1602.

UNIVERSITAT ROVIRA I VIRGILI
BOTTOM-UP SURFACE ENGINEERING FOR THE CONSTRUCTION OF (BIO) SENSORING SYSTEMS: DESIGN STRATEGIES
AND ANALYTICAL APPLICATIONS
Hossam Metwally Ahmed Nassef
ISBN:978-84-692-3235-4/DL:T-932-2009

CHAPTER 3: (Art 2)

Electrocatalytic sensing of NADH on a glassy carbon electrode modified with electrografted *o*-aminophenol film

(Hossam M. Nassef, Abd-Elgawad Radi, Ciara K. O'Sullivan,

Electrochemistry Communications 8 (2006) 1719–1725.)

Available online at www.sciencedirect.com
ScienceDirect
Electrochemistry Communications 8 (2006) 1719 1725
electrochemistry communications
www.elsevier.com/locate/elecom

Electrocatalytic sensing of NADH on a glassy carbon electrode modified with electrografted *o*-aminophenol film

Hossam M. Nassef [a], Abd-Elgawad Radi [a,*], Ciara K. O'Sullivan [a,b,*]

[a] *Nanobiotechnology and Bioanalysis Group, Department of Chemical Engineering, Universitat Rovira i Virgili, Tarragona, Spain*
[b] *Institució Catalana de Recerca i Estudis Avançats, Passeig Lluís Companys 23, 08010 Barcelona, Spain*

Received 3 July 2006; received in revised form 27 July 2006; accepted 31 July 2006
Available online 6 September 2006

Abstract

A simple and sensitive method for the electrocatalytic detection of NADH on a glassy carbon electrode modified with electrografted *o*-aminophenol film (*o*-AP) is presented. The modification of a glassy carbon electrode surface with an *o*-AP film was achieved by electrochemical reduction of the corresponding, in situ generated nitrophenyl diazonium cation. The functionalized electrode shows an efficient electrocatalytic activity towards the oxidation of NADH with activation overpotential, which is ca. 350 mV lower than that at the bare electrode. The stability and the electrocatalytic activity of the modified electrode have been critically addressed. The formation of an intermediate charge transfer complex is proposed for the charge transfer reaction between NADH and adsorbed *o*-AP. The second-order rate constant for electrocatalytic oxidation of NADH, k_{obs}, and the apparent Michaelis–Menten constant K_M, at pH 7.0 were evaluated with rotating disk electrode (RDE) experiments, using the Koutecky–Levich approach. Using the *o*-AP-GC electrode, at an applied potential of +150 mV (vs. Ag–AgCl) with amperometric detection of NADH, a calibration range from 7.5×10^{-7} to 2.5×10^{-6} with a detection limit of 1.5×10^{-7} M was obtained, and excellent reproducibility was demonstrated with an RSD% = 2.1, $n = 10$ using a concentration of 1.0×10^{-6} M NADH.

Keywords: Electrocatalytic oxidation; NADH; Diazonium salt; Surface modification; NADH sensor; Nanostructured selectively catalytic surface

1. Introduction

The electrochemical detection of NADH is of great interest because the pyridine nucleotides NAD and NADP are ubiquitous in all living systems and are required for the reactions of more than 450 oxidoreductases [1]. Although the formal potential of NADH/NAD^+ couple in neutral pH at 25 °C is estimated to be −0.56 vs. SCE [2–4], significant overpotential is often required for the direct oxidation of NADH at bare electrodes [5,6]. In addition, the direct oxidation of NADH is often accompanied by electrode fouling due to the polymerization oxidation products on the electrode surface [7]. Different attempts have been made to decrease the overpotential for the oxidation of NADH, by using mediators in homogeneous solution and by modifying the electrode surface [8–59]. Among the mediators used so far are quinones [8], diimines [9], ferrocene [10], thionine [11] oxometalates [12], polymetallophthalocyanines [13], ruthenium complexes [14], pyrroloquinoline quinone [15–17], fluorenones [18], and quinonoid redox dyes such as indamines, phenazines, phenoxazines and phenothiazines [19–23]. To design an NADH sensor, the mediator has to be immobilized on the electrode surface or within the electrode material. Mediators can be immobilized by chemisorption [24], by covalent attachment directly to

* Corresponding authors. Address: Nanobiotechnology and Bioanalysis Group, Department of Chemical Engineering, Universitat Rovira i Virgili, Tarragona, Spain. Tel.: +34 977 558740/8722; fax: +34 977 559621/8205.
E-mail addresses: ciara.osullivan@urv.net, ckosulli@etse.urv.es (C.K. O'Sullivan).

1388-2481/$ - see front matter © 2006 Elsevier B.V. All rights reserved.
doi:10.1016/j.elecom.2006.07.045

the electrode surface [25,26] or by electrochemical polymerization of the mediators at the electrode surface [27–31] or, alternatively via covalently attached/physically entrapment in polymers, incorporation in carbon paste [32], grown at electrode surface [33] or deposited on the electrodes by drop coating [34]. One of the promising developments in the modification of electrode surface is the formation of self-assembled monolayers (SAMs) of electroactive or electroinactive mercaptans on gold (Au) electrode [35–39]. An alternative methodology is the modification of an electrode substrate with carbon nanotubes [40–42,55]. The majority of these chemically mediator-modified electrodes are based on solid electrodes; recently, however, the use of various materials such as composites [43–46,55], silica gel [47–49], zeolites [50,51] or conducting polymers [52–54] has become increasingly popular for electrode modification.

Diazonium salts are easily and rapidly prepared in one step from a wide range of aromatic amines many of which are commercially available. As a number of different groups can be attached to the aromatic ring of the starting amine it is possible to obtain surfaces bearing a wide variety of functions. These different characteristics make the method appealing for the modification of a variety of surfaces by many different organic functional groups [60,61] for a diverse range of applications. Biological applications include their use as a platform to link biomolecules or as a layer to control protein adsorption and to develop electrochemical sensors, for example, an amperometric glucose sensor [62], flow detectors [63], voltammetric differentiation of dopamine and ascorbic acid [64], and detection of alkaline phosphatase [65,66], modified glassy carbon electrode for alkali metal cation recognition [67] and, preparation of quinone-modified electrodes with high electrocatalytic activity for reduction of oxygen [68–74].

In this work, we report a very simple modification route for the glassy carbon electrodes with *o*-aminophenol (*o*-AP) film grafted by the electrochemical reduction of a diazonium salt generated in situ. The immobilized *o*-AP was reversibly oxidized to the *o*-quinoneimine form, which serves as two-electron acceptor mediator, efficient for the electrocatalytic oxidation of NADH [75]. A noticeable reduction of the overpotential for NADH oxidation at the *o*-AP-GC electrode was observed. The kinetic of the mediated electrooxidation of NADH at the mediator-modified glassy carbon electrode was investigated under defined mass transport conditions, using a RDE at various concentrations of NADH. The use of the developed modified electrode as an amperometric sensor, with a remarkably rapid response time is finally presented.

2. Experimental section

2.1. Chemicals and reagents

All chemicals used were of analytical grade and used as received without any further purification. β-Nicotinamide adenine dinucleotide, reduced disodium salt hydrate, (NADH ~ 98%) was obtained from Sigma. All measurements were carried out in 0.1 M phosphate buffer (pH 7.0) as supporting electrolyte. All solutions were prepared freshly prior to each experiment. Solutions were prepared with Milli-Q water (Millipore Inc., $\Omega = 18$ m Ohms).

2.2. Apparatus

All electrochemical experiments were carried out using an Autolab model PGSTAT 12 potentiostat/galvanostat controlled with the General Purpose Electrochemical System (GPES) software (Eco Chemie B.V., The Netherlands), equipped with a BASi C-3 Stand (RF-1085) three-electrode cell. This configuration contains a bare or chemically modified glassy carbon electrode (BAS model MF-2012, 3.0 mm diameter) working electrode, a platinum wire (BAS model MW-1032) counter electrode and an Ag–AgCl–3 M NaCl (BAS model MF-2078) reference electrode. All potentials were reported with respect to this reference electrode. A magnetic stirrer provided the convective transport during the amperometric experiments. A glassy carbon disk electrode with geometrical area of 0.0314 cm^2 and speed control unit (Pine Instrument Company, USA) were employed for the rotating disk electrode (RDE) measurements.

2.3. Electrode preparation and modification

The electrode was polished before use to a mirror finish with 1.0 and 0.3 μm alumina slurries (Buehler) and cleaned by sonication in Milli-Q water for 5 min. The carbon electrode surface modification with in situ generated diazonium cation was performed by potential cycling between 0.6 and 0.0 V in a mixture of ice-cold solution of 2-nitro-4-aminophenol (4.624 mg, 0.03 mmol) in 4 ml HCl (2 mM) and sodium nitrite (2.07 mg, 2.0 mmol). Following modification, the electrode was sonicated in Nanopure water for 60 s and transferred to 0.1 M H_2SO_4 and subjected to 10 potential scans between 0.0 and −0.85 V at 50 mV s^{-1}, for complete reduction of the nitro group, providing an electrografted film of *o*-aminophenol on the electrode surface. The electrode was reactivated between every voltammetric measurement by the ultrasonic cleaning in ethanol for 30 s.

3. Results and discussion

3.1. Catalytic activity for NADH electrooxidation

The electrocatalytic activity for NADH oxidation at the *o*-AP-GC electrode was investigated initially with cyclic voltammetry (CV). Fig. 1a shows the typical CV obtained for *o*-AP in phosphate buffer pH 7.0. As we have previously reported [66], a reversible signal is observed at $E^{0\prime} = 200$ mV (vs. Ag–AgCl) for *o*-aminophenol (*o*-AP)/*o*-quinoneimine (*o*-QI) redox couple. The peak currents

UNIVERSITAT ROVIRA I VIRGILI
BOTTOM-UP SURFACE ENGINEERING FOR THE CONSTRUCTION OF (BIO) SENSORING SYSTEMS: DESIGN STRATEGIES
AND ANALYTICAL APPLICATIONS
Hossam Metwally Ahmed Nassef
ISBN:978-84-692-3235-4/DL:T-932-2009

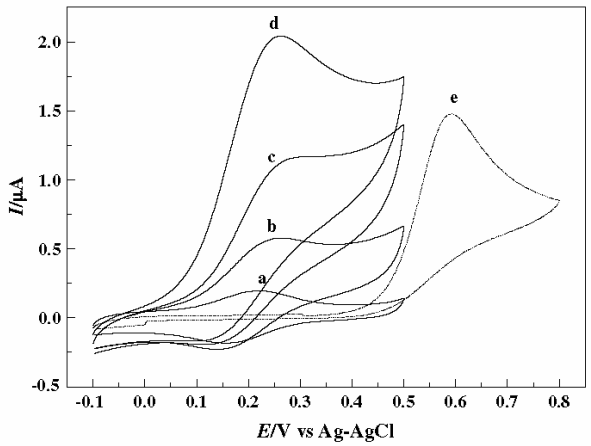

Fig. 1. Cyclic voltammograms of the *o*-AP modified GC electrode in phosphate buffer (a) in the absence and in the presence of increasing concentrations of NADH/mM: (b) 0.1, (c) 0.3 and (d) 0.5; and (e) 0.6 at bare GC in phosphate buffer (0.1 M, pH 7.0). Scan rate = 10 mV s^{-1}.

are linearly proportional to the scan rates at least up to 200 mV, consistent with that anticipated for an electrochemically reversible reaction involving a surface confined species. The reversible couple could be used for the purpose of catalysis. The surface coverage (Γ) of *o*-AP on the carbon surface averaged ca. 4.2×10^{-10} mol cm^{-2} as calculated by the graphical integration of the anodic wave, assuming a two-electron oxidation process. This value is lower than that corresponding to a close-packed monolayer of phenyl groups ($\Gamma_{CPML} = 1.5\times10^{-9}$ mol cm^{-2}) on the GC surface [61].

As can be seen in Fig. 1, in the presence of NADH the oxidation peak is significantly increased and the reduction peak decreased, eventually completely disappearing in the presence of higher concentrations of NADH, indicating an efficient electrocatalytic effect. Moreover, a 350 mV decrease in overpotential for the oxidation of NADH is observed at *o*-AP modified electrode as compared to the bare electrode (Fig. 1e). When carrying out cyclic voltammetry, an ECE mechanism was shown for the electrocatalytic reaction [59]. Initially, the mediator was electrochemically kept in its reduced state (*o*-aminophenol, $o\text{-AP}_{red}$). When a positive scan was applied, approaching and beyond the $E^{0\prime}$ value of the surface-bound mediator, the mediator was transferred into its catalytically active, oxidized form (quinoneimine, QI_{ox}), Eq. (1):

$$o\text{-AP}_{red} \overset{k_s}{\rightleftharpoons} o\text{-QI}_{ox} + 2e + 2H^+ \quad (1)$$

where k_s is the electron transfer rate between the immobilized mediator and the electrode and k_{obs} is the second-order rate constant.

Catalysis is then a result of the diffusion of NADH to the electrode surface, where it reduces QI_{ox} to form NAD^+ and $o\text{-AP}_{red}$, Eq. (2):

$$o\text{-QI}_{ox} + NADH \overset{k_{obs}}{\rightarrow} o\text{-AP}_{red} + NAD^+ \quad (2)$$

where k_{obs} is the second-order rate constant, and is in turn followed by the electrochemical reoxidation of $o\text{-AP}_{red}$ (Eq. (2)), closing the ECE cycle [59].

The cyclic voltammograms for 0.5 mM NADH in phosphate buffer solution (0.1 M, pH 7.0) were recorded at different sweep rates. The catalytic oxidation peak potential gradually shifts towards more positive potentials with increasing the scan rate, suggesting a kinetic limitation for the reaction between the *o*-aminophenol and NADH. However, the oxidation currents increase linearly with the square root of the scan rate, suggesting that at sufficient overpotential, the process is diffusion controlled. Also, a plot of the scan rate-normalized current $I_p/v^{1/2}$ vs. scan rate v, exhibits the characteristic shape typical of an EC catalytic sequence process.

Tafel analysis of voltammograms recorded at the *o*-AP electrode corresponding to the oxidation of 0.5 mM NADH (at a scan rate of 10 mV s^{-1}) plotted as potential vs. log 10 (current) produced a slope value of 144 mV per decade using Eq. (3):

$$b = \frac{2.303RT}{\alpha n_a F} \quad (3)$$

where b is the Tafel slope, α is the transfer coefficient for the potential-determining heterogeneous electron transfer and n_a is the number of electrons transferred in the rate-determining step. A value of 0.41 for αn_a was obtained suggesting that in the overall two-electron oxidation of NADH, the first electron transfer is the rate-determining step.

From the slope value of the plot of the current vs. scan rate, the total number of electrons n in the overall oxidation of NADH can be calculated using the following equation for diffusion controlled electrochemically irreversible reaction in which the first electron transfer is rate-determining [76]:

$$I_p = 3.01\times10^5 n[(1-\alpha)n_a]^{1/2} A C_{NADH} D^{1/2} v^{1/2} \quad (4)$$

where D is the diffusion coefficient (2.4×10^{-6} cm^2 s^{-1}) [77], C_{NADH} is the bulk concentration of NADH, A is the electrode area, v is the scan rate, with values for α and n_a which are deduced from Eq. (3) were 0.41 and 1, respectively. This produced an approximate value for n to be 2.15, i.e. the electrode reaction is governed by a single one-electron step in an overall two-electron process. The mechanism of the oxidation of NADH is thought to be the following [59,78]:

$$NADH \rightarrow NADH^{\cdot+} + e^- \quad (5)$$

$$NADH^{\cdot+} \rightarrow NAD^{\cdot} \quad (6)$$

$$NAD^{\cdot} \rightarrow NAD^+ + e^- \quad (7)$$

where NADH is irreversibly oxidized through loss of an electron to produce a cation radical $NADH^{\cdot+}$, Eq. (5), which then de-protonates to produce a neutral radical $NAD^{\cdot}$, Eq. (6). $NAD^{\cdot}$ is immediately oxidized to NAD^+ at the electrode surface at the positive potential involved as described by Eq. (7). $NAD^{\cdot}$ can also exchange an electron with the cation radical in the bulk solution. The net

electrochemical oxidation of NADH could be described by the following equation:

$$NADH \rightarrow NAD^+ + H^+ + 2e^- \quad (8)$$

3.2. Stability and catalytic activity of the o-AP modified electrode

It is well known that electrode fouling is a problem associated with NADH oxidation and the development of long-term catalytic stability using chemically modified electrodes is an important goal to be pursued. The electrografted *o*-AP film itself is extremely stable and retains its coverage even when subjected to extensive sonication in water or organic solvents. It is unchanged following exposure to ambient air for several weeks. Unfortunately, the catalytic activity of this electrode could not be maintained for more than a few cycles in the presence of high concentrations of NADH. For utilizing such CME electrode for analytical purposes, the partial deleterious effect of the presence of high concentrations of NADH could be circumvented by the ultrasonic cleaning in ethanol for 30 s.

Typical CVs for the *o*-AP modified electrode in the absence and presence of NADH are shown in Fig. 2. The modified electrode itself is quite stable during 500 or more repetitive cycles in pure supporting electrolyte. Curves (1–10) are 10 CV scans of this electrode in the presence of 0.3 mM NADH. A progressive decrease in the peak current can be seen as the electrode is successively cycled. Subsequently, the *o*-AP modified electrode was sonicated in ethanol for 30 s and then abundantly rinsed with water. The CVs obtained before and after this treatment are quite similar in terms of the amount of bound mediator as well as the catalytic activity towards the NADH. This suggests that those species, which cause the partial electrode fouling, are not strongly bound to the electrode surface.

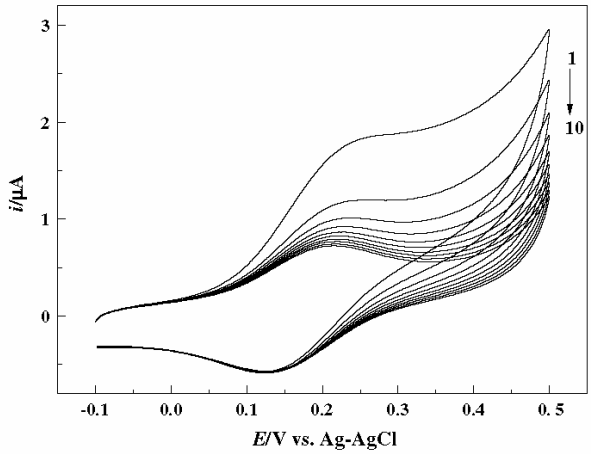

Fig. 2. Repetitive cyclic voltammograms of the *o*-AP modified electrode in phosphate buffer (0.1 M, pH 7.0) of the same electrode in the presence of 0.3 mM NADH (1 10), Scan rate = 20 mV s^{-1}.

3.3. Hydrodynamic voltammetry

In an EC catalytic mechanism, the current function is determined by the kinetic rate of electron transfer from the electrode to the redox catalyst and by the kinetic rate of charge transfer from this catalyst to the solution species. When both k_s, and k_{obs} are very large, the peak current, i_{cat}, becomes limited by the diffusional rate of the solution species to the electrode surface. The electrografted monolayer can be thought of as continuing into the electrode material rather than the abrupt change from electrons being in a metallic environment to an organic environment. The continuity of the electrode material into the monolayer has resulted in the mixing of delocalized electrons between the electrode material and the monolayer allowing more rapid electron transfer for the system [79]. The heterogeneous rate constant [66] is high enough to ensure that the kinetic of electron transfer from the electrode to the redox catalyst will not be the rate-limiting step.

For a better quantitative evaluation of the electrocatalytic behavior, kinetic measurements of NADH electro-oxidation at *o*-AP-modified graphite electrodes were performed at different NADH concentrations in pH 7 using the RDE technique. The experiments with the aim of studying the reaction mechanism and evaluating rate constants were deliberately performed with Γ-value less than the surface concentration of closed-packed monolayer of phenyl groups, where each mediator molecule at the surface of the GC electrode should be directly accessible for NADH molecules diffusing from the contacting solution. The choice of pH 7 is also rationalized since enzyme-catalysed reactions of NADH and NADPH-dependent dehydrogenases are pH dependent with pH optimal at pH 7 and above [52]. It is also the pH where both NADH and NAD^+ show highest stability when dissolved in aqueous solution [2] and most previous values of k_{obs} were reported for pH 7 [80].

Fig. 3A shows the Levich plots obtained for the *o*-AP-GC modified electrode for five different NADH concentrations, 1.00, 0.65, 0.45, 0.30 and 0.10 mM, in phosphate buffer (0.1 M, pH 7.0). The oxidation current of NADH at the modified electrode can be limited by the mass-transfer of NADH to the electrode surface and/or by the kinetics step. For the rotating disk electrode, the mass-transfer limited current (i_{lim}) depends on the angular velocity, ω, and the bulk concentration of NADH, according to the Levich equation [81]:

$$i_L = 0.62nFAD_{NADH}^{2/3}\nu^{-1/6}C_{NADH}\omega^{1/2} \quad (9)$$

For a mediated catalysed reaction, the kinetically limited current (i_k) is generally given by the following expression:

$$i_k = nFAK_{cat}\Gamma C_{NADH} \quad (10)$$

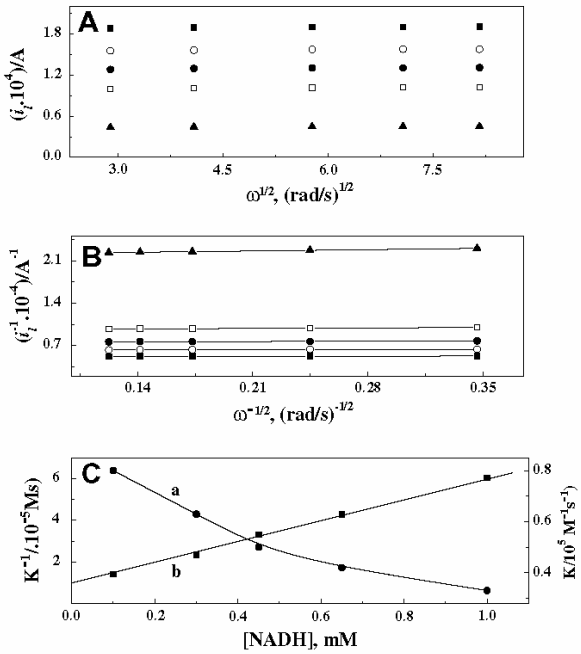

Fig. 3. (A) Levich (B) Koutecky Levich plots for the steady state electrocatalytic response for a GC-RDE modified with electrografted *o*-AP at different NADH concentrations, 1.00, 0.65, 0.45, 0.30 and 0.10 mM, in phosphate buffer (0.1 M, pH 7.0). (C) Dependence of the second-order rate constant: (a) k_{obs} and (b) $1/k_{obs}$, on NADH concentration.

A linear dependence of the catalytic current on $\omega^{1/2}$ is expected from the Levich equation [82]. The observed deviation from the Levich dependence can result from the chemical-limiting step.

The Koutecky–Levich plot of i_{lim}^{-1} vs. $\omega^{-1/2}$ shows linear dependence (Fig. 3B) and therefore, can be used for the calculation of the kinetic parameter according to the following equation:

$$\frac{1}{i_{lim}} = \frac{1}{i_L} + \frac{1}{i_k} = \frac{1}{0.62nFAD_{NADH}^{2/3}\nu^{-1/6}C_{NADH}\omega^{1/2}} + \frac{1}{nFAk_{obs}\Gamma C_{NADH}} \quad (11)$$

where n is the number of electrons transferred, A the electrode area, F the Faraday constant, D the diffusion coefficient of NADH (2.4×10^{-6} cm^2 s^{-1}) [78], ν (0.01 cm^2 s^{-1}) [83] the kinematic viscosity of the solution, Γ the surface coverage of *o*-AP. From the slope, the number of electrons (n) participating in the reaction can be evaluated and knowing that then from the intercept, the second-order rate constant for electrocatalytic oxidation of NADH, k_{obs} at infinite rotation rate can also be evaluated. For all cases, the calculated value of the number of electrons was close to 2. The values of k_{obs} were, however, strongly dependent on [NADH] for the *o*-AP-GC modified electrode as revealed in Fig. 3C. Such behavior has been previously reported for other mediators of the oxidation of NADH and supports an electrocatalytic reaction that proceeds through a mechanism similar to the Michaelis–Menten model. The catalyst and NADH form a charge transfer (CT) complex that dissociates to give rise to the reduced catalyst and NAD^+ [17].

$$QI_{ox} + NADH \underset{k_{-1}}{\overset{k_{+1}}{\rightleftharpoons}} \text{CT-complex} \xrightarrow{k_{+2}} NAD^+ + o\text{-}AP_{red} \quad (12)$$

where k_{+1} and k_{-1} represent the formation and dissociation rate constants for the complex, k_{+2} represents the catalytic rate constant for the breakdown of the complex into products and K_M, the Michaelis constant, which describes the affinity of the mediator for NADH can be defined as:

$$K_M = \frac{k_{-1} + k_{+2}}{k_{+1}} \quad (13)$$

The heterogeneous second-order reaction rate, k_{obs}, for any concentration of NADH can thus be expressed as [84]:

$$k_{obs} = \frac{k_{+2}}{K_M + [NADH]} \quad (14)$$

Inverting Eq. (14) yields an expression:

$$\frac{1}{k_{obs}} = \frac{K_M}{k_{+2}} + \frac{[NADH]}{k_{+2}} \quad (15)$$

Plots of $1/k_{obs}$ vs. [NADH] yielded linear relationship (Fig. 3C, curve b) strongly supporting the belief that a CT-complex is formed between the mediator and NADH. From the slope of these graphs values of k_{+2} can be calculated, and by extrapolation to zero NADH concentrations ([NADH] = 0), i.e., from the intercept, values of K_M can be evaluated. The k_{obs} value was found to be 1.1×10^5 M^{-1} s^{-1}, k_{+2} 18 s^{-1}, and K_M 2.2×10^{-5} mM. The k_{obs} value is relatively larger than those of other mediators with the same catalytic functionality [85,86].

3.4. Amperometric detection of NADH

Amperometric measurements at constant applied potential (+150 mV vs. Ag–AgCl–3 M NaCl), performed in a magnetic stirred solution at pH 7, clearly demonstrated that *o*-AP-GC modified electrode works well as an NADH amperometric sensor. Fig. 4 shows the current response at the immobilized *o*-AP electrode upon the addition of NADH. The current response was extremely rapid and reached a steady-state current within 1–2 s. It is seen that a non linear dependence of the anodic current on coenzyme concentration in the whole calibration range from 1.0 to 100.0 μM is obtained (inset A), as would be anticipated for a Michaelis–Menten type process. Sensitivity was calculated as the slope of the initial linear part of the calibration graph to be ~0.014 μA μM^{-1} (inset B), with the error bars representing the standard deviation of four individual measurements at each concentration. The limit of detection was estimated to be 1.5×10^{-7} M. The precision of the method

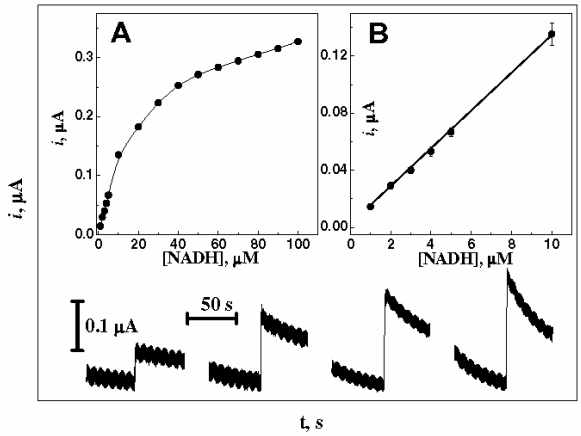

Fig. 4. Amperometric response to successive injections of NADH concentration in 5.0, 10, 20 and 30 μM steps (final cell concentration) to stirred 5 ml of phosphate buffer solution (0.1 M, pH 7.0). Insets show (A) typical calibration graph and (B) the linear range. Error bars represent the standard deviation of each concentration tested, $n = 4$.

was excellent, shown by a R.S.D. of 2.1% for 10 replicate determinations of 1.0×10^{-6} M NADH.

4. Conclusions

In this work a simple and optimal methodology to immobilize *o*-AP electrocatalyst on a glassy carbon electrode surface has been reported. The electrografted *o*-AP surface could be oxidized reversibly to *o*-quinoneimine form, which exhibits effective electrocatalytic activity towards the oxidation of NADH with an overpotential 350 mV lower than at the bare GC electrode. To overcome partial fouling of the modified electrode, brief sonication in ethanol was used to fully reactivate the electrode thus restoring catalytic activity. A mechanism for the electrocatalytic oxidation of NADH at the modified electrode explained by a complex formation of the charge transfer complex intermediate between NADH and immobilized *o*-AP has been proposed. The *o*-AP-modified electrode enables sensitive and remarkably fast amperometric measurements of NADH, suggesting it as a very interesting transducer candidate in dehydrogenase-based biosensors. Future directions for research will include the development of methods to immobilize dehydrogenase enzymes on these modified surfaces to produce integrated devices incorporating the mediator sites and the enzyme with a view to utilizing these structures as amperometric biosensors.

Acknowledgements

This work has been carried out with financial support from the Commission of the European Communities, specific RTD programme 'Smart Integrated Biodiagnostic Systems for Healthcare, SMARTHEALTH, FP6-2004-IST-NMP-2-016817'. It does not necessarily reflect its views and in no way anticipates the Commission's future policy in this area.

References

[1] H.B. White, Evolution of coenzymes and the origin of pyridine nucleotides, in: J. Everse, B. Anderson, K.-S. You (Eds.), The Pyridine Nucleotide Cofactors, Academic Press, New York, 1982, pp. 1 17.
[2] H.K. Chenault, G.M. Whitesides, Appl. Biochem. Biotechnol. 14 (1987) 147.
[3] F.L. Rodkey, J. Biol. Chem. 213 (1955) 777.
[4] F.L. Rodkey, J. Biol. Chem. 234 (1959) 188.
[5] A. Kitani, Y-H. So, L.L. Miller, J. Am. Chem. Soc. 103 (1981) 7636.
[6] J. Moiroux, P.J. Elving, Anal. Chem. 50 (1978) 1056.
[7] W.J. Blaedal, R.A. Jenkins, Anal. Chem. 47 (1975) 1337.
[8] B.W. Carlson, L.L. Miller, J. Am. Chem. Soc. 107 (1985) 479.
[9] A. Katani, Y. So, L.L. Miller, J. Am. Chem. Soc. 103 (1981) 7636.
[10] T. Matsue, M. Suda, I. Uchida, T. Kato, U. Akiba, T. Osa, J. Electroanal. Chem. 234 (1987) 163.
[11] K. Hajizadeh, H.T. Tang, H.B. Halsall, W.R. Heineman, Anal. Lett. 24 (1991) 1453.
[12] K. Essaadi, B. Keita, L. Nadjo, R. Contant, J. Electroanal. Chem. 367 (1994) 275.
[13] F. Xu, H. Li, S.J. Cross, T.F. Guarr, J. Electroanal. Chem. 368 (1994) 221.
[14] M. Somasundrum, J. Hall, J.V. Bannister, Anal. Chim. Acta 295 (1994) 47.
[15] M. Yamashita, C.A. Pessôa, L.T. Kubota, J. Colloid Interf. Sci. 263 (2003) 99.
[16] Y. Hiraku, S. Kawanishi, FEBS Lett. 393 (1996) 317.
[17] E. Katz, T. Lötzbeyer, D.D. Schlereth, W. Schuhmann, H.-L. Schmidt, J. Electroanal. Chem. 373 (1994) 189.
[18] N. Mano, A. Kuhn, J. Electroanal. Chem. 498 (2000) 58.
[19] B. Persson, L. Gorton, J. Electroanal. Chem. 292 (1990) 115.
[20] W. Schuhmann, J. Huber, H. Wohlschlaeger, B. Strehlitz, B. Gruendig, J. Biotechnol. 27 (1993) 129.
[21] L. Gorton, E. Csöregi, E. Domínguez, J. Emnéus, G. Jönsson-Pettersson, G. Marko-Varga, B. Persson, Anal. Chim. Acta 250 (1991) 203.
[22] L. Gorton, G. Bremle, E. Csoeregi, G. Joensson-Pettersson, B. Persson, Anal. Chim. Acta 249 (1991) 43.
[23] D.D. Schlereth, E. Katz, H.-L. Schmidt, Electroanalysis 7 (1995) 46.
[24] A. Torstensson, L. Gorton, J. Electroanal. Chem. 130 (1981) 199.
[25] C. Degrand, L.L. Miller, J. Am. Chem. Soc. 102 (1980) 5728.
[26] D.C.-S. Tse, T. Kuwana, Anal. Chem. 50 (1978) 1315.
[27] C.-X. Cai, K.-H. Xue, Anal. Chim. Acta 343 (1997) 69.
[28] D.-M. Zhou, J.-J. Sun, H.-Y. Chen, H.-Q. Fang, Electrochim. Acta 43 (1998) 1803.
[29] F. Pariente, F. Tobalina, M. Darder, E. Lorenzo, H.D. Abruña, Anal. Chem. 68 (1996) 3135.
[30] L. Mao, K. Yamamoto, Talanta 51 (2000) 187.
[31] Q. Wu, M. Maskus, F. Pariente, F. Tobalina, V.M. Fernandez, E. Lorenzo, H.D. Abruna, Anal. Chem. 68 (1996) 3688.
[32] E. Dominguez, H.L. Lan, Y. Okamoto, P.D. Hale, T.A. Skotheim, L. Gorton, B. Hahn-Hägerdahl, Biosens. Bioelectron. 8 (1993) 229.
[33] A. Curulli, I. Carelli, O. Trischitta, G. Palleschi, Talanta 44 (1997) 1659.
[34] K. Ravichandran, R.P. Baldwin, J. Electroanal. Chem. 126 (1981) 293.
[35] C.R. Raj, T. Ohsaka, Electrochem. Commun. 3 (2001) 633.
[36] C.R. Raj, T. Ohsaka, Bioelectrochemistry 53 (2001) 251.
[37] J.-J. Sun, J.-J. Xu, H.-Q. Fang, H.-Y. Chen, Bioelectrochem. Bioenerg. 44 (1997) 45.
[38] H.-Y. Chen, D.-M. Zhou, J.-J. Xu, H.-Q. Fang, J. Electroanal. Chem. 422 (1997) 21.
[39] M. Ohtani, S. Kuwabata, H. Yoneyama, J. Electroanal. Chem. 422 (1997) 45.

UNIVERSITAT ROVIRA I VIRGILI
BOTTOM-UP SURFACE ENGINEERING FOR THE CONSTRUCTION OF (BIO) SENSORING SYSTEMS: DESIGN STRATEGIES
AND ANALYTICAL APPLICATIONS
Hossam Metwally Ahmed Nassef
ISBN:978-84-692-3235-4/DL:T-932-2009

[40] M. Musameh, J. Wang, A. Merkoci, Y. Lin, Electrochem. Commun. 4 (2002) 743.
[41] J. Chen, J. Bao, C. Cai, T. Lu, Anal. Chim. Acta 516 (2004) 29.
[42] C.E. Banks, R.G. Compton, Analyst 130 (2005) 1232.
[43] A.R. Vijayakumar, E. Csöregi, A. Heller, L. Gorton, Anal. Chim. Acta 327 (1996) 223.
[44] J. Wang, P.V.A. Pamidi, Anal. Chem. 69 (1997) 4490.
[45] J. Wang, P.V.A. Pamidi, M. Jiang, Anal. Chim. Acta 360 (1998) 171.
[46] L. Gorton, Electroanalysis 7 (1995) 23.
[47] L.T. Kubota, Y. Gushikem, Electrochim. Acta 37 (1992) 2477.
[48] A. Walcarius, Electroanalysis 10 (1998) 1217.
[49] A. Walcarius, Electroanalysis 13 (2001) 701.
[50] H. Kotte, B. Gründig, K.D. Vorlop, B. Strehlitz, U. Stottmeister, Anal. Chem. 67 (1995) 65.
[51] A. Walcarius, Anal. Chim. Acta 384 (1999) 1.
[52] P.N. Bartlett, P.R. Birkin, E.N.K. Wallace, J. Chem. Soc., Faraday Trans. 93 (1997) 1951.
[53] P.N. Bartlett, E.N.K. Wallace, J. Electroanal. Chem. 486 (2000) 23.
[54] P.N. Bartlett, E. Simon, Phys. Chem. Chem. Phys. 2 (2000) 2599.
[55] M. Pumera, A. Merkoçi, S. Alegret, Sensor. Actuator. B 113 (2006) 617.
[56] B. Limoges, D. Marchal, F. Mavré, J.-M. Saveánt, J. Am. Chem. Soc. 128 (2006) 2084.
[57] S.-M. Chen, M.-I. Liu, Electrochim. Acta 51 (2006) 4744.
[58] K.-C. Lin, S.-M. Chen, J. Electroanal. Chem. 589 (2006) 52.
[59] I. Katakis, E. Domínguez, Microchim. Acta 126 (1997) 11.
[60] A.J. Downard, Electroanalysis 12 (2000) 1085.
[61] J. Pinson, F. Podvorica, Chem. Soc. Rev. 34 (2005) 429.
[62] C. Bourdillon, M. Delamar, C. Demaille, R. Hitmi, H. Moiroux, J. Pinson, J. Electroanal. Chem. 336 (1992) 113.
[63] A.J. Downard, A.D. Roddick, Electroanalysis 9 (1997) 693.
[64] A.J. Downard, A.D. Roddick, A.M. Bond, Anal. Chim. Acta 317 (1995) 303.
[65] M. Dequaire, C. Degrand, B. Limoges, J. Am. Chem. Soc. 121 (1999) 6946.
[66] A. Radi, J.M. Montornes, C.K. O'Sullivan, J. Electroanal. Chem. 587 (2006) 140.
[67] K. Morita, A. Yamaguchi, N. Teramae, J. Electroanal. Chem. 563 (2004) 249.
[68] K. Tammeveski, K. Kontturi, R.J. Nichols, R.J. Potter, D.J. Schiffrin, J. Electroanal. Chem. 515 (2001) 101.
[69] A. Sarapuu, K. Vaik, D.J. Schiffrin, K. Tammeveski, J. Electroanal. Chem. 541 (2003) 23.
[70] K. Vaik, D.J. Schiffrin, K. Tammeveski, Electrochem. Commun. 6 (2004) 1.
[71] K. Vaik, A. Sarapuu, K. Tammeveski, F. Mirkhalaf, D.J. Schiffrin, J. Electroanal. Chem. 564 (2004) 159.
[72] F. Mirkhalaf, K. Tammeveski, D.J. Schiffrin, Phys. Chem. Chem. Phys. 6 (2004) 1321.
[73] A. Sarapuu, K. Helstein, D.J. Schiffrin, K. Tammeveski, Electrochem. Solid-State Lett. 8 (2005) E30.
[74] K. Vaik, U. Mäeorg, F.C. Maschione, G. Maia, D.J. Schiffrin, K. Tammeveski, Electrochim. Acta 50 (2005) 5126.
[75] L. Gorton, E. Domínguez, Rev. Mol. Biotechnol. 82 (2002) 371.
[76] S. Antoniadou, A.D. Jannakoudakis, E. Theodoridou, Synth. Met. 30 (1989) 295.
[77] F. Pariente, E. Lorenzo, H.D. Abruña, Anal. Chem. 66 (1994) 4337.
[78] J. Moiroux, P.J. Elving, J. Am. Chem. Soc. 102 (1980) 6533.
[79] S. Ranganathan, I. Steidel, F. Anariba, R.L. McCreery, Nanoletters 1 (2001) 491.
[80] L. Gorton, E. Dominguez, Electrochemistry of $NAD(P)^+$/NAD(P)H, in: A.J. Bard, M. Stratmann (Eds.), Encyclopedia of Electrochemistry, vol. 9, Wiley-VCH, New York, 2002, p. 67.
[81] A.J. Bard, L.R. Faulkner, Electrochemical Methods: Fundamental and Applications, second ed., Wiley & Sons, New York, 2001.
[82] R.W. Murray, in: R.W. Murray (Ed.), Introduction to the Chemistry of Molecularly Designed Electrode Surfaces, Techniques of Chemistry Series, vol. XXII, John Wiley and Sons, New York, 1992, pp. 1 48.
[83] D.R. Lide (Ed.), CRC Handbook of Chemistry and Physics, 82nd ed., CRC Press, Boca Raton, 2001.
[84] L. Gorton, J. Chem. Soc., Faraday Trans. 182 (1986) 1245.
[85] N. de los Santos Álvarez, P. Muñiz Ortea, A. Montes Pañeda, M.J. Lobo Castañón, A.J. Miranda Ordieres, P. Tuñón Blanco, J. Electroanal. Chem. 502 (2001) 109.
[86] N. de los Santos Álvarez, M.J. Lobo-Castañón, A.J. Miranda-Ordieres, P. Tuñón-Blanco, H.D. Abruña, Anal. Chem. 77 (2005) 2624.

UNIVERSITAT ROVIRA I VIRGILI
BOTTOM-UP SURFACE ENGINEERING FOR THE CONSTRUCTION OF (BIO) SENSORING SYSTEMS: DESIGN STRATEGIES
AND ANALYTICAL APPLICATIONS
Hossam Metwally Ahmed Nassef
ISBN:978-84-692-3235-4/DL:T-932-2009

CHAPTER 4: (Art 3)

Simultaneous detection of ascorbate and uric acid using a selectively catalytic surface

(Hossam M. Nassef, Abd-Elgawad Radi, Ciara O'Sullivan,

Analytica Chimica Acta 583 (2007) 182–189.)

Available online at www.sciencedirect.com
ScienceDirect
Analytica Chimica Acta 583 (2007) 182–189
ANALYTICA CHIMICA ACTA
www.elsevier.com/locate/aca

Simultaneous detection of ascorbate and uric acid using a selectively catalytic surface

Hossam M. Nassef[a], Abd-Elgawad Radi[a,*], Ciara O'Sullivan[a,b,*]

[a] Department of Chemical Engineering, University of Rovira I Virgili, Av.Paisos Catalan, 26, 43007 Tarragona, Spain
[b] Institució Catalana de Recerca i Estudis Avançats, Passeig Lluís Companys 23, 08010 Barcelona, Spain

Received 3 July 2006; received in revised form 28 September 2006; accepted 4 October 2006
Available online 7 October 2006

Abstract

The direct and selective detection of ascorbate at conventional carbon or metal electrodes is difficult due to its large overpotential and fouling by oxidation products. Electrode modification by electrochemical reduction of diazonium salts of different aryl derivatives is useful for catalytic, analytical and biotechnological applications. A monolayer of *o*-aminophenol (*o*-AP) was grafted on a glassy carbon electrode (GCE) via the electrochemical reduction of its in situ prepared diazonium salts in aqueous solution. The *o*-aminophenol confined surface was characterized by cyclic voltammetry. The grafted film demonstrated an excellent electrocatalytic activity towards the oxidation of ascorbate in phosphate buffer of pH 7.0 shifting the overpotential from +462 to +263 mV versus Ag/AgCl. Cyclic voltammetry and d.c. amperometric measurements were carried out for the quantitative determination of ascorbate and uric acid. The catalytic oxidation peak current was linearly dependent on the ascorbate concentration and a linear calibration curve was obtained using d.c. amperometry in the range of 2–20 μM of ascorbate with a correlation coefficient 0.9998, and limit of detection 0.3 μM. The effect of H_2O_2 on the electrocatalytic oxidation of ascorbate at *o*-aminophenol modified GC electrode has been studied, the half-life time and rate constant was estimated as 270 s, and 2.57×10^{-3} s^{-1}, respectively. The catalytically selective electrode was applied to the simultaneous detection of ascorbate and uric acid, and used for their determination in real urine samples. This *o*-AP/GCE showed high stability with time, and was used as a simple and precise amperometric sensor for the selective determination of ascorbate.

Keywords: Ascorbate; Uric acid; Diazonium salt; Modified electrode; Electrocatalysis

1. Introduction

Ascorbate (Vitamin C) is a water-soluble substance present in a wide number of foods, such as fruits and vegetables. [1]. Due to the presence of ascorbate in the mammalian brain, it has an important role in bioelectrochemistry, neurochemistry and clinical diagnostics applications. It is also necessary for the formation of collagen, and has been used for the prevention and treatment of common cold, metal illness, scurvy and cancer [2–4]. The content of ascorbate in biological fluids can be used to assess the amount of oxidation stress in human metabolism, and excessive oxidative stress has been linked to cancer, diabetes mellitus and hepatic disease [5]. Therefore, the determination of ascorbate contents is particularly important in the pharmaceutical and food industry at different concentration levels.

The direct oxidation of ascorbate at conventional (carbon or metal) electrodes is irreversible [6,7], and it is thus difficult to determine ascorbate directly due to its large overpotential and fouling by oxidation products [8–11]. So, the development of voltammetric methods for the selective determination of ascorbate has been a major target of electroanalytical research. Therefore, numerous attempts have been made to reduce the large overpotentials by using various active mediators immobilized at the electrode surface for the catalysis of electrooxidation of ascorbate [11–20].

Uric acid (UA) and other oxypurines are the principal final products of purine metabolism in the human body [21]. Abnormal levels of UA are symptoms of several diseases, including gout, hyperuricemia, and Lesch–Nyan disease [22]. Thus the determination of the concentration of UA in human blood or

* Corresponding authors at: Department of Chemical Engineering, University of Rovira I Virgili, Av.Paisos Catalan, 26, 43007 Tarragona, Spain.
Fax: +34 977 559621.
E-mail address: ciara.osullivan@urv.net (C. O'Sullivan).

0003-2670/$ – see front matter © 2006 Elsevier B.V. All rights reserved.
doi:10.1016/j.aca.2006.10.004

UNIVERSITAT ROVIRA I VIRGILI
BOTTOM-UP SURFACE ENGINEERING FOR THE CONSTRUCTION OF (BIO) SENSORING SYSTEMS: DESIGN STRATEGIES
AND ANALYTICAL APPLICATIONS
Hossam Metwally Ahmed Nassef
ISBN:978-84-692-3235-4/DL:T-932-2009

urine is a powerful indicator in diagnosing diseases caused by any alteration in purine metabolism which leads to raising or lowering the UA level and in controlling it during the use of chemotherapeutic drugs [23–25]. UA and ascorbate commonly coexist in biological fluids of humans, mainly in serum, blood and urine. The major obstacle in monitoring UA is interferences from other electroactive constituents, such as ascorbate, which oxidizes close to the potential of UA on various types of electrodes [26–28]. Therefore electrochemists still devote their studies mainly to develop a simple and rapid method for the simultaneous determination of UA and ascorbate [29–31].

The covalent modification of carbon is of the utmost importance for carbonaceous materials used in electrocatalysis [32–35]. The modification of conductive surfaces through the electrografting of organic groups [36,37] via electrochemical reduction of aryl diazonium was first reported by Pinson, et al., which results in a strongly attached layer [38], forming a monolayer or sub-monolayer [39–41]. Electrodes modified via the electrochemical reduction of diazonium salts of different aryl derivatives have been used for many analytical applications [42–56].

In this work we describe the electrocatalytic behavior of a grafted *o*-AP film towards the oxidation of ascorbate. In addition, the kinetics of the mediated electrooxidation of ascorbate at *o*-AP of modified glassy carbon electrode is investigated using cyclic voltammetry, chronoamperometry and chronocoulometry. The application of the modified electrode as electrocatalytic sensors in the amperometric detection of ascorbate, and for the selective detection of UA in presence of ascorbate were investigated. The *o*-AP/GCE not only exhibited strong catalytic activity toward ascorbate but also provided remarkable stable and a quantitatively reproducible analytical performance.

2. Experimental section

2.1. Reagents and chemicals

L-Ascorbic acid (99%) and uric acid, purchased from the Sigma–Aldrich (Spain) and 2-nitro-4-aminophenol (Acros) were used as received. All other chemicals were of analytical-reagent grade. All solutions were prepared with Milli-Q water. L-Ascorbic acid solutions were prepared immediately prior to use. Fresh urine samples were collected from adult persons.

2.2. Instrumentation

All electrochemical experiments were carried out using an Autolab model PGSTAT 12 potentiostat/galvanostat controlled with the general purpose electrochemical system (GPES) software (Eco Chemie B.V., The Netherlands), equipped with a BASi C-3 Stand (RF-1085) three-electrode cell. This configuration contains a bare or chemically modified glassy carbon electrode (BAS model MF-2012, 3.0 mm diameter) as working electrode, a platinum wire (BAS model MW-1032) counter electrode and an Ag-AgCl-3M NaCl (BAS model MF-2078) reference electrode. All potentials were reported with respect to this reference electrode. A magnetic stirrer provided the convective transport during the amperometric experiments.

2.3. Electrode modification

Prior to electrode modification, the electrode was polished to a mirror finish with 0.3 μm alumina slurries (Buehler) and cleaned by sonication in ethanol for 5 min. To a stirred, ice-cold solution of 2-nitro-4-aminophenol (4.624 mg, 0.03 mmol) in 4 mL HCl (2 mM) and sodium nitrite (2.07 mg, 2.0 mmol) was added. After the mixture was stirred for 1.0 h at 4 °C, a polished

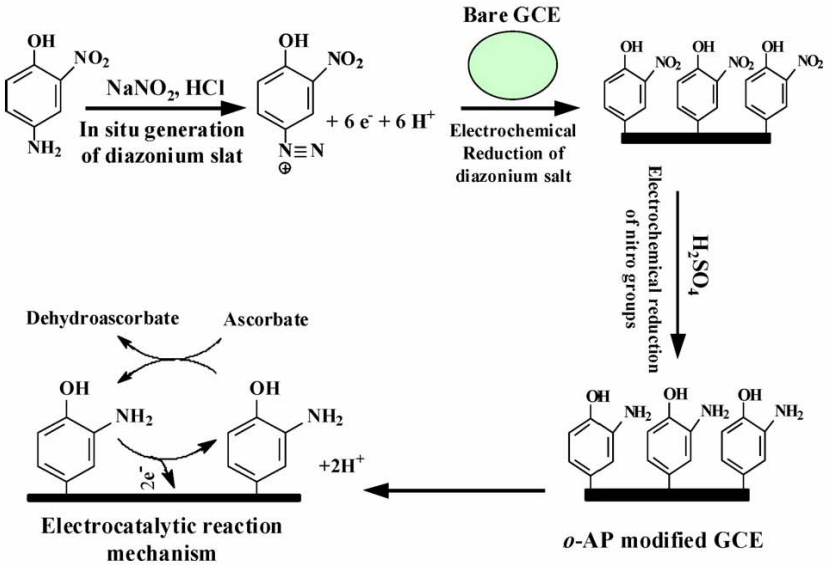

Scheme 1.

GC electrode was immersed in the mixture and the potential cycling was carried out between 0.6 and 0.0 V to electrochemically reduce the "in situ" generated *o*-nitrophenol diazonium salt (Scheme 1). The electrode was then washed and transferred to 0.1 M H_2SO_4 solution and subjected to 10 potential scans between 0.0 and −0.85 V at 50 mV s^{-1} for complete reduction of the nitro group to have a modified film of *o*-aminophenol on the electrode surface (Scheme 1) [57,58]. The modified electrodes were sonicated in ethanol and water to remove physically adsorbed compounds. O_2-free nitrogen was used to remove oxygen from the solution and a continuous flow of nitrogen was maintained during the voltammetric measurements. All experiments were carried out at ambient temperature.

3. Results and discussion

3.1. Electrochemistry of ascorbate at o-AP modified GCE

The cyclic voltammograms of the *o*-AP-modified GC electrode (Fig. 1) present a relatively large peak-to-peak separation, even at low sweep rate. The large peak-to-peak separation obtained is unexpected for compounds attached to a surface and the possible reasons are the slow kinetics for the charge transfer, including the slow direct electron transfer between the GC electrode and the *o*-AP film and the transport of the protons between the modified layer and the bulk solution, or the slow electrostatic charge compensation during the redox process. The oxidation mechanism may likely correspond to the formation of cation radical at the nitrogen or the oxygen at the amino or the hydroxyl group, respectively, the probable oxidation centres in the *o*-aminophenol molecule. This complies with the oxidation route proposed for the anodic oxidation of aromatic amine or phenolic compounds [59].

The surface coverage was evaluated from the equation $\Gamma = Q/nFA$, where Q is the charge from the area under the *o*-AP oxidation peak corrected for the baseline; (at a low scan rate of 5 mV s^{-1}) and other symbols have their usual meanings. In the present case, by assuming the number of electrons exchanged per reactant molecule: $n = 2$ (n is obtained from Eq. (2), and by chronocoulometry as below), the calculated value of Γ is 4.2×10^{-10} mol cm^{-2}. This is consistent with the coverage found for the formation of close pack monolayer of grafted 4-nitophenyl groups on glassy carbon electrode [38]. The *o*-aminophenol molecules should be align axially on the glassy carbon electrode and lateral to each other as shown in Scheme 1. All experiments reported herein have been carried out with the above mentioned surface coverage.

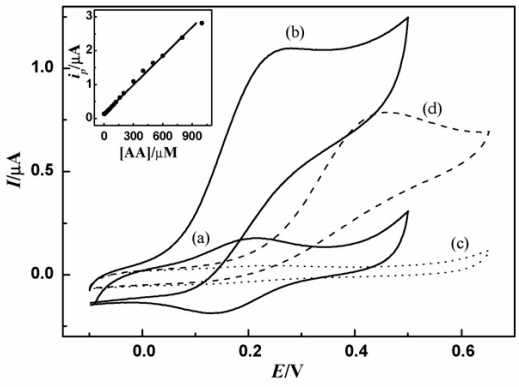

Fig. 1. Cyclic voltammograms of *o*-AP modified (a and b) and bare (c and d) GC electrodes in phosphate buffer (0.1 M, pH 7.0) at a scan rate of 5 mV s^{-1}: (a and c) in the absence and (b and d) in the presence 200 μM ascorbate. Also shown as inset the current–concentration calibration graph.

The electrocatalytic behavior of the grafted *o*-AP was investigated by cyclic voltammetry at bare and *o*-AP modified glassy carbon electrode at 5 mV s^{-1} in phosphate buffer solution (0.1 M, pH 7.0) in the absence and presence of ascorbate (Fig. 1). At a bare glassy carbon electrode the oxidation of ascorbate occurs at a highly positive potential of +462 mV versus Ag/AgCl, while at the *o*-AP modified electrode a significant enhancement in the anodic current was observed at potentials close to the formal potential of *o*-aminophenol/quinoneimine redox couple with a decrease of ≅200 mV in overpotential. A concomitant disappearance of the cathodic current was achieved, which indicates that *o*-AP is an effective mediator in the electrocatalytic oxidation of ascorbate. The effect of different concentrations (2–1000 μM) of ascorbate was studied using cyclic voltammetry, and a linear relationship was obtained between anodic peak current (I_p) and ascorbate concentration (Fig. 1 inset), suggesting that the grafted *o*-AP is suitable for the sensing and quantitative determination of ascorbate.

Fig. 2A shows the cyclic voltammograms of 200 μM ascorbate at different sweep rates in phosphate buffer solution (0.1 M, pH 7.0). The catalytic oxidation peak potential gradually shifts towards more positive potentials with increasing scan rate, suggesting a kinetic limitation for the reaction between the redox site of the *o*-aminophenol and ascorbate. However, a linear relationship between the catalytic peak current and the square root of the scan rate (Fig. 2B, curve a) suggested that at sufficient overpotential the reaction is diffusion controlled process. Moreover, the plot of the sweep rate-normalized current ($I_p/\nu^{1/2}$) versus sweep rate (Fig. 2B, curve b) exhibits the characteristic shape typical of an EC_{cat} process [60], in which the electrochemically formed *o*-quinoneimine chemically reacts with the ascorbate diffused toward the electrode surface, while the simultaneous oxidation of the regenerated *o*-aminophenol causes an increase in the anodic current. For the same reason, in the presence of ascorbate the cathodic current of the modified electrode is smaller than in phosphate buffer. These results show that the overall electrochemical oxidation of ascorbate at the modified electrode is controlled by the cross-exchange process between ascorbate and the redox site of the *o*-aminophenol and diffusion of ascorbate.

The number of electrons in the overall reaction can be calculated from the slope of the I_p versus $\nu^{1/2}$ plot (Fig. 2A, curve a), according to the following equation for a totally irreversible diffusion-controlled process [61]:

$$I_P = 3.01 \times 10^5 n[(1-\alpha_a)n_\alpha]^{1/2} A c_o D^{1/2} \nu^{1/2} \quad (1)$$

The number of electrons (n) involved in the oxidation of ascorbate calculated from the slope of the linear plot $I_p - \nu^{1/2}$

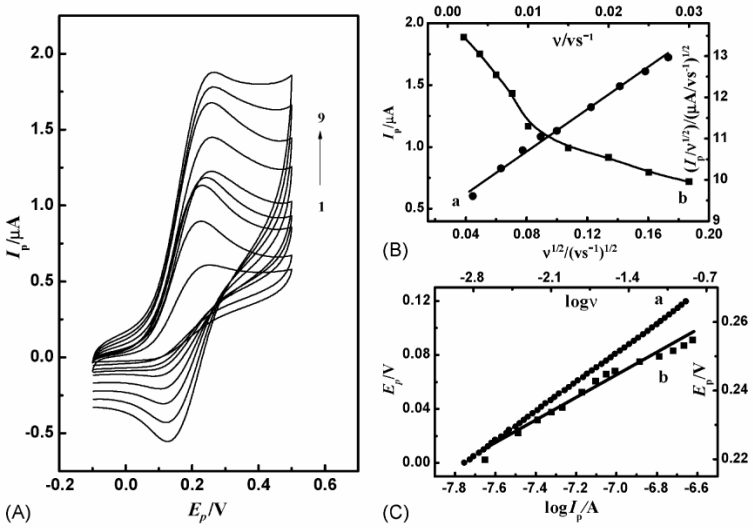

Fig. 2. (A) Cyclic voltammograms of *o*-AP modified GC electrodes in presence of 200 μM ascorbate, in phosphate buffer (0.1 M, pH 7.0) at different scan rate of 2, 4, 6, 8, 10, 12, 15, 20, 25, and 30 mV s^{-1} (1–9), respectively. (B) Curve a: plot of the electrocatalytic current I_p with the square root of scan rate and curve b: plot of the scan rate-normalized current $I_p/v^{1/2}$ with scan rate. (C) Curve a: Tafel plot derived from the rising part of voltammograms recorded at a scan rate 2 mV s^{-1} and curve b: plot of E_p vs. log v.

was found to be about 1.8 (≅2.0), considering $(1-\alpha)n_\alpha = 0.46$, $D = 2.7 \times 10^{-6}$ cm^2 s^{-1}, $A = 0.071$ cm^2 and $c_o = 200$ μM.

A theoretical model was developed by Andrieux and Savéant [62] for deriving a relation between the peak current and the concentration of the substrate for the case of a slow rate, v, and a large catalytic rate constant, k_h:

$$I_{cat} = 0.496nFAc_s v^{1/2}(nFDRT)^{1/2} \quad (2)$$

where D and c_s are the diffusion coefficient (cm^2 s^{-1}) and the bulk concentration (mol cm^{-3}) of ascorbate, respectively. Low values of k_h result in values lower than 0.496 for the constant. Based on computations, a working curve showing the relationship between numerical values of the constant, $I_{cat}/nFAc_s v^{1/2}(nFDRT)^{1/2}$, and log $[k_h\Gamma/(DnFvRT)^{1/2}]$ (Fig. 1 of [62]) is given. The value of k_h can thus be calculated from such a working curve. For low scan rates (2–30 mV s^{-1}), the value of the constant $(I_{cat}/nFAc_s v^{1/2}(nFDRT)^{1/2})$ is found to be 0.324 for modified *o*-AP, with a coverage of $\Gamma = 4.2 \times 10^{-10}$ mol cm^{-2}, a geometric area (A) of 0.071 cm^2 and considering $D = 2.7 \times 10^{-6}$ cm^2 s^{-1} (D is obtained by chronoamperometry as below), in the presence of 200 μM ascorbate. The estimated value of k_h was found to be 3.79×10^3 M^{-1} s^{-1} for 10 mV s^{-1} scan rate [63], which represent the catalytic rate constant of the charge transfer interaction between the grafted *o*-AP and the electrode surface, explain well the sharp feature of the catalytic peak observed for catalytic oxidation of ascorbate at the modified *o*-AP GCE.

In order to obtain some information on the rate-determining step, the Tafel plot is a useful tool for evaluating kinetic parameters. Therefore, a Tafel-like plot was drawn using the data derived from the rising part of the current–voltage curve recorded at a scan rate of 2 mV s^{-1} for 200 μM ascorbate (Fig. 2C, curve a). The slope b for the linear part of the plot was equal to 0.108 V decade^{-1}, the charge transfer coefficient (α), estimated from the slope was found to be 0.54, indicating that a one electron process was involved in the rate determining step. The exchange current density (j_o) can also be estimated from the intercept of the Tafel plot [64], it was found to be 0.2347 μA cm^{-2}. The Tafel slope b can be obtained by another method [65], as shown in Fig. 2C (curve b), E_p is linearly dependent on log v for scan rates in the range 2–30 mV s^{-1}, assuming the number of electrons transferred in the rate-limiting step one, the charge transfer coefficient (α) was estimated 0.54, and the results obtained from the two different methods are in good agreement. These data suggests that, during the catalytic oxidation of ascorbate at the *o*-AP modified GCE, the total number of transferred electrons is two, since only one electron is included in the rate determining step (slow step), and remained electron is contributed in the fast step.

3.2. Chronoamperometric and chronocoulometric measurements

Double step potential chronoamperometry and chronocoulometry are useful tools for investigation of the electrochemical processes at chemically modified electrodes [64,66–68]. The electrocatalytic oxidation of ascorbate at the glassy carbon electrode modified with *o*-AP was studied also using double step potential chronoamperometry. Fig. 3A shows the current–time curves of the modified *o*-AP GCE obtained by setting the working electrode potential at 400 mV (at first potential step) and 0.0 mV (at second potential step) versus Ag|AgCl for various concentration of ascorbate in aqueous buffered solution (pH7.0). As can be seen, there is no net cathodic current corresponding to the reduction of the mediator in the presence of ascorbate, but the forward and backward potential step chronoamperometry of the modified electrode in the blank buffered solution show very sym-

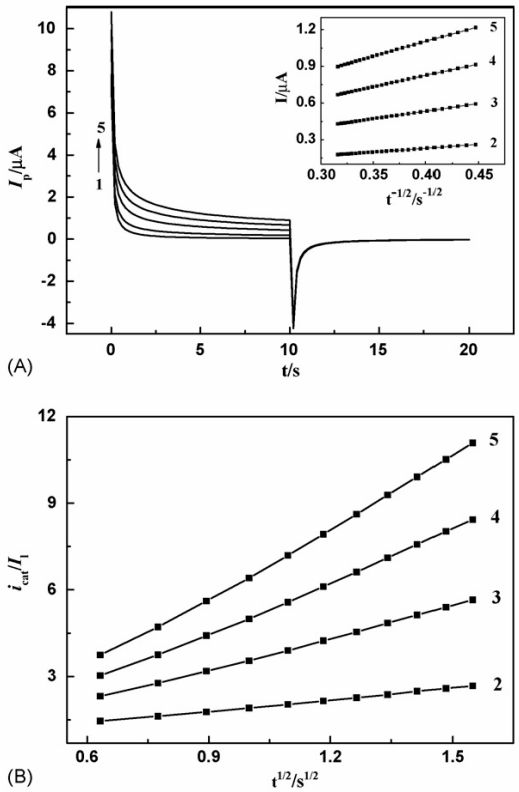

Fig. 3. (A) Double-potential step chronoamperometry response of *o*-AP modified GC electrode in phosphate buffer solution (0.1 M, pH 7.0) under double voltage steps (from 0.0 to 0.4 to 0.0 V) for different concentration of ascorbate: 0, 20, 60, 100 and 140 μM (1–5). Inset: plots of I_P vs. $t^{-1/2}$ (2–5) and (B) plot of I_{cat}/I_l on $t^{1/2}$.

metrical chronoamperograms with an equal charge consumed for the oxidation and reduction of incorporated *o*-aminophenol and quinoneimine on the GCE surface (Fig. 3A). However, in the presence of ascorbate, the current value associated with forward chronoamperometry is greater than that observed for the backward chronoamperometry, and the increase in concentration of ascorbate was accompanied by an increase in anodic currents obtained for a potential step of 400 mV, and in addition, the level of the Cottrell current increased. At higher concentrations, there appears to be a levelling off of the response, presumably due to kinetic limitations. The diffusion coefficient of ascorbate for the modified electrode can be determined using the Cottrell equation [64]:

$$I_p = nFAD^{1/2}\frac{C}{\pi^{1/2}}t^{1/2} \quad (3)$$

where D and C are the diffusion coefficient ($cm^2\,s^{-1}$) and the bulk concentration ($mol\,cm^{-3}$), respectively. Using the Cottrell equation, a plot of I_p versus $t^{-1/2}$ shows a linear relation with a slope of 7.64 μA $decade^{-1}$, and the estimated diffusion coefficient was 2.7×10^{-6} $cm^2\,s^{-1}$ for ascorbate. This result is similar to that reported in the literature [67].

The rate constant for the chemical reaction between ascorbate and redox sites in the grafted *o*-AP film on the surface of GCE, k_h can be evaluated by chronoamperometry according to the method described in [68]:

$$\frac{i_{cat}}{I_l} = \gamma^{1/2}\left(\pi^{1/2}\mathrm{erf}(\gamma^{1/2}) + \frac{\exp(-\gamma)}{\gamma^{1/2}}\right) \quad (4)$$

where i_{cat} is the catalytic current of *o*-AP in the presence of ascorbate and I_l is the limited current in the absence of ascorbate, and $\gamma = k_h C_o t$ (C_o is the bulk concentration of ascorbate, $mol\,cm^{-3}$) is the argument of the error function. In the cases where γ exceeds 2, the error function is almost equal to 1 and the above equationcan be reduced to:

$$\frac{i_{cat}}{I_l} = \pi^{1/2}\gamma^{1/2} = (\pi k c_o t)^{1/2} \quad (5)$$

where k_h and t are the catalytic rate constant ($l\,mol^{-1}\,s^{-1}$) and time elapsed (s), respectively. Employing Equation (5), the rate constant of the catalytic process, k_h, has been calculated using the slope of the plot I_{cat}/I_l versus $t^{1/2}$ (Fig. 3B), the estimated value was of 3.13×10^3 $M^{-1}\,s^{-1}$. This value of k_h is in agreement and in the same order of magnitude with that estimated from Andrieux and Savéant equation [62]. Moreover, the heterogeneous rate constant of catalytic reaction between ascorbate and *o*-AP was also calculated as $K'_h = 1.32 \times 10^{-3}$ $cm\,s^{-1}$.

The electrocatalytic behavior of *o*-AP modified electrode was also studied by the double potential-step chronocoulometry technique in the absence and presence of various concentrations of ascorbate. In the absence of ascorbate, the *o*-AP modified GC electrode in a blank buffered solution, exhibits a symmetrical forward and backward chronocoulogram (Fig. 4A) with equal charges consumed for the oxidation (Q_f) and reduction (Q_b) of the *o*-AP modified system. In the presence of ascorbate, the charge value associated with forward chronocoulometry (Q_f) is significantly high, and there is no net cathodic current corresponding to the reduction of the *o*-AP mediator in the presence of ascorbate (Fig. 4A). This behavior is typical of that expected for a mediated oxidation. The number of electrons n involved in ascorbate oxidation at the modified electrode is evaluated from the slope of Q versus $t^{1/2}$ plots (Fig. 4B) using the Cottrell equation, i.e.,

$$Q = 2nFAc_o D^{1/2}\pi^{-1/2}t^{1/2} \quad (6)$$

where $c_o = 0.6$ mM, $A = 0.071$ cm^2 and $D = 2.7 \times 10^{-6}$ $cm^2\,s^{-1}$. The calculated n value was 1.86 (≅2.0), in agreement with value determined from cyclic voltammetry.

3.3. Hydrodynamic amperometric detection of ascorbate in presence of uric acid

Owing to the fact that amperometry under stirred conditions has a much higher current sensitivity than cyclic voltammetry [69], it was adopted to estimate the lower limit of detection of ascorbate at an *o*-AP modified GCE. Fig. 5A shows a typical amperometric *i*–*t* response for step-wise injections of 1, 5, 10 μL of (0.01 M) ascorbate (a–c, respectively), into phosphate

UNIVERSITAT ROVIRA I VIRGILI
BOTTOM-UP SURFACE ENGINEERING FOR THE CONSTRUCTION OF (BIO) SENSORING SYSTEMS: DESIGN STRATEGIES
AND ANALYTICAL APPLICATIONS
Hossam Metwally Ahmed Nassef
ISBN:978-84-692-3235-4/DL:T-932-2009

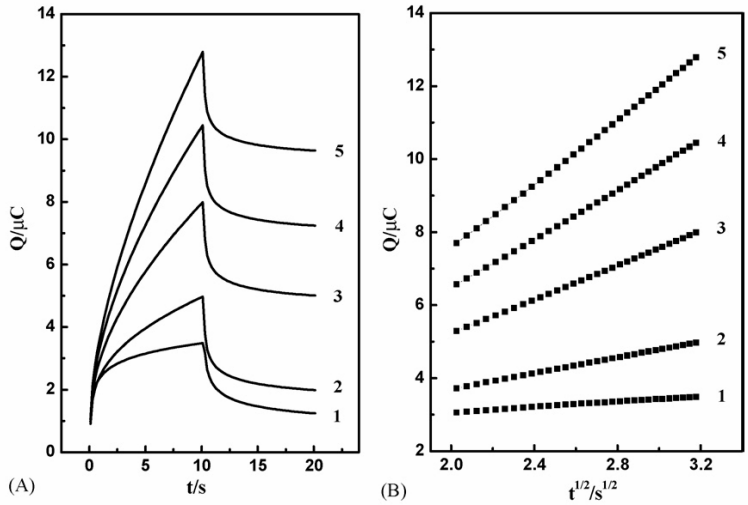

Fig. 4. (A) Double-potential step chronocoulometry response of *o*-AP modified GC electrode in phosphate buffer solution (0.1 M, pH 7.0) in absence (1) and presence of ascorbate (2–5). (B) plot of Q vs. $t^{1/2}$. All conditions as in Fig. 3.

buffer (0.1 M, pH 7.0) at the *o*-AP modified GC electrode at a constant potential of 150 mV. It can be seen that the oxidation current increases with addition of ascorbate and reaches steady state within few seconds. The current responses showed a linear relationships with the concentration of ascorbate over the ranges

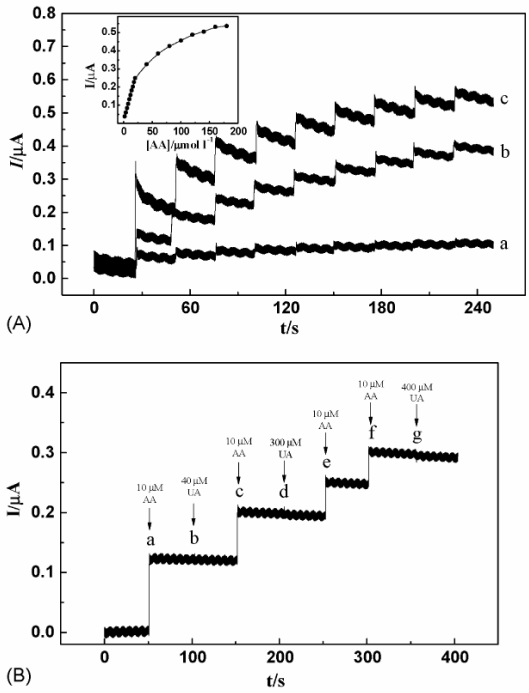

Fig. 5. (A) Current-time response of *o*-AP modified GC electrode to the successive injections of ascorbate concentration in (a) 2 μM, (b) 10 μM and (c) 20 μM steps in 0.1 M phosphate buffer (pH 7.0); Inset shows current–concentration calibration graph; (B) amperometric response of the sequential additions of ascorbate and UA to final cell concentration in μM; (a) 10 ascorbate, (b) 40 UA, (c) 10 ascorbate, (d) 300 UA, (e) 10 ascorbate, (f) 10 ascorbate, and (g) 400 UA.

of 2–20 μM with a sensitivity of 0.01186 μA μM^{-1}, intercept 0.01354 μA, and with a correlation coefficient, $r = 0.99987$. After 20 μM of ascorbate concentration, a plateau was obtained and the current–concentration response deviates from linearity. From the analysis of the data obtained from the calibration curve, the estimated limit of detection (LOD) of ascorbate was 0.3 μM. The precision was estimated from 10 repetitive measurements of 0.01 M ascorbate solution, and the relative standard deviations (R.S.D.) was 2.5%. These results indicate that the *o*-AP modified electrode has a good accuracy for the determination of ascorbate. The good reproducibility demonstrated the high stability of the *o*-AP modified GCE in the analytical applications.

The interfering effect of UA on the amperometric determination of ascorbate has been studied in phosphate buffer (0.1 M, pH 7.0). Fig. 5B represents the amperogram of the sequential additions of ascorbate and UA, a significant increase in the oxidation current was obtained with each addition of 10 μM ascorbate, while no response could be detected with the injection of different concentrations of UA (40–400 μM). This behavior demonstrates that UA does not interfere in the amperometric determination of ascorbate.

The stability tests were carried out by measuring the response from day to day. A *o*-AP modified GC electrode kept under vacuum at room temperature for 30 days showed a maintainance of 90% of its initial activity.

3.4. Determination of UA in real urine sample in presence of ascorbate

In view of the fact that it is normally difficult to obtain separate voltammetric waves for ascorbate and UA in the presence of each other, the ability of the *o*-AP modified electrode to achieve the voltammetric resolution of ascorbate and UA was investigated (Fig. 6). The resolution is due to the mediated oxidation of ascorbate at a sufficiently negative potential. In order to demonstrate the capability of this modified GC electrode for the

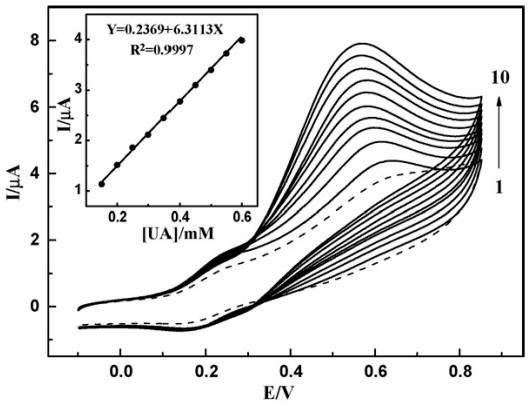

Fig. 6. Cyclic voltammograms (1–10) of different concentrations of UA, 150, 200, 250, 300, 350, 400, 450, 500, 550, and 600 μM, respectively, and real urine sample (- - -) at *o*-AP modified GC electrode in 0.1 M phosphate buffer (pH 7.0) in presence of 300 μM ascorbate at 50 mV s^{-1} scan rate vs. Ag/AgCl.

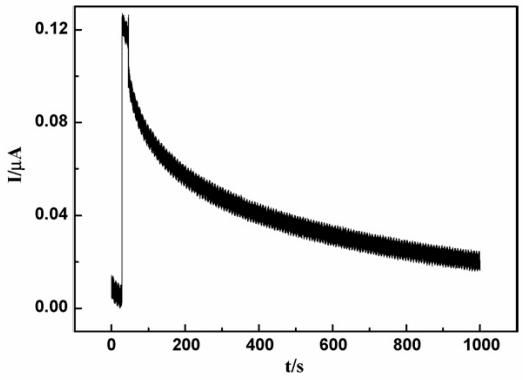

Fig. 7. Amperometric response of *o*-AP modified GC electrode of two consequent injections of 10 μM ascorbate and 6.0 mM H_2O_2, to final cell concentration 5 mL of phosphate buffer solution (0.1 M, pH 7.0).

selective determination of UA in presence of ascorbate, cyclic voltammograms were carried out in 0.1 M phosphate buffer (pH 7.0) for different concentrations of UA in presence of 300 μM ascorbate (Fig. 6). The voltammograms showed that the oxidation peak current of uric acid was increased with increasing UA concentration, while the peak current attributed to the electrocatalytic oxidation of ascorbate remained constant (Fig. 6). As shown in Fig. 6 inset, the oxidation peak current of UA has linear relationship with UA concentrations over the range of 150–600 μM, with a slope, intercept, and correlation (r), of 6.3113 μA μM^{-1}, 0.2369 μA, and 0.9997, respectively. The limit of detection of UA was estimated to be 14 μM. As an example for the analytical performance of the *o*-AP modified GC electrode, and for the selective determination of UA contents in real urine sample, CV was carried out at the modified electrode in 5 mL 0.1 M phosphate buffer (pH 7.0) containing 100 μL urine sample of adult person and 1.5 μmol ascorbate (Fig. 6, dashed line), the estimated UA content was 3.45 mM. This behavior indicates the potential usefulness of the *o*-AP modified GC electrode for the practical determination of UA in real samples in presence of ascorbate, and vice versa.

3.5. The reaction kinetics of H_2O_2 and ascorbate at *o*-AP/GCE

The kinetics of the reaction between H_2O_2 and ascorbate has been studied at the *o*-AP modified GCE, and is described as follows:

$$H_2O_2 + \text{ascorbate} \rightarrow 2H_2O + \text{dehydroascorbate}$$

Fig. 7 shows a current–time response observed for two immediately consecutive injections of 10 μM ascorbate and 6 mM H_2O_2 at *o*-AP in phosphate buffer (0.1 M, pH 7). The initial increase in current is due to addition of ascorbate, while after injection of H_2O_2 the current start to decay with a half-life time of approximately 270 s due to the consumption of electroactive species of ascorbate, and production of the electro-inactive dehydroascorbic acid (DAA). However, a very high concentration of H_2O_2 was used with respect to the ascorbate concentration, to obtain a reaction of pseudo-first order with rate constant (k) of 2.57×10^{-3} s^{-1}, very close to the reported values [70,71]. This kinetics is very useful for sensors in which the elimination of ascorbate is necessary for detection of another analyte interfering with ascorbate. Moreover, many ascorbate-detecting sensors have been developed, and successful efforts have been made to reduce the direct faradaic interference between H_2O_2 and ascorbate by endogenous electroactive species [72]. However, the homogeneous interference and kinetics of H_2O_2 and ascorbate interaction are important and questions the suitability of this type of sensor in systems, which contain continuously changing levels of H_2O_2.

4. Conclusion

Glassy carbon electrodes were modified with *o*-aminophenol by electrochemical reduction of in situ prepared diazonium salt, and was characterized by CV. This modified electrode was used to study the electrocatalytic oxidation of ascorbate in phosphate buffer of pH 7.0, and showed excellent enhancement in the anodic current of ascorbate/dehydroascorbate redox couple with a decrease of ≅ 200 mV versus Ag/AgCl in overpotential. Double potential step chronoamperometry and chronocoulometry also showed a very good response with different concentrations of ascorbate, and it was used to estimate the diffusion coefficient (2.7×10^{-6} cm^2 s^{-1}) and catalytic rate constant (3.13×10^3 M^{-1} s^{-1}). Cyclic voltammetry showed a linear relationship between anodic peak current and ascorbate concentration (2–1000 μM). Moreover, from d.c. amperometry the catalytic oxidation peak current was also linearly dependent on ascorbate concentration in the range of 2–20 μM with limit of detection (0.3 μM). In the amperometric detection of ascorbate, UA has no current response and does not interfere in ascorbate determination. The half-life time and rate constant of the reaction between H_2O_2 and ascorbate was estimated as 270 s, and 2.57×10^{-3} s^{-1}, respectively. The oxidation peak current of UA has a linear relationship with UA concentrations over the range of 150–600 μM, and applied for determination of UA

in real samples in presence of ascorbate, indicating the potential usefulness of the *o*-AP modified GC electrode for practical applications. The *o*-AP modified glassy carbon electrode not only exhibited strong catalytic activity toward ascorbate but was also demonstrated to have remarkable stability and quantitatively reproducible analytical performance, and could be used as simple, selective and precise amperometric sensor for the determination of ascorbate in presence of uric acid and vice versa, thus allowing their facile simultaneous detection.

Acknowledgment

This work has been carried out with financial support from the Commission of the European Communities specific RTD programme 'Smart Integrated Biodiagnostic Systems for Healthcare, SMARTHEALTH, FP6-2004-IST-NMP-2-016817'.

References

[1] S. Lupu, A. Mucci, L. Pigani, R. Seeber, C. Zanardi, Electroanalysis 14 (2002) 519.
[2] L.R. Faulkner, Chem. Eng. News 62 (1984) 28.
[3] O. Arrigoni, M.C.D. Tullio, Biochem. Biophys. Acta 1569 (2002) 1.
[4] D.W. Martin Jr., in: D.W. Martin Jr., P.A. Mayes, V.W. Rodwell (Eds.), Harper's Review of Biochemistry, 19th ed., Lange, Los Altos, CA, 1983, p. 112.
[5] K.J. Stutts, R.M. Wightman, Anal. Chem. 55 (1983) 1576.
[6] Z. Gao, A. Ivaska, T. Zha, G. Wang, P. Li, Z. Zhao, Talanta 40 (1993) 399.
[7] J. Facci, R.W. Murray, Anal. Chem. 54 (1982) 772.
[8] M.A. Kutnik, W.C. Hawkes, E.E. Schaus, S.T. Omage, Anal. Biochem. 66 (1982) 424.
[9] L.A. Pachla, D.L. Reynolds, P.T. Kissinger, J. Assoc. Off. Anal. Chem. 68 (1985) 1.
[10] S.A. Wring, J.P. Hart, Anal. Chim. Acta 229 (1989) 63.
[11] L. Falat, H.-Y. Cheng, J. Electroanal. Chem. 157 (1983) 393.
[12] M.H. Pournaghi-Azar, R. Ojami, Talanta 42 (1995) 1839.
[13] A.P. Doherty, M.A. Stanley, J.G. Vos, Analyst 120 (1995) 2371.
[14] M.H. Pournaghi-Azar, H. Razmi-Nerbin, J. Electroanal. Chem. 488 (2000) 17.
[15] L. Angnes, R.C. Matos, M.A. Augelli, C.L. Lago, Anal. Chim. Acta 404 (2000) 151.
[16] J.B. Raoof, R. Ojani, A. Kiani, J. Electroanal. Chem. 515 (2001) 45.
[17] P.N. Bartlett, E.N.K. Wallace, Phys. Chem. Chem. Phys. 3 (2001) 1491.
[18] M.H. Pournaghi-Azar, R. Ojani, J. Solid State Electrochem. 4 (2000) 75.
[19] I. Koshiishi, T. Imanari, Anal. Chem. 69 (1997) 216.
[20] R. Pauliukaite, M.E. Ghica, C.M.A. Brett, Anal. Bioanal. Chem. 381 (2005) 972.
[21] G. Dryhurst, Electrochemistry of Biological Molecules, Academic Press, New York, 1977.
[22] J.M. Zen, J.J. Jou, G. Ilangovan, Analyst 123 (1998) 1345.
[23] T.E. Smith, in: T.M. Devlin (Ed.), Textbook of Biochemistry with Clinical Correlations, Wiley-Liss, New York, 1992, p. 544.
[24] H.A. Harper, Review of Physiological Chemistry, 13th ed., Lange Medical Publications, Los Atlos, CA, 1977, p. 406.
[25] V.V.S.E. Dutt, H.A. Mottola, Anal. Chem. 46 (1974) 1777.
[26] R. Aguilar, M.M. Davila, M.P. Elizalde, J. Mattusch, R. Wennrich, Electrochim. Acta 49 (2004) 851.
[27] S.B. Khoo, F. Chen, Anal. Chem. 74 (2002) 5734.
[28] E. Popa, Y. Kubota, D.A. Tryk, A. Fujishima, Anal. Chem. 72 (2000) 1724.
[29] W. Ren, H.Q. Luo, N.B. Li, Biosens. Bioelectron. 21 (2006) 1086.
[30] H.R. Zare, N. Rajabzadeh, N. Nasirizadeh, M.M. Ardakani, J. Electroanal. Chem. 589 (2006) 60.
[31] C.-X. Li, Y.-L. Zeng, Y.-J. Lui, C.-R. Tang, Anal. Sci. 22 (2006) 393.
[32] O. Ghodbone, G. Chamouloud, O. Be'langer, Electrochem. Commun. 6 (2004) 254.
[33] R.W. Murray, in: A.J. Bard (Ed.), Electroanalytical Chemistry, vol. 13, M. Dekker, New York, 1984, p. 191.
[34] R.L. McCreery, in: A.J. Bard (Ed.), Electroanalytical Chemistry, vol. 17, M. Dekker, New York, 1991, p. 221.
[35] A.A. İsbir, A.O. Solak, Z. Üstündağ, S. Bilge, A. Natsagdorj, E. Kiliç, Z. Kiliç, Anal. Chim. Acta 547 (2005) 59.
[36] A.J. Downard, A.D. Roddick, Electroanalysis 7 (1995) 376.
[37] H. Maeda, Y. Yamauchi, H. Ohmori, Curr. Top. Anal. Chem. 2 (2001) 121.
[38] M. Delamar, R. Hitmi, J. Pinson, J.M. Saveant, J. Am. Chem. Soc. 114 (1992) 5883.
[39] P. Allongue, M. Delamar, B. Desbat, O. Fagebaume, R. Hitmi, J. Pinson, J.M. Saveant, J. Am. Chem. Soc. 119 (1997) 201.
[40] J.K. Kariuki, M.T. McDermot, Langmuir 17 (2001) 5947.
[41] G. Lui, J. Lui, T. Böcking, P.K. Eggers, J.J. Gooding, Chem. Phys. 319 (2005) 136.
[42] M. Kullapere, G. Jürmann, T.T. Tenno, J.J. Paprotny, F. Mirkhalaf, K. Tammeveski, J. Electroanal. Chem., in press.
[43] A. Radi, J.M. Montornés, C.K. O'Sullivan, J. Electroanal. Chem. 587 (2006) 140.
[44] S. Baik, M. Usrey, L. Rotkina, M. Strano, J. Phys. Chem. B 108 (2004) 15560.
[45] A. Adenier, E. Cabet-Deliry, T. Lalot, J. Pinson, F. Podvorica, Chem. Mater. 14 (2002) 4576.
[46] X. Yang, S.B. Hall, S.N. Tan, Electroanalysis 15 (2003) 885.
[47] T. Matrab, M.M. Chehimi, C. Perruchot, A. Adenier, A. Guillez, M. Save, B. Charleux, E. Cabet-Deliry, J. Pinson, Langmuir 21 (2005) 4686.
[48] N. Ferreyra, L. Coche-Guérente, P. Labbé, Electrochim. Acta 49 (2004) 477.
[49] R. Blankespoor, B. Limoges, B. Schöllhorn, J.L. Syssa-Magalé, D. Yazidi, Langmuir 21 (2005) 3362.
[50] V. Vijaikanth, J.F. Capon, F. Gloaguen, P. Schollhammer, J. Talarmin, Electrochem. Commun. 7 (2005) 427.
[51] A. Sarapuu, K. Vaik, D.J. Schiffrin, K. Tammeveski, J. Electroanal. Chem. 541 (2003) 23.
[52] B.P. Corgier, C.A. Marquette, L.J. Blum, J. Am. Chem. Soc. 127 (2005) 18328.
[53] M. Dequaire, C. Degrand, B. Limoges, J. Am. Chem. Soc. 121 (1999) 6946.
[54] A. Chaussé, M.M. Chehimi, N. Karsi, J. Pinson, F. Podvorica, C. Vautrin-Ul, Chem. Mater. 14 (2002) 392.
[55] B. Šljukić, C.E. Banks, R.G. Compton, Electroanalysis 17 (2005) 1025.
[56] K. Tammeveski, K. Kontturi, R.J. Nichols, R.J. Potter, D.J. Schiffrin, J. Electroanal. Chem. 515 (2001) 101.
[57] E. Theodoridou, J.O. Besenhard, H.P. Fritz, J. Electroanal. Chem. 124 (1981) 87.
[58] K.W. Leitner, B. Gollas, M. Winter1, J.O. Besenhard, Electrochim. Acta 50 (2004) 199.
[59] H. Lund, M.M. Baizer, Organic Electrochemistry, 3rd ed., Marcel Dekker, NY, 1991, p. 601.
[60] S.A. Wring, J.P. Hart, B.J. Birch, Analyst 114 (1989) 1563.
[61] S. Antoniadou, A.D. Jannakoudakis, E. Theodoridou, Synth. Met. 30 (1989) 295.
[62] C.P. Andrieux, J.M. Savéant, J. Electroanal. Chem. 93 (1978) 163.
[63] A.B. Florou, M.I. Prodromidis, M.I. Karayannis, S.M. Tzouwara-Karayanni, Anal. Chim. Acta 409 (2000) 113.
[64] A.J. Bard, L.R. Faulkner, Electrochemical Methods, Fundamentals and Applications, Wiley, New York, 2001.
[65] J.A. Harrison, Z.A. Khan, J. Electroanal. Chem. 28 (1970) 131.
[66] J.-B. Raoof, R. Ojani, S. Rashid-Nadimi, Electrochim. Acta 49 (2004) 271.
[67] S.M. Golabi, L. Irannejad, Electroanalysis 17 (2005) 985.
[68] Z. Galus, Fundamentals of Electrochemical Analysis, Ellis Horwood, New York, 1994.
[69] D.A. Skoog, F.J. Holler, T.A. Nieman, Principles of Instrumental Analysis, 5th ed., Saunders College Publishing, 1998.
[70] I. Losito, C.G. Zambonin, J. Electroanal. Chem. 410 (1996) 181.
[71] A.O. Dekker, R.G. Dickinson, J. Am. Chem. Soc. 62 (1940) 2165.
[72] J.P. Lowry, R.D. O'Neill, Anal. Chem. 64 (1992) 453.

Analytica Chimica Acta 632 (2009) 315

Contents lists available at ScienceDirect

Analytica Chimica Acta

journal homepage: www.elsevier.com/locate/aca

Corrigendum

Corrigendum to "Simultaneous detection of ascorbate and uric acid using a selectively catalytic surface" [Anal. Chim. Acta 583 (2007) 182–189]

Hossam M. Nassef[a], Abd-Elgawad Radi[a,*], Ciara O'Sullivan[a,b,*]

[a] Department of Chemical Engineering, University of Rovira I Virgili, Av. Paisos Catalan, 26, 43007 Tarragona, Spain
[b] Institució Catalana de Recera I Estudis Avançats, Passeig Lluís Companys 23, 08010 Barcelona, Spain

The author regrets that in the original printing of the above article Scheme 1 appeared incorrectly. Here follows the corrected figure.

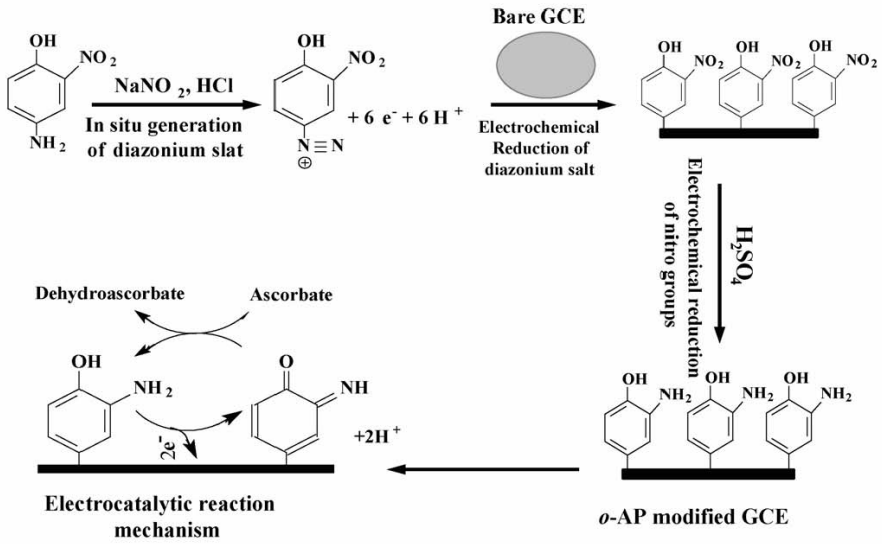

Scheme 1.

DOI of original article: 10.1016/j.aca.2006.10.004.
* Corresponding authors at: Department of Chemical Engineering, University of Rovira I Virgili, Av. Paisos Catalan, 26, 43007 Tarragona, Spain. Fax: +34 977 559621.

0003-2670/$ – see front matter
doi: 10.1016/j.aca.2008.10.040

UNIVERSITAT ROVIRA I VIRGILI
BOTTOM-UP SURFACE ENGINEERING FOR THE CONSTRUCTION OF (BIO) SENSORING SYSTEMS: DESIGN STRATEGIES AND ANALYTICAL APPLICATIONS
Hossam Metwally Ahmed Nassef
ISBN:978-84-692-3235-4/DL:T-932-2009

CHAPTER 5: (Art 4)

Amperometric sensing of ascorbic acid using a disposable screen-printed electrode modified with electrografted *o*-aminophenol film

(Hossam M. Nassef, Laia Civit, Alex Fragoso and Ciara K. O'Sullivan, Analyst, 2008, 133, 1736–1741.)

UNIVERSITAT ROVIRA I VIRGILI
BOTTOM-UP SURFACE ENGINEERING FOR THE CONSTRUCTION OF (BIO) SENSORING SYSTEMS: DESIGN STRATEGIES
AND ANALYTICAL APPLICATIONS
Hossam Metwally Ahmed Nassef
ISBN:978-84-692-3235-4/DL:T-932-2009

Amperometric sensing of ascorbic acid using a disposable screen-printed electrode modified with electrografted *o*-aminophenol film

Hossam M. Nassef,[a] Laia Civit,[a] Alex Fragoso*[a] and Ciara K. O'Sullivan*[ab]

Received 20th May 2008, Accepted 11th August 2008
First published as an Advance Article on the web 27th September 2008
DOI: 10.1039/b808499h

Electrode modification by electrochemical reduction of diazonium salts of different aryl derivatives is useful for catalytic, analytical and biotechnological applications. A simple and sensitive method for the electrocatalytic detection of ascorbic acid using disposable screen-printed carbon electrodes modified with an electrografted *o*-aminophenol film, *via* the electrochemical reduction of its *in situ* prepared diazonium salts in aqueous solution, is presented. The performance of two commercial SPEs as substrates for grafting of diazonium films has been compared and the grafting process optimized with respect to deposition time and diazonium salt concentration, with the modified surfaces being characterised using cyclic voltammetry. The functionalised screen-printed electrodes demonstrated an excellent electrocatalytic activity towards the oxidation of ascorbic acid shifting the overpotential from 298 and 544 mV to 160 and 244 mV, respectively *vs.* Ag/AgCl. DC amperometric measurements were carried out for the quantitative determination of ascorbic acid using the modified electrodes. The catalytic oxidation peak current was linearly dependent on the ascorbic acid concentration in the range of 2–20 μM, with a correlation coefficient 0.998, and a limit of detection of 0.86 μM was obtained with an excellent reproducibility (RSD% = 1.98, $n = 8$). The functionalised screen-printed electrodes exhibited notable surface stability, and were used as a simple and precise disposable sensor for the selective determination of ascorbic acid.

Introduction

Ascorbic acid (vitamin C) is naturally present in a wide number of foods, such as fruits and vegetables. Additionally it is added to foodstuffs as an antioxidant, for the stabilization of color and aroma. Pharmaceuticals also often contain ascorbic acid, as a supplementary source to human diets as a free-radical scavenger.[1] It has been used for the prevention and treatment of the common cold, mental illness, scurvy and cancer.[2–4] The content of ascorbic acid in biological fluids is used to assess the amount of oxidation stress in human metabolism, and excessive oxidative stress has been linked to cancer, diabetes mellitus and liver disease.[5] Additionally, ascorbic acid derivatives are exploited to stimulate the growth of dermal papilla cells and to promote the elongation of hair shafts in hair follicles,[6] and also for the suppression of growth of malignant leukemia cells.[7] In human beings, ascorbic acid can also be used for the therapy and treatment of a variety of bone diseases associated with over-activation of osteoclastogenesis, such as menopausal osteoporosis,[8] and also effectively suppresses ultraviolet-induced skin pigmentation, through its anti-oxidative activity.[9] There is thus a clear need for an easy-to-use, inexpensive method for the detection of ascorbic acid, particularly in the pharmaceutical and food industries. A considerable effort has been devoted for many years to the development of voltammetric methods for the determination of ascorbic acid (AA).[10,11] The direct oxidation of ascorbic acid at conventional (carbon or metal) electrodes is irreversible,[12,13] and it is thus difficult to determine ascorbic acid directly due to its large overpotential and fouling by oxidation products.[10] Therefore, numerous attempts have been made to reduce the large overpotentials using various active mediators immobilised at the electrode surface for the catalysis of the electro-oxidation of ascorbic acid.[10,11] Different approaches have been recently used for electrode modification and applied to the detection of ascorbic acid, such as the copolymerization of aniline and *o*-aminophenol on glassy carbon electrodes (GCEs),[14] mechanical attachment of terbium hexacyanoferrate to the surface of the carbon ceramic electrode[15] and modification of GCEs with a cellulose acetate polymeric film bearing 2,6-dichlorophenolindophenol.[16]

Screen-printing is a well-established technique for the fabrication of mechanically robust electrochemical transducers, due to its low cost, applicability to mass production, and ease of use.[17] Three-electrode configurations can be printed on a single substrate, to produce a microelectrochemical cell onto which the target sample can be directly added for analysis.[18] The surface of carbon screen-printed electrodes (SPEs) can be easily modified to enhance selectivity and/or sensitivity by surface deposition of various substances such as metal films, polymers, enzymes, *etc.*,[19] using different approaches, including chemical reduction of chloro-metallate anions,[20] electrochemical deposition,[21] metal vapour synthesis,[22] and reactive magnetron sputtering.[23] SPEs have been used as electrochemical sensors and as substrates for biosensors due to the broad exploitable potential window of

[a]*Nanobiotechnology and Bioanalysis Group, Department of Chemical Engineering, Universitat Rovira I Virgili, Avd. Països Catalans, 26, 43007 Tarragona, Spain. E-mail: ciara.osullivan@urv.cat; alex.fragoso@urv.cat; Fax: +34-977-559621; Tel: +34-977-558740*
[b]*Institució Catalana de Recerca i Estudis Avançats, Passeig Lluís Companys 23, 08010 Barcelona, Spain. E-mail: ciara.osullivan@icrea.es*

carbon, as well as the low background current, and its chemical inertness, ease of chemical derivatization and modification; carbon electrodes are thus suitable for a variety of applications.[24,25] Coupling the advantages of SPEs and electrochemical sensors/biosensors[26,27] results in a highly useful analytical tool with application in clinical, environmental, industrial, and food analysis.[19] As previously mentioned, carbonaceous materials can be easily covalently modified to produce tailored surfaces for use in electrocatalysis.[28,29] The modification of conductive surfaces through the grafting of organic groups[30] *via* the electrochemical reduction of aryl diazonium salts was first reported by Pinson and co-workers in 1992.[31] The electrografted layer (complete monolayer or submonolayer)[32–34] of aryl groups is very strongly attached and extremely stable, and due to this stability, several attempts have been made to construct electrochemical sensors or biosensors on glassy carbon,[35–38] SPEs,[39–41] and recently on gold[42] for a range of analytical applications.

We have recently demonstrated the electrochemistry of an *o*-aminophenol (*o*-AP) film grafted onto glassy carbon electrodes and its application to the electrocatalytic oxidation of ascorbic acid.[11] In the work reported here, we wish to extend our previous work to move closer to a practical application *via* the use of disposable screen-printed electrodes. Commercial screen-printed carbon electrodes (DropSens and BVT) were grafted with *o*-AP *via* electro-reduction of the *in situ*-generated diazonium salt. The electrografted film of *o*-AP was reversibly oxidized to the *o*-quinoneimine form, which serves as a two-electron acceptor mediator, efficient for the electrocatalytic oxidation of ascorbic acid.[11] A noticeable reduction of the overpotential for ascorbic acid oxidation at the *o*-AP-SPE was observed, and the modified SPEs were applied to the analysis of ascorbic acid. A linear relationship between the catalytic oxidation peak current and ascorbic acid concentration in the range of 2–20 μM was obtained with a limit of detection of 0.86 μM and excellent reproducibility, $n = 8$ and RSD% = 1.98. The disposable *o*-AP-SPEs not only exhibited strong catalytic activity toward ascorbic acid but also demonstrated remarkable stability with a highly reproducible quantitative analytical performance for at least three months, with sensors stored under vacuum at room temperature.

Experimental

Chemicals and reagents

All chemicals used were of analytical grade and used as received without any further purification. L-Ascorbic acid (99%) was purchased from Sigma Aldrich (Spain) and 2-nitro-4-aminophenol was obtained from Acros. L-Ascorbic acid solutions were prepared immediately prior to use. All measurements were carried out in 0.1 M phosphate buffer (pH 7.2) as supporting electrolyte, unless specifically stated otherwise. All solutions were prepared with Milli-Q water (Millipore Inc., $\Omega = 18$ mOhm).

Apparatus

All electrochemical experiments were carried out using an Autolab model PGSTAT 12 potentiostat/galvanostat controlled with the General Purpose Electrochemical System (GPES) software (Eco Chemie B.V., The Netherlands). A three-configuration system was used for all the electrochemical measurements in a 5 ml volume. Two kinds of commercially available SPE were used as working electrodes from BVT Technologies (single electrode, model AC3.W4, batch 5914, $\varnothing = 1.25 \pm 0.05$ mm) and from DropSens (three-electrode system, ref. 110, $\varnothing = 4$ mm), a platinum wire (BAS model MW-1032) counter electrode and an Ag/AgCl-3 M NaCl (BAS model MF-2078) reference electrode. All potentials were reported with respect to this reference electrode. A magnetic stirrer provided the convective transport during the amperometric experiments.

Modification of the screen-printed electrodes

Prior to modification, an electrochemical pre-treatment of the screen-printed electrodes was carried out by cycling the potential between −0.5 and 1.0 V at 100 mV s^{-1} in 1 M H_2SO_4 for eight cycles. After activation, the SPEs were washed with Milli-Q water and dried with dry nitrogen gas. The SPEs were electrochemically characterised by cyclic voltammetry (CV) in 1 mM $[Fe(CN)_6]^{4-}$/$[Fe(CN)_6]^{3-}$ in 0.1 M KCl. The surface areas of the clean SPEs were measured by carrying out cyclic voltammetry in the potential range −0.25 to 0.5 V at different scan rates (100, 81, 64, 49, 36 mV s^{-1}) in 1 mM $[Fe(CN)_6]^{4-}$/$[Fe(CN)_6]^{3-}$ solution.

After cleaning and measuring the surface areas of the SPEs, the grafting of the SPEs with *o*-AP was optimized with respect to the concentration of the 2-nitro-4-aminophenol (and thus the corresponding diazonium salt concentration), as well as the number of potential cycles for the electrochemical grafting of the *o*-aminophenol film. Different concentrations of diazonium salts (6, 10, 13 mM) were prepared *in situ* by adding HCl (6 mM) and sodium nitrite (138 mg, 2.0 mmol) to a stirred, ice-cold solution of 2-nitro-4-aminophenol (4.62, 7.71, or 10.02 mg, 0.03, 0.05, or 0.07 mmol, respectively) in 5 ml, and the mixture was stirred for 25 min at 4 °C. For surface modification, the DropSens and/or BVT SPEs were immersed in 5 ml of the diazonium salt solution, and potential cycling was carried out between 0.6 and −0.2 V, to electrochemically reduce the *in situ*-generated *o*-nitrophenol diazonium salt for a range of cycle numbers (10, 15, 20, 25, 30, 40, 50, 60, 70 cycles) at 50 mV s^{-1}. Following modification, the electrode was washed with Milli-Q water and transferred to 1 M H_2SO_4 and subjected to five potential scans between −0.1 and −0.85 V at 100 mV s^{-1}, for complete reduction of the nitro group, providing an electrografted film of *o*-aminophenol on the carbon SPE surface.[11,43,44] The modified electrodes were subsequently subjected to potential scanning between −0.1 and 0.6 V for ten cycles at 100 mV s^{-1} *vs.* Ag/AgCl in phosphate buffer (0.1 M, pH 7.2) to remove physically adsorbed compounds. Oxygen-free nitrogen was used to remove oxygen from the solution and a continuous flow of nitrogen was maintained during the voltammetric measurements.

All experiments were carried out at ambient temperature. DC amperometric measurements at both types of the SP modified electrodes (BVT and DropSens) were performed at a fixed potential of 0.2 V *vs.* Ag/AgCl, in 5 ml phosphate buffer and ascorbic acid was injected at different concentration levels (2, 4, 6, 8, 10, 12, 14, 16, 18 and 20 μM in cell) under stirring conditions of 350 rpm.

UNIVERSITAT ROVIRA I VIRGILI
BOTTOM-UP SURFACE ENGINEERING FOR THE CONSTRUCTION OF (BIO) SENSORING SYSTEMS: DESIGN STRATEGIES
AND ANALYTICAL APPLICATIONS
Hossam Metwally Ahmed Nassef
ISBN:978-84-692-3235-4/DL:T-932-2009

Results and discussion

Activation and measurements of the surface area of the DropSens and BVT SPEs

In the manufacturing of SPEs, high amounts of polymer in the ink result in slower kinetics of heterogeneous reactions, and quasi-reversible or irreversible redox processes. Therefore, the activation of the SPEs is necessary for optimum electrochemical performance *via* mild electrochemical activation.[45] A short electrochemical pre-anodization of the unmodified SPE at a high positive polarization potential increases the heterogeneous transfer constant for the $[Fe(CN)_6]^{4-}/[Fe(CN)_6]^{3-}$ couple, enhancing electrochemical reversibility, and improving their analytical performance[45] due to an increase in their surface functionalities, surface roughness and the removal of surface contaminants. The SPEs were thus cleaned and activated by carrying out a potential cycling in 1 M H_2SO_4 between −0.5 and 1.0 V at 100 mV s^{-1} for eight cycles. CV was used to access the electrochemical reactivity of the electrode surface by comparing the peak-to-peak separation.[45,46] Broad oxidation and reduction peaks with small peak heights were obtained before cleaning, whereas after electrochemical activation in H_2SO_4, well-defined oxidation and reduction peaks were observed corresponding to the Fe^{II}/Fe^{III} couple.

Similarly, well-defined cyclic voltammograms of $[Fe(CN)_6]^{4-}/[Fe(CN)_6]^{3-}$ were obtained for both DropSens (DS) (Fig. 1) and BVT (not shown) SPEs, with peak-to-peak separation corresponding to a Nernstian one-electron transfer reaction.

In order to assay the electrode-to-electrode area reproducibility, the surface areas of the DS and BVT SPEs were measured following cleaning and prior to modification with the aminophenol film. Typical cyclic voltammograms for the $[Fe^{II}(CN)_6]^{4-}/[Fe^{III}(CN)_6]^{3-}$ couple at the activated SPEs at different scan rates (36–100 mV s^{-1}) in the potential range −0.15 to 0.55 V are shown in Fig. 1. The separation between the anodic and cathodic peaks increases with increase in the scan rate, from 70 mV at 36 mV s^{-1} to 74 mV at 100 mV s^{-1}, compared with ΔE_p values of 60–80 mV for treated glassy carbon electrodes,[47] with lower values of ΔE_p indicating a faster electron transfer.[48] The SPE surface areas were calculated from the slope of the I_p *vs.* $v^{1/2}$ plot (Fig. 1 inset), as previously reported[48,49] using a diffusion coefficient (D) value of 7.63×10^{-6} cm^2 s^{-1} for the $Fe(CN)_6^{3-}$ probe.[47] The surface areas of the DS and BVT SPEs were 0.087 and 0.012 cm^2 with RSD% = 16.54 and 22.52, for $n = 174$ and 84, respectively. Owing to the low reproducibility in electrode area, responses were corrected with respect to its electrode surface area, to obtain the normalized current intensity (I_p/A, μA cm^{-2}).

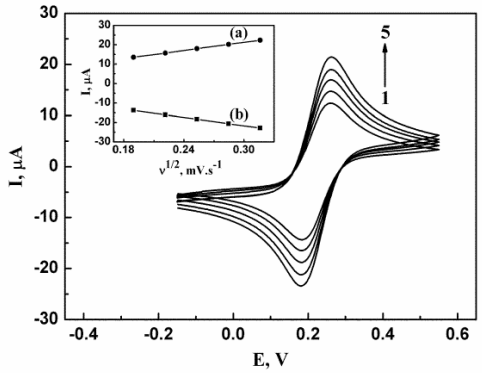

Fig. 1 Cyclic voltammograms of 1 mM $[Fe(CN)_6]^4$ /$[Fe(CN)_6]^3$ in 0.1 M KCl at a clean DS SPE at different scan rates of 36, 49, 64, 81, and 100 mV s^{-1} (1→5), respectively. Inset curves (a,b): plot of the anodic ($I_{p,a}$) and cathodic ($I_{p,c}$) current with the square root of scan rate.

Electrocatalytic activity of ascorbic acid at modified SPEs

The cyclic voltammograms of the *o*-AP-modified DS and BVT SPEs present a relatively large peak-to-peak separation, even at a low scan rate. The large peak-to-peak separation obtained is unexpected for surface-attached molecules and possible reasons for this separation are slow charge transfer kinetics, including slow direct electron transfer between the SPEs and the *o*-AP film and the transport of the protons between the modified layer and the bulk solution. A slow electrostatic charge compensation during the redox process may also contribute.[11]

The electrocatalytic behaviour of the modified *o*-AP was investigated by cyclic voltammetry at bare and *o*-AP-modified BVT (not shown) and DS SPEs at 10 mV s^{-1} in phosphate buffer solution (0.1 M, pH 7.2) in the absence and presence of ascorbic acid as shown in Fig. 2A.

At bare DS and BVT SPEs the oxidation of ascorbic acid occurs at a highly positive potential of +298 and +544 mV, respectively, while at the *o*-AP-modified SPEs a significant

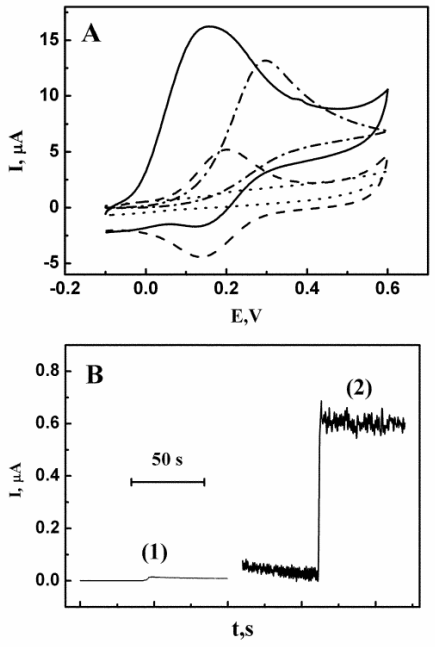

Fig. 2 (A) Cyclic voltammograms of *o*-AP-modified DS SPEs in the absence (----) and in the presence (—) of 1 mM ascorbic acid, and of bare SPE in the absence (···) and in the presence (-·-·-) of ascorbic acid in phosphate buffer (0.1 M, pH 7.2) at a scan rate of 10 mV s^{-1}. (B) Amperometric response at *o*-AP-modified (1) BVT and (2) DS SPEs in the presence of 20 μM ascorbic acid.

enhancement in the anodic current was observed at potentials close to the formal potential of the *o*-aminophenol/quinoneimine redox couple with a decrease in overpotential of ≅138 and 300 mV obtained for the *o*-AP-modified DS and BVT SPEs, respectively. The difference in overpotential between the two commercial SPEs may be due to the different composition of their manufacturing materials. The fact that there is less overpotential in DS would be an indication that the main factoring material is of *better* quality, and thus another advantage of their use. At both modified electrodes, a concomitant disappearance of the cathodic current was achieved, which indicates that *o*-AP is an effective mediator in the electrocatalytic oxidation of ascorbic acid in which the electrochemically formed *o*-quinoneimine chemically reacts with the ascorbic acid, while the simultaneous oxidation of the regenerated *o*-aminophenol causes an increase in the anodic current.[11] Fig. 2B represents the amperometric response at *o*-AP-modified BVT and DS SPEs in the presence of 20 μM ascorbic acid. The normalized catalytic current (I_p/A) calculated from the amperometric response, due to the catalytic oxidation of 20 μM ascorbic acid at *o*-AP-modified DS and BVT SPEs was 6.78 and 4.98 μA cm^{-2}, respectively, indicating a much more sensitive response at the modified DS SPEs than at the modified BVT SPEs. Owing to the better performance of the DS SPE in terms of response, reproducibility, as well as their low cost/sensor, we selected them for further experiments.

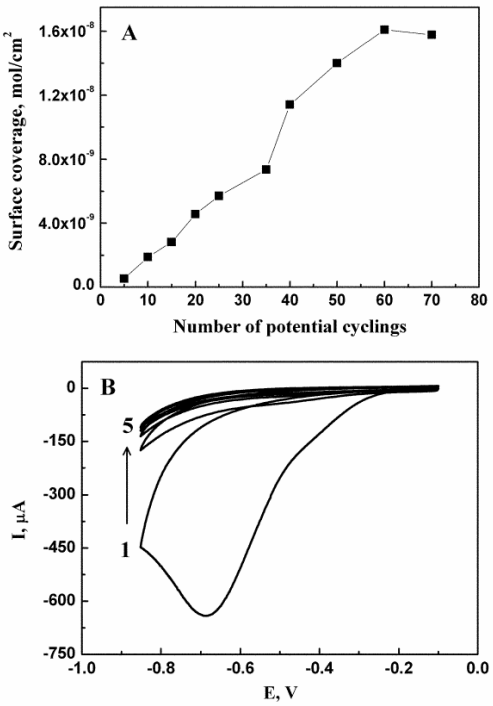

Fig. 3 (A) Influence of the number of the potential cycling on the surface coverage of the DS SPEs at 6 mM of *o*-nitro-*p*-aminophenol. (B) Cyclic voltammograms in 1.0 M H_2SO_4 at the *o*-nitrophenol-modified DS SPEs of five cycles (1→5) in the potential range of −0.1 to −0.85 V at a scan rate 100 mV s^{-1}.

Optimization of the grafting of the DropSens SPEs with *o*-AP

In order to achieve maximum sensitivity, a full surface coverage of *o*-AP active sites is desirable, and the parameters for electrografting of the *o*-AP film were optimized to achieve this goal. Two basic parameters are crucial to the success of the construction, operation and sensitivity of the ascorbic acid sensor: (i) the concentration of *o*-nitro-*p*-aminophenol which corresponds to the concentration of the '*in situ*'-generated *o*-nitrophenol diazonium salt concentration, and (ii) the deposition time (*i.e.* number of potential cycling, 10–70 cycles in the potential range 0.6 to −0.2 V) required for the electrochemical reduction of the diazonium salt.[32] As depicted in Fig. 3A, saturation of surface coverage is achieved after 60 cycles (corresponding to 32 min), with a high closely packed monolayer or multilayers of *o*-AP obtained. The possibility of using different concentrations of diazonium salts (6, 10, 13 mM) to optimize the SPE surface coverage was tested but it was found that at concentrations of 10 and 13 mM of diazonium salts a precipitation was observed during deposition, leading to the choice of the 6 mM concentration of *o*-nitro-*p*-aminophenol and 60 potential cycles at 50 mV s^{-1} as optimal. The modification of the SPEs surface using 60 potential sweeps could potentially produce a multilayer of *o*-AP film, but this did not affect the sensor performance.

Fig. 3B represents the cyclic voltammograms of the *o*-nitrophenol-modified DS SPEs, in 1 M H_2SO_4 solution at a 100 mV s^{-1} scan rate. The first reductive sweep gave a sharp irreversible cathodic peak at −0.688 V *vs.* Ag/AgCl, corresponding to the six-electron reduction reaction of the nitro groups to the amino group.[50] After the initial reduction of *o*-nitrophenol to *o*-aminophenol, a new oxidation/reduction peak pair appears on cycling into the positive potential range (−0.85 to +0.4 V) of the second scan (not shown) in a blank aqueous solution of H_2SO_4, attributable to the *o*-aminophenol/*o*-quinoneimine redox system. As shown in Fig. 3B, the cathodic peak completely disappeared in the second to the fifth reduction cycles. Therefore, the reduction of the nitro group of the *o*-nitrophenol film could be achieved by continuous potential cycling in H_2SO_4 between −0.1 and −0.85 V *vs.* Ag/AgCl-3 M NaCl, and five sweeps at the scan rate of 100 mV s^{-1} ensured complete reduction.

The surface coverage, Γ, of *o*-AP-modified DS and BVT SPEs was evaluated by cyclic voltammetry (not shown) in phosphate buffer (0.1 M, pH 7.2) in the potential range 0.6 to −0.1 V at a scan rate of 100 mV s^{-1}, from the equation $\Gamma = Q/nFA$, where Q is the charge from the area under the *o*-AP oxidation peak obtained in for the baseline, and other symbols have their usual meanings. In the present case, by assuming the number of electrons exchanged per reactant molecule: $n = 2$,[11] the mean value of the calculated Γ was 11.09 × 10^{-9} mol cm^{-2}, which is higher than the coverage calculated from theoretical calculations (5.0 × 10^{-10} mol cm^{-2}) and the coverage found for the formation of a close-packed monolayer of grafted 4-nitrophenyl groups on a glassy carbon electrode with a relatively close surface area.[11,31] As reported previously, the *o*-aminophenol molecules should be laterally aligned in an axial manner on the SPE.[11] The high surface coverage obtained was presumably due to the formation of multilayers of *o*-AP film.[33,34]

UNIVERSITAT ROVIRA I VIRGILI
BOTTOM-UP SURFACE ENGINEERING FOR THE CONSTRUCTION OF (BIO) SENSORING SYSTEMS: DESIGN STRATEGIES
AND ANALYTICAL APPLICATIONS
Hossam Metwally Ahmed Nassef
ISBN:978-84-692-3235-4/DL:T-932-2009

After modification, the CV of *o*-AP/SPEs in phosphate buffer showed that the oxidation peak height of the first scan was large, which rapidly decreased in the second scan, indicating the desorption of the physisorbed molecules. Therefore, repetitive cyclic voltammograms were carried out at the *o*-AP-modified SPEs in the potential range −0.1 to 0.6 V *vs.* Ag/AgCl-3 M NaCl, in phosphate buffer pH 7.2, in order to remove the physically adsorbed components until stable reproducible voltammograms were obtained.

Hydrodynamic amperometric detection of ascorbic acid

Amperometric measurements of ascorbic acid (2–20 μM) at constant applied potential (+200 mV *vs.* Ag/AgCl-3 M NaCl), performed in a magnetically stirred solution at pH 7.2, were carried out, and as can be seen in Fig. 4A, the current response was extremely rapid, achieving steady-state current within 1–2 s.

The current responses showed a linear relationship with the concentration of ascorbic acid (Fig. 4B) over the ranges of 2–20 μM with a sensitivity of 0.32 μA μM^{-1}, and a correlation coefficient of $r^2 = 0.998$. From the analysis of the data obtained from the calibration curve, the estimated limit of detection (LOD) of ascorbic acid was 0.86 μM. The precision of the method was excellent, with an RSD of 1.98% for eight repetitive measurements.

By comparing *o*-AP/DS SPEs with the reported sensors using poly(*N*-methylaniline)-modified Pt[51] and copper hexacyanoferrate deposited on carbon[52] for the detection of ascorbic acid, these reported sensors[51,52] have a higher LOD, of 5 and 2.1 μM, respectively, than our proposed sensor (0.82 μM), a value very similar to our previously reported *o*-AP/GCE[11] system (LOD = 0.3 μM). In addition, the use of *o*-AP-modified DS SPEs for the detection of ascorbic acid was found to be advantageous with respect to previously reported sensors[11,51,52] because DS-modified SPEs are cheap, easy and fast to prepare, highly reproducible and disposable, and therefore could be used in field applications.

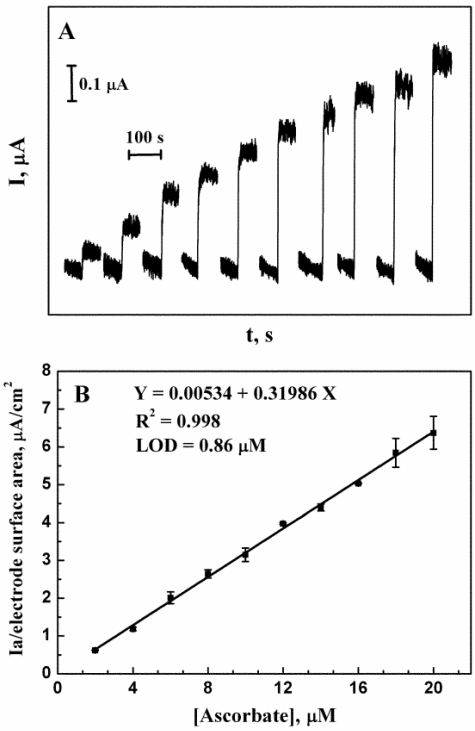

Fig. 4 (A) Amperometric response to successive injections of ascorbic acid concentration in 2, 4, 6, 8, 10, 12, 14, 16, 18 and 20 μM steps (final cell concentration) to stirred 5 ml of phosphate buffer solution (0.1 M, pH 7.2) at DS SPEs modified with *o*-AP; (B) typical calibration graph.

Stability of the *o*-AP-SPE sensor

The grafted *o*-aminophenol screen-printed electrodes were prepared according to the optimized conditions and were stored under vacuum at room temperature, and the stability of the grafted layer was tested on a weekly basis over a two month period and no loss of activity was observed. The operational stability of the sensors was studied by continuous exposure to the working buffer, measuring the produced current after injection of a 15 μM solution of ascorbic acid. The responses after one and three months of continuous use were 91.4 and 87% of the initial responses, respectively.

Conclusions

Commercial screen-printed electrodes from BVT Technologies and DropSens were grafted with a film of *o*-aminophenol, *via* the electrodeposition of the *in situ*-generated *o*-nitrophenol diazonium salt. Parameters for optimal grafting of the aminophenol film were determined by varying the length of electrodeposition time and concentration of the diazonium salt. These modified electrodes were used to study the electrocatalytic oxidation of ascorbic acid in phosphate buffer of pH 7.2, and showed excellent enhancement of the anodic current of ascorbic acid/dehydroascorbic acid redox couple with a decrease of ≅138 and 300 mV *vs.* Ag/AgCl in overpotential for the modified DS and BVT SPEs respectively. The resulting catalytic electrodes were applied to the determination of ascorbic acid, and their performances compared. Normalizing for the different areas of the SPEs, the DropSens-modified electrode showed much higher sensitivity and was used for further studies. In DC amperometry, the catalytic oxidation peak current was linearly dependent on ascorbic acid concentration in the range of 2–20 μM with a limit of detection of 0.86 μM. The *o*-AP DS SPE not only exhibited strong catalytic activity toward ascorbic acid but was also demonstrated to have excellent storage and operational stability, as well as a quantitatively reproducible analytical performance, and could be used for the facile, selective, rapid and precise determination of ascorbic acid. Future work will focus on the application of the disposable *o*-AP DS sensor for the detection of ascorbic acid in different vegetable and fruit samples, where the specificity of the sensor in complex matrices will be evaluated.

Acknowledgements

This work has been carried out with financial support from the Commission of the European Communities specific RTD programme 'Smart Integrated Biodiagnostic Systems for Healthcare', SMARTHEALTH, FP6-2004-IST-NMP-2-016817.

A. F. thanks Ministerio de Ciencia y Tecnología, Spain, for a 'Ramón y Cajal' Research Professorship. H. M. N. wishes to thank the Universitat Rovira i Virgili for a BRDI scholarship, and Abd Radi for his previous help.

References

1 S. Lupu, A. Mucci, L. Pigani, R. Seeber and C. Zanardi, *Electroanalysis*, 2002, **14**, 519.
2 L. R. Faulkner, *Chem. Eng. News*, 1984, **62**, 28.
3 O. Arrigoni and M. C. D. Tullio, *Biochem. Biophys. Acta*, 2002, **1569**, 1.
4 D. W. Martin, Jr., in *Harper's Review of Biochemistry*, ed. D. W. Martin, Jr., P. A. Mayes and V. W. Rodwell, Lange, Los Altos, CA, 19th edn, 1983, p. 112.
5 K. J. Stutts and R. M. Wightman, *Anal. Chem.*, 1983, **55**, 1576.
6 Y. K. Sung, S. Y. Hwang, S. Y. Cha, S. R. Kim, S. Y. Park, M. K. Kim and J. C. Kim, *J. Dermatol. Sci.*, 2006, **41**, 150.
7 M. W. Roomi, D. House, M. Eckert-Maksić, Z. B. Maksić and C. S. Tsao, *Cancer Lett.*, 1998, **122**, 93.
8 T. Takarada, E. Hinoi, Y. Kambe, K. Sahara, S. Kurokawa, Y. Takahata and Y. Yoneda, *Eur. J. Pharmacol.*, 2007, **575**, 1.
9 Y. Ochiai, S. Kaburagi, K. Obayashi, N. Ujiie, S. Hashimoto, Y. Okano, H. Masaki, M. Ichihashi and H. Sakurai, *J. Dermatol. Sci.*, 2006, **44**, 37.
10 L. Falat and H.-Y. Cheng, *J. Electroanal. Chem.*, 1983, **157**, 393.
11 H. M. Nassef, A. Radi and C. K. O'Sullivan, *Anal. Chim. Acta*, 2007, **583**, 182.
12 Z. Gao, A. Ivaska, T. Zha, G. Wang, P. Li and Z. Zhao, *Talanta*, 1993, **40**, 399.
13 J. Facci and R. W. Murray, *Anal. Chem.*, 1982, **54**, 772.
14 L. Zhang and J. Lian, *J. Electroanal. Chem.*, 2007, **611**, 51.
15 Q. Sheng, H. Yu and J. Zheng, *J. Electroanal. Chem.*, 2007, **606**, 39.
16 A. B. Florou, M. I. Prodromidis, M. I. Karayannis and S. M. Tzouwara-Karayanni, *Anal. Chim. Acta*, 2000, **409**, 113.
17 O. Bagel, B. Limoges, B. Schöllhorn and C. Degrand, *Anal. Chem.*, 1997, **69**, 4688.
18 A. Erlenkötter, M. Kottbus and G. C. Chemnitius, *J. Electroanal. Chem.*, 2000, **481**, 82.
19 O. D. Renedo, M. A. Alonso-Lomillo and M. J. A. Martínez, *Talanta*, 2007, **73**, 202.
20 H. J. Wang, H. Yu, F. Peng and P. Lv, *Electrochem. Commun.*, 2006, **8**, 499.
21 M. S. El-Deab, T. Sotomura and T. Ohsaka, *Electrochem. Commun.*, 2005, **7**, 29.
22 P. J. Collier, J. A. Iggo and R. Whyman, *J. Mol. Catal. A: Chem.*, 1999, **146**, 149.
23 F. Ghamouss, P.-Y. Tessier, A. Djouadi, M.-P. Besland and M. Boujtita, *Electrochim. Acta*, 2007, **52**, 5053.
24 R. L. McCreey and K. K. Cline, in *Laboratory Techniques in Electroanalytical Chemistry*, ed. P. T. Kissinger and W. R. Heinemann, Dekker, New York, 2nd edn, 1996, pp. 293 332.
25 J. Wang, *Analytical Electrochemistry*, VCH, New York, 1994.
26 J. Gonzalo-Ruiz, M. A. Alonso-Lomillo and F. J. Muñoz, *Biosens. Bioelectron.*, 2007, **22**, 1517.
27 B. Prieto-Simon, J. Macanas, M. Muñoz and E. Fabregas, *Talanta*, 2007, **71**, 2102.
28 R. W. Murray, in *Electroanalytical Chemistry*, ed. A. J. Bard, M. Dekker, New York, 1984, vol. 13, p. 221.
29 R. L. McCreery, in *Electroanalytical Chemistry*, ed. A. J. Bard, M. Dekker, New York, 1991, vol. 17, p. 221.
30 A. J. Downard and A. D. Roddick, *Electroanalysis*, 1995, **7**, 376.
31 M. Delamar, R. Hitmi, J. Pinson and J. M. Saveant, *J. Am. Chem. Soc.*, 1992, **114**, 5883.
32 P. Allongue, M. Delamar, B. Desbat, O. Fagebaume, R. Hitmi, J. Pinson and J. M. Saveant, *J. Am. Chem. Soc.*, 1997, **119**, 201.
33 J. K. Kariuki and M. T. McDermot, *Langmuir*, 2001, **17**, 5947.
34 F. Anariba, S. H. DuVall and R. L. McCreery, *Anal. Chem.*, 2003, **75**, 3837.
35 A. Radi, J. M. Montornés and C. K. O'Sullivan, *J. Electroanal. Chem.*, 2006, **587**, 140.
36 B. Ortiz, C. Saby, G. Y. Champagne and D. Bélanger, *J. Electroanal. Chem.*, 1998, **455**, 75.
37 H. M. Nassef, A. Radi and C. K. O'Sullivan, *Electrochem. Commun.*, 2006, **8**, 1719.
38 H. M. Nassef, A. Radi and C. K. O'Sullivan, *J. Electroanal. Chem.*, 2006, **592**, 139.
39 B. P. Corgier, C. A. Marquette and L. J. Blum, *Biosens. Bioelectron.*, 2007, **22**, 1522.
40 A. Vakurov, C. E. Simpson, C. L. Daly, T. D. Gibson and P. A. Millner, *Biosens. Bioelectron.*, 2004, **20**, 1118.
41 M. D. Carlo and M. Mascini, *Field Anal. Chem. Technol.*, 1999, **3**, 179.
42 R. Polsky, J. C. Harper, D. R. Wheeler, S. M. Dirk, D. C. Arango and S. M. Brozik, *Biosens. Bioelectron.*, 2008, **23**, 757.
43 E. Theodoridou, J. O. Besenhard and H. P. Fritz, *J. Electroanal. Chem.*, 1981, **124**, 87.
44 K. W. Leitner, B. Gollas, M. Winter1 and J. O. Besenhard, *Electrochim. Acta*, 2004, **50**, 199.
45 J. Wang, M. Pedrero, H. Sakslund, O. Hammerich and J. Pingarron, *Analyst*, 1996, **121**, 345.
46 G. Cui, J. H. Yoo, J. S. Lee, J. Yoo, J. H. Uhm, G. S. Cha and H. Nam, *Analyst*, 2001, **126**, 1399.
47 I. Hu, D. H. Karweik and T. Kuwana, *J. Electroanal. Chem.*, 1985, **188**, 59.
48 A. J. Bard and L. R. Faulkner, *Electrochemical Methods Fundamentals and Applications*, Wiley, New York, 2nd edn, 2001.
49 S. Antoniadou, A. D. Jannakoudakis and E. Theodoridou, *Synth. Met.*, 1989, **30**, 295.
50 M. Delamar, G. DeAsarmot, O. Fagebaume, R. Hitmi, J. Pinson and J.-M. Saveant, *Carbon*, 1997, **35**, 801.
51 K. Brazdziuviene, I. Jureviciute and A. Malinauskas, *Electrochim. Acta*, 2007, **53**, 785.
52 R. Pauliukaite, M. E. Ghica and C. M. A. Brett, *Anal. Bioanal. Chem.*, 2005, **381**, 972.

UNIVERSITAT ROVIRA I VIRGILI
BOTTOM-UP SURFACE ENGINEERING FOR THE CONSTRUCTION OF (BIO) SENSORING SYSTEMS: DESIGN STRATEGIES
AND ANALYTICAL APPLICATIONS
Hossam Metwally Ahmed Nassef
ISBN:978-84-692-3235-4/DL:T-932-2009

CHAPTER 6: (Art 5)

Amperometric determination of ascorbic acid in real samples using a disposable screen-printed electrode modified with electrografted *o*-aminophenol Film

(Laia Civit, Hossam M. Nassef, Alex Fragoso, and Ciara K. O'Sullivan, J. Agric. Food Chem., 2008, 56 (22), 10452-10455.)

10452 J. Agric. Food Chem. 2008, 56, 10452–10455

JOURNAL OF AGRICULTURAL AND FOOD CHEMISTRY

ARTICLES

Amperometric Determination of Ascorbic Acid in Real Samples Using a Disposable Screen-Printed Electrode Modified with Electrografted *o*-Aminophenol Film

LAIA CIVIT,[†] HOSSAM M. NASSEF,[†] ALEX FRAGOSO,*[,†] AND CIARA K. O'SULLIVAN*[,†,‡]

Nanobiotechnology and Bioanalysis Group, Department of Chemical Engineering, Universitat Rovira i Virgili, Tarragona 43007, Spain, and Institució Catalana de Recerca i Estudis Avançats, Passeig Lluís Companys 23, Barcelona 08010, Spain

Ascorbic acid (AA) is an antioxidant considered to play a crucial role in human health. Therefore, diverse methods for the determination of AA in foods have been developed, most of them time-consuming and requiring costly instrumentation. A simple and sensitive method for the quantification of AA in fresh fruits and vegetables and commercial juices using an amperometric sensor is presented on the basis of disposable screen-printed carbon electrodes (SPEs) modified with an *o*-aminophenol (*o*-AP) film selective for the detection of AA. The sensor exhibited a linear response for AA from 2−20 μM, with a correlation coefficient $r^2 = 0.998$ and a limit of detection of 0.86 μM. Common possible interferents of the sample matrices were tested, and results showed high selectivity of the *o*-AP SPEs toward AA. The sensor exhibited an excellent reproducibility (RSD% = 1.98, $n = 8$) and surface stability. The method was validated by a comparison to a reference method, and excellent correlation is obtained.

KEYWORDS: Amperometric sensor; ascorbic acid; electrocatalytic oxidation; diazonium salt; modified electrode; screen-printed electrodes; fruits; vegetables; commercial juices

INTRODUCTION

Ascorbic acid (AA, vitamin C) is a water-soluble antioxidant essential for life with widely recognized benefits (*1*). It is present in relatively high amounts in fresh fruit and vegetables and it is also added to pharmaceutical products and foodstuffs as an antioxidant and a stabilizer of aroma and color. Additionally, AA is used to cure scurvy (*2*). The content of AA in biological fluids is used to assess the amount of oxidative stress in human metabolism, a process that has been linked to cancer, diabetes mellitus, and several liver diseases (*3*). Epidemiological studies have shown that diets high in fruits and vegetables are associated with lower risk of cardiovascular failure, stroke, and cancer and with increased longevity, supporting the hypothesis that antioxidant activity may help to decrease the risk of such diseases (*4*). Thus, the development of inexpensive and easy methods for the determination of AA is particularly important in the pharmaceutical and food industry.

There are several reported methods for the detection of AA in foodstuffs, such as chromatography (*5*), spectrophotometry (*6*), capillary electrophoresis (*7*), and most recently, electrochemical methods (*8, 9*). Electrochemical methods have been performed using different electrode materials. The amperometric determination of AA is based on its electrochemical oxidation, which occurs at high potentials at carbon or metal electrodes, and fouling by oxidation products leads to poor reproducibility (*10*). Numerous attempts to decrease the high working potentials and improve reproducibility have been made by modifying the electrode surface with various active mediators for the electrochemical oxidation of AA (*10, 11*). Different approaches have been recently used for electrode modification and applied to the detection of AA, such as glassy carbon electrodes (GCEs) modified with a cellulose acetate film bearing 2,6-dichlorophenolindophenol (*12*) or by electropolymerization of *N*,*N*′-dimethylaniline (*13*), as well as carbon paste electrodes modified with calixarenes (*14*) and congo red dye absorbed on a silica/aniline xerogel (*15*). However, electrochemical AA determina-

* To whom correspondence should be addressed. Fax: +34-977-559621. E-mail: alex.fragoso@urv.cat (A.F.); ciara.osullivan@urv.cat (C.K.O.).
[†] Universitat Rovira i Virgili.
[‡] Institució Catalana de Recerca i Estudis Avançats.

10.1021/jf802536k CCC: $40.75
Published on Web 10/25/2008

UNIVERSITAT ROVIRA I VIRGILI
BOTTOM-UP SURFACE ENGINEERING FOR THE CONSTRUCTION OF (BIO) SENSORING SYSTEMS: DESIGN STRATEGIES
AND ANALYTICAL APPLICATIONS
Hossam Metwally Ahmed Nassef
ISBN:978-84-692-3235-4/DL:T-932-2009

Table 1. Weight and Volumes Extracted from Fresh Fruits and Vegetables for the Preparation of the Samples

sample	weight (g)	volume extracted (mL)
	Fruits	
apple	310.1	120
kiwi	143.7	74
lemon	130.3	90
orange	146.4	45
pineapple	387.6	224
strawberry	83.3	50
	Vegetables	
green pepper	302	197
tomato	266.2	224

tion in foodstuffs has been very limited (*16*−*18*). In particular, to the best of our knowledge, there is only one report on the application of the screen-printing technique for AA determination in fruits, despite the several advantages that they offer in terms of large-scale fabrication of disposable sensors, low cost, versatility, and miniaturization (*19*).

The modification of conductive surfaces through the grafting of organic groups (*20*) via the electrochemical reduction of aryl diazonium salts was first reported by Pinson in 1992 (*21*). We have recently use this strategy to electrograft *o*-aminophenol (*o*-AP) films on GCEs (*22*) and studied the electrocatalytic oxidation of AA in the presence of uric acid (*11*). Here, we report the applicability of modified *o*-AP screen-printed carbon electrodes (SPEs) for the detection of AA in a wide variety of fresh fruits and vegetables and commercial juices. Sensor selectivity, reproducibility, and stability have also been tested.

MATERIALS AND METHODS

Reagents. All chemicals were of analytical grade and used as received without any further purification. Solutions were prepared with MilliQ water (Millipore, Inc.; $\Omega = 18\ M\Omega\ cm^{-1}$). L-Ascorbic acid (99%) was purchased from Sigma Aldrich (Spain); 2-amino-4-nitrophenol was purchased from Acros (Spain); and disodium oxalate was purchased from Probus (Spain). Stock solutions of AA (1 mM) were prepared daily in degassed 0.1 M phosphate buffer at pH 7.2. For the spectrophotometric measurements, 2,6-dichlorophenolindophenol disodium salt (DCIP) was purchased from Fluka (Spain).

Instrumentation. Electrochemical experiments were carried out using an Autolab model PGSTAT 12 potentiostat/galvanostat controlled with the general purpose electrochemical system (GPES) software (Eco Chemie B.V., The Netherlands). The commercial screen-printed electrodes used (DropSens, Oviedo, Spain, ref 110) consisted of a carbon working electrode (4.0 mm in diameter), a Ag pseudo-reference electrode, and a carbon counter electrode.

Spectrophotometric measurements were performed with a Cary 100 Bio (Varian), UV−vis spectrophotometer at 520 nm.

Sample Preparation. Fresh fruits (apple, kiwi, lemon, orange, pineapple, and strawberry) and vegetables (green pepper and tomato) samples were obtained from a local supermarket (Mercadona). The commercial juices analyzed were lemon juice (Lemonada, Minute Maid), tomato juice (Hacendado), and refrigerated orange juice (Hacendado).

Fruit juices were first mixed with an extraction solution [1% (w/v) disodium oxalate] and centrifuged prior to dilution with the working buffer solution (0.1 M phosphate buffer at pH 7.2). For fruit and vegetable samples, a specific amount (**Table 1**) was weighed and mixed with 25 mL of 1% (w/v) disodium oxalate. The mixture was homogenized for 5 min with a Braun homogenizer. The extract was centrifuged at 3000 rpm for 15 min, and the supernatant was filtered through a 0.22 μm nylon filter. An aliquot of the recovered filtrate volume was diluted according to the AA content of the sample in 10 mL of 0.1 M phosphate buffer at pH 7.2 and applied to the electrochemical cell.

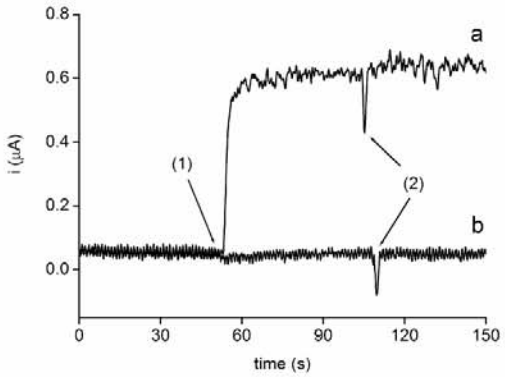

Figure 1. Amperometric response of *o*-AP-modified electrodes to 15 μM AA (1) followed by the addition of 0.15 mM citric acid (2). The arrows indicate the moment of the additions.

Electrode Modification. Briefly, surface-activated Dropsens SPEs of known area were immersed in 5 mL of a 6 mM 2-amino-4-nitrophenol diazonium salt solution, and 60 potential cycles were carried out between 0.6 and −0.2 V at 50 mV s^{-1} to electrochemically reduce the in situ generated *o*-nitrophenol diazonium salt. After modification, electrodes were washed with Milli-Q water, transferred to 1 M H_2SO_4, and subjected to five potential scans between −0.1 and −0.85 V at 100 mV s^{-1}, for complete reduction of the nitro group, providing an electrografted film of *o*-AP on the carbon SPE surface (*11*). The modified electrodes were subsequently subjected to a potential scan between −0.1 and 0.6 V for 10 cycles at 100 mV s^{-1} versus Ag in phosphate buffer (0.1 M, pH 7.2) to remove any physically adsorbed compounds and used.

Electrochemical Measurements. Hydrodynamic amperometric measurements were performed at a fixed potential of +200 mV (versus Ag) in a magnetically stirred solution at pH 7.2. After baseline stabilization, an aliquot of the AA containing solution was added to the stirred buffer solution, and the current response was measured after achieving steady state (typically 1−2 s).

Spectrophotometric Measurements (*6*). The instrument was adjusted to zero using a mixture of disodium oxalate 0.6% (w/v) (125 μL) and acetate buffer (300 g of anhydrous sodium acetate plus 700 mL of miliQ water plus 1000 mL of glacial acetic acid) (125 μL). The absorbance (A_1) of a mixture of disodium oxalate (50 μL) plus acetate buffer (50 μL) plus 12 mM DCIP (400 μL) was recorded at 15 s. The absorbance of a 10 ppm standard AA solution (50 μL) plus acetate buffer (50 μL) plus 12 mM DCIP (400 μL) was recorded as A_2. Values for A_2 were recorded for standard solutions (20, 30, 40, and 50 ppm). $A_1 - A_2$ values (the absorbance for each working standard) were calculated, and a calibration graph was constructed plotting $A_1 - A_2$ versus the AA concentration (data not shown). For the absorbance measurements of the samples, A_2 was the absorbance of sample solution (50 μL) plus acetate buffer (50 μL) plus 12 mM DCIP (400 μL). All of the measurements were recorded at 520 nm.

RESULTS AND DISCUSSION

Effect of Interference on the Determination of AA. To evaluate the selectivity of the *o*-AP SPE sensor, the effect of common potentially interfering compounds present in vegetable, fruit, and juice samples (organic acids, antioxidants, and sugars) was investigated. Concentrations typically higher than those of the natural levels expected in the food samples were tested by measuring the AA content of a 15 μM stock solution in the presence of the potential interferent (**Figure 1**). **Table 2** summarizes the percent of signal recovery of the determination of 15 μM AA in the presence of several organic hydroxyacids and sugars (citric acid, tartaric acid, glutamic acid, and oxalate and glucose, fructose, and sucrose). The average recovery ranged from 97.3 to 103.3%, indicating that the tested species did not

UNIVERSITAT ROVIRA I VIRGILI
BOTTOM-UP SURFACE ENGINEERING FOR THE CONSTRUCTION OF (BIO) SENSORING SYSTEMS: DESIGN STRATEGIES
AND ANALYTICAL APPLICATIONS
Hossam Metwally Ahmed Nassef
ISBN:978-84-692-3235-4/DL:T-932-2009

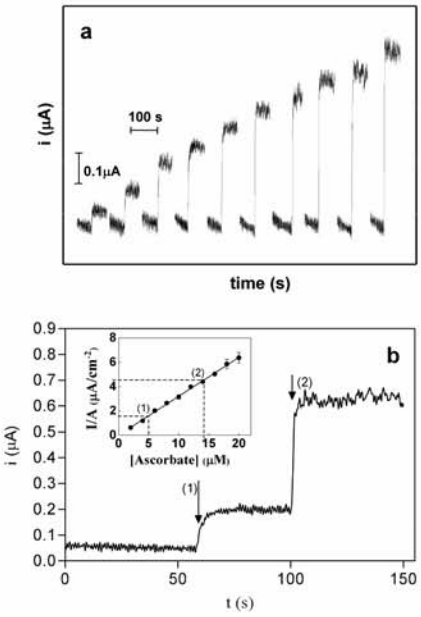

Figure 2. (a) Amperometric responses in 0.1 M phosphate buffer at pH 7.2 to successive injections of AA (2−20 μM) at *o*-AP-modified SPEs. (b) Amperometric response of (1) a diluted sample ($^{1.5}/_{1000}$) of freshly prepared orange juice sample and (2) a recovery test for the addition 15 μM AA. (Inset) Interpolation of the current values obtained in 1 and 2 in the calibration plot.

Table 2. Recovery of AA in the Presence of Some Possible Interferents at *o*-AP-Modified Screen-Printed Electrodes

additive	concentration (mM)	AA concentration (μM) added	AA concentration (μM) found	recovery of AA (%)
glucose	1.5	15	14.9	99.3
fructose	1.5	15	14.8	98.7
sucrose	1.5	15	14.6	97.3
citric acid	0.15	15	15.5	103.3
tartaric acid	0.15	15	14.8	98.7
glutamic acid	0.15	15	14.9	99.3
disodium oxalate	0.15	15	14.7	98.0

cause any interference and demonstrating the specificity and selectivity of the *o*-AP SPCE sensors to AA over a wide number of interfering compounds.

Sensor Calibration. Plots of the current response versus the concentration of AA over a dynamic range of 2−20 μM were obtained in triplicate (**Figure 2a**). They showed a linear behavior in the studied range with a sensitivity of 0.32 μA μM^{-1} (r^2 = 0.998). The precision of the method was excellent, with RSD of 1.98% (n = 8). The limit of detection (LOD) was 0.86 μM, which is lower than other reported methods using poly(*N*-methylaniline)-modified Pt (*23*) and copper hexacyanoferrate deposited on carbon (*24*) (LOD = 5 and 2.1 μM, respectively). Although there are also methods describing lower LOD values than that obtained in this work [0.015 (*16*), 0.2 (*25*), and 0.3 μM (*11*)], it allows for detection of AA at levels to $^{1}/_{10}$ those deemed permissible by regulatory agencies. In addition, our aim has been to optimize the method based on accuracy and precision rather that seeking very low detection limits, which would require higher dilution factors, thus introducing potential errors and possibly increasing the time required for the determination.

Table 3. Determination of the Content of AA in Fresh Fruit and Vegetables and Commercial Juices (n = 3) Using *o*-AP-Modified Sensor and Recovery Test Results

sample	amount of AA found (μM)	added (μM)	total (μM)	recovery (%)	total amount (mg/kg)	using reference method (mg/kg)
			Fruits			
lemon	4.3 ± 0.1	15	19.2	99.5	351 ± 4	343 ± 14
orange	5.0 ± 0.1	15	20.3	101.5	182 ± 4	174 ± 2
pineapple	15 ± 2	15	29.7	99.0	371 ± 8	363 ± 12
strawberry	4.7 ± 0.2	15	19.7	100.0	547 ± 6	565 ± 7
apple	3.4 ± 0.1	15	18.2	98.9	116 ± 1	118 ± 20
kiwi	3.4 ± 0.1	15	18.3	99.5	205 ± 3	ND[a]
			Vegetables			
tomato	15 ± 2	15	29.8	99.3	148 ± 13	115 ± 8
green pepper	1.7 ± 0.1	15	15.5	92.8	13.0 ± 0.4	13.8 ± 0.3
			Commercial Juices			
lemon	4.3 ± 0.1	15	19.3	100.0	15.1 ± 0.6[b]	12.2 ± 0.8[b]
orange[c]	3.9 ± 0.6	15	18.4	97.4	28 ± 1[b]	26 ± 1[b]
tomato	2.8 ± 0.2	15	17.9	100.6	13.2 ± 0.8[b]	14.02.8 ± 0.5[b]

[a] Not determined (see the text for details). [b] In units of mg/100 mL. [c] Refrigerated sample.

Analysis of Fruit Juices and Fresh Fruits and Vegetables. All amperometric measurements exhibited a stable and extremely rapid response (1−2 s) for AA oxidation at the selected potential. **Figure 2b** shows a typical amperometric response obtained for the sequential addition of orange juice and an AA stock solution and the interpolation of the response in the calibration plot. Verification of the method was carried out by measuring the AA content of the samples using a spectrophotometric method as indicated in ref *6*.

The AA content of the samples analyzed is detailed in **Table 3**. The method was applied to fruits and vegetables containing between 10 and 300 mg of AA per 100 g of the fresh sample. The comparison of the results obtained by the proposed method to those of the reference method demonstrated an excellent correlation. In the case of kiwi, the spectrophotometric measurement of AA contents was not possible because of a persistent turbidity on the extracted (homogenized) samples, which could not be possible to remove by either centrifugation (at 16 000 rpm for 30 min) or filtration through 0.2 μm nylon filters. This resulted in extremely high absorbance values for the blank solution (>2.5), making the measurement impossible to carry out. However, the obtained value for kiwi (205 mg/kg) matches well with the reported content of AA (40−260 mg/kg) in different species of this fruit (*26*).

In addition, different types of commercial juices were tested to determine the potential interfering effect of preservatives contained in the fruit juices. The results (**Table 3**) show that the detected amount of AA with the *o*-AP SPE of the refrigerated orange juice sample, which is the most natural juice of the tested ones, is in good agreement with the expected values. For lemon and tomato juice samples, which are more treated to ensure a longer shelf life of the products, the amounts of AA found were in good correlation with those given by the reference method.

To validate the sensor performance, recovery studies were carried out by adding standard solutions of AA to the sample and measuring the response of the sum of both the sample and standard concentrations. In all cases, recoveries of 92.8−101.5% were obtained, as shown in **Table 3**.

Stability of the *o*-AP SPE. To test the stability of the sensors, *o*-AP-modified electrodes were prepared and stored under vacuum at room temperature. Amperometric measurements were carried out weekly over a 5 months period, and a loss of 16%

of the initial activity was observed at the end of the fifth month. This characteristic indicates a high degree of robustness of the *o*-AP SPE, making them an attractive tool for the analytical determination of AA.

In conclusion, the applicability of the newly developed amperometric *o*-AP SPE sensor for the detection of AA in real samples has been demonstrated. The sensor exhibited high sensitivity and selectivity toward AA with excellent storage and operational stability, as well as a quantitatively reproducible analytical performance. It could be used for the facile, selective, rapid, and precise determination of AA in a large number of fruits and vegetables containing any amount of AA.

LITERATURE CITED

(1) Padayatty, S. J.; Katz, A.; Wang, Y.; Eck, P.; Kwon, O.; Lee, J. H.; Chen, S.; Corpe, C.; Dutta, A.; Dutta, S. K.; Levine, M. Vitamin C as an antioxidant: Evaluation of its role in disease prevention. *J. Am. Coll. Nutr.* **2003**, *22*, 18–35.

(2) Arrigoni, O.; De Tullio, M. C. Ascorbic acid: Much more than just an antioxidant. *Biochim. Biophys. Acta* **2002**, *1569*, 1–9.

(3) Stutts, K. J.; Wightman, R. M. Electrocatalysis of ascorbate oxidation with electrosynthesized, surface-bound mediators. *Anal. Chem.* **1983**, *55*, 1576–1579.

(4) Yokoyama, T.; Date, C.; Kokubo, Y.; Yoshiike, N.; Matsumura, Y.; Tanaka, H. Serum vitamin C concentration was inversely associated with subsequent 20-year incidence of stroke in a Japanese rural community. The Shibata study. *Stroke* **2000**, *31*, 2287–2294.

(5) Brause, A. R.; Woollard, D. C.; Indyk, H. E. Determination of total vitamin C in fruit juices and related products by liquid chromatography: Interlaboratory study. *J. AOAC Int.* **2003**, *86*, 367–374.

(6) Dürüst, N.; Sümengen, D.; Dürüst, Y. Ascorbic acid and element contents of food of Trabzon (Turkey). *J. Agric. Food Chem.* **1997**, *45*, 2085–2087.

(7) Wu, T.; Guan, Y.; Ye, J. Determination of flavonoids and ascorbic acid in grapefruit peel and juice by capillary electrophoresis with electrochemical detection. *Food Chem.* **2007**, *100*, 1573–1579.

(8) Pournaghi-Azar, M. H.; Razmi-Nerbin, H.; Hafezi, B. Amperometric determination of ascorbic acid in real samples using an aluminium electrode, modified with nickel hexacyanoferrate films by simple electroless dipping method. *Electroanalysis* **2002**, *14*, 206–212.

(9) Guanghan, L.; Yu, W.; Leiming, Y.; Shuanglong, H. Determination of ascorbic acid in fruits and vegetables by stripping voltammetry on a glassy carbon electrode. *Food Chem.* **1994**, *51*, 237–239.

(10) Falat, L.; Cheng, H.-Y. Electrocatalysis of ascorbate and NADH at a surface modified graphite-epoxy electrode. *J. Electroanal. Chem.* **1983**, *157*, 393–397.

(11) Nassef, H. M.; Radi, A.; O'Sullivan, C. K. Simultaneous detection of ascorbate and uric acid using a selectively catalytic surface. *Anal. Chim. Acta* **2007**, *583*, 182–189.

(12) Florou, A. B.; Prodromidis, M. I.; Karayannis, M. I.; Tzouwara-Karayanni, S. M. Flow electrochemical determination of ascorbic acid in real samples using a carbon electrode modified with a cellulose acetate film bearing 2,6-dichlorophenolindophenol. *Anal. Chim. Acta* **2000**, *409*, 113–121.

(13) Roy, P. R.; Saha, M. S.; Okajima, T.; Ohsaka, T. Electrooxidation and amperometric detection of ascorbic acid at GC electrode modified by electropolymerization of *N*,*N*-dimethylaniline. *Electroanalysis* **2004**, *16*, 289–297.

(14) Ijeri, V. S.; Algarra, M.; Martins, A. Electrocatalytic determination of vitamin C using calixarene modified carbon paste electrodes. *Electroanalysis* **2004**, *16*, 2082–2086.

(15) Pavan, F. A.; Ribeiro, E. S.; Gushikem, Y. Congo red immobilized on a silica/aniline xerogel: Preparation and application as an amperometric sensor for ascorbic acid. *Electroanalysis* **2005**, *17*, 625–629.

(16) Tian, L.; Chen, L.; Liu, L.; Lu, N.; Song, W.; Xu, H. Electrochemical determination of ascorbic acid in fruits on a vanadium oxide polypropylene carbonate modified electrode. *Sens. Actuators, B* **2006**, *113*, 150–155.

(17) Hasebe, Y.; Akiyama, T.; Yagisawa, T.; Uchiyama, S. Enzymeless amperometric biosensor for L-ascorbate using poly-L-histidine-copper complex as an alternative biocatalyst. *Talanta* **1998**, *47*, 1139–1147.

(18) Guorong, Z.; Xiaolei, W.; Xingwang, S.; Tianling, S. β-Cyclodextrin–ferrocene inclusion complex modified carbon paste electrode for amperometric determination of ascorbic acid. *Talanta* **2000**, *51*, 1019–1025.

(19) Kulys, J.; D'Costa, E. J. Printed electrochemical sensor for ascorbic acid determination. *Anal. Chim. Acta* **1991**, *243*, 173–178.

(20) Downard, A. J.; Roddick, A. D. Protein adsorption at glassy carbon electrodes: The effect of covalently bound surface groups. *Electroanalysis* **1995**, *7*, 376–378.

(21) Delamar, M.; Hitmi, R.; Pinson, J.; Saveant, J. M. Covalent modification of carbon surfaces by grafting of functionalized aryl radicals produced from electrochemical reduction of diazonium salts. *J. Am. Chem. Soc.* **1992**, *114*, 5883–5884.

(22) Radi, A.; Montornés, J. M.; O'Sullivan, C. K. Reagentless detection of alkaline phosphatase using electrochemically grafted films of aromatic diazonium salts. *J. Electroanal. Chem.* **2006**, *587*, 140–147.

(23) Brazdziuviene, K.; Jureviciute, I.; Malinauskas, A. Amperometric ascorbate sensor based on conducting polymer: Poly(*N*-methylaniline) versus polyaniline. *Electrochim. Acta* **2007**, *53*, 785–791.

(24) Pauliukaite, R.; Ghica, M. E.; Brett, C. M. A. A new, improved sensor for ascorbate determination at copper hexacyanoferrate modified carbon film electrodes. *Anal. Bioanal. Chem.* **2005**, *381*, 972–978.

(25) Wang, S.; Du, D. Differential pulse voltammetry determination of ascorbic acid with ferrocene–L-cysteine self-assembled supramolecular film modified electrode. *Sens. Actuators, B* **2004**, *97*, 373–378.

(26) Ferguson, A. R.; MacRae, E. A. Vitamin C in *Actinidia*. *Acta Hortic.* **1991**, *297*, 481–487.

Received for review June 19, 2008. Revised manuscript received September 22, 2008. Accepted September 23, 2008. This work has been carried out with financial support from Agència de Gestió d'Ajuts Universitaris i de Recerca to the Grup de Recerca de la Interfície Físico/biologica (INTERFIBIO), Grant 2005SGR00851. A.F. thanks Ministerio de Ciencia y Tecnología, Spain, for a "Ramón y Cajal" Research Professorship. L.C. and H.M.N. thank the European Communities specific RTD program Smart Integrated Biodiagnostic Systems for Healthcare, SmartHEALTH (FP6-2004-IST-NMP-2-016817) for a project and BRDI scholarship, respectively.

JF802536K

UNIVERSITAT ROVIRA I VIRGILI
BOTTOM-UP SURFACE ENGINEERING FOR THE CONSTRUCTION OF (BIO) SENSORING SYSTEMS: DESIGN STRATEGIES AND ANALYTICAL APPLICATIONS
Hossam Metwally Ahmed Nassef
ISBN:978-84-692-3235-4/DL:T-932-2009

CHAPTER 7: (Art 6)

Electrochemical Immunosensor for Detection of Celiac Disease Toxic Gliadin in Foodstuff

(Hossam M. Nassef, M. Carmen Bermudo Redondo, Paul J. Ciclitira, H. Julia Ellis, Alex Fragoso, and Ciara K. O'Sullivan, Anal. Chem., 2008, 80 (23), 9265-9271.)

Anal. Chem. **2008**, *80*, 9265–9271

Electrochemical Immunosensor for Detection of Celiac Disease Toxic Gliadin in Foodstuff

Hossam M. Nassef,[†] M. Carmen Bermudo Redondo,[†] Paul J. Ciclitira,[‡] H. Julia Ellis,[‡] Alex Fragoso,*[,†] and Ciara K. O'Sullivan*[,†,§]

Nanobiotechnology & Bioanalysis Group, Department of Chemical Engineering, Universitat Rovira i Virgili, Avinguda Països Catalans 26, 43007 Tarragona, Spain, Division of Nutritional Sciences, Rayne Institute, King's College London, St. Thomas' Hospital, Westminster Bridge Road, London SE1 7EH, U.K., and Institució Catalana de Recerca i Estudis Avançats (ICREA), Passeig Lluís Companys 23, 08010 barcelona, Spain

Celiac disease is a gluten-sensitive enteropathy that affects as much as 1% of the population. Patients with celiac disease should maintain a lifelong gluten-free diet, in order to avoid serious complications and consequences. It is essential to have methods of analysis to reliably control the contents of gluten-free foods, and there is a definitive need for an assay that is easy to use, and can be used on site, to facilitate the rapid testing of incoming raw materials or monitoring for gluten contamination, by industries generating gluten-free foods. Here, we report on the development of an electrochemical immunosensor exploiting an antibody raised against the putative immunodominant celiac disease epitope, for the measurement of gliadin content and potential celiac toxicity of a foodstuff. To develop the gliadin immunosensor, we explored the use of two surface chemistries, based on the use of dithiols, 22-(3,5-bis((6-mercaptohexyl)oxy)phenyl)-3,6,9,12,15,18,21-heptaoxadocosanoic acid (1) and 1,2-dithiolane-3-pentanoic acid (thioctic acid) (2), for anchoring of the capture antibody. The different surface chemistries were evaluated in terms of time required for formation of self-assembled monolayers, stability, susceptibility to nonspecific binding, reproducibility, and sensitivity. The thioctic acid self-assembled monolayer took more than 100 h to attain a stable surface and rapidly destabilized following functionalization with capture antibody, while the heptaoxadocosanoic acid surface rapidly formed (less than 3 h) and was stable for at least 5 days, stored at room temperature, following antibody immobilization. Both surface chemistries gave rise to highly sensitive immunosensors, with detection limits of 5.5 and 11.6 ng/mL being obtained for 1 and 2, respectively, with nonspecific binding of just 2.7% of the specific signal attained. The immunosensors were extremely reproducible, with RSD of 5.2 and 6.75% obtained for 1 and 2 (n = 5, 30 ng/mL), respectively. Finally, the immunosensor was applied to the analysis of commercial gluten-free and gluten-containing raw and processed foodstuffs, and excellent correlation achieved when its performance compared to that of an ELISA.

Gluten sensitivity, manifesting as celiac disease (CD), affects possibly 1:100 people in Northern Europe and North America.[1,2] Celiac disease is an inflammatory disease of the upper small intestine, results from gluten ingestion in genetically susceptible individuals, and is the only lifelong nutrient-induced enteropathy.[3,4] The small bowel abnormalities are reversed on withdrawal of gluten from the diet. CD is a familial condition with ~10−15% of first degree relatives being similarly affected.[5]

Celiac disease, when untreated or poorly treated, that is with continued ingestion of gluten, leads to a large number of complications, [6,7] which can result in considerable morbidity and repeated hospital visits. In children, symptoms such as growth retardation among others are observed[8,9] and patients with osteoporosis have a higher prevelance of CD,[10] with bone mineral density in CD patients improving with a gluten-free diet.[11] Up to 50% of women with untreated celiac disease experience miscarriage, and long-term, silent undiagnosed celiac disease can lead to infertility.[12] The condition is also strongly associated with other autoimmune conditions.[13,14] Celiac disease sufferers who do not adhere to a strict gluten-free diet have an increased incidence of a fatal small intestinal lymphoma,[15,16] and the standardized mortality rate is twice that of the general population, non-Hodgkin lymphoma being the main cause of death.[17]

Dieterich and colleagues identified tissue transglutaminase as the autoantigen of celiac disease,[18] which was supported by a publication by Arentz-Hanson et al.,[19] the sequence identified was further backed up by Anderson et al., and it was later shown that

* To whom correspondence should be addressed. E-mail: alex.fragoso@urv.cat; ciara.osullivan@urv.cat.
[†] Universitat Rovira i Virgili.
[‡] King's College London.
[§] Institució Catalana de Recerca i Estudis Avançats (ICREA).

10.1021/ac801620j CCC: $40.75 © 2008 American Chemical Society
Published on Web 10/29/2008

(1) Lee, S. K.; Green, P. H. R. *Curr. Opin. Rheumatol.* **2006**, *18*, 101.
(2) Dube, C.; Rostom, A.; Sy, R.; Cranney, A.; Salojee, N.; Garritty, C.; Sampson, M.; Zhang, L.; Yazdi, F.; Mamaladze, V.; Pan, I.; MacNeil, J.; Mack, D.; Patel, D.; Moher, D. *Gastroenterology* **2005**, *128*, S57.
(3) Maki, M.; Collin, P. *Lancet* **1997**, *34*, 9–1755.
(4) Turski, A.; Georgetti, G.; Brandimarte, G.; Rubino, E.; Lombardi, D. *Hepatogastroenterology* **2001**, *48*, 462.
(5) Marsh, M. N. *Gastroenterology* **1992**, *102*, 330.
(6) Fasano, A.; Catassi, C. *Gastroenterology* **2001**, *120*, 636.
(7) Green, P. H. R. *Gastroenterology* **2005**, *128*, S74.
(8) Farrell, R. J.; Kelly, C. P. *N. Engl. J. Med.* **2002**, *346*, 180.
(9) Catassi, C.; Fabiani, E. *Baillieres Clin. Gastroenterol.* **1997**, *11*, 485.
(10) Stenson, W.; Newberry, R.; Lorenz, R.; Baldus, C. *Civitelli R. Arch. Intern. Med.* **2005**, *28*, 393.
(11) Mustalahti, K.; Collin, P.; Sievanen, H.; Salmi, J.; Maki, M. *Lancet* **1999**, *2*, 8–744.
(12) Rostami, K.; Steegers, E. A. P.; Wong, W. Y.; Braat, D. D.; Steegers-Theunissen, R. P. M *Eur. J. Obstet. Gynecol. Reprod. Biol.* **2001**, *96*, 146.
(13) Ventura, A.; Magazzu, G.; Greco, L. *Gastroenterology* **1999**, *117*, 297.
(14) Corrao, G.; Corazza, G. R.; Bagnardi, V.; Brusco, G.; Ciacci, C.; Cottone, M.; Sattegna Guidetti, C.; Usai, P.; Cesari, P.; Pelli, M.; Loperfido, S.; Volta, U.; Calabro, A.; Certo, M. *Lancet* **2001**, *4*, 356.
(15) Cooper, B.; Holmes, G.; Cooke, W. *Digestion* **1982**, *23*, 89.
(16) West, J.; Logan, R.; Smith, C.; Hubbard, R.; Card, T. *Br. Med. J.* **2004**, *25*, 716.

UNIVERSITAT ROVIRA I VIRGILI
BOTTOM-UP SURFACE ENGINEERING FOR THE CONSTRUCTION OF (BIO) SENSORING SYSTEMS: DESIGN STRATEGIES
AND ANALYTICAL APPLICATIONS
Hossam Metwally Ahmed Nassef
ISBN:978-84-692-3235-4/DL:T-932-2009

a 19-mer peptide formed by the two overlapping peptides of Arentz-Hansen is indeed disease activating to the small intestines of celiac disease patients in vivo, causing the classic parameters of the condition.[21]

The development of legislation on levels of gluten permissible in foods labeled as gluten-free has been hampered by lack of a suitable assay system. The present standard has stood since 1981 (Codex Stan 118−1981) and is very nonspecific.[22,23] Codex Alimentarius have recently approved new standards for gluten-free foods (July 2008). The new benchmark states that foods labeled "gluten-free" may not exceed a gluten content of 20 ppm, while those with a gluten content to a level between 20 and 100 ppm may be called "low gluten" or "reduced gluten". A range of methods for the detection of gliadin have been reported, such as the use of gluten-specific PCR,[24,25] and SDS-PAGE in combination with immunoblotting, counter-immunoelectrophoresis, or mass spectroscopy and MALDI-TOF analysis.[26] High-performance liquid chromatography and capillary electrophoresis have been widely used to analyze prolamins in food,[27,28] and gel permeation high-performance liquid chromatography has been described for the quantitative determination of gliadin. More recent reports have looked at the use of flow cytometry detecting as low as 10 pg/mL levels of gliadin,[29] as well as the first report of a biosensor for gliadin detection, which exploited the use of a recombinant glutamine-binding protein.[30] The same group have gone on to report a fluorescence correlation spectroscopy assay, reporting a detection limit of 0.006 ppm, which would require huge dilution of extracts from gluten-free samples for detection.[31]

The most common method of measurement of gliadin is that of the enzyme-linked immunosorbent assay (ELISA). Early assays used whole gliadin as the immunogen to produce polyclonal antisera and gave rise to antibodies that were insufficiently specific, for example, giving spurious cross-reactivities with nontoxic maize.[32] Later, advantage was taken of monoclonal antibody technology to produce more precisely targeted reagents.[33] The first toxic sequence to be identified in vivo was A-gliadin 31−49,[34] and a monoclonal antibody has been raised against the celiac-toxic 19-mer A-gliadin peptide (LGQQQPFP-PQQPYPQPQPF) and used for detection of gliadin and gluten hydrolysates.[35,36]

Two commercial immunoassays are currently available. The first is based on a monoclonal antibody to the heat-stable ω-gliadin fraction;[37] however, measurement of this subfraction with extrapolation to total gliadin has theoretical errors of −44 to +80%.[38] The R5 method[39] has been proposed as the standard method of gluten analysis to back up the Draft Codex Standard (2003) on gluten-free foods, but this method weakly recognizes the immunodominant gliadin T cell stimulating epitope,[19,20] and measurement of this important epitope is highly pertinent. It can be argued that measurement of the immunodominant T cell epitope is the method more likely to give a true indication of the potential celiac toxicity of a foodstuff. Moreover, there is a definitive need for an assay that is easy to use and can be used on site, so that industries generating gluten-free foods can rapidly test incoming raw materials as well as checking for gluten contamination throughout the food production process.

Here, we report the use of an electrochemical immunosensor exploiting an antibody, coined CDC5, which was raised against the putative immunodominant celiac disease toxic epitope of α-gliadin, 56−75. Immunosensors offer the advantages of being easy to use, inexpensive, rapid, and in this particular case, importantly they can be used in situ allowing rapid assay turnaround time in labeled or labeless formats.[40,41] This facilitates punctual measurement of gliadin levels throughout a food production lifetime as well as control of raw materials. The immunosensor we report herein is highly sensitive, detecting low ppb levels of gliadin, and a reliable quantitative detection of gliadin content can be attained within 90 min, with minimal requirement of operator manipulation. Moreover, the immunosensor exploits a monoclonal antibody that can be correlated with celiac disease toxic gliadin, giving a correct indication of toxicity, rather than total gliadin content. Furthermore, the reported immunosensor is extremely reproducible, compatible with solvents required for extraction of gliadin from foodstuffs, and demonstrates excellent correlation with ELISA when applied to the detection of real samples.

EXPERIMENTAL SECTION

Chemicals and Materials. 1. Materials. Dithiol **1** (22-(3,5-bis((6-mercaptohexyl)oxy)phenyl)-3,6,9,12,15,18,21-heptaoxadocosanoic acid) was purchased from SensoPath Technologies (Bozeman, MT) and used as received. One mM stock solution

(17) Jacobson, D. L.; Gange, S. J.; Rose, N. R.; Graham, N. M. *Clin. Immunol. Immunopathol.* **1997**, *84*, 223.
(18) Dieterich, W.; Ehnis, T.; Bauer, M.; Donner, P.; Volta, U.; Riecken, E. O.; Schuppan, D. *Nat. Med.* **1997**, *3*, 797.
(19) Arentz-Hansen, H.; Körner, R.; Molberg, O.; Quarsten, H.; Vader, W.; Kooy, Y. M.; Lundin, K. E.; Koning, F.; Roepstorff, P.; Sollid, L. M.; McAdam, S. N. *J. Exp. Med.* **2000**, *191*, 603.
(20) Anderson, R. P.; Degano, P.; Godkin, A. J.; Jewell, D. P.; Hill, A. V. S. *Nat. Med.* **2000**, *6*, 337.
(21) Fraser, J. S.; Engel, W.; Ellis, H. J.; Moodie, S. J.; Pollock, E. L.; Wieser, H.; Ciclitira, P. J. *Gut* **2003**, *52*, 1698.
(22) Skerritt, J. H.; Hill, A. S. *Cereal Chem.* **1992**, *69*, 110.
(23) Codex Alimentarius Commission. Standard for Gluten-Free Foods. FAO/WHO 1981; p 118.
(24) Allmann, M.; Candrian, U.; Hofelein, C.; Luthy, J. *Z. Lebensm. Unters. Forsch.* **1993**, *196*, 248.
(25) Köppel, E.; Stadler, M.; Luthy, J.; Hubner, P. *Z. Lebensm. Unters. Forsch.* **1998**, *206*, 399.
(26) Méndez, E.; Valdés, I.; Camafeita, E. *Methods Mol. Biol.* **2000**, *146*, 355.
(27) Nicolas, Y.; Martinant, J.-P.; Denery-Papini, S.; Popineau, Y. *J. Sci. Food Agric.* **1998**, *77*, 96.
(28) Wieser, H.; Seilmeier, W.; Belitz, H.-D. *J. Cereal Sci.* **1994**, *19*, 149.
(29) Capparrelli, R.; Ventimaglia, I.; Longobardo, L.; Iannelli, D. *Cytometry A* **2006**, *63A*, 108.
(30) De Stefano, L.; Rossi, M.; Staiano, M.; Mamone, G.; Parracino, A.; Rotirotti, L.; Rendina, I.; Rossi, M.; D'Auria, S. *J. Proteome Res.* **2006**, *5*, 1241.
(31) Varriale, A.; Rossi, M.; Staiano, M.; Terpetschnig, E.; Barbieri, B.; Rossi, M.; D'Auria, S. *Anal. Chem.* **2007**, *79*, 4687.
(32) Troncone, R.; Vitale, M.; Donatiello, A.; Farris, E.; Rossi, G.; Auricchio, S. *J. Immunol. Methods* **1986**, *92*, 21.
(33) Freedman, A. R.; Galfre, G.; Gal, E.; Ellis, H. J.; Ciclitira, P. J. *J. Immunol. Methods* **1987**, *98*, 123.
(34) Sturgess, R. P.; Day, P.; Ellis, H. J.; Lundin, K.; Gjertsen, H.; Kontakou, M.; Ciclitira, P. J. *Lancet* **1994**, *343*, 756.
(35) Ellis, H. J.; Rosen-Bronson, S.; O'Reilly, N.; Ciclitira, P. J. *Gut* **1998**, *43*, 190.
(36) Bermudo-Redondo, M. C.; Griffen, P. B.; Garzon Ranaz, M.; Ellis, H. J.; Ciclitira, P. J.; O'Sullivan, C. K. *Anal. Chim. Acta* **2005**, *551*, 105.
(37) Skerritt, J.; Hill, A. *J. Assoc. Off. Anal. Chem.* **1991**, *74*, 257.
(38) Wieser, H.; Seilmeier, W.; Belitz, H.-D. *J. Cereal Sci.* **1994**, *19*, 149.
(39) Valdes, I.; Garcia, E.; Llorente, M.; Mendez, E. *Eur. J. Gastroenterol. Hepatol.* **2003**, *15*, 465.
(40) Warsinke, A. *Adv. Biochem. Eng. Biotechnol.* **2008**, *109*, 155.
(41) Fragoso, A.; Laboria, N.; Latta, D.; O'Sullivan, C. K. *Anal. Chem.* **2008**, *80*, 2556.

was prepared in absolute ethanol, purged with argon, and kept at −20 °C when stored. The Prolamin Working Group (PWG, martin.stern@med.unituebingen.de) provided a gliadin preparation[42] to be used as a basis for standardizing the analysis and detection of gliadin. Monoclonal antigliadin CDC5 antibody[43] and rabbit polyclonal antigliadin[44] (PAb) were developed by Ellis and Ciclitira as previously reported. Goat antimouse IgG (Fc specific) alkaline phosphatase conjugate, (±)-1,2-dithiolane-3-pentanoic acid (lipoic acid, **2**), N-(3-dimethylaminopropyl)-N′-ethylcarbodiimide (EDC), *N*-hydroxysuccinimide (NHS), bovine serum albumin (BSA), and phosphate-buffered saline (PBS) with 0.05% Tween 20 (dry powder) were purchased from Sigma-Aldrich. *p*-Aminophenylphosphate monosodium salt (*p*-APP) was purchased from LKT laboratories Inc. and was used as received. All aqueous solutions were prepared with Milli-Q water (Millipore Inc., Ω = 18 MΩ·cm). Gliadin stock solutions were freshly prepared in PBS−Tween containing 60% (v/v) ethanol and diluted in the appropriate buffer. Prostate-specific antigen (PSA) and anti-PSA monoclonal antibody (α-PSA) were provided by Fujirebio Diagnostics AB, Sweden.

2. Electrochemical Instrumentation. All the electrochemical measurements were performed using a PGSTAT12 potentiostat (Autolab) controlled with the General Purpose Electrochemical System software, with built-in frequency response analyzer FRA2 module. A three-electrode configuration of Ag/AgCl−3 M NaCl as a reference (CH Instruments., model CHI111), Pt wire as a counter (BAS model MW-1032), and bare or modified Au (BAS model MF-2014, 1.6-mm diameter) as working electrode was used. All the impedance measurements were carried out in 0.1 M PBS (pH 7.4) containing 1 mM $Fe(CN)_6^{3-}$ and 1 mM $Fe(CN)_6^{4-}$ within the frequency range of 0.1 Hz−100 kHz at a bias potential of +0.22 V and ac amplitude of 5 mV.

Surface Chemistry. 1. Optimization of Time Required for Self-Assembled Monolayer (SAM) Formation. Prior to the electrode modification, the gold surfaces were extensively cleaned by polishing in a slurry of alumina powder of 0.3 μm to a mirror finish and then sonicated in Milli-Q water and in ethanol for 5 min to remove any alumina remnants. The electrodes were placed in hot (∼70 °C) Piranha's solution (1:3 v/v, 30% H_2O_2, in concentrated H_2SO_4) for 5 min, thoroughly washed with Milli-Q water, and ethanol, and then dried with dry nitrogen. (*Warning:* Piranha solution is highly corrosive and violently reactive with organic materials; this solution is potentially explosive and must be used with extreme caution.) The bare electrodes were characterized using cyclic voltammetry (CV) and faradic impedance spectroscopy in $Fe(CN)_6^{3-/4-}$ in PBS (0.1 mM, pH 7.4). The formation of self-assembled monolayers was facilitated by immersion of the cleaned Au electrodes in 1 mM ethanolic solutions **1** or **2**, and the time dependence of EIS variations was recorded between 0 and 180 min for **1** and 0.5 and 312 h for **2**. R_{ct} values were calculated for different exposure times using the Autolab impedance analysis software.

2. Stability of Antibody-Modified SAMs of 1 and 2. Clean electrodes were immersed in an ethanolic solution of **1** and **2** for 3 and 120 h, respectively. The carboxylic acid groups of the SAM of both **1** and **2** modified electrodes were activated by stirring in 0.1 M MES buffer (pH 5) containing 0.2 M EDC and 50 mM NHS for 15 min, followed by incubation of the electrode with 100 μg/mL PAb in PBS (pH 7.4) for 1 h at 4 °C. The residual activated carboxylic groups were blocked with 1 M ethanolamine solution (pH 8.5) for 15 min. The EIS was recorded in $Fe(CN)_6^{3-/4-}$ in PBS (0.1 mM, pH 7.4) every day for seven days.

3. Nonspecific Binding and Cross-Reactivity Studies of the SAMs. The nonspecific binding and cross-reactivity studies were carried out using EIS in $Fe(CN)_6^{3-/4-}$ in PBS (0.1 M, pH 7.4) solution. Different conditions were used to study the nonspecific binding, using 20 μg/mL PWG: (i) EIS was recorded before and after incubation of the corresponding SAM with PWG for 30 min; (ii) the SAM-modified electrodes were first immersed in 0.05 M PBS−Tween (in the absence and in the presence of 0.1% w/v BSA) for 30 min followed by incubation with PWG; (iii) the modified gold electrodes were EDC/NHS activated for 15 min followed by immersion in a 100 μg/mL solution of PAb or anti-PSA (as nonspecific antibody) in PBS pH 7.4 for 1 h at 4 °C. The remaining carboxyl groups for both SAMs **1** and **2** were then blocked with 1 M ethanolamine hydrochloride (pH 8.5) for 15 min, followed by a second blocking step by incubation in 0.05 M PBS−Tween and 0.1% w/v BSA (in PBS−Tween), respectively, for 30 min. EIS of the antibody-modified surface was recorded in $Fe(CN)_6^{3-/4-}$ before and after incubation with 20 μg/mL of the corresponding protein (PSA or PWG, respectively) for 30 min.

Biosensor Fabrication and Calibration. 1. Formation and Characterization of the Sandwich Assay. SAM formation was carried out at their corresponding optimal times, followed by activation of the carboxylic groups and immobilization of PAb as previously described. Following blocking in ethanolamine hydrochloride, the modified surfaces of **1** or **2** were incubated in PBS−Tween (0.05 M, pH 7.4) and in 0.1% w/v BSA (in PBS−Tween) solutions, respectively, for 30 min. The electrodes were then exposed to different concentrations of PWG (10−60 ng/mL) in PBS−Tween solution for 30 min, followed by incubation with 100 μg/mL CDC5 in PBS for 30 min and 100 μg/mL α-mouse-ALP in PBS for 15 min. Each building step during the fabrication of the biosensor was characterized by CV and EIS using $Fe(CN)_6^{3-/4-}$ in PBS solution as electroactive marker.

2. Optimization of Incubation Time of PWG. The incubation time of the specific recognition between PWG and the immobilized PAb was optimized as follows. The SAM-modified electrodes were biofunctionalized with PAb and blocked as described in the previous section. The electrodes were then incubated with 20 μg/mL PWG in PBS−Tween solution at different incubation times (2, 10, 15, 20, 30, and 45 min), followed by sequential interaction with 100 μg/mL CDC5 for 30 min and 100 μg/mL α-mouse-ALP for 15 min. The immunosensors were subsequently immersed in Tris buffer solution (0.1 M, pH 9) containing 0.1 mM $MgCl_2$ and 0.1 mM $ZnSO_4$ in the presence of 10 mM *p*-APP. The differential pulse voltammetry (DPV) response was then recorded after 10 min of stirring in *p*-APP solution in

(42) van Eckert, R.; Berghofer, E.; Ciclitira, P. J.; Chirdo, F.; Denery-Papini, S.; Ellis, H. J.; Ferranti, P.; Goodwin, P.; Immer, U.; Mamone, G.; Méndez, E.; Mothes, T.; Novalin, S.; Osman, A.; Rumbo, M.; Stern, M.; Thorell, L.; Whim, A.; Wieser, H. *J. Cereal Sci.* **2006**, *43*, 331.

(43) Ciclitira, P. J.; Dewar, D. H.; Suligoj, T.; O'Sullivan, C. K.; Ellis, H. J. *Proceedings of the 12th International Celiac Symposium*, 2007, New York. In press.

(44) Ciclitira, P. J.; Ellis, H. J.; Evans, D. J.; Lennox, E. S. *Br. J. Nutr.* **1985**, *53*, 39.

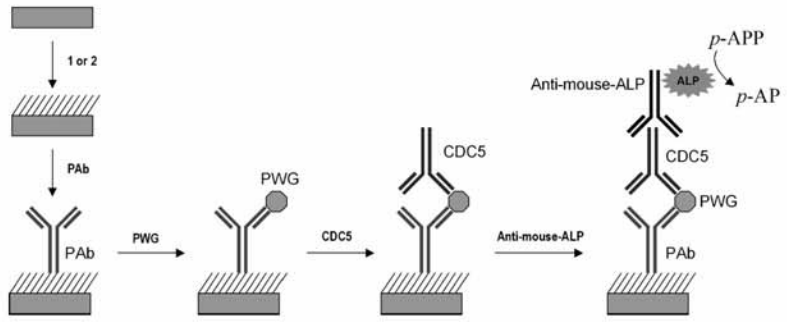

Figure 1. Stepwise construction of the gliadin immunosensor.

the potential range −0.2 to +0.6 V versus Ag/AgCl using a modulation amplitude of 25 mV), a step potential of 5 mV, and a scan rate of 50 mV·s^{-1}).

3. Electrochemical Detection of PWG. Detection of PWG on the modified electrodes (see the section Formation and Characterization of the Sandwich Assay) was carried out using EIS and DPV. EIS measurements were carried out in 1 mM $Fe(CN)_6^{3-/4-}$ in PBS (0.1 M, pH 7.4) in the frequency range of 0.1 Hz−100 kHz at a bias potential of +0.22 V and 5 mV amplitude before and after binding of different concentrations of PWG (10, 20, 30, 40, 50, and 60 ng/mL). The obtained spectra were fitted to an equivalent electrical circuit using the Autolab impedance analysis software. DPV responses were recorded in Tris buffer solution (0.1 M, pH 9) containing 0.1 mM $MgCl_2$ and 0.1 mM $ZnSO_4$, in absence and in presence of 10 mM *p*-APP (after 10 min stirring) using the same parameters described in the section Optimization of Incubation Time of PWG.

Real Sample Analysis. 1. Extraction. Four commercial gluten-free samples were chosen: (i) raw materials, "mix B" bread mix (from Dr. Schär Srl, Italy) and "Damhert Nutrition" cake mix (from Damhert NV, Belgium); (ii) processed foods, "Glutafin" Sweet Biscuits (from Nutricia Dietary Care, UK) and "Harisín" dietetic pasta (from Sanavi, S.A., Spain); as well as (iii) a gluten-containing sample, "Tostagrill" toasted bread (from Diatosta España, S.L.). To extract the gliadin from the commercial gluten-free samples, an extraction buffer consisting of 60% v/v ethanol in the presence of reducing agent in Tris-HCl 50 mM pH 7.4 was prepared. The sample was blended to homogenity, and five portions of this (combined weight 100 mg) was added to 1 mL of the prepared extraction solution. The mixture was then vortexed, before heating under stirring conditions at 60 °C for 10 min, and finally centrifuged for 5 min at room temperature. The supernatant was recovered and divided into two aliquots—one aliquot for analysis using ELISA and the other for analysis using the developed immunosensor.

2. Enzyme-Linked Immunosorbent Assay Analysis of Commercial Gluten Free Samples. Rabbit antigliadin polyclonal antibody (1 μg/mL in carbonate buffer, pH 9.5) was added to each well of a Nunc Immunosorp microtiter plate and incubated for 1 h at 37 °C. Following thorough washing with PBS−Tween (pH 7.4, 50 mM 0.05% v/v Tween), the plate was then blocked by addition of 200 μL of PBS−Tween with 1% w/v BSA and incubated for 1 h at 37 °C, before thorough washing of the plate. In the immunorecognition step, 50 μL of a 1 in 10 or 1 in 25 dilution as well as 1 in 50 000 or 1 in 70 000 dilution (prepared by a 1 in 2500 or 1 in 3500 dilution in 60% v/v ethanol in PBS−Tween and a subsequent 1 in 20 dilution in PBS−Tween) of a range of concentrations of gliadin stock solutions prepared in 60% v/v ethanol in PBS buffer, pH 7.4, 50 mM, was used to prepare a calibration curve with a dynamic linear range between 1 and 150 ng/mL. The extracts from the four gluten-free samples were diluted 1 in 10 and 1 in 25 and the gluten-containing sample diluted 1 in 50 000 and 1 in 70 000 (again prepared by a 1 in 2500 or 1 in 3500 dilution in 60% v/v ethanol in PBS−Tween and a subsequent 1 in 20 dilution in PBS−Tween) to avoid precipitation of the gliadin. Analysis of both standards and samples was carried out in triplicate. The plate was again incubated, under stirring conditions for 1 h at 37 °C, and subsequently thoroughly washed with PBS−Tween, prior to exposure to 50 μL of 1 μg/mL CDC 5 antibody, and again left to incubate under stirring conditions for 1 h at 37 °C. Following a further thorough washing, a 1 in 10 000 dilution of commercial alkaline phosphatase-labeled antimouse antibody was added to each well of the microtiter plate, and the plate incubated under stirring conditions for 1 h at 37 °C. After a final washing, 50 μL of the enzyme substrate *p*-nitrophenylphosphate was added to each well and product formation allowed to proceed for 2 h at 37 °C, the reaction was finally stopped by addition of 1 M H_2SO_4, and the absorbance read at 450 nm, the complete indirect sandwich assay requiring more than 8 h to be completed.

3. Immunosensor Detection. The detection of gliadin in real samples was carried out using gold electrodes modified with a SAM of **1**, as previously described in the section Formation and Characterization of the Sandwich Assay. The extracts (see the section Extraction) from the four gluten-free samples were diluted 1/25 v/v in PBS−Tween buffer (0.1 M, pH 7.4), while the gluten-containing sample was diluted 1/3500 v/v in PBS−Tween buffer (0.1 M, pH 7.4) containing 60% (v/v) ethanol, followed by a subsequent 1/20 v/v dilution in PBS−Tween (0.1 M, pH 7.4). The modified electrodes were then incubated with the diluted extracts for 30 min at room temperature. The rest of the sandwich assay biocomponents were built up (see the section Formation and Characterization of the Sandwich Assay), and the DPV responses were recorded as previously described in the section Optimization of Incubation Time of PWG.

RESULTS AND DISCUSSION

Surface Chemistry. Figure 1 shows the strategy employed for the construction of the gliadin immunosensor. SAMs of dithiol **1** or **2** (Scheme 1) were used as supports for the capture PAb, which was covalently linked to the COOH groups of the SAM via carbodiimide chemistry.

UNIVERSITAT ROVIRA I VIRGILI
BOTTOM-UP SURFACE ENGINEERING FOR THE CONSTRUCTION OF (BIO) SENSORING SYSTEMS: DESIGN STRATEGIES
AND ANALYTICAL APPLICATIONS
Hossam Metwally Ahmed Nassef
ISBN:978-84-692-3235-4/DL:T-932-2009

Scheme 1

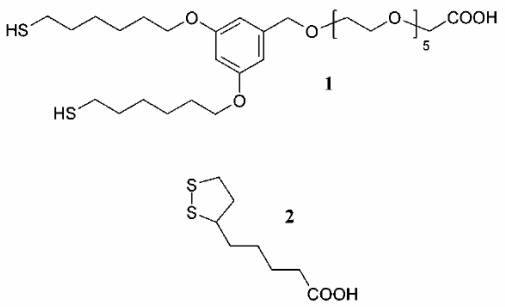

1. Formation of Dithiol Self-Assembled Monolayers. Prior to polyclonal antibody immobilization, the SAMs were optimized in terms of time of formation and minimization of nonspecific interactions. Figure 2 shows the variation of charge-transfer resistance obtained at a SAM of **2** in the presence of 1 mM $Fe(CN)_6^{3-/4-}$ at different lengths of exposure time to the thiol solution. Impedance values increased steadily with time before reaching a constant value after 100 h, in stark contrast with the 3 h needed to form a SAM of **1** (Figure 2, inset). This impedance increase does not account for multilayer formation since each point represents the constant impedance value obtained after repeated washings with ethanol in order to remove physically adsorbed molecules and indicates that the formation of a complete lipoic acid monolayer on gold is an extremely slow process. This apparent disadvantage is compensated in part by the immobilization of a higher number of biorecognition units in comparison to **1** (see below), which could be the result of the presence of a higher number of carboxylate groups in the surface due to its smaller molecular footprint (28 Å^2 for **2**, 49 Å^2 for **1**).

2. Immobilization of Capture Antibody and Stability of Biofunctionalized SAM. Immobilization of the capture antibody was achieved via activation of the COOH groups of the SAMs as labile NHS esters followed by covalent coupling of the PAb through its amino groups. The stability of antibody-modified SAMs was tested by recording the impedance variations daily for one week for electrodes kept in PBS buffer at room temperature (Figure 3). An impedance decrease for the SAM of **2** in the first three days of interaction was observed, which could be related with the partial loss of some physisorbed antibody material or destabilizing effect of the antibody immobilization on the thioctic acid SAM. In contrast, electrodes modified with **1** showed a slight

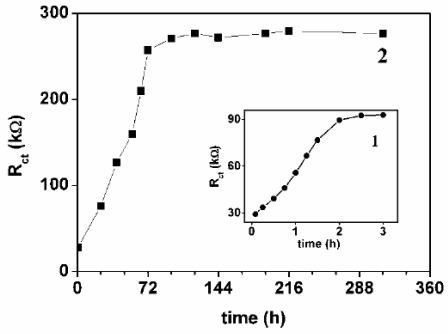

Figure 2. Time dependence of R_{ct} values (obtained from simulation) for the formation of SAMs of dithiols **1** (●) and **2** (□).

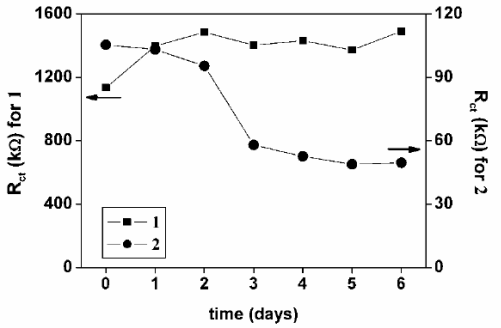

Figure 3. Time dependence of the charge-transfer resistance of SAMs of **1** and **2** modified with PAb.

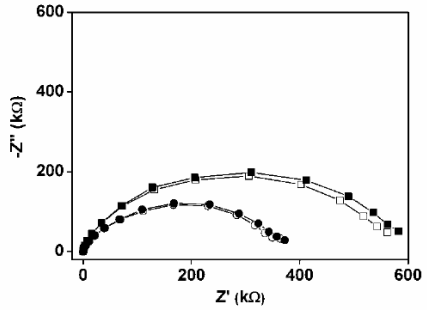

Figure 4. Complex impedance plots (in 1 mM $K_3Fe(CN)_6$ solution in PBS pH 7.4) recorded at a SAM of **2** modified with the following: PAb (□), PAb in the presence of 2 μg/mL PSA (■), anti-PSA (○), and anti-PSA in the presence of 20 μg/mL PWG (●).

impedance increase in the first day, remaining constant during the rest of the stability study.

3. Evaluation of Nonspecific Interactions. Using EIS we evaluated nonspecific interactions on SAMs of **1** and **2** as well as modified SAMs carrying specific and nonspecific antibodies against gliadin or using PSA as a nonspecific analyte. Impedance measurements showed the occurrence of a relatively high degree (>50%) of nonspecific adsorption on a bare SAM of **2** as compared with **1** (15%) when they are exposed to 20 μg/mL PWG. The degree of nonspecific interactions of both surfaces toward PWG was 2-fold reduced when this SAM was further incubated with 0.1% BSA in PBS−Tween. In a situation more akin to the true final immunosensor format, where antibodies are immobilized on the SAMs of **1** or **2** and incubated with a nonspecific antigen, nonspecific binding values were markedly decreased to below 10%, with values of 2.7 and 6.6% observed when PWG was allowed to interact with a SAM of **1** or **2**, respectively, modified with a monoclonal nonspecific PSA antibody (Figure 4).

Electrochemical Detection of Gliadin. 1. Labeless Impedance Detection. Figure 5 represents the impedance spectra of the successive building steps leading to the construction of the gliadin immunosensors using **1** and **2**. As shown in Figure 5, the charge-transfer resistance was increased with the binding of each corresponding protein layer, providing evidence of the successful formation of the immunocomplex. Interestingly, in spite of the relative complexity of the formed sandwich structure, the surface is capable of detecting a hydrophobic redox probe such as *p*-aminophenol even at submicromolar levels (LOD = 15 nM) as evidenced by DPV titration experiments in the concentration range

UNIVERSITAT ROVIRA I VIRGILI
BOTTOM-UP SURFACE ENGINEERING FOR THE CONSTRUCTION OF (BIO) SENSORING SYSTEMS: DESIGN STRATEGIES
AND ANALYTICAL APPLICATIONS
Hossam Metwally Ahmed Nassef
ISBN:978-84-692-3235-4/DL:T-932-2009

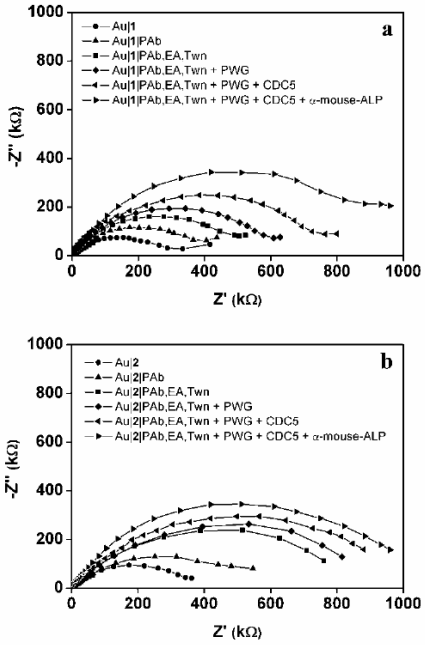

Figure 5. Complex impedance plots (in 1 mM $K_3Fe(CN)_6$ solution in PBS pH 7.4) recorded at a SAM of **1** (a) and **2** (b) for the sequential immobilization of biocomponents in the sandwich assay.

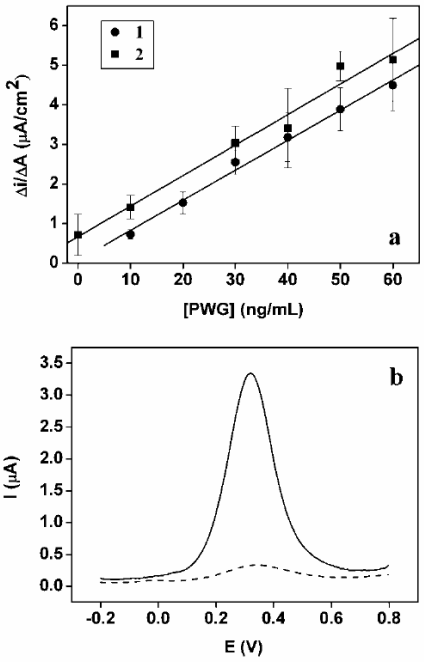

Figure 6. (a) Calibration plots for the detection of PWG on surfaces modified with **1** and **2**. (b) Differential pulse voltammograms of surfaces modified with **1** (—) and **2** (- - -) after 3-h SAM formation, followed by antibody immobilization and formation of sandwich immunocomplex and final addition of 10 mM *p*-aminophenylphosphate substrate in 100 mM Tris buffer, pH 7.4.

of 0−10 μM. However, the R_{ct} values showed no linear relationship with increasing PWG concentrations in the range of 10−60 ng/mL, indicating that the impedance technique is not suitable for gliadin detection under the studied conditions. This might be provoked by a dampening effect of the physically adsorbed BSA blocking agent, which makes impedance measurements irreproducible as it is very sensitive, not only to analyte binding but also to the occurrence of minimal changes in the biointerface structure.[45]

2. Optimization of Incubation Time. The current response of the immunosensor at different incubation times (2, 10, 15, 20, 30, and 45 min) of 50 ng/mL PWG was increased with increasing reaction time and then maintained the maximum value after 30-min incubation. Therefore, this incubation time was used in further experiments.

3. Differential Pulse Voltammetry Detection. Figure 6a represents the calibration plots obtained for PWG detection for immunosensors based on both SAMs **1** and **2**. The current peak height showed a linear relationship with the concentration of PWG over the range of 10−60 ng/mL for both **1** and **2** modified biosensors. As further proof of the requirement to allow the SAM of **2** to form for 100 h prior to biofunctionalization, the SAMs of both **1** and **2** were allowed to form for 3 h before immobilization of the capture antibody, and exposure to a saturating concentration of gliadin and subsequent formation of the complete sandwich immunocomplex and detection, as previously described. As can be seen in Figure 6b, a markedly lower signal is obtained at 0.32 V for the immunosensor based on SAM **2** when the SAM is only allowed to form for 3 h, similar measurements were made for various formation times of SAM **2** at periodic times between 0 and 100 h, and it was clearly observed that only after 100 h were comparable responses obtained (data not shown). Table 1 shows the analytical parameters obtained for the immunosensors based on SAM **1** formed after 3 h and SAM **2** formed after 100 h. As can be seen, the sensitivity of each immunosensor was similar for both surfaces, although electrodes modified with a SAM of **1** showed a lower limit of detection (LOD) when compared with **2** and the value of the LOD obtained for both is applicable to detection of gluten in gluten-free food samples.

Table 1. Analytical Parameters for Gliadin Detection Using 1 and 2

surface	sensitivity (μA ng^{-1} mL^{-1})	LOD (ng/mL)	r
Au|**1**	75 ± 3	5.5	0.996
Au|**2**	77 ± 6	11.6	0.989

4. Real Sample Analysis. The developed immunosensor was then applied to the detection of commercial gluten-free food products, as well as to a commercial gluten-containing food product. Extracts from gluten-free samples were diluted 1 in 25 and from the gluten-containing sample 1 in 70 000. As can be seen in Table 2, an excellent correlation was obtained between the immunosensor and the ELISA, but with the former representing a dramatic reduction in assay time from more than 8 h to less than 90 min, demonstrating the applicability of the immunosensor to in situ use, and work is ongoing to further reduce the required assay time.

(45) Pänke, O.; Balkenhohl, T.; Kafka, J.; Schäfer, D.; Lisdat, F. *Adv. Biochem. Eng. Biotechnol.* **2008**, *109*, 195.

Table 2. Comparison of Gliadin Detection in Real Samples Using Two Methods

sample	immunosensor (ppm)	ELISA (ppm)
"Glutafin" Sweet Biscuits (from Nutricia Dietary Care, UK)	0.56 ± 0.09	0.24 ± 0.08
"Harisin" dietetic pasta (from SANAVI, S.A., Spain)	12.4 ± 1.5	11.2 ± 1.3
"mix B" bread mix (from Dr. Schär Srl, Italy)	2.26 ± 0.04	1.60 ± 0.40
"Damhert Nutrition" cake mix (from Damhert NV, Belgium)	0.8 ± 0.1	1.65 ± 0.04
"Tostagrill" toasted bread (from Diatosta España, S. L.)	29000 ± 8000	33000 ± 9000

CONCLUSIONS

An electrochemical immunosensor for the measurement of potential celiac toxicity in raw and processed foodstuffs has been developed. The use of two different surface chemistries for the anchoring of the capture antibody has been compared in terms of time required for formation of self-assembled monolayers, stability, susceptibility to nonspecific binding, reproducibility, and sensitivity. The thioctic acid self-assembled monolayer took more than 100 h to attain a stable surface, and rapidly destabilized following functionalization with capture antibody, while the heptaoxadocosanoic acid surface rapidly formed (less than 3 h) and was stable for at least 5 days, stored at room temperature, following antibody immobilization. Both surface chemistries gave rise to highly sensitive immunosensors, with detection limits of 5.5 and 11.6 ng/mL being obtained for **1** and **2**, respectively, and nonspecific binding was significantly lower for the heptaoxadocosanoic acid based immunosensor, at just 2.7% of the specific signal. Better reproducibility was attained with **1** with RSD of 5.2% as compared with an RSD of 6.75% obtained for **2** ($n = 5$). Finally, the immunosensor was applied to the analysis of commercial gluten-free and gluten-containing raw and processed foodstuffs, its performance compared to that of an ELISA, and excellent correlation achieved. Ongoing work is looking at the use of antibody fragments as compared to whole antibodies as a means of improving sensitivity, as well as exploring formats to reduce assay time.

ACKNOWLEDGMENT

This work has been carried out as part of the Commission of the European communities specific RTD programme 'Quality of Life and Management of Living Resources' QLKI-2002-02077, the Plan Nacional GLUTACATCH and was partly financed by the Grup Emergente INTERFIBIO, 2005SGR00851. A.F. acknowledges the Ministerio de Ciencia y Tecnología, Spain, for a "Ramón y Cajal" Research Professorship.

Received for review July 31, 2008. Accepted September 29, 2008.

AC801620J

UNIVERSITAT ROVIRA I VIRGILI
BOTTOM-UP SURFACE ENGINEERING FOR THE CONSTRUCTION OF (BIO) SENSORING SYSTEMS: DESIGN STRATEGIES
AND ANALYTICAL APPLICATIONS
Hossam Metwally Ahmed Nassef
ISBN:978-84-692-3235-4/DL:T-932-2009

CHAPTER 8: (Art 7)

Amperometric immunosensor for detection of celiac disease toxic gliadin based on Fab fragments

(Hossam M. Nassef, Laia Civit, Alex Fragoso, and Ciara K. O'Sullivan, Submitted to Anal. Chem., 2009.)

UNIVERSITAT ROVIRA I VIRGILI
BOTTOM-UP SURFACE ENGINEERING FOR THE CONSTRUCTION OF (BIO) SENSORING SYSTEMS: DESIGN STRATEGIES
AND ANALYTICAL APPLICATIONS
Hossam Metwally Ahmed Nassef
ISBN:978-84-692-3235-4/DL:T-932-2009

Amperometric immunosensor for detection of celiac disease toxic gliadin based on Fab fragments

Hossam M. Nassef,[1] Laia Civit,[1] Alex Fragoso,[1*] and Ciara K. O' Sullivan[1,2*]

AUTHOR EMAIL ADDRESS alex.fragoso@urv.cat, ciara.osullivan@urv.cat,

RECEIVED DATE

[1] Nanobiotechnology & Bioanalysis Group, Department of Chemical Engineering, Universitat Rovira i Virgili, Avinguda Països Catalans 26, 43007 Tarragona, Spain.

[2] Institució Catalana de Recerca i Estudis Avançats (ICREA), Passeig Lluís Companys 23, 08010 Barcelona, Spain

UNIVERSITAT ROVIRA I VIRGILI
BOTTOM-UP SURFACE ENGINEERING FOR THE CONSTRUCTION OF (BIO) SENSORING SYSTEMS: DESIGN STRATEGIES AND ANALYTICAL APPLICATIONS
Hossam Metwally Ahmed Nassef
ISBN:978-84-692-3235-4/DL:T-932-2009

ABSTRACT

Immunosensor sensitivity is strongly dependent on the density of free active epitopes per surface area, which could be achieved via well-oriented immobilization of antibody fragments as bioreceptor molecules. Here, we report on the development of an electrochemical gliadin immunosensor based on the spontaneous self-assembly of anti-gliadin Fab fragments (CDC5-Fab) on Au surfaces. The analytical performance of this immunosensor is compared with a similar containing whole CDC5 antibodies previously modified with thiol groups (CDC5-SH) as recognition element. Fab fragments were generated by reduction of the disulfide bond of $F(ab)_2$ fragments obtained by bromelain digestion of CDC5 antibody. Surface Plasmon Resonance (SPR) was used to evaluate the degree of immobilization and recognition ability of immobilized CDC5-Fab and CDC5-SH on gold surfaces. The studied surface chemistries were evaluated in terms of time required for SAM formation , stability, susceptibility to non-specific interactions, and sensitivity using Surface Plasmon Resonance (SPR), electrochemical impedance spectroscopy (EIS) and amperometry. CDC5-Fab formed a stable monolayer on gold after 15 min and retained >90% of antigen recognition ability after 2 month of storage at 4ºC.Detection of gliadin of Fab modified electrodes was evaluated by impedance and amperometry. Labeless impedimetric detection achieved a LOD of 0.42 μg/mL while the amperometric immunosensor based on Fab fragments showed a highly sensitive response with LOD 3.29 ng/mL. The Fab based immunosensor offers the advantages of being highly sensitive, easy and rapid to prepare, with a low assay time.

KEYWORDS: Antibody fragments, Immunosensor, Self-assembled monolayer, Gliadin, Celiac disease

UNIVERSITAT ROVIRA I VIRGILI
BOTTOM-UP SURFACE ENGINEERING FOR THE CONSTRUCTION OF (BIO) SENSORING SYSTEMS: DESIGN STRATEGIES AND ANALYTICAL APPLICATIONS
Hossam Metwally Ahmed Nassef
ISBN:978-84-692-3235-4/DL:T-932-2009

INTRODUCTION

Protein/peptide molecules strongly interact with a wide variety of solid surfaces through hydrophobic, electrostatic, and hydrogen bond interactions.[1] Many studies have compared methods of antibody attachment to biosensor surfaces including physicochemical adsorption and covalent attachment.[2,3] Covalent methods improve the uniformity and reproducibility of the bound proteins and have been applied for immobilizing proteins onto different solid substrate surfaces using defined linkages or strong Au-S bonds to form self-assembled monolayers (SAM),[4,5] generally addressing the lysine residues randomly present in the antibodies. This gives rise to a random orientation of the antigen binding site toward the sensor surface[5,6] and may also lead to loss of the biological activity of the antibody.[7]

An alternative to whole antibodies is the use of antibody fragments as recognition element. Recombinant Fab fragments, as well as the even smaller Fv and single-chain Fv fragments can be readily generated using robust engineering approaches, such as phage display. Whilst the generated fragments possess definitive advantages over their whole antibody counterpart, they are generally labelled with a histidine or biotin tail for linking to a functionalized surface rather than by direct chemisorptionfor subsequent immunoassay/immunosensing. In an alternative approach, the production of $F(ab')_2$ and Fab fragments using enzymatic proteolysis is a well established technique.[8]

Fab fragments can be directly generated using thiol proteases such as papain or ficin, or, alternatively, $F(ab')_2$ fragments can be generated using bromelain, pepsin, or ficin, and the disulphide hinge subsequently cleaved using a reducing agent, generating Fab fragments.[9,10] Pepsin is not applicable to all antibody types (e.g. it cannot be used for mouse IgG1 subclasses) and the low pH required for pepsin digestion can destroy antibodies.[11] Bromelain or ficin provide significantly higher yields than pepsin,[12] and with more rapid and reproducible digestion (Scheme 1).[13] The $F(ab')_2$ fragments are dimeric structures of two Fab units linked together by a disulfide bridge that can be cleaved generating two Fab fragments with active thiol groups, which are located on the opposite side of the molecule with respect to the binding site.[14] These thiol groups can interact with gold surfaces leading to a monolayer of Fab fragments displaying a highly controlled orientation that is expected to maximize their antigen-binding efficiency with a concomitant increase in sensitivity and selectivity[15,16] when compared to randomly immobilized whole antibodies (Figure 1).[17] Lu et. al, have demonstrated that the antigen binding activity of the Fab fragments immobilized in oriented form on

ISBN:978-84-692-3235-4/DL:T-932-2009

derivatized silica surfaces is 2.7 times higher than that of the random form.[15] Vikholm-Lundin[18] reported on a generic platform where the spaces in between chemisorbed Fab fragments is filled with the disulfide bearing polymer of *N*-[tris(hydroxyl-methyl)methyl]-acrylamide, resulting in a marked decrease in non-specific binding. The same group went on to apply the developed platform to the detection of C-reactive protein, comparing $F(ab')_2$ and Fab immunocapture layers, with a five-fold improvement in specific binding observed with the Fab monolayer.[19] The self assembly of Fab onto a gold surface, followed by surface plasmon resonance transduction was applied to the detection of insulin[20], with another report detailing the detection of differentiated leukocyte antigens for immunophenotyping of acute leukaemia via the direct adsorption of Fab fragments onto gold nano-particles with piezoelectric transduction.[21] In last two examples, the authors did not compare their approach with a full length antibody strategy.

In some cases, the use of $F(ab')_2$ fragments has resulted in lower detection limits as compared to whole antibodies.[22] There have also been reports of the exploitation of Fab fragments, but without taking direct advantage of the ordered monolayer that can be formed via the direct chemisorption of the thiolated Fab onto a gold surface, but rather focusing on antibody orientation as a means of increasing sensitivity. Examples of this are the immobilization of biotinylated anti-atrazine Fab on neutravidin modified gold electrodes[23,24] for the detection of atrazine, and monobiotinylated Fab against human chorionic gonadotropin and using surface plasmon fluorescence measurements, the biotin-Fab achieved a detection limit of 6×10^{-13}M as compared to 4×10^{-12}M when biotinylated whole antibody was used.[25] Additionally, exchange reactions between disulfide-terminated SAMs and thiolated Fab fragments have also been employed to generate sensor surfaces with well oriented Fab fragments.[15-17,26] However, the preferred method for Fab immobilization is the spontaneous adsorption of Fab motifs on gold, giving rise to surfaces of higher epitope density, high antigen-binding constants and operational stability or adhesion.[27-29]

UNIVERSITAT ROVIRA I VIRGILI
BOTTOM-UP SURFACE ENGINEERING FOR THE CONSTRUCTION OF (BIO) SENSORING SYSTEMS: DESIGN STRATEGIES AND ANALYTICAL APPLICATIONS
Hossam Metwally Ahmed Nassef
ISBN:978-84-692-3235-4/DL:T-932-2009

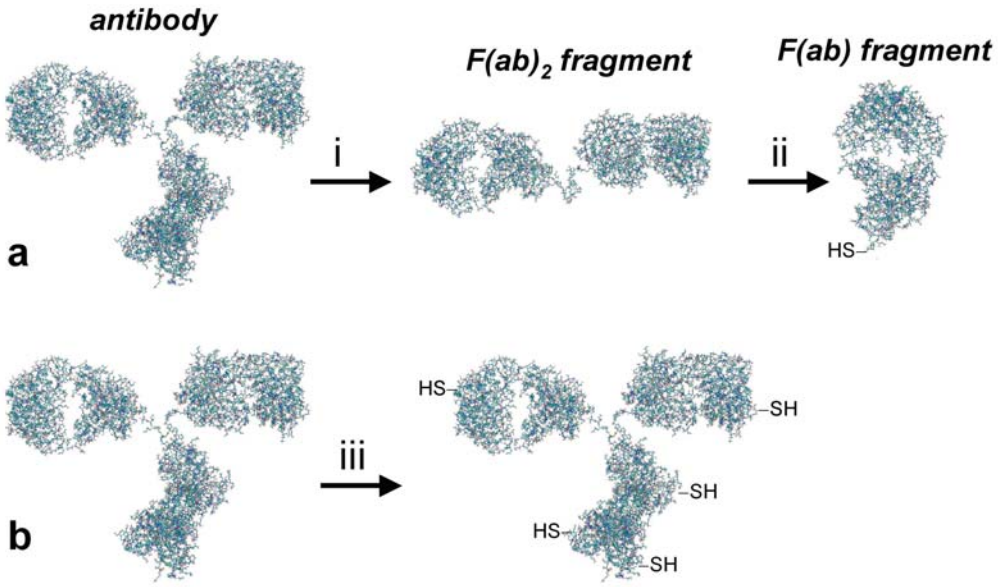

Scheme 1. Preparation of: (a) Fab fragments (i: bromelain, ii: cysteine), b) SATA-modified antibody (iii: SATA, hydrolysis).

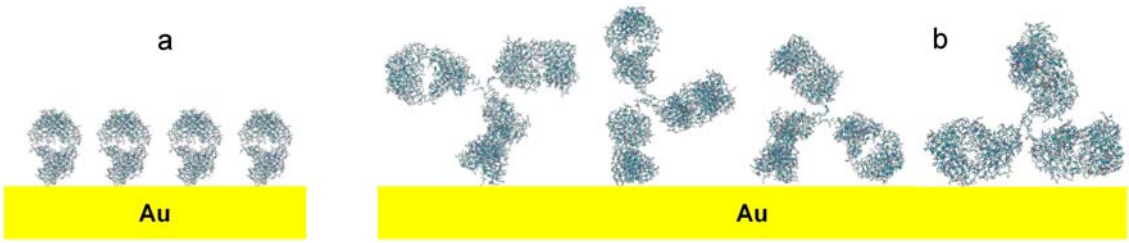

Figure 1. Comparison of oriented disposition of F(ab) fragments on gold surface (left) with randomly-oriented SATA-modified antibody (right).

Celiac disease (CD) is a condition associated with the ingestion by susceptible individuals of gluten from wheat, barley, rye and oats triggered causing histological changes in the small intestine mucosa and leading to a mal-absorption syndrome.[30, 31] CD affects possibly 1:100 people in Northern Europe and Northern America[32, 33] and symptoms revert when a strict gluten-free diet is established, being the only treatment available thus far. Therefore, accurate assays for detecting gluten in foodstuffs are mandatory. The new benchmark recently approved by Codex Alimentarius (July 2008) states that "gluten-free" foods may not exceed 20 ppm of gluten, whilst those with a

gluten content to a level between 20 ppm - 100 ppm may be referred to as "low gluten" or "reduced gluten".

Industries generating gluten-free foods have a definitive need for on site and easy to use gluten assays so that incoming raw materials and possible gluten contamination throughout the production process can be rapidly tested. Biosensors could provide a rapid and convenient alternative to conventional analytical methods for monitoring substances under interest in various application fields. Our group has recently reported an electrochemical immunosensor for the detection of gliadin with a detection limit of 5.5 ng/mL which exploits a gold electrode functionalised with a dithiol self-assembled monolayer. This sensor was based on an antibody, coined CDC5, which was raised against the putative immunodominant celiac disease toxic epitope of α-gliadin, 56−75[34] and applied to the analysis of gliadin in real food samples.[35]

In this paper, we exploit the spontaneous self-assembly of CDC5 Fab fragments on gold surfaces for the construction of a sandwich electrochemical immunosensor for gliadin and compare its performance with the corresponding whole antibody in which thiol groups have been selectively introduced using the N-hydroxysuccinimide ester of S-acetylthioacetic acid (SATA). Surface modification and antigen affinities were studied by surface plasmon resonance (SPR) and the electrochemical assay was optimized in terms of deposition and incubation times. The immunosensor we report herein is highly sensitive, easy and rapid to prepare, with a lower assay time and improved detection limit as compared to our previous reported method,[35] with minimal requirement of operator manipulation.

EXPERIMENTAL SECTION

Chemicals and Materials. 1. Materials. The Prolamin Working Group (PWG, martin.stern@med.uni-tuebingen.de) provided a gliadin preparation[36] to be used as a basis for standardizing the analysis and detection of gliadin. Monoclonal antigliadin CDC5 antibody was kindly provided by H. J. Ellis and P. J. Ciclitira.[37] Monoclonal anti-gliadin horseradish peroxidase conjugate was used as received. 1-(Mercaptoundec-11-yl)-tetra(ethyleneglycol) (PEG) was purchased from Aldrich. Antibody $F(ab)_2$ and Fab fragments of CDC5 were prepared according to a method provided by Fujirebio Diagnostics AB. Gliadin stock solutions were freshly prepared in PBS-Tween® containing 60% (v/v) ethanol and diluted in the appropriate buffer. All other reagents were of analytical grade and used without further purification.

ISBN:978-84-692-3235-4/DL:T-932-2009

2. Electrochemical Instrumentation. All the electrochemical measurements were performed using a PGSTAT12 potentiostat (Autolab, The Netherlands) controlled with the General Purpose Electrochemical System (GPES) software, with built-in frequency response analyzer FRA2 module. A three electrode configuration of Ag/AgCl-3M NaCl as a reference (CH Instruments., model CHI111), Pt wire as a counter (BAS model MW-1032), and bare or modified Au (BAS model MF-2014, 1.6 mm diameter) as working electrode was used. The working surface was cleaned as reported previously.[35]

Faradaic impedimetric measurements were carried out in 0.1 M phosphate buffer saline (PBS) (pH 7.4) containing 1 mM $Fe(CN)_6^{3-}$ and 1 mM $Fe(CN)_6^{4-}$ within the frequency range of 0.1 Hz-100 kHz at a bias potential of +0.22 V and ac amplitude of 5 mV. The non-faradaic measurements were carried out in PBS (pH 7.4) at 0.0 V and ac amplitude of 5 mV. All amperometric measurements were carried out at fixed potential (-0.2 V) under continuous stirring at 350 rpm.

3. SPR Instrumentation. A Biacore3000® SPR instrument was used for all the SPR studies. It was operated at a constant temperature of 20°C. A gold (Au) sensor chip was used as a solid support for immobilization of CDC5-Fab and CDC5-SH. The data were evaluated with the Biacore3000® control software version 4.1.

Preparation and Characterization of Antibody Fragments 1. Preparation of F(ab')$_2$ Fragments. CDC5 antibody was purified by YM 100 kDa microcon and washed four times with 0.15 M NaCl. To 500 μL of the purified CDC5 antibody (1 mg/mL), 50 μL of 0.5 M Tris buffer containing 50 mM EDTA (pH 7) was added. To the previous mixture, 50 μL (10 mg/mL) bromelain solution in PBS (pH 7.2) was added. The mixture was incubated at 37 ºC overnight. The produced F(ab')$_2$ fragments were separated with a Sephacryl S-100 column using 0.15 M NaCl as eluting agent. The fractions with maximum absorbance at 280 nm were concentrated using a YM10 KDa microcon, washed several times with PBS (pH 7.4) and stored at -20 ºC.

2. Preparation and Characterisation of Fab Fragments (CDC5-Fab). Fab fragments were always freshly prepared before use, using 1500 μL of 10 mM cysteine in phosphate buffer (pH 10.3) treated with 60 μL (0.483 mg/mL) F(ab')$_2$ was added. The mixture was incubated for 2 hours at room temperature under gentle shaking and the excess of cysteine was removed using a YM 10 kDa microcon. The obtained Fab fragments were washed four times with PBS (pH 7.4), and spectrophotometrically

ISBN:978-84-692-3235-4/DL:T-932-2009

quantified at 280 nm and the number of free sulfhydryl groups was determined using Ellman`s reagent using a molar absorptivity of 14150 $M^{-1}.cm^{-1}$ at 412 nm.[38]

CDC5-Fab were characterized by non-reducing sodium dodecyl sulfate-polyacrylamide gel electrophoresis analysis (SDS-PAGE, 12% acrylamide in TRIS-glycine gel).[39] A precision protein standard marker (Bio-Rad, Nazareth Eke, Belgium) was used as molecular weight reference. The protein fragments were stained with Coomassie brilliant blue R250 (Sigma, Spain).

3. Modification of CDC5 with Thiol Groups (CDC5-SH). To 100 μL of CDC5 (4 mg/mL)**,** 5.4 μL of SATA (1 mg/0.9 mL in DMSO) was added and the mixture was incubated for 30 minutes at room temperature under gentle shaking. Then, 100 μL of deacetylation solution (0.5 M hydroxylamine hydrochloride containing 25 mM EDTA in PBS, pH 7.4) was added and the mixture was incubated at room temperature for 2 hours under gentle shaking. The produced SATA modified antibody (CDC5-SH) was dialyzed in PBS (pH 7.4) overnight and concentrated using a YM 30 KD microcon. The final concentration of CDC5-SH was determined spectrophotometrically at 280 nm, and then stored at -20 ºC.

4. Enzyme Linked Immunosorbent Assay (ELISA) Characterization of the Prepared Fab Fragments and the SATA Modified Antibody. The ELISA analysis was performed as reported previously[35] with the following modifications. The capture layer was formed using 100 μg/mL of CDC5-Fab or CDC5-SH in carbonate buffer, pH 9.6. In the immunorecognition step, 50 μL of 1 μg/mL PWG in PBS-Tween prepared from PWG stock solution prepared in 60% v/v ethanol in PBS buffer (pH 7.4, 0.1 M), was added for each well. Detection was carried out with 100 μg/mL of commercial HRP- labelled monoclonal anti-gliadin antibody. The analysis was carried out in triplicate.

Surface Chemistry. 1. Optimization of Time Required for SAM Formation. Clean Au electrodes were modified by direct immersion in 100 μg/mL CDC5-Fab or CDC5-SH in PBS solution (pH 7.4), and the time dependence of impedance variations was recorded for selected immobilization times. CDC5-Fab immobilization was monitored between 0-60 min by non-faradaic impedance while faradaic responses were recorded between 0-180 min for CDC5-SH. R_{ct} values were calculated for different exposure times using the Autolab impedance analysis software.

ISBN:978-84-692-3235-4/DL:T-932-2009

2. Immobilization of CDC5-Fab and CDC5-SH on SPR Au Chips. A 100 μg/mL solution of CDC5-Fab and CDC5-SH in PBS (pH 7.4) was injected onto a clean Biacore SIA Au chip during the immobilization phase until a saturation level was obtained. 100 μg/mL of CDC5-Fab or CDC5-SH in PBS pH 7.4 were injected directly over the sensor chip for 20 min, at a flow rate of 5 μL/min. The free space of modified gold chip was then backfilled with 25 μl of 1 mM PEG in PBS-Tween.

3. Impedimetric Study of the Stability and Affinity of the Antibody Fragments with Time. Clean electrodes were immersed in 100 μg/mL of CDC5-Fab or CDC5-SH in PBS (pH 7.4) for 15 min. The modified Au electrode was then stored in PBS (pH 7.4) at 4 ºC. The non-faradaic EIS was recorded weekly during two months in PBS for the modified electrodes with Fab fragments at a bias potential of 0.0 V (frequency range: 0.1 Hz-100 kHz, ac amplitude 5 mV) and log Z‘ was calculated at fixed frequency (1.1 Hz)

4. Non-Specific Binding Study. Firstly, the EIS response was recorded before and after incubation of a pure SAM of PEG, which is used as the backfiller with the Fab fragments, with 30 μg/mL PWG for 30 min.

Different conditions were used in the amperometric study at fixed potential (-0.2 V) in PBS (0.1 M, pH 7.4) solution with two consecutive injections of 2 mM H_2O_2 and 2 mM HQ, using 30 μg/mL PWG and 100 μg/mL anti-gliadin-HRP;

(i) PEG-modified electrodes with were first immersed in 0.05 M PBS-Tween for 30 min followed by incubation with anti-gliadin-HRP in the absence and in the presence of PWG;

(ii) CDC5-Fab modified electrodes were first backfilled with PEG followed by immersion in 0.05 M PBS-Tween for 30 min followed by incubation with anti-gliadin-HRP.

Cross-Reactivity Studies 1. Amperometric Detection. Amperometric measurements were carried out using the same conditions explained in the previous section. The clean gold electrodes were modified with different antibody Fab fragments, by immersion in a 100 μg/mL solution of CDC5-Fab or CEA-Fab (as non-specific antibody) in PBS pH 7.4 for 15 min. The remaining free space of the gold surfaces were then blocked with 1 mM PEG for 10 min, followed by incubation in 0.05 M PBS-Tween for 30 min. Subsequently, 30 ng/mL of the corresponding protein (CEA or

PWG, respectively) were incubated for 30 min. After incubation with 100 μg/mL of anti-gliadin HRP for another 30 min, the amperometric response was recorded.

2. Surface Plasmon Resonance. Five μg/mL of different non-specific analytes such as recombinant high molecular weight glutenin (r-HMW-Glu), CEA and PSA (prostate specific antigen) were injected during 6 min to a CDC5-Fab and CDC5-SH modified Au chip and the SPR responses were measured. Before each measurement, three regeneration steps were carried out by injecting 20 μL glycine (10 mM, pH 2.2) for 1 minute. Specific signals were recorded using 5 μg/mL of PWG or gliadin (from Sigma) dissolved in PBS pH 7.4.

Immunosensor Construction and Calibration. 1. Formation and Characterization of the Sandwich Assay. SAM formation of the Fab and CDC5-SH were carried out at their corresponding optimal times and following blocking with 1mM PEG, the modified surfaces were incubated in PBS-Tween (0.05 M, pH 7.4) solution for 30 min. The electrodes were then exposed to different concentrations of PWG (1-20 μg/mL) in PBS-Tween solution for 10 min. Each building step during the fabrication of the biosensor was characterized by CV and EIS using $Fe(CN)_6^{3-/4-}$ in PBS solution as an electroactive marker. In the case of the Fab modified surfaces, an additional amperometric measurement were carried out at different concentrations of PWG (5-30 ng/mL) after an additional layer of labelled antibody was incubated with 100 μg/mL anti-gliadin-HRP in PBS for 30 min at room temperature under stirring conditions.

2. Optimization of Incubation Times. The incubation time of the specific recognition between PWG and the immobilized Fab was optimized as follows. The modified electrodes with Fab were blocked with PEG and PBS-Tween as described in the previous section. The electrodes were then incubated with 30 ng/mL PWG in PBS-Tween solution at 12 different incubation times (between 0- 45 min), the non-faradaic EIS was measured at each incubation time in PBS (pH 7.4) in the frequency range of 0.1 Hz-100 kHz at a bias potential of 0.0 V and 5 mV amplitude. The influence of the incubation time on the logarithm of impedance of the real part at fixed frequency (0.0383 Hz) was investigated.

For the optimization of incubation with labeled anti-gliadin-HRP in the sandwich assay, the Fab modified gold surface was blocked with PEG and PBS-Tween, followed by incubation with 10 ng/mL PWG in PBS-Tween. The electrodes were then incubated with 100 μg/mL MAb-HRP solution at different incubation times (between 0- 60 min).

ISBN:978-84-692-3235-4/DL:T-932-2009

The amperometric responses were then recorded at fixed potential (-0.2V vs Ag/AgCl) in PBS (0.1 M, pH 7.4) in the absence and presence of 2mM H_2O_2 and 2mM HQ.

Electrochemical Detection of PWG. 1. Impedimetric Detection. Detection of PWG on the modified electrodes (see Section 2.7.1) was carried out using EIS and Amperometry. EIS measurements were carried out in the presence of the redox probe 1 mM $Fe(CN)_6^{3-/4-}$ in PBS (0.1 M, pH 7.4) in the frequency range of 0.1 Hz-100 kHz at a bias potential of +0.22 V and 5 mV amplitude before and after binding of different concentrations of PWG (5, 10, 15, 20, 25, and 30 ng/mL). The obtained spectra were fitted to an equivalent electrical circuit using the Autolab impedance analysis software.

2. Amperometric Detection. Clean gold electrodes were modified with Fab as previously explained. The free surfaces were then blocked with PEG and PBS-Tween, followed by incubation of the modified electrodes in different concentrations of PWG (5, 10, 15, 20, 25, and 30 ng/mL) in PBS-Tween for 10 min. Followed by a final incubation with 100 μg/mL of MAb-HRP for 30 min, the amperometric response of the antibody-modified surface was recorded in PBS before and after the two consecutive injections of 2 mM H_2O_2 and 2 mM HQ.

RESULTS AND DISCUSSION

Preparation of CDC5 Fragments and Characterization Using Non-Reducing Electrophoresis (SDS-PAGE). Scheme 1 shows the strategy employed for the preparation of Fab fragments and for the introduction of thiol groups in CDC5 using SATA. Whole CDC5 antibody was first digested with bromelain to obtain the corresponding $(Fab')_2$ after chromatographic purification. Purified $(Fab')_2$ fragments kept in PBS (0.1 M, pH 7.4) at -20ºC were stable for more than six months, which allowed the preparation of a large batch of $(Fab')_2$ from which Fab fragments were generated when needed.

The fragmentation process of CDC5 and the chemical reductions of the produced mouse MAb CDC5 $(Fab')_2$ to Fab fragments using cysteine as a reducing agent were characterized by non-reducing electrophoresis. The mouse MAb CDC5 $(Fab')_2$ were successfully reduced to Fab fragments. Figure 2 illustrates the SDS-PAGE (12 %) analysis of the full length CDC5 antibody and their $(Fab')_2$ and Fab fragments under the non-reducing conditions. Lane 1 of Figure 2 clearly shows one major band around 40 kDa, indicating that a significant amount of Fab was produced. In lane 1, there were no significant bands less than 40 kDa, indicating that the produced Fab fragments were not

UNIVERSITAT ROVIRA I VIRGILI
BOTTOM-UP SURFACE ENGINEERING FOR THE CONSTRUCTION OF (BIO) SENSORING SYSTEMS: DESIGN STRATEGIES AND ANALYTICAL APPLICATIONS
Hossam Metwally Ahmed Nassef
ISBN:978-84-692-3235-4/DL:T-932-2009

further reduced into smaller inactive peptides. Lanes 2 and 3 present major bands around 120 and 150 kDa, respectively, which can be attributed to the prepared $(Fab')_2$ fragments and whole CDC5 antibody, respectively. In Lane 2, a few faint bands were visible around 40 kDa, indicating that some Fab was produced due to further reduction of $F(ab')_2$ during the enzymatic fragmentation process, which is expected. The successful cysteine-mediated reduction of CDC5 $F(ab')_2$ to Fab fragments was also demonstrated using Ellman`s reagent. The concentration of free sulfhydryl groups after reduction was 1.697 μM, a value 2.35-fold higher than that of $F(ab')_2$ (0.722 μM). This indicates a successful reduction of the $F(ab')_2$ fragments. The biorecognition affinity of the prepared Fab and modified CDC5-SH was further studied by ELISA. The ELISA results indicated that the Fab and CDC5-SH are still active and easily recognize PWG, and the preparation processes for both biocomponents does not affect their activity.

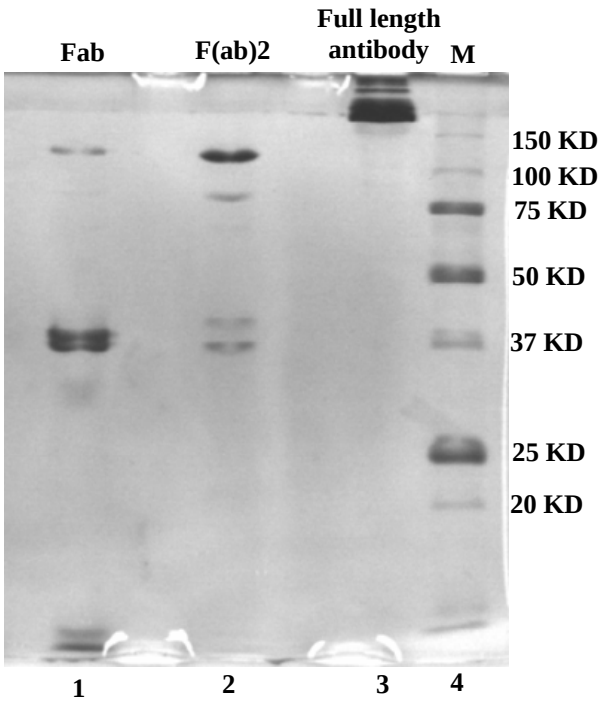

Figure 2. SDS-PAGE analysis (12% gel; non-reducing conditions) of the full length CDC5 antibody their F(ab)2 and Fab fragments. a) Lane 1: Cysteine reduction of F(ab)2 to F(ab) fragments, lane 2: F(ab)2 fragments (obtained by enzymatic bromelain fragmentation), lane 3: full-length CDC5, and lane 4: molecular weight marker.

Surface Chemistry. 1. Surface Plasmon Resonance Study. The deposition of CDC5-Fab and CDC5-SH onto Au surfaces was primarily studied using SPR. Figure 3

UNIVERSITAT ROVIRA I VIRGILI
BOTTOM-UP SURFACE ENGINEERING FOR THE CONSTRUCTION OF (BIO) SENSORING SYSTEMS: DESIGN STRATEGIES AND ANALYTICAL APPLICATIONS
Hossam Metwally Ahmed Nassef
ISBN:978-84-692-3235-4/DL:T-932-2009

represents the SPR sensograms of consecutive immobilization, blocking and recognition steps for both CDC5 forms and Table 1 details the RU values obtained for the immobilization and recognition steps. The surface mass density obtained for CDC5-Fab and CDC5-SH after the immobilization step were 109 and 171 ng/cm^2, respectively. These values translate into molar concentrations of 2.72 and 0.85 pmol/cm^2, considering a molecular weight of 40 kDa for CDC5-Fab and 200 kDa for CDC5-SH as revealed by SDS-PAGE. Hence, an antigenic CDC5-Fab monolayer contains about 1.6 times more recognition epitopes per square centimeter than a monolayer of full antibodies (considering two binding sites per whole antibody molecule). It has been recently estimated that a full monolayer contains between 130–650 ng/cm^2 of whole antibodies of approximate size 15×15×3 nm^3) and 260–700 ng/cm^2 of Fab fragments (8.2×5.0×3.8 nm^3).[17] Therefore the observed RU values indicate that an incomplete monolayer was obtained with the Fab fragments in contrast with the whole antibody.

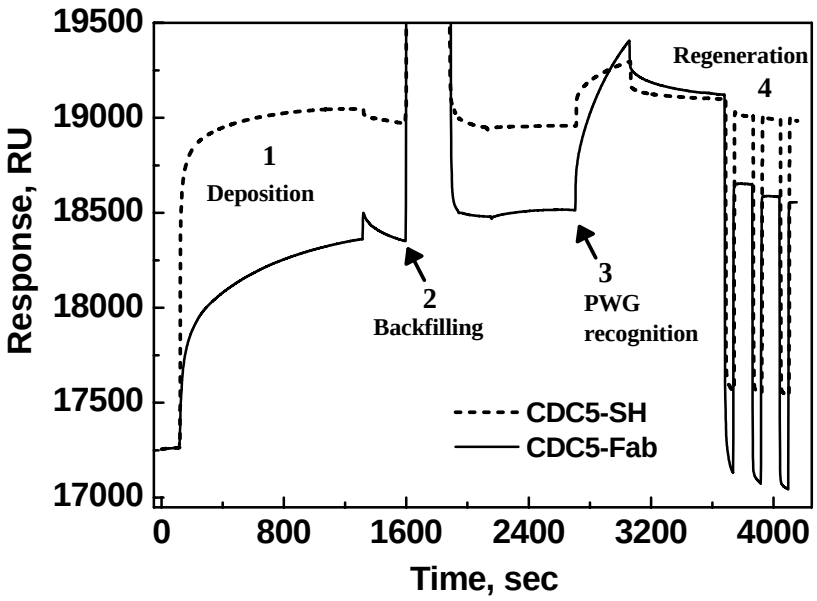

Figure 3. SPR sensorgrams obtained at CDC5-Fab (—) and CDC5-SH (---) modified Au chips. (1) SAM formation, (2) Blocking step with 1 mM PEG and PBS-Tween, (3) injection of 5 μg/mL PWG for antigen binding, (4) regeneration with 3 pulses of glycine (10 mM, pH 2.2).

ISBN:978-84-692-3235-4/DL:T-932-2009

SPR was also used also to assess antigen (PWG) binding to the immobilized full-length antibodies and fragments. Figure 3 shows the antigen binding responses on the covalently immobilized CDC5-Fab and CDC5-SH. The Fab fragment showed the highest antigen binding response (606 RU for 5 μg/mL of PWG) (Table1) in comparison to the 136 RU for immobilized CDC5-SH, i.e. a decrease of about 77% antigen recognition ability was observed for CDC5-SH. This is presumably due to the fact that the modification process of the full length antibody with SATA reagent converts the free amines distributed throughout the antibody structure to sulfhydryl groups, resulting in a randomly oriented immobilization of CDC5-SH which leads to a decrease in antigen accessibility to the recognition epitope (Figure 1). An additional factor could be the steric hindrance of the whole antibody onto the sensor surface, since it has larger dimensions (15×15×3 nm^3) and consequently consumes a larger space on the sensor surface, which can therefore negatively influence antigen binding efficiency, as compared to the smaller receptor molecules (Fab), well oriented on Au which resulted in a higher number of accessible active epitopes.[27]

Table 1. SPR Responses (ΔRU) Values for the Immobilization of CDC5-Fab and CDC5-SH and the Corresponding Binding with 5 μg/mL PWG

Surface	**Immobilization**	**PWG recognition**
CDC5-Fab	1091	606
CDC5-SH	1708	136

2. Immobilization of CDC5-Fab and CDC5-SH on Gold Electrodes. The immobilization of CDC5-Fab and CDC5-SH on Au electrode was optimized in terms of time of formation and minimization of non-specific interactions using impedance spectroscopy. Faradic impedance was used to follow CDC5-SH deposition, while the non-faradic technique was used for CDC5-Fab since it gave a more sensitive response variation than faradic impedance.

UNIVERSITAT ROVIRA I VIRGILI
BOTTOM-UP SURFACE ENGINEERING FOR THE CONSTRUCTION OF (BIO) SENSORING SYSTEMS: DESIGN STRATEGIES AND ANALYTICAL APPLICATIONS
Hossam Metwally Ahmed Nassef
ISBN:978-84-692-3235-4/DL:T-932-2009

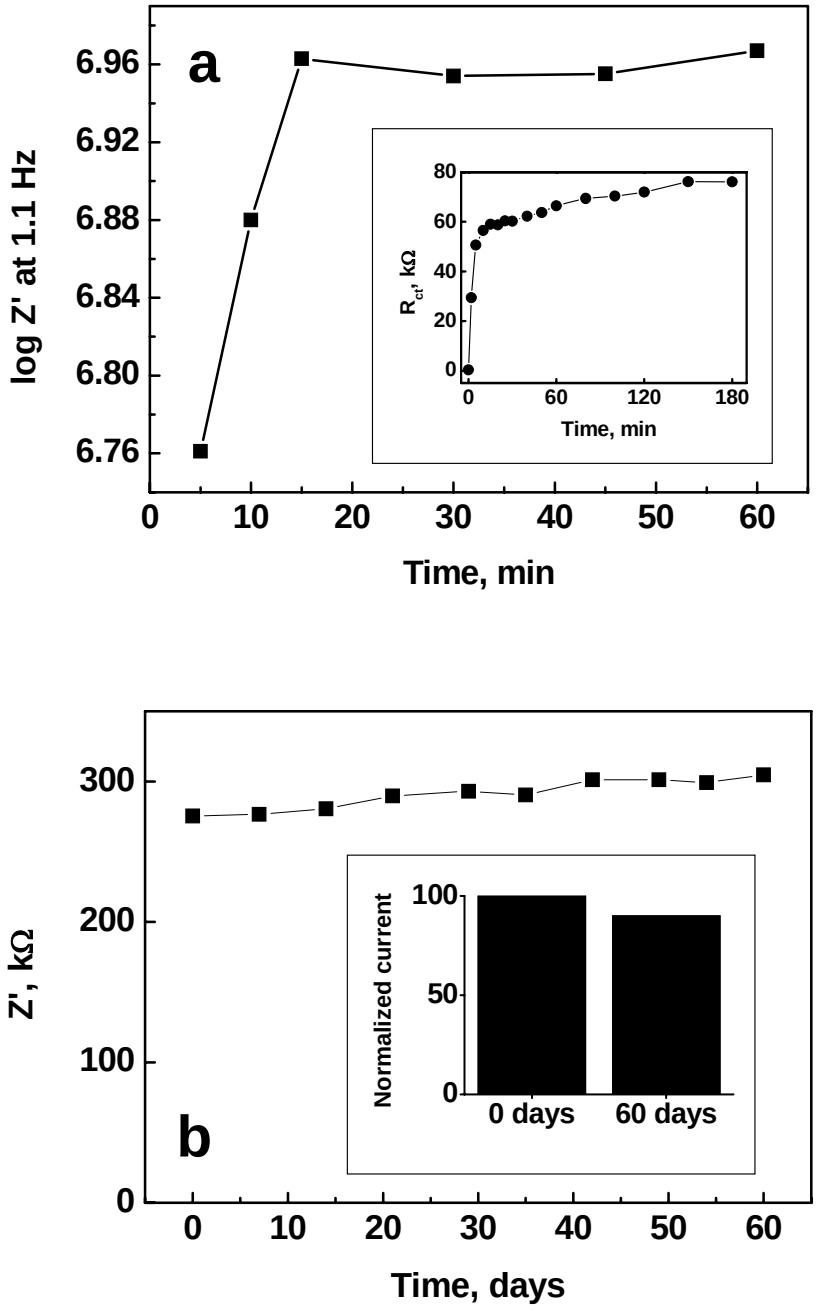

Figure 4. a) Impedance variations obtained upon formation of SAMs of CDC5-Fab (■) and CDC5-SH (●). b) Time dependence of the impedance response obtained for Au electrodes immobilized CDC5-Fab stored in PBS (0.1 M, pH 7.4) at 4 ºC. Inset: amperometric responses obtained to test the recognition ability of stored electrodes.

In both cases, the impedance response increased steadily with time (Figure 4a), reaching a saturation after 15 min for CDC5-Fab and 3 h for CDC5-SH. In both cases, the impedance increase does not account for multilayer formation since each point

ISBN:978-84-692-3235-4/DL:T-932-2009

represents the constant impedance value obtained after repeated washings to remove physically-adsorbed molecules. This difference in deposition time highlights the advantage of using Fab fragments for biosensor construction, where SAM formation is notably faster than that achievable using the whole antibody, or chemical crosslinking to alkanethiol SAMs.[35]

3. Stability of CDC5-Fab and CDC5-SH Modified Electrodes. The stability of Fab-modified Au was tested by recording the non-faradaic impedance variations weekly for two months for electrodes stored in PBS buffer at 4 ºC (Figure 4b). The electrodes modified with CDC5-Fab showed a slight impedance increase at fixed frequency (1.1 Hz) in the first two weeks, remaining constant during the rest of the stability study. A similar behavior was obtained for the CDC5-SH modified electrodes with (not shown) indicating a stable antibody layer was attached to the Au surface. After two months of storage, < 10% lost of antigen recognition activity was observed for the Fab modified Au electrodes as revealed by amperometric measurements, indicating the high stability of the immobilized Fab fragments.

4. Evaluation of Non-Specific Interactions. In immunosensors, it is critical to avoid the interaction of the target analyte or labeled reporter antibody with the surface (non-specific binding) while maximizing the recognition by the immobilized biocomponent (specific binding). In this study (1-mercaptoundec-11-yl)-tetra-(ethyleneglycol) and Tween® 20 were used to prevent non-specific adsorption. EIS and amperometry have been used to evaluate the occurrence of non-specific interactions on SAMs of PEG further blocked with Tween® (0.05 % w/v), as well as gold surfaces modified with specific and non-specific Fab fragments against gliadin, using CEA as a non-specific analyte.

Impedance measurements (Figure 5) shows the occurrence of a very low degree (< 3%) of non-specific adsorption on a bare SAM of PEG when exposed to 20 μg/mL of PWG for 30 min. Similarly, amperometric measurements (Table 2) carried out using 30 ng/mL PWG are in agreement with the EIS results. In a situation more comparable to the final immunosensor format, where antibody Fab fragments are immobilized on gold and incubated with a non-specific antigen (carcinoembryonic antigen, CEA), the non-specific binding value was 4.4%.

UNIVERSITAT ROVIRA I VIRGILI
BOTTOM-UP SURFACE ENGINEERING FOR THE CONSTRUCTION OF (BIO) SENSORING SYSTEMS: DESIGN STRATEGIES AND ANALYTICAL APPLICATIONS
Hossam Metwally Ahmed Nassef
ISBN:978-84-692-3235-4/DL:T-932-2009

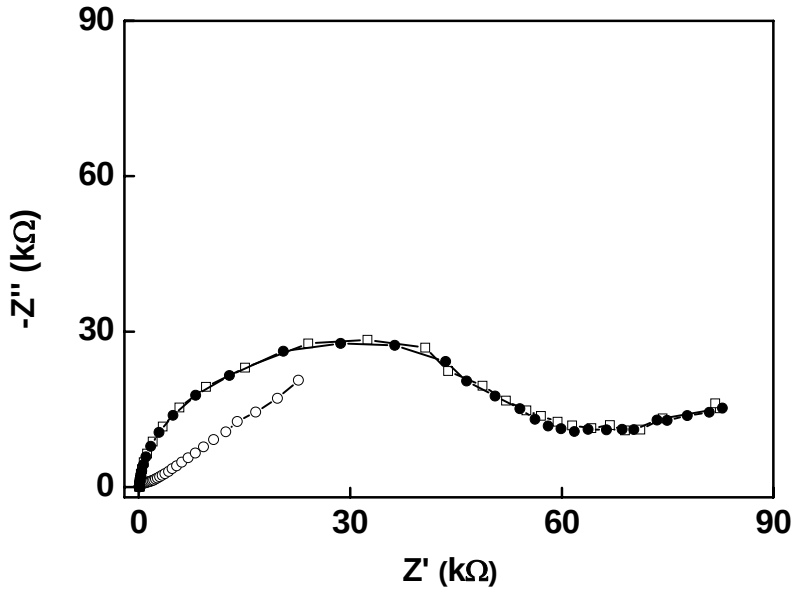

Figure 5. Complex impedance plots (in 1 mM $K_3Fe(CN)_6$ solution in PBS pH 7.4) recorded at bare Au (○), PEG modified Au covered with Tween 20 (●), and after incubation with 20 μg/mL PWG (□).

In addition, the SPR responses corresponding to the binding of 5 μg/mL of the non-specific analytes recombinant high molecular weight peptic triptic gluten (r-HMW PTGlu), carcinoembryonic antigen (CEA), and prostate specific antigen (PSA) with the immobilized Fab molecules resulted in a very small increase in SPR responses of 8.2, 5.2 and 6.2 RUs, respectively (Table 3), which represents 0.86–1.35% of the signals observed for the specific antigen. These results indicating that the Fab modified Au surfaces are highly specific to PWG antigen. Moreover, the presence of non-specific proteins in the detection media does not interfere with PWG. Therefore, this immunosensor could have a wide range of applications for the detection of PWG in real samples.

UNIVERSITAT ROVIRA I VIRGILI
BOTTOM-UP SURFACE ENGINEERING FOR THE CONSTRUCTION OF (BIO) SENSORING SYSTEMS: DESIGN STRATEGIES AND ANALYTICAL APPLICATIONS
Hossam Metwally Ahmed Nassef
ISBN:978-84-692-3235-4/DL:T-932-2009

Table 2. Amperometric Responses at Different Surfaces Corresponding to Non-Specific Binding and Cross-Reactivity

Surface	**Δi (nA)**	**%NSB**[1]
Au|PEG&Tween|30 ng/mL PWG	0	0
Au|Fab (CDC5)|30 ng/mL CEA	7	4.4
Au|Fab (CEA)|30 ng/mL PWG	25	15.8
Au|Fab (CDC5)|30 ng/mL PWG	158	-

[1] NSB = 100 × ($\Delta i^{non\text{-}analyte}$ / $\Delta i^{analyte}$), where NSB is the degree of non-specific binding and Δi represents the change in the amperometric current responses before and after injection of hydroquinone.

Table 3. Observed RU Values for CDC5-Fab and CDC5-SH Modified Au Surface After Incubation with Different Non-Specific Analytes.

	Surface	
Sample	**CDC5-Fab (%NSB)**[1]	**CDC5-SH (%NSB)**[1]
Sigma gliadin	376.8 (62.12)	0 (0)
r-HMW PTGlu	8.2 (1.35)	6.7 (4.9)
CEA	5.2 (0.86)	-
PSA	6.2 (1.02)	-

[1]NSB = 100 × ($RU^{non\text{-}analyte}$ / $RU^{analyte}$), where NSB is the degree of non-specific binding and ΔRU represents the change in RU values before and after incubation of the surface with 5 μg/mL of the selected analyte.

Electrochemical Detection of Gliadin. 1. Immunosensor Construction. Figure 6 represents the impedance spectra of the successive building steps leading to the construction of the gliadin immunosensors using CDC5-Fab and CDC5-SH. The impedance spectra of each building step of both biosensors consisted of a semicircle whose extrapolation to the x axis gives the charge-transfer resistance (R_{ct}) of each layer. This value is closely related with the hindering of the flux of the redox couple towards the electrode surface and, therefore, addition of successive layers increases this value. As shown in figure 6, the diameter of the semicircle was increased with the binding of

UNIVERSITAT ROVIRA I VIRGILI
BOTTOM-UP SURFACE ENGINEERING FOR THE CONSTRUCTION OF (BIO) SENSORING SYSTEMS: DESIGN STRATEGIES AND ANALYTICAL APPLICATIONS
Hossam Metwally Ahmed Nassef
ISBN:978-84-692-3235-4/DL:T-932-2009

each corresponding protein layer, providing evidence of the successful formation of the immunocomplex.

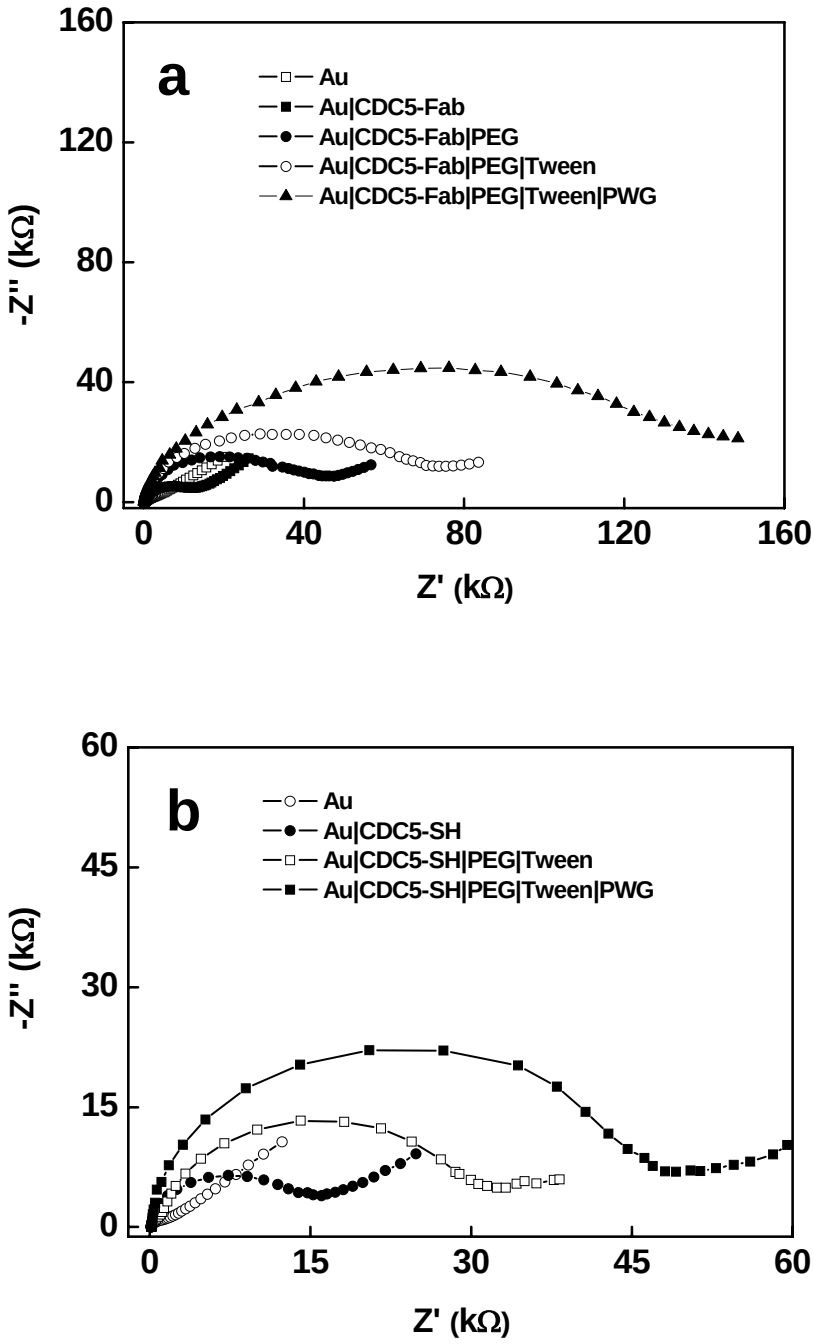

Figure 6. Complex impedance plots (in 1 mM $K_3Fe(CN)_6$ solution in PBS pH 7.4) recorded at a SAM of CDC5-Fab (a) and CDC5-SH (b) modified Au electrodes for the sequential immobilization steps of the immunosensors.

UNIVERSITAT ROVIRA I VIRGILI
BOTTOM-UP SURFACE ENGINEERING FOR THE CONSTRUCTION OF (BIO) SENSORING SYSTEMS: DESIGN STRATEGIES AND ANALYTICAL APPLICATIONS
Hossam Metwally Ahmed Nassef
ISBN:978-84-692-3235-4/DL:T-932-2009

2. Optimization of Incubation Times of Recognition and Detection Steps for Fab-Based Biosensor. Since the analytical performance of the immunosensor is directly related to its ability to recognize the target PWG, it is essential to optimize the time required for the complete reaction between the antigen and the immobilized biorecognition probe. Figure 7a shows the influence of incubation time (0-45 min) on the impedance response of the system in the presence of 30 ng/mL PWG. The log Z' values improved with increasing incubation time and then maintained the maximum value after 10 min incubation. Therefore, this incubation time was used in further experiments.

The incubation time required for the complete interaction between the detecting conjugate (anti-gliadin-HRP) and the CDC5-Fab/PWG complex was studied using amperometry (Figure 7b). After modification of the Au surfaces with CDC5-Fab fragments, blocking and incubation with 30 ng/mL PWG for 10 minutes, the system was exposed to 100 μg/mL R5-HRP at different incubation times (0-60 min). The amperometric responses were then recorded reaching saturation after 30 min incubation. Therefore, this incubation time was used for the amperometric detection of PWG.

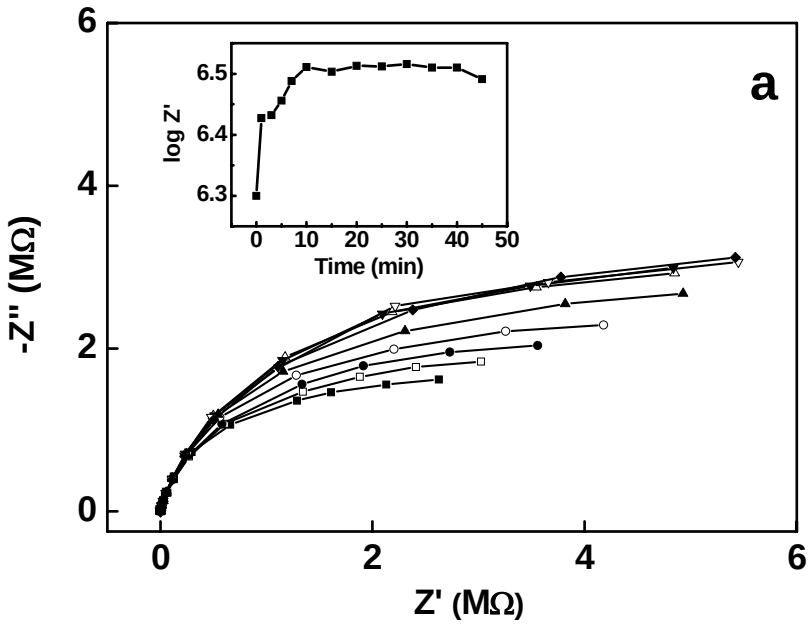

UNIVERSITAT ROVIRA I VIRGILI
BOTTOM-UP SURFACE ENGINEERING FOR THE CONSTRUCTION OF (BIO) SENSORING SYSTEMS: DESIGN STRATEGIES AND ANALYTICAL APPLICATIONS
Hossam Metwally Ahmed Nassef
ISBN:978-84-692-3235-4/DL:T-932-2009

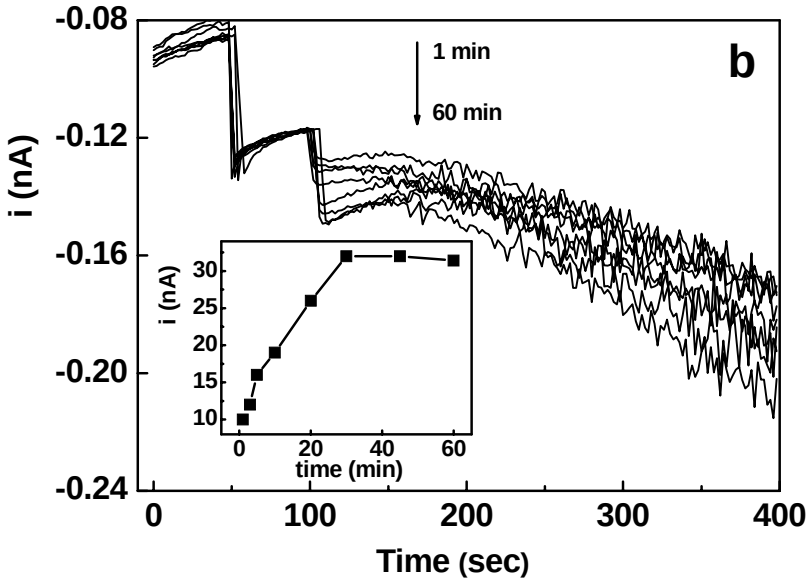

Figure 7. (a) Nyquist plots of the non-faradaic impedance in PBS (pH 7.4) at CDC5-Fab modified electrodes after interaction with 30 ng/mL PWG at incubation times; 0(■), 1(□), 3(●), 5(○), 7(▲), 10(Δ), 15(▼), 20(∇), and 25(♦) minutes,. Inset, the time dependence of log Z` 0.0383 Hz. (b) Amperometric responses at CDC5-Fab modified immunosensor in PBS (pH 7.4) at different incubation times with 10 ng/mL R5-HRP; (0, 1, 3, 5, 10, 20, 30, 45 and 60 minutes) Inset: time dependence of current responses.

3. Electrochemical Detection of PWG. The impedance technique allows a fast, direct labeless detection of targets. We have investigated the possibility of using this technique for PWG detection using the constructed immunosensors. Figure 8a shows the calibration plots obtained using both CDC5-Fab and CDC5-SH modified electrodes. At higher concentration levels of PWG (μg/mL), R_{ct} values were linearly correlatable with PWG concentrations (1-20 μg/mL) using the Fab immunosensor, with an LOD of 0.42 μg/mL. At lower concentration levels of PWG (ng/mL), the impedance technique was not sensitive enough to detect the minimal changes in the biointerface structure and not suitable for gliadin detection with the CDC5-Fab fragments. However, with using CDC5-SH, the R_{ct} variations were substantially less sensitive, which may be due to non-controlled orientations of the modified antibody.

Detection of very low PWG concentrations levels (ng/mL) was achieved with the CDC5-Fab biosensor using amperometric detection. Figure 8b shows the amperometric calibration curve, in which the current response showed a linear relationship with the

UNIVERSITAT ROVIRA I VIRGILI
BOTTOM-UP SURFACE ENGINEERING FOR THE CONSTRUCTION OF (BIO) SENSORING SYSTEMS: DESIGN STRATEGIES AND ANALYTICAL APPLICATIONS
Hossam Metwally Ahmed Nassef
ISBN:978-84-692-3235-4/DL:T-932-2009

concentration of PWG over the range of 5–30 ng/mL with a limit of detection of 3.29 ng/mL. This value is twice lower than that previously obtained by our group using a CDC5 covalently immobilized on a bipodal alkanethiol based self-assembled monolayer[35] and highlights the advantage of using antibody fragments for the detection of lower levels of target.

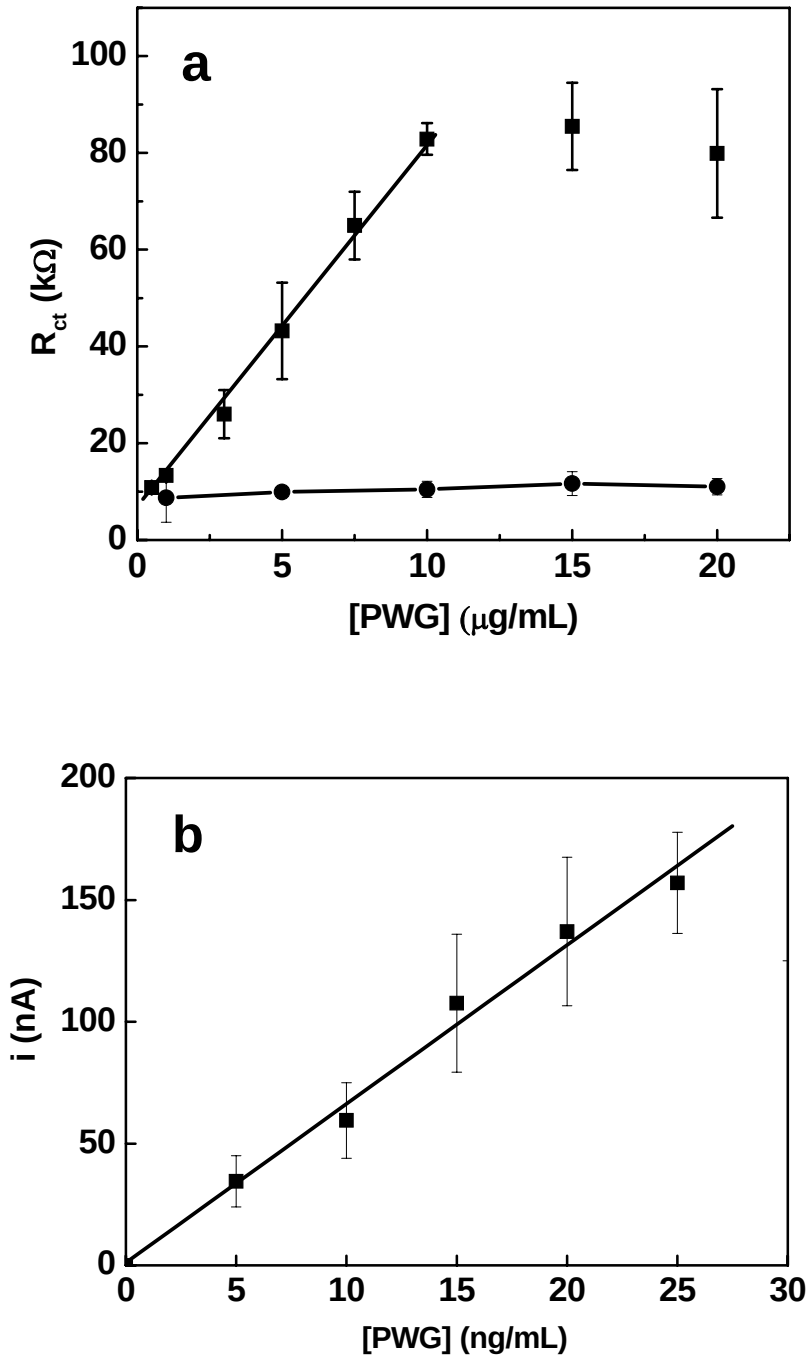

Figure 8. a) Impedimetric calibration curves for CDC5-Fab (■) and CDC5-SH (●); (b) Amperometric calibration plot at CDC5-Fab modified immunosensor.

ISBN:978-84-692-3235-4/DL:T-932-2009

CONCLUSIONS

An electrochemical gliadin immunosensor based on the spontaneous adsorption of anti-gliadin Fab fragments on Au surfaces has been developed and compared with whole antibody modified electrodes. SPR results revealed that the antigenic CDC5-Fab monolayer contains about 3 times more epitopes per square centimeter than CDC5-SH. CDC5-Fab formed a stable monolayer on gold after 15 min and retained >90% of antigen recognition ability after 2 month of storage at 4ºC. Detection of gliadin of Fab modified electrodes was evaluated by impedance and amperometry. Labeless impedimetric detection achieved a LOD of 0.42 μg/mL while the amperometric immunosensor based on Fab fragments showed a highly sensitive response with LOD 3.29 ng/mL. The Fab based immunosensor offer the advantages of being highly sensitive, easy and rapid to prepare, with a low assay time.

ACKNOWLEDGEMENTS

This work has been carried out as part of the Commission of the European communities specific RTD programme ‘Quality of Life and Management of Living Resources’ QLKI-2002-02077, the Plan Nacional GLUTACATCH and was partly financed by the Grup Emergente INTERFIBIO, 2005SGR00851. A.F. acknowledges the Ministerio de Ciencia e Innovación, Spain, for a “Ramón y Cajal” Research Professorship.

ISBN:978-84-692-3235-4/DL:T-932-2009

REFERENCES

(1) Holtz, B., Wang, Y., Xiao-Yang Z., Guo, A. *Proteomics* **2007**, *7*, 1771-1774.

(2) Danczyk, R., Krieder, B. *Biotechnol. Bioeng.* **2003**, *84*, 215-223.

(3) Shinkai, M., et al. *J. Biosci. Bioeng* **2002**, *94*, 606-613.

(4) Cass, T., Ligler, F.S. In *Immobilized Biomolecules in Analysis: A Practical Approach*; Oxford University Press: New York., 1998.

(5) Hermanson, G. T. In *Bioconjugate Techniques*; Academic Press: San Diego, 1996.

(6) Vijayendran, R. A., Leckband, D.E. *Anal. Chem.* **2001**, *73*, 471.

(7) Babacam, S., Pivarnik, P. *Biosen. Bioelectron.* **2000**, *15*, 615-621.

(8) King, D. J. In *Antibody Engineering: Design for Specific Applications in Applications and Engineering of Monoclonal Antibodies*; Routledge Taylor & Francis, 1998, pp 40-43.

(9) Coulter, A.; Harris, R. *J. Immunol. Meth.* **1983**, *59*, 199-203.

(10) Rousseaux, J.; Biserte, G.; Bazin, H. *Mol. Immunol.* **1980**, *17*, 469-482.

(11) Beale, D. *Dev.Comp. Immunol.* **1987**, *11*, 287-296.

(12) Bia, M.; Li, W.; Lia, L.; Yian, Z.; Zo, Y. *Chin. Med. Sci. J.* **1995**, *10*, 78-81.

(13) Mariant, M.; Camagna, M.; Tarditi, L.; Seccamani, E. *Mol. Immunol.* **1991**, *28*, 69-77.

(14) Saerens, D.; Huang, L.; Bonroy, K.; Muyldermans, S. *Sensors* **2008**, *8*, 4669-4686.

(15) Lu, B.; Xie, J.; Lu, C.; Wu, C.; Wei, Y. *Anal. Chem.* **1995**, *67*, 83-87.

(16) Vikholm, I., Albers, W.M., Välimäki, H., Helle, H. *Thin Solid Films* **1998**, *643*, 327-329.

(17) Bonroy, K., Frederix, F., Reekmans, G., Dewolf, E., De Palma, R., Borghs, G., Declerck, P., Goddeeris, B. *J. Immunol. Meth.* **2006**, *312*, 167-181.

(18) Vikholm-Lundin, I. *Langmuir* **2005**, *21*, 6473-6477.

(19) Vikholm-Lundin, I.; Albers, W. M. *Biosens. Bioelectron.* **2006**, *21*, 1141-1148.

(20) Lee, W.; Oh, B. K.; Lee, W. H.; Choi, J. W. *Coll. Surf. B: Biointerfaces* **2005**, *40*, 143-148.

(21) Wang, H.; Zeng, H.; Liu, Z.; Yang, Y.; Deng, T.; Shen, G.; Yu, R. *Anal. Chem.* **2004**, *76*, 2203-2209.

(22) Song, S.; Li, B.; Wang, L.; Wu, H.; Hu, J.; Li, M.; Fan, C. *Mol. Biosys.* **2007**, *3*, 151-158.

(23) Esseghaier, C., Helali, S., Fredj, H.B., Tlili, A., Abdelghani, A. *Sens. Act. B: Chemical* **2008**, *131*, 584-589.

(24) Hleli, S.; Martelet, C.; Abdelghani, A.; Burais, N.; Jaffrezic-Renault, N. *Sens. Act. B: Chemical* **2006**, *113*, 711-717.

(25) Vareiro, M. M. L. M.; Liu, J.; Knoll, W.; Zak, K.; Williams, D.; Jenkins, A. T. A. *Anal. Chem.* **2005**, *77*, 2426-2431.

(26) Ihalainen, P.; Peltonen, J. *Langmuir* **2002**, *18*, 4953-4962.

(27) O'Brien, J. C.; Jones, V. W.; Porter, M. D.; Mosher, C. L.; Henderson, E. *Anal. Chem.* **2000**, *72*, 703-710.

(28) Harada, Y., Kuroda, M., Ishida, A. *Langmuir* **2000**, *16*, 708.

(29) Brogan, K. L., Wolfe, K.N., Jones, P.A., Schoenfish, M.H. *Anal. Chim. Acta* **2003**, *496*, 73.

(30) Maki, M., Collin, P. *Lancet* **1997**, *349*, 1755.

(31) Turski, A., Georgetti, G., Brandimarte, G., Rubino, E., Lombardi, D. *Hepatogastroenterology* **2001**, *48*, 462.

(32) Lee, S. K. P. H. R. G. *Curr. Opin. Rheumatol.* **2006**, *18*, 101.

(33) Dube, C., Rostom, A., Sy, R., Cranney, A., Salojee, N., Garritty, C., Sampson, M., Zhang, L., Yazdi, F., Mamaladze, V., Pan, I., MacNeil, J., Mack, D., Patel, D., Moher, D. *Gastroenterol.* **2005**, *128*, S57.

(34) Ellis, H. J., Rosen-Bronson, S., O'Reilly, N., Ciclitira, P.J. *Gut* **1998**, *43*, 190.

(35) Nassef, H. M.; Bermudo Redondo, M. C.; Ciclitira, P. J.; Ellis, H. J.; Fragoso, A.; O`Sullivan, C. K. *Anal. Chem.* **2008**, *80*, 9265-9271.

(36) van Eckert, R., Berghofer, E., Ciclitira, P.J., Chirdo, F., Denery-Papini, S., Ellis, H.J., Ferranti, P., Goodwin, P., Immer, U., Mamone, G., Méndez, E., Mothes, T., Novalin, S., Osman, A., Rumbo, M., Stern, M., Thorell, L., Whim, A., Wieser, H. *J. Cer. Sci.* **2006**, *43*, 331.

(37) Ciclitira, P. J., Dewar, D.H., Suligoj, T., O'Sullivan, C. K., Ellis, H. J. In *Proceedings of the 12th International Celiac Symposium*: New York 2008.

(38) Riddles, P. W. *Meth. Enzymol* **1983**, *91*, 49-60.

(39) Laemmli, U. K. *Nature* **1970**, *227*, 680.

UNIVERSITAT ROVIRA I VIRGILI
BOTTOM-UP SURFACE ENGINEERING FOR THE CONSTRUCTION OF (BIO) SENSORING SYSTEMS: DESIGN STRATEGIES AND ANALYTICAL APPLICATIONS
Hossam Metwally Ahmed Nassef
ISBN:978-84-692-3235-4/DL:T-932-2009

CHAPTER 9:

Evaluation of electrochemical grafting of full length antibody onto gold via diazonium reduction as surface chemistry for immunosensor construction

UNIVERSITAT ROVIRA I VIRGILI
BOTTOM-UP SURFACE ENGINEERING FOR THE CONSTRUCTION OF (BIO) SENSORING SYSTEMS: DESIGN STRATEGIES AND ANALYTICAL APPLICATIONS
Hossam Metwally Ahmed Nassef
ISBN:978-84-692-3235-4/DL:T-932-2009

Evaluation of electrochemical grafting of full length antibody onto gold via diazonium reduction as surface chemistry for immunosensor construction

Abstract

In the work presented here, we report on the electrochemical reduction of the in situ prepared diazonium cations of conjugate prepared from the monoclonal full length anti-gliadin antibody (CDC5) and the linker 3,5-bis(aminophenoxy)benzoic acid (DAPBA) onto gold surface. The deposition of CDC5-DAPBA diazonium cations was carried out electrochemically using cyclic voltammetry using different numbers of potential cycles and via application of fixed potential at various deposition times, as well as non-electrochemically for several lengths of exposure. Cyclic voltammetry showed two ill defined reduction peaks at +0.047 and +0.414 V in the first scan due to the diazonium depositon of CDC5-DAPBA. Extensive washing process in PBS-Tween (0.01 M, pH 7.4, with 0.05% v/v Tween) was carried out to remove the formed multilayers and non-specifically adsorbed species. Following the surface modification with CDC5-DAPBA, the remaining free spaces on the electrode surface was blocked via electrochemical reduction of diazonium cations of aminophenylacetic acid (APAA) applied for three potential cycles. The surface chemistries were evaluated using cyclic voltammetry and electrochemical impedance spectroscopy (EIS). The modified CDC5-DAPBA surface showed high amperometric response with a sensitivity 0.082 $nA.ng^{-1}$ ml, after incubation with 5 μg/ml gliadin indicating the excellent specificity toward gliadin, while no response was observed in the absence of gliadin. Whilst the approach was demonstrated for the formation of an immunoactive surface, further research is required to understand the formation of mono and multilayers using the diazonium approach, so as to deposit biocomponents in a controllable fashion.

UNIVERSITAT ROVIRA I VIRGILI
BOTTOM-UP SURFACE ENGINEERING FOR THE CONSTRUCTION OF (BIO) SENSORING SYSTEMS: DESIGN STRATEGIES AND ANALYTICAL APPLICATIONS
Hossam Metwally Ahmed Nassef
ISBN:978-84-692-3235-4/DL:T-932-2009

1. Introduction

Pinson and co-workers first demonstrated that diazonium salts could be reduced onto glassy carbon surfaces to yield very stable functional layers [1], and since then this technique has been widely studied and used to modify a variety of substrates, such as carbon [2,3], carbon nanotubes [4,5], metals [6-9] and semi-conductors [10-14]. The reduction of diazonium salts is recognised to be a very versatile and simple way to graft a wide variety of functional groups onto conductive surfaces using specific aryl derivatives. The reduction can occur in aqueous and organic media, and can be either spontaneous via simple dipping of the material into a solution of the diazonium salt [9,15] or electro-induced [1,9]. The mechanism for the electro-induced deposition involves the formation of an aryl radical at the vicinity of the surface following the reduction of the diazonium salt, leading to the evolution of an N_2 molecule and formation of a covalent bond [16] between the aryl group and the substrate allowing a strong attachment of the deposited layers, requiring mechanical abrasion to remove them from the surface. This mechanism can yield coatings of variable thickness (from monolayer to multilayers) depending on the charge allowed to reduce the diazonium, concentration of the diazonium and/or the reaction time.

Gold is important relative to carbon as it has a lower capacitance, and it can be produced very flat or as a single crystal, and is compatible with many microfabrication technologies. The attraction of Au-thiol chemistry is that well ordered and densely-packed monolayers can be easily formed, with a reasonably strong bond formed between the immobilized molecule and the electrode, and furthermore, a diverse range of molecules can be synthesized with a vast number of functional groups to modify the electrode surface [17-19]. One of the disadvantages of the Au-thiol system is that alkanethiols can be oxidatively or reductively desorbed at potentials typically outside the window defined by -800 to +800 mV versus Ag/AgCl [20], as well as the fact that alkanethiols are desorbed at temperatures over 100 ºC [21,22]. Additionally, as gold is a highly mobile surface, this results in monolayers moving across the electrode surface. Furthermore, the Au-thiolate bond is prone to UV photooxidation [23] and the Au/thiol junction creating large tunneling barrier (≈ 2 eV) which affects on the rate of electron transfer from the organic monolayer to the electrode [24]. Futhermore, the formation of a stable alkanethiol based SAM can require between 3 and 120 hours to allow organisation into an energetically favourable monolayer [25].

The electrochemical reduction of aryl diazonium salts is one possible alternative which has recently been reported as a method for the covalent derivatization of carbon or gold electrodes, forming a covalent bond which is strong, stable over both time and temperature, non-polar and conjugated [20].

The advantages of the diazonium reduction approach as compared to alkanethiol self-assembled monolayers, include a highly stable surface over time and over a wide potential window, ease of preparation, and the ability to synthesize diazonium salts with a wide range of functional groups [2,26]. In addition, the ability to create a diazonium-modified surface by the application of a potential bias allows the selective functionalization of closely spaced microelectrode surfaces. While the use of carbon surfaces have dominated the majority of studies relating to the electrodeposition of aryl diazonium salts, Au surfaces have also been shown to be suitable for diazonium grafting [8,27]. The selective functionalization of Au electrodes with control over surface functional group density and electron transfer kinetics employing diazonium chemistry has been reported [28]. In contrast to the more common thiol–Au chemistry, diazonium modification on Au surfaces yields increased stability with respect to long-term storage in air, potential cycling under acidic conditions, and a wider potential window for subsequent electrochemistry [29], which has been proved by the calculated bonding energy; 24, 70, and 105 kcal/mol on Au, Si, and carbon, respectively [30,31]. The reductive deposition of aryl diazonium salts onto gold electrodes is superior for electrochemical sensors than either alkanethiol modified gold electrodes or aryl diazonium salt modified GC electrodes [29].

Some obvious advantages of the use of diazonium-functionalized antibodies and the electrically addressable deposition procedure are simplicity, fewer reagents and preparation steps; a strong covalent bond between antibody and electrode; the ability to selectively coat and control deposition onto electrode platforms and finally, a reduced number of chemical reactions on a surface relative to attaching a protein to a surface that has been diazonium-functionalized. The use of diazonium modification also allows for attachment to a variety of substrates including conducting and semiconducting substrates as well as carbon nanotubes [32]. Recently, Marquette and co-workers introduced a technique for the direct and electroaddressable immobilization of proteins consisting of coupling 4-carboxymethylaniline to antibodies followed by diazotination of the aniline derivative to form an aryl diazonium functional group [33]. However, much of the work has been devoted to the study of a variety of aryl derivatives for

ISBN:978-84-692-3235-4/DL:T-932-2009

possible applications of the process [34] but little has been published about the influence of the experimental conditions (potential range, eletrochemical techniques, etc.) on the deposition mechanism onto gold surfaces and the potential formation of multilayers [20,27,29,32,35-40].

In the work reported here, we exploit the deposition of full length antibody raised against gliadin, CDC5, coupled to the linker 3,5-bis(aminophenoxy)benzoic acid (DAPBA) onto gold via the electrochemical reduction of corresponding in situ prepared diazonium salt and non-electrochemical adsorption of the same salt respectively. DAPBA has a bipodal structure featuring two aniline groups linked to a COOH-terminated central benzene ring (see Figure 1a). This structure, with two points of connection to the electrode surface is expected to give a higher stability to the grafted assembly while allowing the covalent attachment of biomolecules through the carboxylic group. The electrochemical graftings were carried out via the application of potential scans with different numbers of potential cycling and/or via the application of fixed potential at different deposition times, while the non-electrochemical (spontaneous) immobilization was carried out by dipping the electrode in diazonium solution at different exposure times. In the modification process, a washing step was optimized at different stirring times in PBS-Tween to remove the non-specifically adsorbed protein molecules. The CDC5-DAPBA modified Au electrodes have been characterized by CV and electrochemical impedance spectroscopy (EIS). The affinity of the immobilized antibody toward PWG was studied using EIS and amperometry.

2. Experimental

2.1. Chemicals and materials

2.1.1. Materials

The Prolamin Working Group (PWG, martin.stern@med.uni-tuebingen.de) provided a gliadin preparation [41] to be used as a basis for standardizing the analysis and detection of gliadin. Monoclonal anti-gliadin antibody (CDC5) was developed by HJ Ellis and PJ Ciclitira as previously reported [42]. Monoclonal antigliadin horseradish peroxidase conjugate was used as received. *N*-(3-dimethylaminopropyl)-*N'*-ethylcarbodiimide (EDC), *N*-hydroxysuccinimide (NHS), hydroquinone, H_2O_2, Trizma base, 4-aminophenyl acetic acid (APAA) and phosphate buffered saline with 0.05% Tween® 20 (dry powder) were purchased from Sigma-Aldrich. 3,5-Bis(aminophenoxy)benzoic acid (DAPBA) was purchased from TCI, Belgium. All

ISBN:978-84-692-3235-4/DL:T-932-2009

aqueous solutions were prepared with Milli-Q water (Millipore Inc., Ω = 18 MOhms·cm). Gliadin stock solutions were freshly prepared in PBS-Tween containing 60% (v/v) ethanol and diluted in the appropriate buffer.

2.1.2. Electrochemical Instrumentation

All the electrochemical measurements were performed using a PGSTAT12 potentiostat (Autolab, The Netherlands) controlled with the General Purpose Electrochemical System (GPES) software, with built-in frequency response analyzer FRA2 module. A three electrode configuration of Ag/AgCl-3M NaCl as a reference (CH Instruments., model CHI111), Pt wire as a counter (BAS model MW-1032), and bare or modified Au (BAS model MF-2014, 1.6 mm diameter) as working electrode was used. All the Faradaic impedimetric measurements were carried out in 0.1 M phosphate buffer saline (PBS) (pH 7.4) containing 1 mM $Fe(CN)_6^{3-}$ and 1 mM $Fe(CN)_6^{4-}$ within the frequency range of 0.1 Hz-100 kHz at a bias potential of +0.22 V and ac amplitude of 5 mV. All amperometric measurements were carried out at fixed potential (-0.2 V) under continuous stirring at 350 rpm.

2.2. Preparation of the conjugate CDC5-DAPBA.

Twenty five milligrammes of DAPBA were dissolved in 5 mL (0.1 M) HCl, and the carboxylic acid groups of the DAPBA were activated via the addition 0.2 M EDC and 50 mM NHS in 0.1 M MES buffer (pH 5) for 15 min, followed by addition of 200 μL (4.4 mg/ml) CDC5 in PBS (pH 7.4) for 2 h at room temperature. The excess reagents were removed, and the conjugate was purified and concentrated using YM 3 KDa microcon, and the concentration of the conjugate was then measured at 280 nm, and stored at -20 ºC in PBS buffer (pH 7.4, 0.1M). The amino groups of the DAPBA coupled to the full length antibody CDC5, was diazotised in an aqueous solution of 20 mM HCl and 20 mM $NaNO_2$ for 15 min under stirring in ice-cold water. The freshly prepared diazonium salt solution was then immediately used to immobilize the modified CDC5 onto the gold electrode surface.

2.3. Deposition of CDC5-DAPBA on gold surgaces.

Prior to electrode modification, the gold surfaces were extensively cleaned by polishing in a slurry of alumina powder of 0.3 μm to a mirror finish. The electrodes

ISBN:978-84-692-3235-4/DL:T-932-2009

were then sonicated in Milli-Q water and in ethanol for 5 min to remove any alumina remnants. The electrodes were placed in hot (~70 ^{o}C) Piranha's solution (1:3 v/v, 30% H_2O_2, in concentrated H_2SO_4) for 5 minutes, and thoroughly washed with Milli-Q water, ethanol and finally dried with dry nitrogen. [*Warning:* Piranha's solution is highly corrosive and violently reactive with organic materials; this solution is potentially explosive and must be used with extreme caution]. The bare electrodes were characterized using cyclic voltammetry (CV) and faradaic impedance spectroscopy in $Fe(CN)_6^{3-/4-}$ in PBS buffer (0.1 mM, pH = 7.4).

2.3.1. Electrochemical deposition at different potential cycling

The electrochemical deposition of the CDC5-DAPBA onto Au was carried out using cyclic voltammetry by application of different potential cycling. In the three configuration cell, the working electrode was immersed in 2 mL (100 μg/mL) of CDC5-DAPBA. Potential cycling was applied between +0.7 to -0.4 V vs Ag/AgCl at a scan rate of 100 mv/sec. The deposition step was carried out for different numbers of potential cycles (1, 2, 3, 4, 5, 10, and 20 scans).

2.3.2. Electrochemical deposition at fixed potential (-0.4 V) at different deposition times.

The electrochemical reduction of CDC5-DAPBA was also carried out at a fixed potential of -0.4 V vs Ag/AgCl at different deposition times. The working electrode was immersed in 2 mL (100 μg/mL) of freshly prepared diazonium salt solution. A fixed potential (-0.4 V) was applied vs Ag/AgCl at different deposition times (0, 30, 60, 120, 180, 240, 300, 600, 1200 and 1800 sec).

2.3.3. Non-electrochemical deposition at different exposure times

Non-electrochemical deposition was carried out via immersion of a clean gold electrode in a freshly prepared solution of CDC5-DAPBA (100 μg/mL) at different exposure times (0, 30, 60, 300, 600, 1200, 1800, and 3600 sec), without application of any potential at the working electrode.

ISBN:978-84-692-3235-4/DL:T-932-2009

2.4. Surface Chemistry.

2.4.1 Optimization of the washing step required for removal of non-specific adsorption of CDC5-DAPBA conjugate.

During the immobilization process of the conjugate CDC5-DAPBA onto Au surfaces, non-specific adsorption the CDC5-DAPBA (i.e. via passive adsorption) possibly occurred. Therefore, a washing process was carried out to remove the passively adsorbed CDC5-DAPBA. The washing step was carried out via immersion of the modified electrode in PBS-Tween (0.01 M, pH 7.4, with 0.05% v/v Tween) at different times under stirring conditions (5, 10, 20, 30, 40, 50, 60, 70, 80, 90, and 100 min).

2.5. Immunosensing assay construction.

The prepared CDC5-DAPBA was immobilized onto Au electrode surface via the application of one potential cycle between +0.7 to -0.4 V, and the non-specifically adsorbed molecules were removed via stirring in PBS-Tween (0.01 M, pH 7.4, with 0.05% v/v Tween) for 90 min. The immobilization and washing steps were sequentially repeated twice in order to "fill" the free spaces obtained after washing. The remaining free spaces were blocked with 4-aminophenylacetic acid (APAA) (via electrochemical reduction of its in situ prepared diazonium salt in potential range +0.7 to -0.4 V), the carboxyl groups of APAA were converted to hydroxyl via consecutive interactions with EDC/NHS and ethanolamine (1M, pH 8.3) for 15 min, respectively, followed by a second blocking through incubation in PBS-Tween (0.05 M, pH 7.4) solution for 30 min, thus facilitating a mixed layer which incorporated hydrophilic moieties for repulsion of non-specific protein binding. The electrodes were then exposed to gliadin (5 μg/mL) in PBS-Tween solution for 30 min. Each building step during the fabrication of the biosensor was characterized using CV and EIS using $Fe(CN)_6^{3-/4-}$ in PBS solution as electroactive marker. An additional layer of labelled antibody was incubated with 100 μg/mL anti-gliadin-HRP in PBS for 30 min at room temperature under stirring.

2.5.2. Electrochemical detection of gliadin.

2.5.2.1. Impedimetric detection.

Detection of gliadin on the modified electrodes was carried out using EIS and amperometry. EIS measurements were carried out in 1 mM $Fe(CN)_6^{3-/4-}$ in PBS (0.1 M, pH 7.4) in the frequency range of 0.1 Hz-100 kHz at a bias potential of +0.22 V and 5

ISBN:978-84-692-3235-4/DL:T-932-2009

mV amplitude before and after binding of (5 μg/mL) gliadin. The obtained spectra were fitted to an equivalent electrical circuit using the Autolab impedance analysis software.

2.5.2.2. Amperometric detection.

Clean gold electrodes were modified with CDC5-DAPBA as previously outlined. The free surfaces were then blocked with APAA and PBS-Tween and subsequently incubated with 5 μg/mL of gliadin in PBS-Tween for 30 min, followed by a final incubation with 100 μg/mL of anti-gliadin-HRP for 30 min. The amperometric response of the antibody-modified surface was recorded in PBS before and following two consecutive injections of 2 mM hydrogen peroxide (H_2O_2) and 2 mM hydroquinone (HQ).

3. Results and discussion

3.1. Deposition of CDC5-DAPBA on gold surfaces

3.1.1. Electrochemical deposition at different potential cycling

Figure 1a shows the strategy employed for the attachment of DAPBA to CDC5. Gold electrodes were modified with CDC5-DAPBA via electrochemical reduction of an aryl diazonium salt (100 μg/mL) in aqueous solution. Consecutive cyclic voltammograms were carried out in *in situ*-generated diazonium cations of CDC5-DAPBA at clean Au electrodes (Fig. 1b). The first sweep showed two broad ill defined reduction peaks at +0.047 and +0.414 V versus Ag/AgCl with no associated oxidation peaks indicative of the loss of N_2 and the formation of phenyl radicals, which then binds to the gold surface. The appearance of two reduction peaks may be associated with electrochemical reduction onto polycrystalline Au surfaces. This explains the formation of multi-peaks in CV curves due to the reduction of diazonium salts on different crystallographic sites of gold electrodes [39]. Subsequent scans showed a blocking of redox electrochemistry indicative of a passivated electrode, in this case, with an antibody layer.

UNIVERSITAT ROVIRA I VIRGILI
BOTTOM-UP SURFACE ENGINEERING FOR THE CONSTRUCTION OF (BIO) SENSORING SYSTEMS: DESIGN STRATEGIES AND ANALYTICAL APPLICATIONS
Hossam Metwally Ahmed Nassef
ISBN:978-84-692-3235-4/DL:T-932-2009

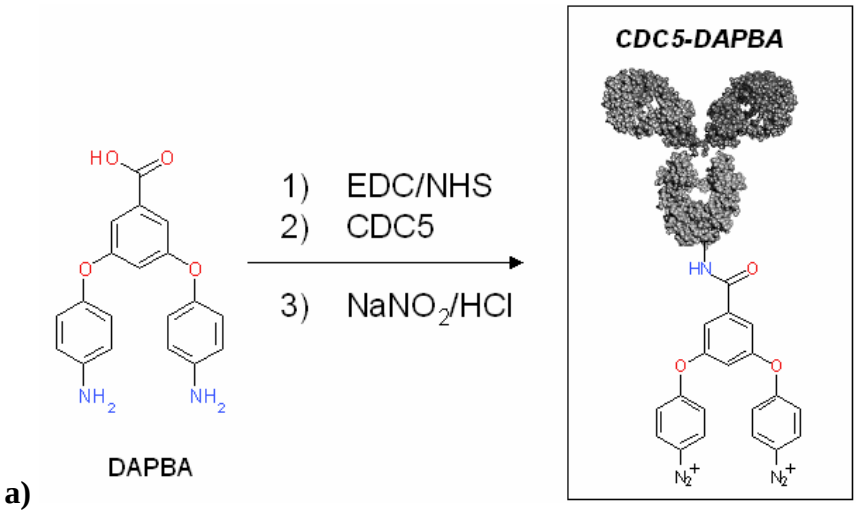

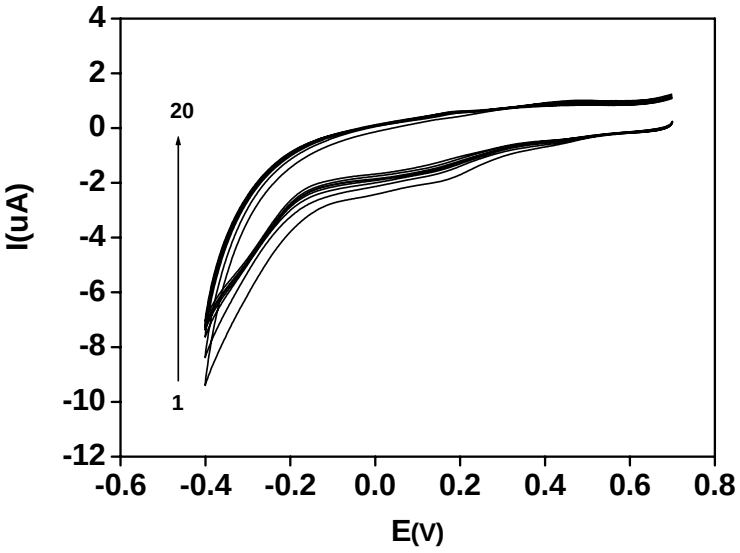

Fig 1. a) Preparation of CDC-DAPBA conjugate. b) Cyclic voltammograms in situ prepared diazonium salt solution of (100 µg/mL) CDC5-DAPBA at gold electrode at 100 mV/sec scan rate, at different number of potential scans (1, 2, 3, 4, 5, 10, and 20 cycles).

The modification processes was characterized using EIS and Figure 2 represents the Nyquist plots of the faradaic impedance in 1 mM $K_3Fe(CN)_6$ / $K_4Fe(CN)_6$ in PBS (pH 7.4) at Au electrodes modified via application of a different number of potential scans. As shown in Figure 2, the diameter of the semicircle representing the electron-transfer resistance (R_{ct}) increased with increasing the number of potential scans applied for the electrochemical reduction of *in situ* generated diazonium cations of CDC5-

UNIVERSITAT ROVIRA I VIRGILI
BOTTOM-UP SURFACE ENGINEERING FOR THE CONSTRUCTION OF (BIO) SENSORING SYSTEMS: DESIGN STRATEGIES AND ANALYTICAL APPLICATIONS
Hossam Metwally Ahmed Nassef
ISBN:978-84-692-3235-4/DL:T-932-2009

DAPBA onto the Au surface. The increase of R_{ct} value after each cycle demonstrates the successful reduction and immobilization of CDC5-DAPBA onto Au.

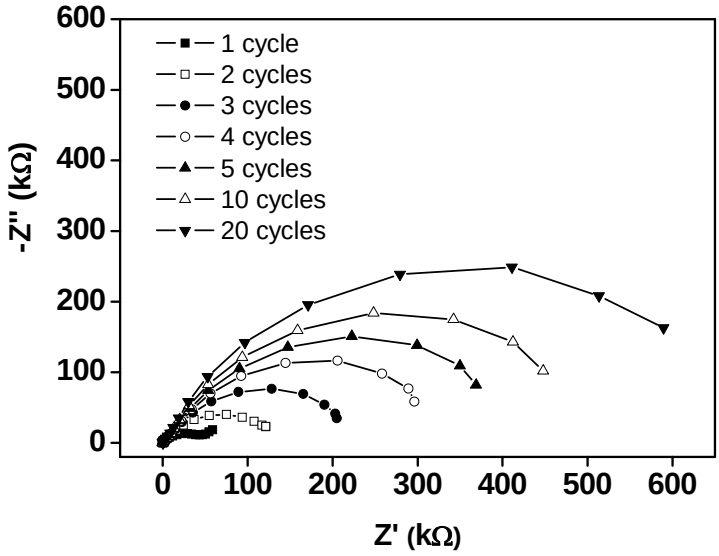

Fig. 2. Nyquist plots of the faradaic impedance in 1 mM $K_3Fe(CN)_6$ / $K_4Fe(CN)_6$ solution PBS (pH 7.4) at Au electrodes modified via application of different number of potential scans; 1(■), 2(□), 3(●), 4(○), 5(▲), 10(Δ), and 20(▼) cycles, between +0.7 and -0.4 V at 100 mV/sec scan rate vs Ag/AgCl, in in situ prepared diazonium salt solution of (100 μg/mL) CDC5-DAPBA

3.1.2. Electrochemical deposition at fixed potential

The modification of an Au surface was also carried out via the electrochemical reduction of CDC5-DAPBA diazonium cations at a fixed potential of -0.4 V at varying exposure times. The value of the applied fixed potential was chosen to be negative enough to allow the effective reduction of the diazonium moieties [36]. The permeability characteristics of the diazonium–antibody modified electrodes were investigated in 1 mM ferricyanide solution using EIS (not shown) and CV. As depicted in Figure 3, CV showed a controlled decrease in redox currents after 1, 2, and 3 electrodeposition cycles of diazonium–antibody when compared to a bare gold surface.

UNIVERSITAT ROVIRA I VIRGILI
BOTTOM-UP SURFACE ENGINEERING FOR THE CONSTRUCTION OF (BIO) SENSORING SYSTEMS: DESIGN STRATEGIES AND ANALYTICAL APPLICATIONS
Hossam Metwally Ahmed Nassef
ISBN:978-84-692-3235-4/DL:T-932-2009

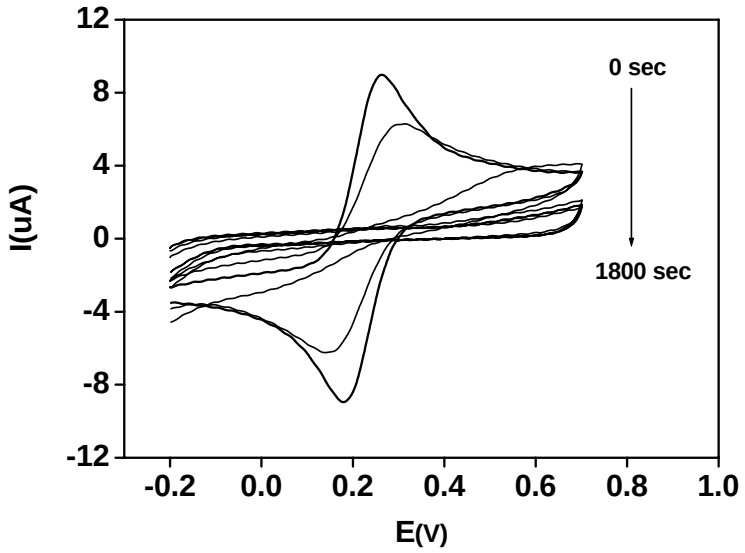

Fig 3. Cyclic voltammograms in 1 mM $K_3Fe(CN)_6$ / $K_4Fe(CN)_6$ solution PBS (pH 7.4) at CDC5-DAPBA modified Au electrode, modified at fixed potential (-0.4 V vs Ag/AgCl) at different deposition times (0, 30, 60, 120, 180, 240, 300, 600, 1200 and 1800 sec) in in situ prepared diazonium salt solution of (100 μg/mL) CDC5-DAPBA.

The apparent kinetics of the deposition of the diazonium-modified antibody is much slower than the deposition of the unconjugated diazonium molecule, which would normally result in complete electrode coverage, even after one cycle. This is probably due to the relatively lower diazonium concentration in the assembly solution and slower diffusion rate of the large diazonium–protein complex as compared to unconjugated diazonium molecules. However, the ferricyanide peak is completely suppressed after one minute, which also could be attributed to the non-spcific binding of biomolecules. Therefore, a detailed washing study was carried out to remove the non-specifically adsorbed molecules (see section 3.2.1.). The EIS results (not shown) were in agreement with the CV results obtained, and the modified Au surface showed a very high charge transfer resistance (≅ 2 MΩ) toward ferricyanide diffusion after electrodeposition.

3.1.3. Non-Electrochemical deposition at different exposure times

Spontaneous grafting of diazonium molecules onto electrodes has been observed and is favoured on easily oxidizable metals [43]. The permeability towards ferricyanide on Au electrodes held at open circuit potential in diazonium–antibody solution for the

UNIVERSITAT ROVIRA I VIRGILI
BOTTOM-UP SURFACE ENGINEERING FOR THE CONSTRUCTION OF (BIO) SENSORING SYSTEMS: DESIGN STRATEGIES AND ANALYTICAL APPLICATIONS
Hossam Metwally Ahmed Nassef
ISBN:978-84-692-3235-4/DL:T-932-2009

spontaneous grafting of the diazonium–antibody, CDC5-DAPBA conjugate was investigated. Figure 4 represents the impedance spectra recorded at Au electrode after immersion in CDC5-DAPBA solution (100 μg/ml) at different exposure times in 1mM $Fe(CN)_6^{3-/4-}$ in PBS (0.1 M, pH 7.4). As shown in Figure 4, the increase in charge transfer resistance was of only 5 kΩ changing the exposure time from 1 to 60 minutes, indicating that the spontaneous reduction of CDC5-DAPBA diazonium cations onto Au was not successful under these conditions as compared with the two previous methods for electrode modification (potential cycling and reduction at fixed potential).

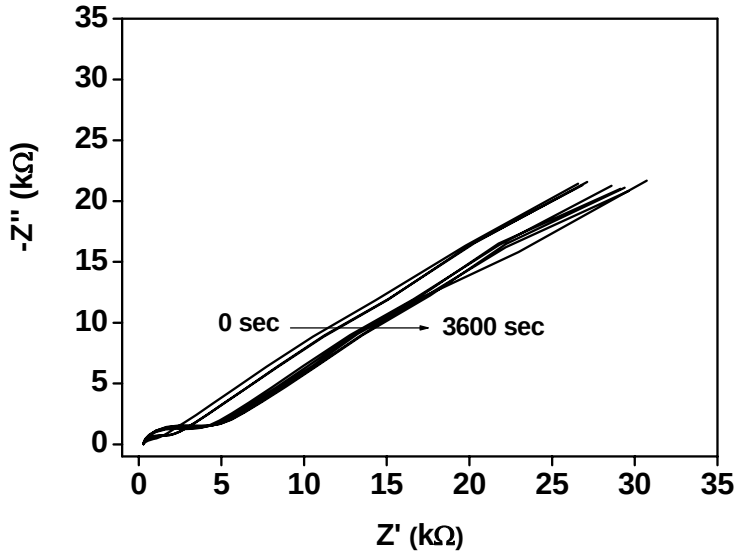

Fig 4. Complex impedance plots in 1 mM $K_3Fe(CN)_6$ / $K_4Fe(CN)_6$ solution in PBS (pH 7.4) recorded at Au electrode after immersion in in situ prepared diazonium salt solution of (100 μg/ml) CDC5-DAPBA, at different exposure times (0, 30, 60, 300, 600, 1200, 1800, and 3600 sec).

3.2. Surface Chemistry.

3.2.1 Optimization of the washing step required for removal of non-specific adsorption of CDC5-DAPBA conjugate.

Centrifugation or stirring is sufficient to remove unconjugated diazonium during diazonium protein modification so that the electrode properties are due to deposited antibody alone [32]. Therefore, to remove the non-specifically adsorbed molecules, washing steps were carried out via stirring in PBS-Tween. Figure 5a represents the Nyquist plots of the faradaic impedance in 1 mM $K_3Fe(CN)_6$ / $K_4Fe(CN)_6$ solution in

ISBN:978-84-692-3235-4/DL:T-932-2009

PBS (pH 7.4) at the CDC5-DAPBA modified gold electrode (modified via application of one potential cycling in diazonium salts solution) after consecutive washing steps. As shown in Fig 5, the charge transfer resistance (R_{ct}) values decreased with increasing washing time, indicating the removal of the non-specifically adsorbed molecules.

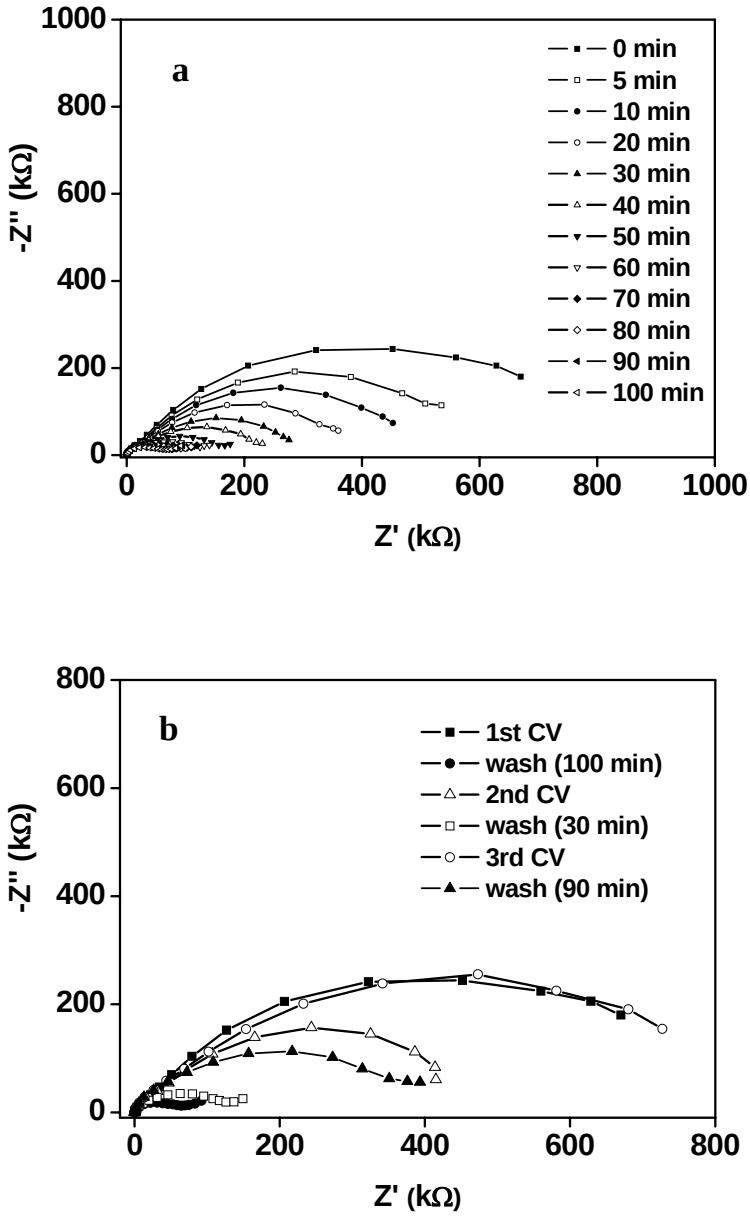

Fig. 5. (a) Nyquist plots of the faradaic impedance in 1 mM $K_3Fe(CN)_6$ / $K_4Fe(CN)_6$ solution in PBS (pH 7.4) at CDC5-DAPBA modified Au electrode (modified via one potential scan in its diazonium salt solution) after washing in PBS-Tween at different times; 0(■), 5(□), 10(●), 20(○), 30(▲), 40(Δ), 50(▼), 60(∇), 70(♦), 80(◊), 90(◄) and

ISBN:978-84-692-3235-4/DL:T-932-2009

100(◁) minutes. (b) Complex impedance plots for the modification process of Au electrode with CDC5-DAPBA, recorded after aaplication of the following consecutive steps; 1st CV for the electrochemical reduction of diazonium salt (■), wash for 100 min in PBS-Tween (●), 2nd CV (Δ), wash for 30 min (□), 3rd CV (○), and finally wash for 90 min (▲), recorded in 1 mM $K_3Fe(CN)_6$ / $K_4Fe(CN)_6$ solution in PBS (pH 7.4).

The resulting free spaces were then backfilled with CDC5-DAPBA via application of a second CV at the same modified electrode in the CDC5-DAPBA diazonium solution, to increase the number of active sites immobilized on the electrode surface to enhance the immunosensing detection. The washing steps were carried out again to remove the non-specifically adsorbed molecules, followed by backfilling with CDC5-DAPBA via application of a third reduction CV of diazonium salt. The modified electrode was then washed in PBS-Tween. The modification processes including the reduction, backfilling, and washing steps were characterized using EIS in in 1 mM $K_3Fe(CN)_6$ / $K_4Fe(CN)_6$ solution in PBS (pH 7.4) (Fig. 5b). As shown in Fig 5b, after each reduction step, the impedance was highly increased, which then decreased dramatically after washing, indicating the presence of a high level of non-specific adsorption or electrostatic multilayer fomation. After washing, the Rct values obtained according to the number of reduction cycles, had the following sequence; Rct (3rd CV) > Rct (2nd CV) > Rct (1st CV), indicating the successful backfilling and immobilization of a higher amount of active sites well oriented on the gold electrode surface. The EIS results shown in Fig 5b indicates that three cyclic voltammograms are enough to fully cover the electrode surface, while washing steps after each reduction are necessary to remove the non-specific adsorption and empty a space for the following specific deposition.

3.3. Immunosensing assay construction and characterization.

As previously explained in section 3.2.1., the modification of Au surface was carried out via electrochemical reduction of diazonium cations by three cyclic voltammograms which was enough to fully cover the electrode surface, and between the

UNIVERSITAT ROVIRA I VIRGILI
BOTTOM-UP SURFACE ENGINEERING FOR THE CONSTRUCTION OF (BIO) SENSORING SYSTEMS: DESIGN STRATEGIES AND ANALYTICAL APPLICATIONS
Hossam Metwally Ahmed Nassef
ISBN:978-84-692-3235-4/DL:T-932-2009

reduction processes, extensive washing steps are necessary to remove the non-specific adsorption and empty a space for the following specific deposition.

Figure 6 shows the strategy employed for immunosensor construction. After surface modification with CDC5-DAPBA, the free spaces resulting from the steric hindrance of the immobilized protein, was backfilled via the electrochemical reduction of phenylacetic acid diazonium cations. Figure 7 shows the consecutive cyclic voltammogram for the electrochemical reduction of phenylacetic acid diazonium cations in the potential range +0.7 to -0.4 V vs Ag/AgCl at 100 mV/sec scan rate at CDC5-DAPBA modified surface. As shown in Fig 7, an irreversible reduction peak was observed at -0.164 V with no associated oxidation peak, indicating the libration of N_2 gas due to the deposition of phenylacetic acid radical onto Au surface. A sequential decrease in reduction peak current associated with a shift in peak position was observed with each CV, indicating the deposition and successful backfilling of organic layer of phenylacetic acid, which is highly useful (after conversion of COOH to OH using EDC/NHS and ethanolamine) to prevent non-specifc adsorption.

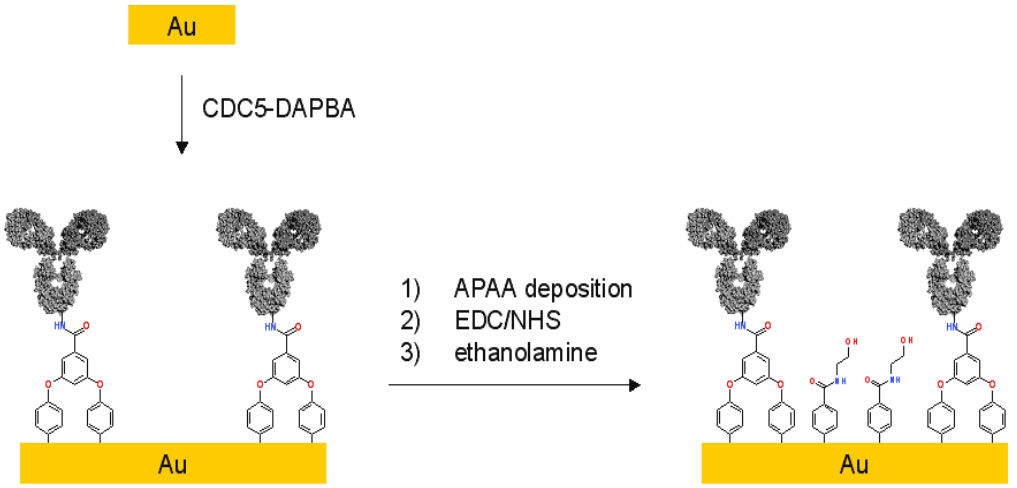

Fig 6. Strategy employed for immunosensor construction.

UNIVERSITAT ROVIRA I VIRGILI
BOTTOM-UP SURFACE ENGINEERING FOR THE CONSTRUCTION OF (BIO) SENSORING SYSTEMS: DESIGN STRATEGIES AND ANALYTICAL APPLICATIONS
Hossam Metwally Ahmed Nassef
ISBN:978-84-692-3235-4/DL:T-932-2009

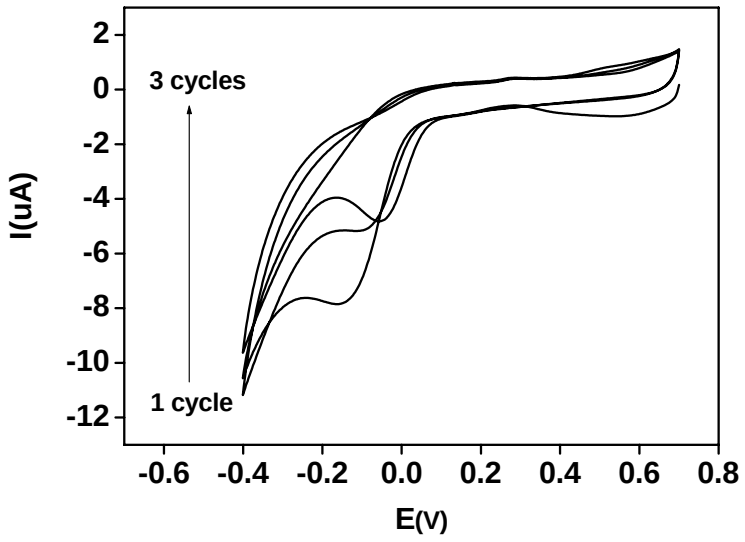

Fig 7. Cyclic voltammograms in in situ prepared diazonium salt solution of 100 mM APAA at CDC5-DAPBA modifed gold electrode for backfilling at 100 mV/sec scan rate via application of 3 continous potential scans vs Ag/AgCl.

Figure 8 represents the impedance spectra of the successive building steps of the immunosensor construction, in 1mM $Fe(CN)_6^{3-/4-}$ in PBS (0.1 M, pH 7.4). As shown in figure 8, the R_{ct} value was increased after immobilization of CDC5-DAPBA onto a clean gold electrode as previously explained in section 3.2.1., and the impedance then decreased after backfilling with APAA film. This decrease in EIS could be attributed to the removal of some specific or non-specific protein molecules from the modified surface and replaced by APAA. The carboxylic groups of APAA were then converted to hydroxyl groups using EDC/NHS and ethanolamine hydrochloride. Following blocking in ethanolamine, the modified surface was incubated in PBS-Tween (0.05 M, pH 7.4) solution for 30 min. The electrode was then exposed to 5 μg/mL gliadin in PBS-Tween solution for 30 min, followed by incubation with 100 μg/mL anti-gliadin-HRP in PBS for 30 min. Completing the sandwich sequence, the diameter of the semicircle increased with binding of each corresponding protein layer, with the increase of its value after each step demonstrating immunocomplex formation [46].

ISBN:978-84-692-3235-4/DL:T-932-2009

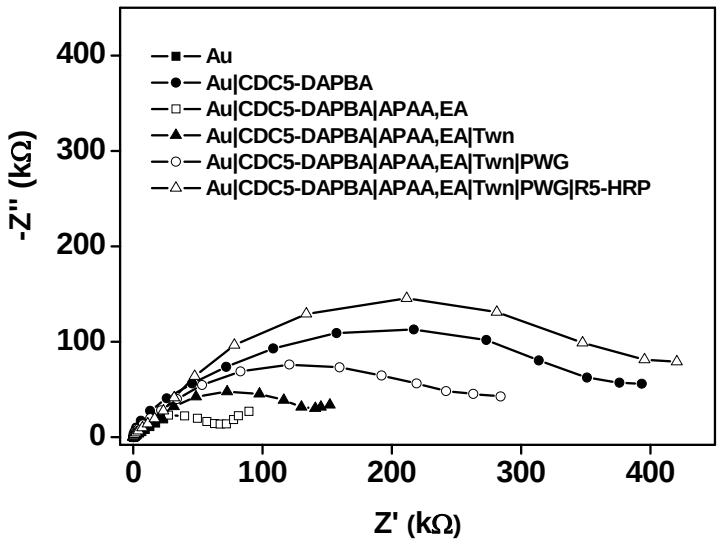

Fig. 8. Complex impedance plots in 1 mM $K_3Fe(CN)_6$ / $K_4Fe(CN)_6$ solution in PBS (pH 7.4) recorded at a SAM of CDC5-DAPBA modified Au electrodes for the sequential immobilization steps of the immunosensing assay.

3.4. Electrochemical detection of PWG.

3.4.1. Impedimetric detection.

Detection of gliadin on the modified electrodes was carried out using EIS and amperometry. EIS measurements were carried out in 1 mM $Fe(CN)_6^{3-/4-}$ in PBS (0.1 M, pH 7.4) in the frequency range of 0.1 Hz-100 kHz at a bias potential of +0.22 V and 5 mV amplitude before and after binding of (0 and 5 μg/ml) PWG in PBS-Tween (0.05 M, pH 7.4). The obtained spectra were fitted to an equivalent electrical circuit using the Autolab impedance analysis software. As shown in Figure 8 the Rct increased after incubation with 5 μg/mL gliadin whilst no response was obtained in absence of gliadin, indicating the specific binding of gliadin with the immobilized CDC5 anti-gliadin antibody.

3.4.2. Amperometric detection.

After modification of the gold electrode with CDC5-DAPBA and complete the construction of the sandwich as previously explained in section 3.3, the amperometric responses (Fig. 9) of the antibody-modified surface toward (0 and 5 μg/mL) gliadin concentrations were recorded at a fixed potential (-0.2 V vs Ag/AgCl) in PBS before and after the two consecutive injections of 2mM H_2O_2 and 2mM HQ under stirring. As

UNIVERSITAT ROVIRA I VIRGILI
BOTTOM-UP SURFACE ENGINEERING FOR THE CONSTRUCTION OF (BIO) SENSORING SYSTEMS: DESIGN STRATEGIES AND ANALYTICAL APPLICATIONS
Hossam Metwally Ahmed Nassef
ISBN:978-84-692-3235-4/DL:T-932-2009

shown in figure 9 (inset), no change in the amperometric current was observed after injection of HQ in the absence of gliadin, indicating the prevention of the non-specific adsorption of the anti-gliadin-HRP. In the presence of 5 μg/mLl gliadin, the reduction current was increased to about 410 nA, indicating the specific recognition of gliadin by the CDC5-DAPBA modified Au surface.

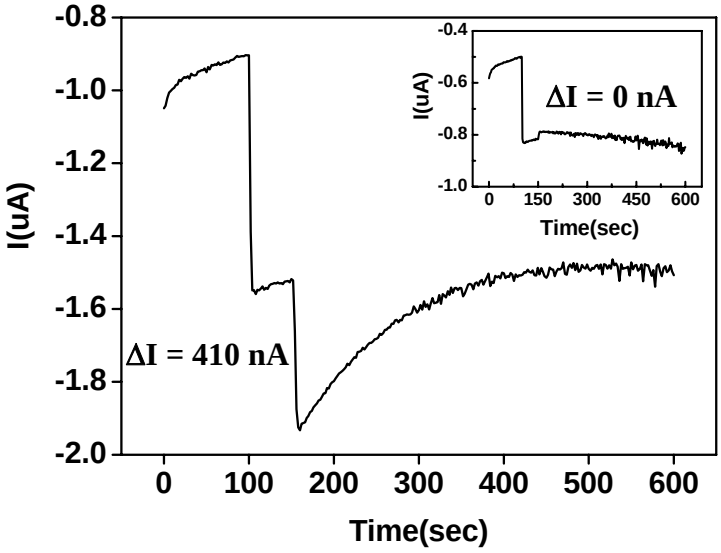

Fig. 9. Amperometric responses at CDC5-DAPBA modified surfaces after two consecutive injections of 2mM H_2O_2 and 2mM hydroquinone in cell; in presence of 0.0 (inset) and 5 μg/ml gliadin, respectively.

4. Conclusions

The full length anti-gliadin antibody CDC5 was coupled to 3,5-bis(aminophenoxy)benzoic acid (DAPBA) via carbodiimide chemistry. The CDC5-DAPBA was immobilized onto gold via the electrochemical reduction and non-electrochemical adsorption of the corresponding in situ prepared diazonium salt, respectively. The spontaneous reduction of CDC5-DAPBA diazonium cations onto Au was not successful. The modification of Au surface was carried out via electrochemical reduction of diazonium cations applying three potential cycles, and between cycles, extensive washing steps were necessary to remove the non-specific adsorption and to liberate spaces for subsequent deposition. Two ill defined reduction peaks were observed in the first scan at +0.047 and +0.414 V, which disappeared in the second and third scans, indicating the successful immobilization of CDC5-DAPBA. The affinity of

the immobilized antibody towards gliadin was studied using EIS and amperometry. The modified CDC5-DAPBA surface showed a reasonable amperometric response after incubation with 5 μg/mL gliadin, while no response was observed in the absence of gliadin, indicating the excellent specificity. The approaches of surface modification via the electrochemical deposition of diazonium salts, either by modification of the surface with a linker and then binding the full length antibody to the immobilized linker using carbodiimide chemistry, or via one step immobilization of the prepared antibody-linker conjugate, are time consumingand very laborious, due to the extensive washing processes needed to remove both the formed multilayers and/or the non-specifically adsorbed protein molecules onto gold surface. Moreover, sequential depositions of the protein-linker conjugate onto the librated spaces, followed by blocking of the remained free surface with a hydrophobic moiety, were necessary to fully prepare the immunosensing surface. This immunosensor model based on diazonium deposition has a lower sensitivity (0.082 $nA.ng^{-1}ml$) toward gliadin detection as compared with the F(ab) based immunosensor model (6.28 $nA.ng^{-1}ml$). Further work is required to elucidate the underlying mechanism of what is going on at the electrode surface suring deposition in order to have a controlled deposition technique for the rational construction of immunosensor architectures.

Acknowledgements

This work has been carried out as part of the Commission of the European communities specific RTD programme ‘Quality of Life and Management of Living Resources’ QLKI-2002-02077, the Plan Nacional GLUTACATCH and was partly financed by the Grup Emergente INTERFIBIO, 2005SGR00851. A.F. acknowledges the Ministerio de Ciencia e Innovación, Spain, for a “Ramón y Cajal” Research Professorship.

ISBN:978-84-692-3235-4/DL:T-932-2009

References

[1] M. Delamar, R. Hitmi, J. Pinson, J.M. Saveant, J. Am. Chem. Soc. 114 (1992) 5883.

[2] P. Allongue, M. Delamar, B. Desbat, O. Fagebaume, R. Hitmi, J. Pinson, J.M. Saveant, Journal of the American Chemical Society 119 (1997) 201.

[3] J.K. Kariuki, M.T. McDermott, Langmuir 15 (1999) 6534.

[4] P.R. Marcoux, P. Hapiot, P. Batail, J. Pinson, New Journal of Chemistry 28 (2004) 302.

[5] J.L. Bahr, J. Yang, D.V. Kosynkin, M.J. Bronikowski, R.E. Smalley, J.M. Tour, Journal of the American Chemical Society 123 (2001) 6536.

[6] A. Adenier, M.-C. Bernard, M.M. Chehimi, E. Cabet-Deliry, B. Desbat, O. Fagebaume, J. Pinson, F. Podvorica, Journal of the American Chemical Society 123 (2001) 4541.

[7] A. Chausse, M.M. Chehimi, N. Karsi, J. Pinson, F. Podvorica, C. Vautrin-Ul, Chemistry of Materials 14 (2002) 392.

[8] M.C. Bernard, A. Chausse, E. Cabet-Deliry, M.M. Chehimi, J. Pinson, F. Podvorica, C. Vautrin-Ul, Chem. Mater. 15 (2003) 3450.

[9] A. Adenier, E. Cabet-Deliry, A. Chausse, S. Griveau, F. Mercier, J. Pinson, C. Vautrin-Ul, Chem. Mater. 17 (2005) 491.

[10] M.P. Stewart, F. Maya, D.V. Kosynkin, S.M. Dirk, J.J. Stapleton, C.L. McGuiness, D.L. Allara, J.M. Tour, J. Am. Chem. Soc. 126 (2004) 370.

[11] P. Hartig, T. Dittrich, J. Rappich, Journal of Electroanalytical Chemistry 524-525 (2002) 120.

[12] P. Allongue, C. Henry de Villeneuve, G. Cherouvrier, R. Cortès, M.C. Bernard, Journal of Electroanalytical Chemistry 550-551 (2003) 161.

[13] J. Charlier, S. Palacin, J. Leroy, D. Del Frari, L. Zagonel, N. Barrett, O. Renault, A. Bailly, D. Mariolle, Journal of Materials Chemistry 18 (2008) 3136.

[14] J. Rappich, P. Hartig, N.H. Nickel, I. Sieber, S. Schulze, T. Dittrich, Microelectronic Engineering 80 (2005) 62.

[15] C. Saby, B. Ortiz, G.Y. Champagne, D. Bélanger, Langmuir 13 (1997) 6805.

[16] K. Boukerma, M.M. Chehimi, J. Pinson, C. Blomfield, Langmuir 19 (2003) 6333.

[17] J.A. Rogers, R.J. Jackman, G.M. Whitesides, J. Microelectromech. Syst. 6 (1997) 184.

[18] J.L. Wilbur, G.M. Whitesides, in Self-assembly and Self-assembled Monolayers in Micro and Nanofabrication nanotechnology, Springer-Verlag, New York, 1999, (Chapter 8).

[19] H.O. Finklea, Electroanal. Chem. 19 (1996) 109.

[20] G. Liu, J. Liu, T. Bo?cking, P.K. Eggers, J.J. Gooding, Chemical Physics 319 (2005) 136.

[21] E. Delamarche, B. Michel, H. Kang, C. Gerber, Langmuir 10 (1994) 4103.

[22] A.B. Horn, D.A. Russell, L.J. Shorthouse, T.R.E. Simpson, J. Chem. Soc. Faraday Trans. 92 (1996) 4759.

[23] M.H. Schoenfisch, J.E. Pemberton, J. Am. Chem. Soc. 120 (1998) 4502.

[24] S. Ranganathan, I. Steidel, F. Anariba, R.L. McCreery, Nano Lett. 1 (2001) 491.

[25] H.M. Nassef, M.C. Bermudo Redondo, P.J. Ciclitira, H.J. Ellis, A. Fragoso, C.K. Oâ€™Sullivan, Analytical Chemistry 80 (2008) 9265.

[26] A.J. Downard, Electroanalysis 12 (2000) 1085.

[27] A. Laforgue, T. Addou, D. Be?langer, Langmuir 21 (2005) 6855.

[28] J.C. Harper, R. Polsky, S.M. Dirk, D.R. Wheeler, S.M. Brozik, Electroanalysis 19 (2007) 1268.

[29] G. Liu, T. Bocking, J.J. Gooding, Journal of Electroanalytical Chemistry 600 (2007) 335.

[30] D.-e. Jiang, B.G. Sumpter, S. Dai, J. Am. Chem. Soc. 128 (2006) 6030.

[31] D.-e. Jiang, B.G. Sumpter, S. Dai, J. Phys. Chem. B 110 (2006) 23628.

[32] R. Polsky, J.C. Harper, D.R. Wheeler, S.M. Dirk, D.C. Arango, S.M. Brozik, Biosensors and Bioelectronics 23 (2008) 757.

[33] B.P. Corgier, C.A. Marquette, L.J. Blum, J. Am. Chem. Soc. 127 (2005) 18328.

[34] A. Vakurov, C.E. Simpson, C.L. Daly, T.D. Gibson, P.A. Millner, Biosensors & Bioelectronics 20 (2004) 1118.

[35] C. Combellas, F. Kanoufi, J. Pinson, F.I. Podvorica, Langmuir 21 (2005) 280.

[36] J. Haccoun, C. Vautrin-Ul, A. Chaussé, A. Adenier, Progress in Organic Coatings 63 (2008) 18.

[37] M.G. Paulik, P.A. Brooksby, A.D. Abell, A.J. Downard, J. Phys. Chem. C 111 (2007) 7808.

[38] S. Griveau, D. Mercier, C. Vautrin-Ul, A. Chausse, Electrochemistry Communications 9 (2007) 2768.

ISBN:978-84-692-3235-4/DL:T-932-2009

[39] A. Benedetto, M. Balog, P. Viel, F. Le Derf, M. Sallé, S. Palacin, Electrochimica Acta 53 (2008) 7117.

[40] C. Combellas, F. Kanoufi, J. Pinson, F.I. Podvorica, J. Am. Chem. Soc. 130 (2008) 8576.

[41] R. van Eckert, Berghofer, E., Ciclitira, P.J., Chirdo, F., Denery-Papini, S., Ellis, H.J., Ferranti, P., Goodwin, P., Immer, U., Mamone, G., Méndez, E., Mothes, T., Novalin, S., Osman, A., Rumbo, M., Stern, M., Thorell, L., Whim, A., Wieser, H., J. Cer. Sci. 43 (2006) 331.

[42] P.J. Ciclitira, D.H. Dewar, T. Suligoj, C.K. O'Sullivan, H.J. Ellis, in Proceedings of the 12th International Celiac Symposium, New York 2008.

[43] A. Adenier, N. Barré, E. Cabet-Deliry, A. Chaussé, S. Griveau, F. Mercier, J. Pinson, C. Vautrin-Ul, Surface Science 600 (2006) 4801.

[44] M. Delamar, G. Desarmot, O. Fagebaume, R. Hitmi, J. Pinsonc, J.M. Saveant, Carbon 35 (1997) 801.

[45] M. Dequaire, C. Degrand, B. Limoges, Journal of the American Chemical Society 121 (1999) 6946.

[46] O. Pänke, T. Balkenhohl, J. Kafka, D. Schäfer, F. Lisdat, in T. Scheper (Editor), Advances in Biochemical Engineering/Biotechnology, Springer-Verlag Berlin Heidelberg, 2008, p. 227.

UNIVERSITAT ROVIRA I VIRGILI
BOTTOM-UP SURFACE ENGINEERING FOR THE CONSTRUCTION OF (BIO) SENSORING SYSTEMS: DESIGN STRATEGIES
AND ANALYTICAL APPLICATIONS
Hossam Metwally Ahmed Nassef
ISBN:978-84-692-3235-4/DL:T-932-2009

CHAPTER 10:

Conclusions and future work

UNIVERSITAT ROVIRA I VIRGILI
BOTTOM-UP SURFACE ENGINEERING FOR THE CONSTRUCTION OF (BIO) SENSORING SYSTEMS: DESIGN STRATEGIES AND ANALYTICAL APPLICATIONS
Hossam Metwally Ahmed Nassef
ISBN:978-84-692-3235-4/DL:T-932-2009

10. Conclusions and future work

10.1. Conclusions

The present PhD is a component of an overall vision to construct a reagentless, washless and ultrasensitive biosensor, as explained in the introduction. The first aim of the main project (reagentless biosensor) can be achieved via the co-immobilization of an enzyme substrate (such as o-aminophenylphosphate) with the capture antibody on the electrode surface. To achieve the objectives of a washless biosensor, target sensitive liposomes can be exploited as the reporter label, encapsulating a large number of enzyme molecules (such as alkaline phosphatase (ALP)) as well as a mediator, which can be used for substrate recycling of the electrochemically oxidized product of the enzymatically dephosphorylated o-aminophenol (o-AP) for signal amplification, achieving the goal of ultrasensitivity.

One of the objectives of the present PhD was to find a suitable mediator that could be used for catalytic recycling of o-AP, and another important objective was to study different design strategies for capture antibody immobilization for the construction of immunosensors and their use for analytical applications. In the work reported here, we used gliadin as a model substrate – however, the generic platform developed could be applied to any target antigen detected using a sandwich format.

Different potential mediators that could be used for the catalytic interaction with the enzymatic product o-AP, were evaluated and due to their well characterized properties, hydrazine, NADH and ascorbic acid were selected for further study. Hydrazine is used as an antioxidant and reducing agent; NADH plays an important rule in oxidoreductases and dehydrogenase systems and ascorbic acid (vitamin C) is an antioxidant whose detection is important in clinical and food applications. The electrocatalytic properties of o-aminophenol films grafted on glassy carbon surfaces have been employed for the electrochemical evaluation of hydrazine, NADH and ascorbic acid, to select the most relevant as a recycling mediator in the planned signal amplification strategy. To evaluate the best mediator, the reaction kinetics between mediators and the o-AP/o-QI were extensively studied using different techniques such as cyclic voltammetry, hydrodynamic voltammetry, double potential step chronoamperometry, and double potential step chronocoulometry. The calculated transfer

UNIVERSITAT ROVIRA I VIRGILI
BOTTOM-UP SURFACE ENGINEERING FOR THE CONSTRUCTION OF (BIO) SENSORING SYSTEMS: DESIGN STRATEGIES AND ANALYTICAL APPLICATIONS
Hossam Metwally Ahmed Nassef
ISBN:978-84-692-3235-4/DL:T-932-2009

coefficients (α) were in the range 0.41 to 0.63 indicating that one electron transfer process is the rate limiting step. The diffusion coefficients (D) of the mediators from the bulk solution to the electrode surface were in the same magnitude, ranging from 2.4×10^{-6} to 5.9×10^{-6} cm^2s^{-1}. The number of electrons transferred in the catalytic reaction was high (n = 4) in case of hydrazine leading to a low limit of detection (0.05 μM). Furthermore, the o-AP catalytic surface showed higher sensitivity (0.016 μA/μM) toward hydrazine oxidation compared to NADH and ascorbic acid, 0.014 and 0.012 μA/μM, respectively. The electrocatalytic rate constants (k) for the NADH system, of 1.1×10^{5} M^{-1} s^{-1} is an order of magnitude higher when compared the rate constants of hydrazine and ascorbic acid, 4×10^{4} M^{-1} s^{-1} and 3.8×10^{4} M^{-1} s^{-1}, respectively, indicating that the reaction between NADH and o-QI is the fastest of the three. In addition, sub-micromolar amounts of these mediators were detected, a property that could be used for highly sensitive analytical purposes. Of the three mediators evaluated, hydrazine is flammable, detonable, corrosive and highly toxic [1-3] and therefore difficult to handle. On the other hand, NADH is unstable and expensive [4,5] and electrode surfaces are easily fouled by the accumulation of reaction products during NADH oxidation [6]. On the other hand, ascorbic acid is cheap, easy to handle, safe, showed excellent electrocatalytic behavior, and is compatible with hydrolases such as ALP for co-encapsulation purposes [7,8]. Therefore, ascorbic acid was selected as the mediator for regeneration of the o-AP film and substrate recycling.

We had thus demonstrated an interesting catalytic system for the oxidation of ascorbic acid, which is stable, sensitive and reproducible, and we decided to explore this system for clinical and food applications. In the first application, we targeted the determination of uric acid (UA) in the presence of ascorbic acid (AA), which commonly co-exist in biological fluids of humans, mainly in blood and urine. It is difficult to electrochemically differentiate between UA and AA at bare electrodes, while the o-AP surface facilitates a selective catalytic activity towards ascorbic acid. To this end, the o-AP modified surface has been used for the detection of ascorbic acid in the presence of uric acid and vice versa, and was applied to the detection of uric acid in real urine sample, with the estimated UA content of that adult person (me) being 3.45 mM,

UNIVERSITAT ROVIRA I VIRGILI
BOTTOM-UP SURFACE ENGINEERING FOR THE CONSTRUCTION OF (BIO) SENSORING SYSTEMS: DESIGN STRATEGIES
AND ANALYTICAL APPLICATIONS
Hossam Metwally Ahmed Nassef
ISBN:978-84-692-3235-4/DL:T-932-2009

indicating normal levels of uric acid, falling within the normal clinical range of 0.79-7.9 mM [9].

The selective electrocatalytic properties of the grafted o-AP film toward ascorbic acid were also applied to its detection in real samples of fruits and vegetables using disposable one-shot screen printed electrodes. The o-AP modified screen printed electrodes showed high catalytic responses toward the electrocatalytic oxidation of ascorbic acid with a decrease in overpotential. The o-AP SPE sensor exhibited high sensitivity and selectivity toward ascorbic acid with excellent storage and operational stability, as well as a quantitatively reproducible analytical performance. The catalytic oxidation peak current of amperometric response was linearly dependent on ascorbic acid concentration in the range of 2–20 μM with a limit of detection of 0.86 μM. The modified screen printed electrode was applied to the determination of ascorbic acid in a large number of fruits, vegetables, and commercial juices, and our sensor exhibited excellent correlation with the standard spectrophotometric method [10].

In the second part of the present thesis, different surface engineering strategies of antibody immobilization for immunosensor construction using a linker or via direct attachment onto a Au surface using a strategy of self assembly. An alternative strategy explored was the direct anchoring of the antibody with or without a linker via the electrochemical reduction of their diazonium cations.

A comparison between these different surface chemistries methodologies for the construction of immunosensors towards the model analyte of coeliac toxic gliadin was carried out. Firstly, the self-assembled monolayer approach was evaluated based on the modification of gold surfaces with two bipodal carboxylic acid terminated thiols (thioctic acid and a benzyl alcohol disubstituted thiol, DT2). A stable SAM of DT2 was rapidly immobilized (3h) on Au as compared with thioctic acid (100h), although both surface chemistries resulted in highly sensitive electrochemical immunosensors for gliadin detection using an anti-gliadin antibody (CDC5), with detection limits of 11.6 and 5.5 ng/mL, respectively. The developed immunosensors were then applied to the detection of gliadin in commercial gluten-free and gluten-containing food products, showing an

excellent correlation when compared to results obtained with ELISA. The antibody-modified SAMs of DT2 showed higher stability compared to thioctic acid; in the first three days of interaction, an impedance decrease for the SAM of thioctic acid was observed, which could be related to the partial loss of some physisorbed antibody material, or destabilising effect of the antibody immobilization on the thioctic acid SAM. In contrast, electrodes modified with DT2 showed a slight impedance increase in the first day, remaining constant during the rest of the stability study.

Exploring approaches to further improving immunosensor sensitivity and stability and furthermore to reduce the time necessary for sensor preparation, the direct attachment of the SATA modified full length antibody, and their F(ab) fragments onto Au electrodes was investigated. Spontaneously adsorbed SAMs of Fab-SH and CDC5-SH onto Au were rapidly formed in just 15 minutes. The amperometric immunosensors based on Fab fragments exhibited vastly improved detection limit as compared to the thiolated antibody with a highly sensitive response toward gliadin detection (LOD, 3.29 ng/ml for amperometric detection and 0.42 μg/ml for labelless (impedimetric) detection). Moreover, the self-assembled monolayer of F(ab) fragments was extremely stable with almost no loss in response after 60 days storage at 4^{o}C, and this combined with the advantages of sensitivity, reduced biosensor preparation time and improved detection limit presents this approach as a very promising surface chemistry for immunosensors.

An alternate surface chemistry approach was explored for the modification of Au electrodes via electrochemical (i.e. CV at different potential cycling or via application of fixed potential at different deposition times) and spontaneous reduction (via dipping at different exposure times) in diazonium cations of a conjugate prepared from the monoclonal full length anti-gliadin antibody (CDC5) and the linker 3,5-bis(aminophenoxy)benzoic acid (DAPBA). Voltammetry cycling was chosen for surface modification via three potential cycles, but it was observed that an extensive washing process was necessary after each potential cycle to remove the non-specifically adsorbed molecules or formed multilayers. The affinity of the immobilized antibody toward gliadin was studied using EIS and amperometry. The modified CDC5-DAPBA surface showed a

UNIVERSITAT ROVIRA I VIRGILI
BOTTOM-UP SURFACE ENGINEERING FOR THE CONSTRUCTION OF (BIO) SENSORING SYSTEMS: DESIGN STRATEGIES AND ANALYTICAL APPLICATIONS
Hossam Metwally Ahmed Nassef
ISBN:978-84-692-3235-4/DL:T-932-2009

reasonable amperometric response after incubation with 5 μg/ml gliadin, and exhibited excellent specificity with no response observed in the absence of the analyte. However, this immunosensor model based on diazonium deposition has a much lower sensitivity (0.082 $nA.ng^{-1}ml$) toward gliadin detection as compared with the F(ab) based immunosensor (6.28 $nA.ng^{-1}ml$).

The approaches of surface modification via the electrochemical deposition of diazonium salts, either by modification of the surface with a linker and followed by cross-linking with the full length antibody, or via one step immobilization of the prepared antibody-linker conjugate, are time consuming and very laborious requiring extensive washing, and further exploration is required to understand how to control deposition to avoid complex multiplayer formation.

From the different surface chemistry strategies evaluated in this work we can conclude that the best approach is the immunosensor based on the spontaneous adsorption of thiolated F(ab) fragments on gold. This surface is easy and fast to prepare, very stable and sensitive and can be stored for long times in the appropriate conditions without lost of affinity. A good alternative to this approach seems to be the electrodeposition of antibody-diazonium conjugates, although further work is needed in order to optimize this system.

Overall, this work has contributed significantly to the vision we have for an immunosensor that avoids washes and reagent addition, where we have selected an excellent mediator for co-encapsulation with alkaline phosphatase enzymes within liposome reporter molecules, for regeneration of surface immobilised substrate following enzymatic dephosporylation, facilitating substrate recycling and increase in sensitivity and reduction in detection limit. Furthermore, we have selected an optimum surface chemistry for co-immobilisation of capture antibody molecules and enzyme substrate via the formation of self-assembled monolayers of antibody fragments on gold surfaces. Future work will focus on combining the selected mediator and surface chemistry into a sandwich immunosensor with a target sensitive liposome reporter molecule, to demonstrate a reagentless, washless ultrasesensitive immunosening platform.

UNIVERSITAT ROVIRA I VIRGILI
BOTTOM-UP SURFACE ENGINEERING FOR THE CONSTRUCTION OF (BIO) SENSORING SYSTEMS: DESIGN STRATEGIES
AND ANALYTICAL APPLICATIONS
Hossam Metwally Ahmed Nassef
ISBN:978-84-692-3235-4/DL:T-932-2009

10.2. Future work

- Preparation of sensitive target liposome encapsulated with ascorbic acid and ALP and/or HRP.
- Co-immobilization of catching antibody F(ab) fragments and o-aminophenylphosphate substrate onto the same electrode surface.
- Optimize the immobilization and detection parameters such as deposition ratio, deposition time, and incubation times for the biosensor construction.
- Use the optimized biosensor model for analytical applications.

ISBN:978-84-692-3235-4/DL:T-932-2009

References

[1] I. Makarovsky, G. Markel, T. Dushnitsky, A. Eisenkraft, Israel Medical Association Journal 10 (2008) 302.

[2] C.J. Waterfield, J. Delaney, M.D.J. Kerai, J.A. Timbrell, Toxicology in Vitro 11 (1997) 217.

[3] A. Tostmann, M.J. Boeree, W.H.M. Peters, H.M.J. Roelofs, R.E. Aarnoutse, A.J.A.M. van der Ven, P.N.R. Dekhuijzen, International Journal of Antimicrobial Agents 31 (2008) 577.

[4] T.W. Barrett, Journal of Raman Spectroscopy 9 (1980) 130.

[5] S.G.A. Alivisatos, F. Ungar, G. Abraham, Nature 203 (1964) 973.

[6] J. Wang, L. Angnes, T. Martinez, Bioelectrochemistry and Bioenergetics 29 (1992) 215.

[7] A.J. Bäumner, R.D. Schmid, Biosens. Bioelectron. 13 (1998) 519.

[8] M. Campas, P. de la Iglesia, M. Le Berre, M. Kane, J. Diogene, J.L. Marty, Biosensors & Bioelectronics 24 (2008) 716.

[9] C.S.H. Joseph C. Fanguy, ELECTROPHORESIS 23 (2002) 767.

[10] N. Durust, D.a. Sumengen, Y. Durust, Journal of Agricultural and Food Chemistry 45 (1997) 2085.